Design, development and experimental trialof a tailored cytotoxic T-cell vaccine againstPorcine Reproductive and RespiratorySyndrome Virus-2

Welner, Simon

Publication date:
2017

Document Version
Publisher's PDF, also known as Version of record

DTU Vet
National Veterinary Institute

Design, development and experimental trial of a tailored cytotoxic T-cell vaccine against Porcine Reproductive and Respiratory Syndrome Virus-2

PhD Thesis
Simon Welner
March, 2017

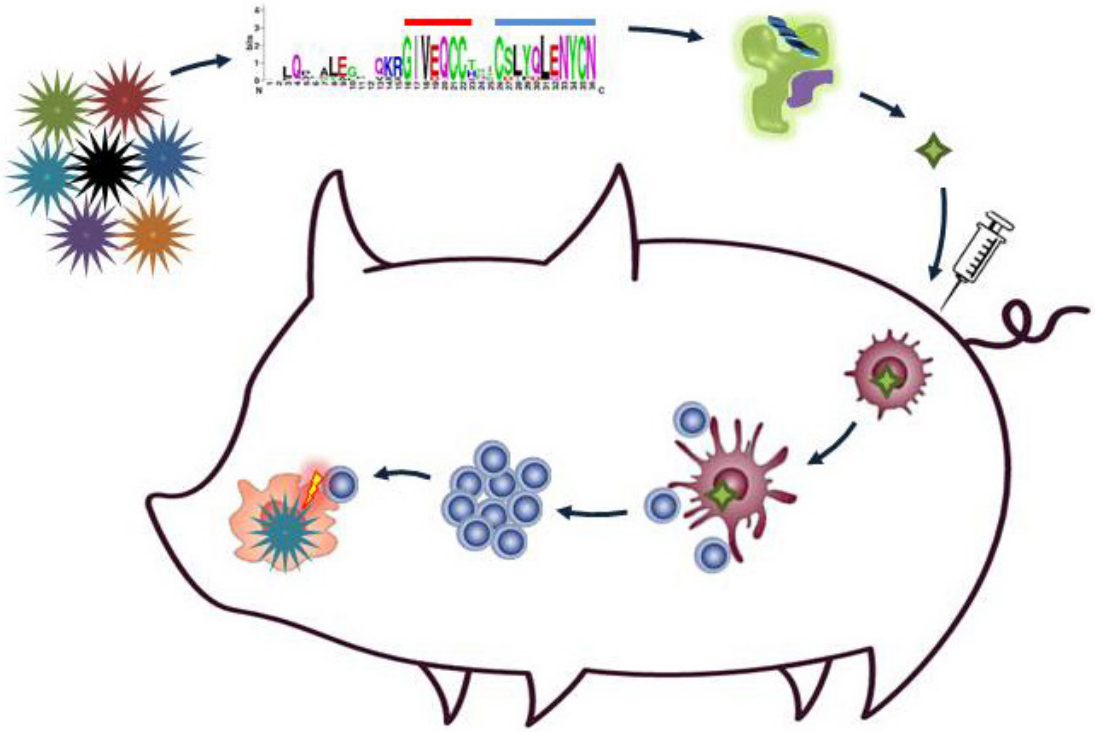

PREFACE

The current PhD project was conducted at the National Veterinary Institute (Vet), Technical University of Denmark (DTU) from September 2013 to March 2017. It was funded by DTU-Vet as a "high impact - high risk" PhD project in an attempt to promote cross-disciplinary DTU projects with high innovative potential. As such, it was erected as a collaboration between Section for Virology (DTU-Vet), Section for Immunology and Vaccinology (DTU-Vet), and Center for Biological Sequence Analysis (DTU-CBS), each represented by a supervisor.

The overall idea of the project was to combine various innovative tools in order to achieve the following milestones:

1. Prediction and prioritization of conserved CD8 T cell epitopes derived from Porcine reproductive and respiratory syndrome (PRRS) virus-2 by using bioinformatic tools developed at DTU-CBS.
2. Verification of the predicted epitopes based on *in vitro* methods developed by DTU-Vet and the Laboratory of Experimental Immunology, University of Copenhagen.
3. Design and generation of a polyepitope-encoding vaccine construct based on a virus replicon particle (VRP) platform developed by the Swiss partner, Institute for Virology and Immunology (IVI).

The generation and verification of the final vaccine VRPs were executed during a 2½ months stay at IVI. Following this, a vaccine-challenge animal experiment for the trial of vaccine efficacy was conducted at the island of Lindholm (DTU-Vet).

The thesis consists of a general introduction to central aspects of importance including the porcine immune system, the mechanisms involved in the induction of a cytotoxic T cell response, and the PRRS virus. This is followed by a description of the applied methods and the experimental setups. Finally, a general discussion is given in which I elaborate on the results presented in the two accompanying papers, both of which are yet to be published.

The two papers, on which my thesis is based, are:

Paper 1: Prediction and in vitro verification of conserved PRRSV type 2 CTL epitopes

Paper 2: Challenge study of pigs immunized with virus replicon particles for the induced expression of conserved PRRSV-2 CTL epitopes

ACKNOWLEDGEMENTS

First of all, I would like to thank DTU-VET for hiring me. I hope that I fulfilled the expectations.

A profound thank you is dedicated to my supervisors, Lars Erik Larsen and Gregers Jungersen. Despite you both being busy scientists, you were always available for advice when I doubted, inspiration when I got stuck and support when I failed. You brought me to great places around the world, enthusiastically presented my work in my absence, and got down and dirty when blood and tissue samples were needed. For this and much more, I am sincerely grateful.

An excited thank you is given to my co-supervisor at DTU-CBS, Ole Lund, and to my bioinformatics guru, Morten Nielsen, especially. You opened up the magical black box to me and introduced me to the intriguing world of bioinformatics. A world rid of inexplicable outliers. A world behaving just the way I wanted it. A world where each line of functional code released endorphins in a constant flow of brain fixes.

A big thank you goes to the wonderful virology people on the second floor. I enjoyed your company at Friday morning breakfasts, at journal clubs, at parties and on a daily basis. A special thanks to Hue Thi Thanh Tran, who helped me with several practical matters; Lise Kirstine Kvisgaard for her expertise in PRRSV; Katrine Fog Thomsen, without whom I never would have completed all the lab work associated with the animal experiment; and Nicole Bakkegård Goecke, who helped during the euthanasia of the pigs, and furthermore was good company in the PhD office.

An equally big thank you goes to the happy people of the Section for Immunology and Vaccinology. You are certainly a dynamic bunch of interesting people, and I have had several rewarding conversations with many of you. A special thanks to Jeanne Toft Jakobsen who skillfully guided my training in several assays and were always good for a chat and a laugh; Lasse Eggers Pedersen, who in many ways was my predecessor and passed on a solid base of experience of porcine SLAs and associated assays; Lien Thi Minh Nguyen, who often helped me with time consuming DNA purification and analysis; and Maria Rathmann Sørensen and Mikael Lenz Strube for your help in conducting and analyzing the NGS-based SLA genotyping even though it didn't really work.

Thank you, Michael Rasmussen, for the analysis of pSLA stability. Those data were central to the thesis.

Heartfelt thanks are sent to all of the fantastic people at IVI in Switzerland. My stay was really a great adventure which was entirely because of your strong scientific foundation, great company and good humor, spiced up with exciting leisure-time activities. I quickly felt welcome and part of the group, and for this, I am utterly grateful. Also, Switzerland is pretty. A special thank goes to Nicolas Ruggli and Artur Summerfield, who functioned as my local supervisors from the virology and immunology sections of the institute, respectively; and to Simea Werder, Markus Gerber and Matthias Liniger from the Ruggli lab, who did most of the VRP generation.

I would also like to thank the persons who fought for making the animal experiment possible. This was a daunting task and required a huge effort by Kirsten Tjørnehøj, the biosafety officer at Lindholm; and Thomas Kledahl, former head of Section for Virology.

Furthermore, I would like to thank the Lindholm people for accepting me to the small island community during the animal experiment. Special thanks to Thomas Bruun Rasmussen for being a great and caring local supervisor; Jani Christiansen for being a splendid life-line, support and good company within the BSL3-ag facility; and Graham Belsham and Jonas Kjær for helping with planning and execution of the western blot, even though it didn't provide the desired results.

Also, the pigs were very grateful for being treated with care during the various experiments. For this, they and I would like to thank the team led by Hans Skåning at Frederiksberg, and the team led by Heidi Lehman at Lindholm. Also, thank you very much, Louise Lohse, for carrying the responsibility for their lives and health at Lindholm.

Finally, I would like to express my greatest love and gratitude to my family. Sandra, my wife, thank you for supporting and nurturing me the whole way through, even in the toughest of times when alone in the new house with a toddler, a dog, and a big belly, while I was partying in Switzerland. Bertram, the toddler, thank you for letting me know whenever you got mad at me that *you* would leave for Switzerland. Leopold, the belly, thank you for being born and for making sure that I didn't waste my time sleeping. I love you all very much.

Lastly, thank you, Otto the dog, for walking me.

LIST OF CONTENT

PREFACE 1

ACKNOWLEDGEMENTS 2

SUMMARY 6

SAMMENDRAG (DANISH SUMMARY) 8

ABBREVIATIONS 10

GENERAL OBJECTIVE 11

1 GENERAL INTRODUCTION 13

1.1 The porcine immune system 13

1.1.1 The innate immune system 13

1.1.1.1 Macrophages 14

1.1.1.2 Dendritic cells 14

1.1.1.3 Natural killer cells 15

1.1.1.4 Neutrophil granulocytes 16

1.1.2 The adaptive immune system 16

1.1.2.1 T cells in general 17

1.1.2.2 γδ T cells 18

1.1.2.3 B cells 19

1.2 The induction of a targeted CTL response 20

1.2.1 The MHC Class I 21

1.2.2 Peptide processing and loading of the MHC 22

1.2.3 CD8β T cell priming 24

1.2.4 CTL effector functions 25

1.2.5 CTL memory 26

1.2.6 Determinants of a functional epitope 27

1.3 The Porcine Reproductive and Respiratory Syndrome Virus 28

1.3.1 Discovery and taxonomy 28

1.3.2 Genomic organization and virion structure 28

1.3.3 Origin, phylogeny and diversity 30

1.3.4 Virus attachment, entry, replication and release 31

1.3.5 Pathogenesis and pathology 33

1.3.6 Virus transmission and epidemiology 33

1.3.7 Prevention and control 34

1.3.8 Immune response and immunoevasion 36

1.3.8.1 Effects on the innate immune response 37

1.3.8.2 Effects on the humoral adaptive immune response 39

1.3.8.3 Effects on the cell-mediated adaptive immune response 40

1.3.9 Upcoming innovative vaccines 41

2 GENERAL MATERIALS AND METHODS 42

2.1 Epitope prediction 42

2.1.1 Selection, curation and preparation of PRRSV sequences 43

2.1.2 Selecting the SLAs 43

2.1.3 Prediction using NetMHCpan 43

2.1.4 Prediction using PSCPL 44

2.1.5 “The Program!” - Python-based program for PSCPL analysis 46

2.1.6 PopCover - prioritizing the epitope candidates 46

2.2 Preparation and storage of the peptides 46

2.3 *In vitro* verification of selected epitopes 47

2.3.1 Peptide-SLA affinity determination by peptide affinity ELISA 47

2.3.2 Peptide-SLA stability determination by scintillation proximity assay 48

2.4 SLA genotyping of pigs ... **49**
2.4.1 DNA-based SLA genotyping ... 50
2.4.2 Next-generation sequencing-based SLA genotyping ... 50
2.5 VRP design, generation and verification ... **51**
2.5.1 The virus replicon particle ... 51
2.5.2 "Juncitope" - Python-based program for neoepitope removal between epitopes in a polyepitope ... 51
2.5.3 Rescue and storage of the VRPs ... 52
2.5.4 Flow cytometry ... 52
2.5.5 Western blot ... 54
2.6 Titration of VRPs and PRRSV ... **55**
2.7 Diagnostic methods ... **57**
2.7.1 ELISA ... 57
2.7.2 qRT-PCR ... 57
2.8 ELISPOT ... **57**
3 EXPERIMENTAL DESIGNS ... **59**
3.1 The VRP vaccine-challenge animal experiment ... **59**
3.2 *Ex vivo* analysis of pigs vaccinated with Ingelvac PRRS Vet (unpublished) ... **61**
4 GENERAL DISCUSSION AND PERSPECTIVES ... **62**
4.1 Discussion of the obtained results ... **62**
4.1.1 Suitability of the selected epitopes ... 63
4.1.2 Compromised CD8β T cell priming ... 66
4.1.2.1 Density of APCs ... 66
4.1.2.2 Density of presented epitopes ... 67
4.1.3 Effects of an established CTL response against a natural infection ... 67
4.2 Discussion of the applied approach ... **69**
4.2.1 Curation and selection of PRRSV sequences ... 69
4.2.2 Prerapation of selected strains prior to epitope prediction ... 69
4.2.3 Identification and selection of epitopes ... 70
4.2.4 The vaccine platform ... 72
4.2.5 The experimental conditions ... 73
4.2.6 The challenge strain ... 74
4.2.7 The readouts ... 74
4.3 Summary and conclusions ... **74**
EPILOGUE ... **76**
PUBLICATIONS ... **77**
Paper 1: Prediction and *in vitro* verification of conserved PRRSV-2 CTL epitopes ... **78**
Paper 2: Challenge study of pigs immunized with virus replicon particles for the induced expression of conserved PRRSV-2 CTL epitopes ... **98**
Supplementary data 1: Nucleotide and amino acid sequences of cassettes inserted in the VRPs ... 123
Supplementary data 2: Verification of VRP infectivity and polyepitope expression and degradation ... 128
APPENDICES ... **129**
Appendix A - "The Program" - code ... **129**
Appendix B - PopCover output ... **134**
Appendix C - "Juncitope" output - VRP1 ... **135**
Appendix D - "Juncitope" - code ... **140**
Appendix E - *Ex vivo* analysis of pigs vaccinated with Ingelvac PRRS Vet ... **153**
REFERENCES ... **158**

SUMMARY

Porcine reproductive and respiratory syndrome virus (PRRSV) is one of the most important threats against the global swine production industry. The virus infects alveolar macrophages that leads to respiratory distress, fever, pneumonia and gives way to secondary respiratory pathogens. Infection of sows in late gestation can lead to late-term abortion, early farrowing and birth of litters mixed with living, stillborn and mummified fetuses. Two species of PRRSV exist that are closely related in evolution and disease: PRRSV-1 and PRRSV-2. PRRSV has a positive sense RNA genome of about 15 kb and exhibits a high mutation rate that has led to a high degree of diversity within each species. Highly pathogenic strains evolve occasionally with large impact on animal health and production economy.

Since its discovery in the late 1980s, massive efforts have been put in the development of an effective vaccine. In spite of this, the most effective commercial vaccines available are only partly capable of protecting against a heterologous challenge. Furthermore, these vaccines are based on modified live virus that at more than one occasion have mutated back to a virulent form and have thus promoted rather that prevented viral spread.

PRRSV exhibits a wide range of immunoevasive mechanisms that manipulate multiple branches of the porcine immune system. However, evidence exist that a cell-mediated immune (CMI) response is capable of clearing the virus from the organism, although this response is somewhat delayed.

In the present PhD thesis, I describe the development of an innovative vaccine for the induction of a cytotoxic T lymphocyte response against PRRSV-2. A major part of the project outline was to design a vaccine that would protect beyond genetic drift, why focus has been on identifying and selecting conserved epitopes specific for swine leukocyte antigen class I (SLA-I). Briefly, all naturally occurring 9- and 10-mer peptides derived from 104 highly curated PRRSV-2 whole genome sequences were analyzed for their predicted binding capacities against five SLA-I alleles. Two methods for epitope prediction was applied (NetMHCpan and Position Scanning Combinatorial peptide library). The outputs of the two methods were combined and the top 2% best candidates were analyzed using the PopCover algorithm, serving to prioritize the candidates according to conservation and SLA allele coverage. Based on this, 53 peptides were purchased for *in vitro* verification. This was done using the assays Peptide Affinity Assay and Scintillation Proximity Assay for the determination of peptide-SLA (pSLA) binding affinity and stability, respectively. From these analyses it was decided to proceed with three of the five SLAs in combination with a total of 33 peptides (/epitopes).

A Classical swine fever virus (CSFV)-based virus replicon particle (VRP) was selected as vaccine platform. This VRP has the same tropism as CSFV and can thus infect dendritic cells that are the major inducers of a CMI response. On basis of this template VRP, 10 vaccine VRPs were designed for the expression of an inserted polyepitope with subsequent degradation via an uncleavable ubiquiting, thereby leading the epitopes into the MHC-I presentation pathway. One VRP was designed as a negative control and encoded an unrelated epitope, while the remaining nine encoded polyepitopes of different combinations of the 33 PRRSV-2 epitopes. Infectivity of the VRPs and the induced polyepitope expression and degradation was verified using flow cytometry.

18 pigs of matching SLA profiles were vaccinated three times over a 10-week period with the control VRP (N=7) or the PRRSV-VRPs (N=11). After this, all pigs were inoculated with a Danish PRRSV-2 field strain and were euthanized after an additional four weeks. Seroconversion for both VRP and PRRSV was confirmed for all pigs. The induction of a CMI response was monitored using interferon-γ (IFN-γ) enzyme-linked immunospot (ELISPOT) assay pre challenge, but did unfortunately not provide any usefull data. The setup was improved and post challenge ELISPOT provided evidence of a VRP-induced CMI. Viral load was measured post challenge in serum, but did not indicate any effects of vaccination. Viral load in lungs did however indicate an effect that was significant in one part of the lungs.

Conclusively, the present study provides proof-of-concept that a peptide-specific CMI can be induced by vaccination with VRPs encoding conserved epitopes, along with indications of a protective effect on viral load in lungs. However, several improvements must be made to the concept before it can be subjected to field trials.

SAMMENDRAG (DANISH SUMMARY)

Porcint reproduktions og respiratorisk syndrom virus (PRRSV) er en af de største trusler mod den globale svineproduktion. Den inficerer lungemakrofager, hvilket fører til åndedrætsbesvær, feber, lungebetændelse og baner desuden vejen for sekundære infektioner. Hos søer inficeret sent i drægtighedsperioden, kan dette føre til abort, for tidlig faring samt fødslen af kuld blandet med levende, dødfødte og mumificerede fostre. Der findes to arter af PRRSV, der er nært beslægtede med hensyn til både genetik og sygdom: PRRSV-1 og PRRSV-2. PRRSV har et positiv strenget RNA genom på ca. 15 kilobaser og har en høj mutationsrate som har ført til stor diversitet indenfor hver art. Højpatogene virusstammer udvikler sig fra tid til anden med stor indflydelse på både dyrevelfærd produktionsøkonomi.

Siden opdagelsen af PRRSV i slutningen af 1980'erne, er der blevet sat massivt ind for at udvikle af en effektiv vaccine. På trods af dette er de mest effektive kommercielle vacciner kun delvist i stand til at beskytte mod en heterolog infektion. Desuden er disse vacciner baseret på modificeret levende virus, som ved mere end én lejlighed har muteret tilbage til en virulent form, og har således fremmet snarere end forhindret spredningen af virus.

PRRSV udviser en lang række mekanismer til manipulation af grisens immunforsvar, der tilsammen betyder at PRRSV ofte kan findes i grisen flere måneder efter infektion. Der findes dog flere eksempler på, at et cellemedieret immunrespons (CMI) er i stand til at udrydde virus fra organismen.

I denne ph.d. afhandling beskriver jeg udviklingen af en innovativ vaccine designet til at inducere et cytotoksisk T-lymfocyt respons mod PRRSV-2. En grundlæggende del af den oprindelige projektbeskrivelse var at designe en vaccine, der ville yde beskyttelse mod et bredt udvalg af forskellige virusstammer, hvorfor fokus har været på at identificere og udvælge konserverede epitoper der binder til svine leukocyt antigen klasse I (SLA-I). Kort fortalt blev alle naturligt forekommende 9- og 10-mer peptider fra i alt 104 udvalgte PRRSV-2 fuld-genomer analyseret for deres prædikterede bindingskapaciteter overfor fem SLA-I alleler. To prædiktionsmetoder blev anvendt til denne analyse (NetMHCpan og Position Scanning Combinatoral Peptide Library). Resultaterne fra de to metoder blev kombineret, hvorefter de 2% bedste kandidater blev analyseret ved hjælp af PopCover algoritmen. Denne prioriterede kandidaterne efter hvor konserverede de var, samt hvor mange af de 5 SLAer, de var prædikteret til at binde med. På basis af dette blev 53 peptider indkøbt til *in vitro*-analyse af de faktiske bindingsværdier. Disse blev mål ved hjælp af metoderne Peptide Affinity Assay og Scintillation Proximity Assay til bestemmelse af henholdsvis bindings affiniteten og -stabiliteten af de enkelte peptid-SLA (pSLA) kombinationer. På baggrund af disse målinger blev det besluttet at gå videre med tre af de fem SLAer i kombination med i alt 33 peptider (/epitoper).

En virus replicon partikel (VRP) baseret på svinepest virus blev valgt som vaccine platform. Denne VRP inficerer celler på samme måde som svinepest og kan dermed inficere dendrit celler, der er centrale for at inducere et adaptivt immunrespons. På basis af denne VRP blev 10 vaccine-VRPer konstrueret, der havde til formål til at inducere ekspressionen af et indsat polyepitop. Et indkodet ubiquitin molekyle hæftet på polyepitopes skulle lede dette til proteasomet, som så ville klippe det i mindre stykker, hvilket i sidste ende skulle føre til, at de enkelte epitoper ville

blive præsenteret på celleoverfladen som pSLAer. Én af de 10 VRPer blev designet som en negativ kontrol og kodede for et urelateret epitop, mens de resterende ni indeholdt forskellige kombinationer af de 33 PRRSV-2-epitoper. VRPernes infektivitet samt den inducerede ekspression og efterfølgende opklipning af polyepitopet blev verificeret ved hjælp af flowcytometri.

18 grise med matchende SLA-profiler blev vaccineret tre gange over en 10-ugers periode med enten kontrol-VRPen (N = 7) eller PRRSV-VRPerne (N = 11). Herefter blev alle grise kunstigt podet med en dansk PRRSV-2 felt stamme og blev aflivet efter yderligere fire uger. Serokonvertering af antistoffer mod både VRP og PRRSV blev bekræftet hos alle svin. Induktionen af et cellemedieret immunrespons blev monitoreret ved hjælp af et interferon-γ enzym-linked immunospot (ELISPOT) assay før podning, hvilket desværre ikke gav nogle brugbare resultater. Forsøgsdesignet blev forbedre, hvilket førte til ELISPOT resultater efter podning, der vidnede om et VRP-induceret immunrespons. Viræmi målt i serum angav ikke nogen effekt af vaccination, hvorimod et lavere antal viruspartikler i lungerne hos de PRRSV-VRP vaccinerede dyr gav antydningerne af en effekt. Specielt i en ud af tre analyserede lungedele var forskellen signifikant.

Det foreliggende PhD studie giver vidnesbyrd om at et peptid-specifikt cellemedieret immunrespons kan blive induceret ved vaccination med VRPer, der koder for konserverede epitoper. Desuden peger resultaterne på en beskeden beskyttende effekt af vaccinen. Der er dog stadig mange forbedringer, der skal gøres, før en endelig VRP-baseret vaccine kan blive testet udenfor laboratoriet.

ABBREVIATIONS

ADE	Antigen-dependent enhancement
ANN	Artificial neural network
AnP	Anchor position
AP	Alkaline phosphatase
APC	Antigen presenting cell
β2m	Beta-2-microglobulin
BCG	Bacillus Calmette-Guérin
BCIP	5-bromo-4-chloro-3'-indolyphosphate p-toluidine
BCR	B-cell receptor
BSL3-ag	Biosafety level 3 agriculture
CBS	Center for biological sequence analysis
cDC	Classical dendritic cells
cDNA	Copy DNA (reverse transcribed mRNA)
CDR	Complementarity determining region
CFSE	Carboxyfluoroscein succinimidyl ester
CMI	Cell mediated immunity
CSFV	Classical swine fever virus
CTL	Cytotoxic T lymphocyte
DC	Dendritic cell
DFR	Distribution free resampling
DMSO	Dimethylsulfoxide
DMV	Double membrane vesicles
DNA	Deoxyribonucleic acid
dpc	Days pos challenge
dpv	Days post vaccination
DTU	Technical University of Denmark
E	Envelope protein
EAV	Equine arteritis virus
EDTA	Ethylenediaminetetraacetic acid
ELISA	Enzyme-linked immunosorbent assay
ELISPOT	Enzyme-linked immunospot assay
EMEM	Eagle's minimum essential medium
ER	Endoplasmic reticulum
FBS	Fetal bovine serum
FCM	Flow cytometry
FMDV	Foot and mouth disease virus
FSC	Forward scatter
GP	Glycoprotein
HA	Haemaglutinin
HC	Heavy chain
HP-PRRSV	High pathogenic PRRSV-2
HRP	Horseradish peroxidase
hβ2m	Human beta-2-microglobulin
IFN	Interferon
IgG	Immunoglobulin G
IL	Interleukin
IRES	Internal ribosome entry site
IRF	IFN regulatory factor
ISG	IFN-stimulated genes
IVI	Institute for Virology and Immunology, Switzerland
K_d	Equilibrium dissociation constrant
LDV	Lactate dehydrogenase elevating virus
M	Membrane protein
mAb	Monoclonal antibody
MEM	Modified eagles medium
MHC	Major histocompatibility complex
MLV	Modified live virus
MOI	Multiplicity of infection
mRNA	Messenger RNA
N	Nucleoprotein
NBT	Nitro-blue tetrazolium chloride
NGS	Next-generation sequencing
NK cell	Natural killer cell
NSP	Non-structural protein
OD	Optical density
ORF	Open reading frame
PAM	Porcine alveolar macrophage
PBMC	Peripheral blood mononucleated cell
PBS	Phosphate buffered saline
PCAD	Porcine Circovirus Associated Disease
PCR	Polymerase chain reaction
pDC	Plasmacytoid dendritic cells
PhD	Potential heavy drinker
pMHC	Peptide-MHC complex
PMT	Photomultiplier tube
PRDC	Porcine Respiratory Disease Complex
PRR	Pattern recognition receptors
PRRSV	Porcine reproductive and respiratory syndrome virus
PSCPL	Positional scanning combinatorial peptide library
pSLA	Peptide-SLA complex
PVDF	Polyvinylidene difluoride
qPCR	Quantitative PCR
qRT-PCR	Quantitative reverse transcription PCR
RB	Relative binding
RFS	Ribosomal frameshifting site
RNA	Ribonucleic acid
RT	Room temperature
RTC	Replication and translation complex
SEB	Staphylococcal enterotoxin B
sgRNA	Sub genomic RNA
SLA	Swine leukocyte antigen
SLO	Secondary lymphoid organ
SNP	Single nucleotide polymorphism
SPA	Scintillation proximity assay
SSC	Side scatter
$t_{½}$	Half-life
TAP	Transporter associated with antigen processing
$TCID_{50}$	50% tissue culture infective dose
TCR	T-cell receptor
Th cell	T helper cell
TNF	Tumor necrosis factor
Treg	Regulatory T cell
Vet	National Veterinary Institute
VRP	Virus replicon particle
WB	Western blot

GENERAL OBJECTIVE

Porcine Reproductive and Respiratory Syndrome virus (PRRSV) is the causative agent of one of the most important porcine diseases with high impact on animal health, welfare and production economy. It primarily infects and replicates within porcine alveolar macrophages causing respiratory distress and facilitating infection by secondary pathogens. Infected macrophages in the placenta can migrate to the fetuses in late gestating sows, leading to late-term abortions, early farrowing and birth of litters mixed with living, stillborn and mummified fetuses. PRRSV exhibits a multitude of immunoevasive mechanisms that, combined with a high mutation rate, has hampered several attempts to develop a vaccine capable of inducing persistent protection against infection with heterologous strains.

A number of studies have shown that cell mediated immunity (CMI) are important for the clearance of PRRSV following infection. Dendritic cells (DC) are the main inducers of CMI by presenting viral epitopes on their class I swine leukocyte antigens (SLA) to T cell receptors of cognate cytotoxic T lymphocytes (CTL). This triggers the activation and proliferation of the mother T cell, whose daughter clones will differentiate into effector CTLs capable of identifying and killing cells infected with the virus.

In the wake of recently emerged technologies including full genome sequencing, epitope prediction, and bulk analysis of peptide-SLA (pSLA) stability and affinity, it is now possible to identify and test the binding capacities of conserved epitopes to relevant SLAs within a reasonable timeframe and with an acceptable budget.

Together, these factors provided the framework for the current thesis, the general objective being to design, develop and test a vaccine capable of inducing a CTL response against PRRSV-2. This was based on the working hypothesis that a virus replicon particle (VRP) could trigger infected cells to present VRP-encoded conserved PRRSV-2 epitopes via their SLA-I molecule, thereby priming cognate T cells to differentiate into effector CTL (figure 1).

The approach was divided into the following milestones:

Described in paper 1:

- Identify and select an ensemble of 9-10 mer peptides conserved among PRRSV-2 strains and predicted to bind to relevant SLA alleles.
- Verify peptide binding affinity and stability *in vitro* using synthetic peptides and recombinant SLA alleles.

Described in paper 2:

- Design a VRP for inducing antigen presentation of transgenic epitopes on SLA-I molecules of infected cells.
- Incorporate transgenes encoding polyepitopes of verified binding peptides into VRP constructs.
- Rescue VRPs and verify their infectivity and polyepitope expression *in vitro*.
- Conduct *in vivo* experiment with pigs of matching SLA-profiles vaccinated with VRPs and subsequently challenged with wild type PRRSV-2.
- Evaluate clinical, serological, virological and immunological parameters.

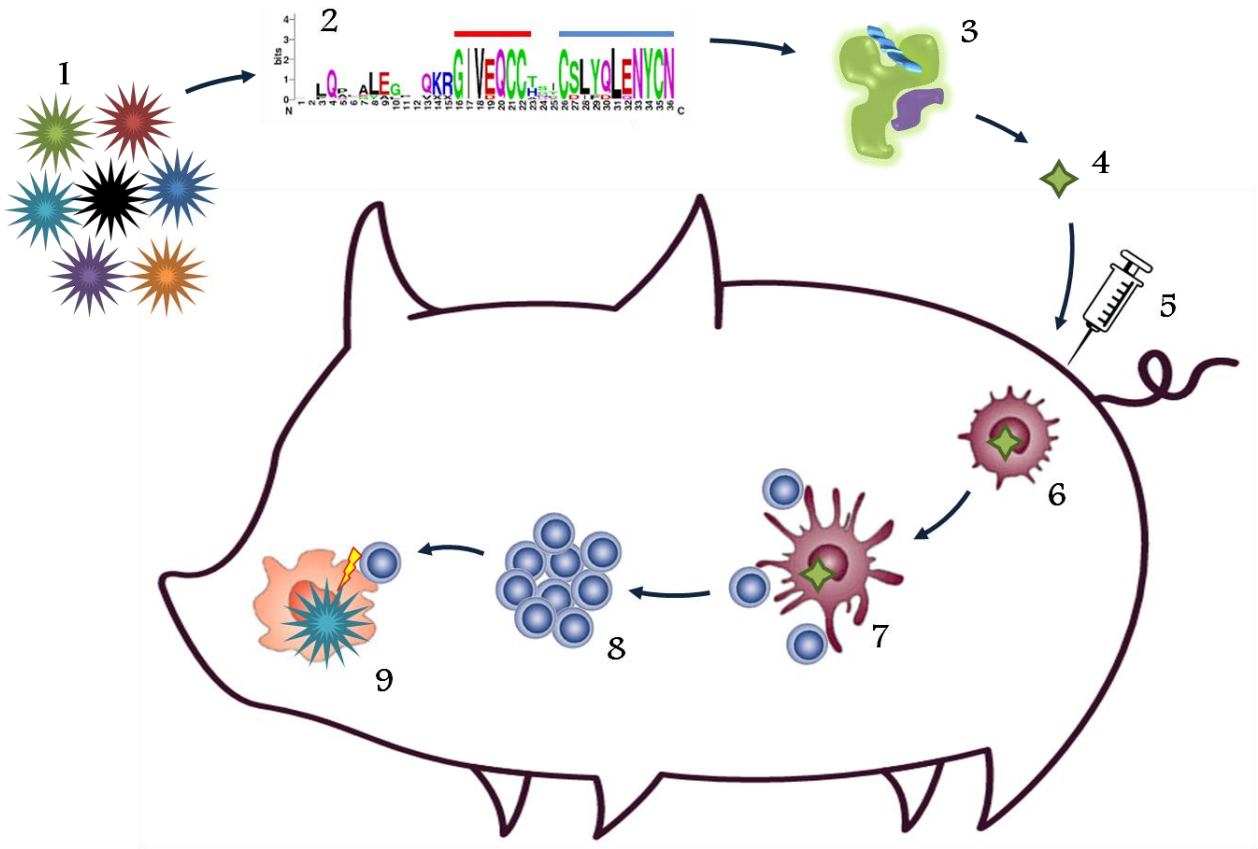

***Figure 1**: Simplified diagram of the PhD working hypothesis. **1**: Collection of available full-genome PRRSV sequences. **2**: Identification of conserved amino acid regions for epitope prediction. **3**: In vitro verification of predicted epitopes. **4**: Integration of verified binders into Virus Replicon Particles (VRP). **5**: Vaccination with VRPs. **6**: Infection of dendritic cells by VRPs. **7**: Dendritic cells become activated by VRP infection and migrate to lymph nodes where they present PRRSV-derived epitopes to naïve CD8 T cells. **8**: Cognate CD8 T cells differentiate into effector cytotoxic T cells (CTL). **9**: A CTL recognizes a PRRSV infected macrophage and kills it.*

1 GENERAL INTRODUCTION

In this chapter, I will give an introduction to the necessary aspects of consideration in order to fulfill the objective of this thesis, namely developing a VRP-based vaccine for the induction of CMI against PRRSV-2. Hence, a description of the porcine immune system is given in section 1.1, in which important components and cells of both the innate and the adaptive immune system in relation to a virus infection are described. This is followed by a detailed description in section 1.2 of the molecular pathways involved in antigen presentation, and the cell-to-cell interactions needed for the recognition and activation of CTLs. Finally, a review of the target virus, PRRSV, is given in section 1.3, encompassing details of its discovery and taxonomy; structural and genomic organization; origin and diversity; means of infection on both the cellular, anatomical and epidemiological level; applied methods for prevention and control; immune response to the virus; and a brief summary of upcoming innovative vaccines.

1.1 The porcine immune system

Despite being almost constantly attacked by vira, bacteria, fungi and parasites, the animal body manages to fight off most of these pathogens even before their incursion. And even so, only a fraction of successful intruders will result in clinical illness. The reason for this is the immune system consisting of mechanical barriers shielding the body from the exterior environment, and a multitude of highly specialized molecules and cells combating the few pathogens that succeed in crossing the barriers. This is the result of a still-ongoing arms race between pathogens and hosts that started millions of years ago when the first organism attacked its neighbor. As a consequence, the immune system has evolved to be an impressively complex meshwork of molecular and cellular interactions regulated by a similarly complex multitude of mechanisms. In concert, these interactions constitute a highly sensitive and powerful system capable of detecting, controlling and/or eliminating virtually all invading threats with a minimum of collateral host tissue destruction and alteration of homeostasis (Goldszmid and Trinchieri 2012).

In vertebrates, the immune system is commonly divided into two major components: the innate and the adaptive immune system. The innate immune system is more primitive and targets everything perceived as a foreign threat. The adaptive immune system is more complex and targets specific threats recalled from past memory. While the two systems are separate they are mutually connected.

In the following sections, introductions to the porcine innate (section 1.1.1) and adaptive (section 1.1.2) immune systems are given with emphasis on the anti-viral response.

1.1.1 The innate immune system

The innate immune system provides a first line of defense against the threats posed by the exterior environment and acts as an immediate response to intruders. It has no memory (although this is being debated) and the onset and level of response to a given infection is therefore not different from time to time. It is constituted by a mechanical, a humoral and a cellular component. The mechanical component is represented by barriers, such as the skin and mucosal lining of the intestinal, respiratory and genital tracts, making it physically difficult for the pathogen to enter

the body. The humoral component is comprised by a multitude of soluble plasma molecules including the complement system, natural antibodies, acute phase proteins, and antimicrobial peptides. The cellular component comprises the granulocytes (neutrophils, eosinophils, basophils and mast cells), natural killer cells (NK), macrophages, and dendritic cells (DC), all having their own specialized role. Most cells of the body express an arsenal of surface and intracellular pattern recognition receptors (PRR) that upon recognition of danger-associated molecular patterns (DAMP) will initiate signaling cascades. These will trigger the production of various cytokines and chemokines for the initiation of an immune response and for the recruitment and activation of relevant cells.

Due to the scope of this thesis, the humoral and mechanical components of the innate immune system will not be discussed further. Regarding the cellular component, only the cells related to viral infection will be described in the following subsections including macrophages (section 1.1.1.1), DCs (section 1.1.1.2), NK cells (section 1.1.1.3) and neutrophil granulocytes (section 1.1.1.4). Despite their functional association with the innate immune system, the γδ T cells are described in context of the adaptive immune system in section 1.1.2.2.

1.1.1.1 Macrophages

Macrophages are, together with DCs, specialized antigen presenting cells (APC) acting as interface between the innate and the adaptive immune system. Macrophages differentiate from hemopoietic progenitor cells either directly or via circulating monocytes after having migrated to different parts of the body (Geissmann et al. 2010). They are able to adapt to the local environment and can hence develop into different phenotypes and reside as Kupffer cells (liver), Langerhans cells (skin) or alveolar macrophages (lung), where they can comprise up to 15% of the total number of cells in tissue (Gordon et al. 2002). After differentiation, macrophages can be primed in either of two ways: 1) The presence of interferon (IFN)-γ produced mainly by activated T helper 1 (Th1) cells or by NK cells will lead to M1 priming, whereas 2) the presence of interleukin (IL)-4 and/or IL-13 will lead to M2 priming (Charley et al. 1990; Stein and Keshav 1992; Dalton et al. 1993). Subsequent recognition of microbes or opsonic stimulation by antibody complexes will lead the macrophage to full activation, after which it will fulfill its role according to priming state. An M1 macrophage will thus carry out pro-inflammatory and antimicrobial/antiviral activities associated with a Th1 response (Fairbairn et al. 2011), whereas an M2 macrophage will promote a Th2 and antibody-mediated immune response. At the end of infection, anti-inflammatory cytokines, such as IL-10, will increase and suppress the pro-inflammatory state of the macrophage leaving it for debris clearance and general repair (Gordon et al. 2010).

During a viral infection the M1 macrophage will promote the expansion, differentiation and survival of T cells and induce IFN-γ production by T and NK cells in a pro-inflammatory feedback loop. This will give rise to increased levels of CD80/86 which provide a co-stimulatory signal during antigen presentation by interacting with the CD28 receptor on T cells, thereby preventing tolerance and promoting a cytotoxic response (Fairbairn et al. 2011).

1.1.1.2 Dendritic cells

DCs play the main role in orchestrating the immune response by virtue of their high efficiency in sensing infection and transporting antigen from the site of entry to the lymphoid tissues. DCs can be subdivided into plasmacytoid DCs

(pDC) that are mainly involved in sensing nucleic acid and are strong inducers of the pro-inflammatory cytokines, IFN-α/β and tumor necrosis factor (TNF)-α; and classical DCs (cDC) that are specialized in antigen presentation. cDCs can be further divided into two subsets of which one is more specialized in stimulating CD8β T cells through major histocompatibility complex (MHC) class I (MHC-I), while the other is more specialized in stimulating Th responses through MHC-II (Miller et al. 2012; Merad et al. 2013). Several other subsets of porcine DCs exist and their diversity is increased further by their phenotypic adaptation to the local environment in the tissue. A review of DC diversity is out of the scope of this thesis but can be found in Summerfield & McCullough (2009).

After activation and migration to the lymphoid tissue, the DCs present their antigen to T cells of the adaptive immune system together with co-stimulatory signals and secreted cytokines. In combination, this will lead to T cell activation and proliferation, thereby mounting an attack suitable for the presented antigen. Depending on the level and type of antigen presentation and on the local cytokines environment, the DCs can polarize the $CD4^+$ T cell responses towards a Th1, Th2, Th17 or regulatory T cell (Treg) profile (Steinbrink et al. 2002; Yamazaki et al. 2006). As with the macrophages, the Th1 profile promotes a cytotoxic response and may involve cross-presentation of engulfed antigen via MHC-I, while the Th2 profile promotes and antibody response. Th17 cells (by virtue of their high IL-17 production) play an essential role in combating bacterial infections, especially in the lungs (Zhang et al. 2016), and Tregs function mainly as immunosuppressive cells responsible for a controlled decline of an immune response against pathogens (Käser et al. 2008; Käser et al. 2011; Käser et al. 2012).

In addition to the capacity of DCs to determine the type of response, they can also manipulate the homing characteristics of the activated T cells by providing information about the location of infection, thus facilitating a fast and efficient immune reaction (Saurer et al. 2007).

DCs also affect B cells of the adaptive immune system through cytokines such as B-cell activating factor (BAFF) and a proliferation-inducing ligand (APRIL) (MacLennan and Vinuesa 2002). Also direct delivery of unprocessed antigen from DCs to B cells has been observed, in addition to the influence of DCs on isotype switching (Wykes et al. 1998; Bergtold et al. 2005; Dubois and Caux 2005).

1.1.1.3 Natural killer cells

Porcine NK cells are small to medium sized lymphocytes capable of inducing an early and rapid immune response, and are therefore considered a first line of defense against microbial pathogens (Denyer et al. 2006). Spontaneous production of effector cytokines and robust cytotoxic activity are important functional characteristics of NK cells (Hamerman et al. 2005; Vivier 2006). In the pig, three different NK-cell subsets have been defined based on their expression of activation receptor, NKp46. The subsets differ in their capacities to produce cytokines and have distinct degranulation properties (Mair et al. 2012; Mair et al. 2013). The abundance of NK cells is highly variable between individual animals, ranging from 1-24% of blood lymphocytes. They reside in relatively low numbers in lymphatic organs, and in high numbers in non-lymphatic organs such as the liver and lungs (Denyer et al. 2006; Mair et al. 2012).

NK cells can execute their effector functions in four ways:

4. Cytotoxicity. NK cell are able to identify and kill cells that reduce or lack the expression of MHC-I through perforin and granzyme secretion (Ljunggren and Kärre 1985; Kärre et al. 1986; Lanier 2005).
5. Antibody-dependent cell-mediated cytotoxicity. Fc receptors present on NK cells have the ability to bind to the fab region of an antibody molecule whose variable region specifically binds to the surface antigen expressed from a pathogen inside an infected cell. Cross-linking of these Fc receptors triggers the release of perforin and granzymes, thereby killing the infected cell (Lanier 2005).
6. Cytokine-induced killing. Activation of NK cells triggers the production of IFN-γ and TNF-α, thus contributing to the activation of infected macrophages to induce antimicrobial killing mechanisms (Bogdan 2001; Stetson et al. 2003; Laouar et al. 2005; Prajeeth et al. 2011).
7. Modulation of DCs. Activated NK cells can induce DC maturation through receptor-ligand interaction and cytokine production. Conversely, activated DCs can promote NK proliferation, cytotoxicity and increase their IFN-γ production (Walzer et al. 2005).

1.1.1.4 Neutrophil granulocytes

Although not directly involved in viral clearance, neutrophils deserve a mention by virtue of their capacity to modulate adaptive immune responses by affecting T-cell function; they can guide their migration in the anatomy of tissue, or they can suppress or support lymphocyte activation and proliferation. An example of the former was described in a study of influenza infection of the respiratory tract in mice. Here, neutrophils preceded and facilitated the recruitment of $CD8^+$ T cells by secreting subcellular fragments enriched in the chemokine CXCL12, thus guiding the lymphocytes along the gradient trail due to their CDCR4 receptor (Lim et al. 2015). Neutrophils have also been shown to possess antigen-presentation properties in a study describing the upregulation of CCR7 in neutrophils activated upon phagocytosis of an antigen. This protein enables homing to the lymph nodes, where the neutrophils bearing antigen-loaded MHC-I could cross-prime T cells and induce effector functions (Beauvillain et al. 2007). As an example of a suppressive function of neutrophils towards T cells, the production and release of reactive oxygen species was shown to result in the impaired formation of the immunological synapse by inactivating the actin-remodeling protein, cofilin (Klemke et al. 2008).

Finally, neutrophils represent a diverse branch of the innate cellular system and can exhibit both pro- and anti-inflammatory responses depending on subtype and context. In general, neutrophils are regarded as the major acute innate specialized phagocytes are the first to combat a variety of infecting pathogens (reviewed in Kumar and Sharma 2010).

1.1.2 The adaptive immune system

In contrast to the innate immune response, the adaptive response is highly specific and is customized to the particular pathogen. The adaptive response is triggered by the innate response, after which the pathogen is weighed and measured before an adaptive response is initiated. Consequently, this response is relatively slow, and to

compensate for that, the adaptive immune system has the capacity of memory, and can thus provide long-lasting and sometimes even lifelong protection. In such cases where the pathogen is recognized by memory cells, the attack can be initiated immediately, thus clearing infection without any clinical signs.

Similar to the innate immune response, the adaptive response has a humoral and a cell-mediated component. The humoral component is comprised of antibodies secreted by activated B cells (plasma cells), whereas the cell-mediated component is comprised of a wide spectrum of different T cells.

In the following sections, a brief description is given of the cells of the adaptive immune system with emphasis on viral infection. First, a general description T cells is given in section 1.1.2.1. This is followed by a description of γδ T cells in section 1.1.2.2. Finally, a description B cells is given in section 1.1.2.3.

1.1.2.1 T cells in general

T cells originate from the thymus, hence the name, and common to all T cells is their T-cell receptor (TCR) with its tightly associated CD3 molecules responsible for signal transduction from the engaged TCR (Smith-Garvin et al. 2009). The purpose of the TCR is to "taste" the surface of other cells, thereby determining if the cells are infected with an intracellular pathogen. Every cell in the body, except for erythrocytes, display samples of their inner protein metabolism as peptide fragments presented on MHC molecules on their surface. As such, pathogen-derived peptide fragments will also be presented by infected cells. The T cell interacts with peptide-MHC (pMHC) complexes on the surface of APCs and becomes activated in case of recognition. The TCR consists of a disulfide-linked membrane-anchored dimeric protein consisting of two heterogenous chains of the immunoglobulin superfamily. A given TCR will either consist of an α and β chain (αβ T cells) or a γ and δ chain (γδ T cells). Each chain has a short cytoplasmic tail, a transmembrane region, a constant domain and a variable domain. The variable domain is responsible for the interaction with the pMHC.

For the αβ T cells, the TCR is generated in a process of random reassortment of numerous variable (V) and joining (J) genes at the TCR α-locus, and V, diversity (D) and J genes at the TCR β-locus. Further diversity is generated at the V(D)J junctional boundaries via non-nucleotide encoded changes. Before the developing T cells migrate to the periphery, they must first undergo a positive and a negative selection phase in the thymus, ensuring that mature T cells will recognize self-pMHCs but not become activated by self-peptides, respectively. As such, the repertoire of αβ TCRs following thymic selection is estimated in humans to be comprised of 10^7-10^8 unique receptors (Turner et al. 2006). Most of this diversity resides in the complementarity determining regions (CDR), of which each of the two TCR chains have three. Collectively, the six CDR loops constitute the antigen-binding site of the TCR. Despite their unique receptor specificities, T cells exhibit a high degree of promiscuity, meaning that any given T cell can recognize a wide spectrum of peptides (Bhati et al. 2014). Less in known about the γδ TCR diversity, but the discovery of numerous V, D and J genes at the porcine δ locus indicates a potential of an enormous recombinatorial diversity (Uenishi et al. 2009). As a consequence of the above, the specificity of a TCR is completely unique to the particular T cell.

αβ T cells are functionally distinguished based on their expression of two co-receptors, CD4 and CD8 (CD8αα or CD8αβ), determining which MHC, and therefore which cell types the T cells can interact with. CD4 allows the TCR to engage with MHC-II, which is expressed almost exclusively on APCs, whereas CD8 allows engagement with MHC-I, which is expressed on all nucleated cells. CD4 T cells can differentiate into Th1, Th2, Th17, and Treg cells, whose functions were mentioned in the section 1.1.1.2. CD8 T cells expressing the CD8αβ phenotype are the precursors of CTLs and will subsequently be referred to as CD8β T cells. The effector function of CTLs, being to identify and kill infected cells, is a central topic to this thesis why a thorough description of the roles and functions of CTLs will be given in section 1.2.

The distinction between - and classification of - porcine T-cell subsets is quite complex, and well-established paradigms from mouse and human studies cannot be directly adopted by the porcine model. This involves not only various T-cell subsets, such as high numbers of extra-thymic $CD4^+CD8^+$ cells (Zuckermann 1999) and MHC-II expression by resting T cells (Saalmüller et al. 1987) but also anatomical features of the lymphatic system, such as inverted lymph node structures and an unusual route for lymphocyte circulation (Rothkötter 2009). Furthermore, the advent of novel antibodies against a multitude of cell-surface markers and cytokines have facilitated an extensive dissection of the T-cell pool and added subsets in many layers meanwhile demonstrating possible transfers between subsets over time. Due to the scope of this thesis, a detailed description of the whole T-cell family will not be given here, but can be found in Gerner et al. (2009).

1.1.2.2 γδ T cells

Most of the current knowledge of γδ T cells is derived from mouse studies, where it is known that they are able to secrete both pro-and anti-inflammatory cytokines, help to recruit neutrophils and B cells, and maintain homeostasis and repair of mucosal barriers (Witherden and Havran 2013). However, pigs are different from mice and humans due to their large proportion of circulating γδ T cells, which can amount to 50% of the total lymphocyte number in the periphery. In comparison, this number is only about 1-5% in mice and humans (Carding and Egan 2002; Takamatsu et al. 2006). These large differences most likely reflect a broader range of functionalities in the pig. This is supported by the identification of no less than 12 γδ T-cells subsets characterized by the different antigens CD1, CD2, CD4, CD8α, CD8β and CD45RC (Sinkora et al. 2005; Sinkora et al. 2007). In addition, γδ T cells are widely distributed in different organs and can be found in spleen, liver, thymus, lungs, bone marrow, tonsils and lymph nodes (Štěpánová and Šinkora 2012; Sedlak et al. 2014). γδ T cells are the earliest detectable T-cell subset in the porcine thymus appearing in the fetus after 40 days of gestation, while αβ T cells remain absent for an additional 15 days (Šinkora et al. 2000; Sinkora et al. 2005). After birth, the level of γδ T cells increase strongly until 19-25 week of age, indicating an important role during adolescence (Talker et al. 2013).

The activation of γδ T cells is not exclusively triggered by the engagement of their TCR but also by other receptors like NKG2D, NKp46 or Toll-like receptors, which are normally associated with NK cells or myeloid cells (Bonneville et al. 2010; Correia et al. 2011). Hence, γδ T cells display features of both the adaptive and the innate immune system. One study detected enhanced proliferation and IFN-γ production of γδ T cells isolated form *Bacillus Calmette-Guérin*

(BCG) vaccinated pigs upon restimulation with mycobacterial antigens (Lee et al. 2004). The authors also suggested a memory-like cytolytic function, which was subsequently confirmed in 3-week-old BCG vaccinated pigs (Olin et al. 2005b).This is in accordance with human γδ T cells in *Mycobacterium tuberculosis* infections that have shown initial production of IFN-γ and TNF-α, and subsequent memory-like characteristics (Meraviglia et al. 2011). PRRSV infected pigs have also showed higher proliferation and IFN-γ production of γδ T cells, when compared to non-infected pigs (Olin et al. 2005a). In another study, the production of IL-1, IFN-α and granulocyte macrophage-colony stimulating factor (GM-CSF) was detected following *in vitro* stimulation of γδ T cells from naïve pigs with foot and mouth disease virus (FMDV) antigen (Takamatsu et al. 2006). Also antigen presentation has been shown to be a feature of γδ T cells. Especially in some subsets, co-expressed surface molecules associated with APCs (MHC-II, CD80/86, CD40 and CD31) were detected and these cells were further shown to take up ovalbumin within 20 minute, indicative of phagocytosis (Takamatsu et al. 2002).

1.1.2.3 B cells

B cells originate from the bone marrow, hence the name, and similar to T cells, B cells are characterized by their B-cell receptor (BCR) that is unique to the particular B cell due to V(D)J recombination (similar to TCR recombination described in section . The BCRs of mature B cells resemble membrane bound antibodies and function to bind extracellular undigested antigen, such as on the surface of pathogens. Activation of B cells requires three signals. Upon encounter of an extracellular antigen recognized by the B cell, cross-linking of its BCRs will provide the first activation signal. Additionally, it will trigger internalization and processing of the antigen into peptides that are then presented on MHC-II molecules. Subsequent encounter with a $CD4^+$ T cell expressing a TCR cognate to the presented pMHC-II will activate the T cell. In return, the T cell will provide the second and third activation signals to the B cell in terms of stimulation of the CD40 receptor by CD40L on the T cell, and by secreted cytokines. This will allow the B cell to become fully activated. After this, the B cell will undergo dramatic proliferation and the daughter cells will differentiate into plasma cells with the secretion of vast amounts of antibody as their main effector function. The antibodies quickly start circulating the body and efficiently bind to cognate epitopes on the antigen, thus protecting the host in four ways:

1. Neutralization. Antibodies bind to toxic substances preventing their toxicity. Similarly, molecules on the surface of a microbe that are critical to its infectivity may be bound, thereby disarming the microbe.
2. Opsonization. By coating pathogens, antibodies can enable accessory immune cells that recognize the Fc regions of the antibodies to ingest and kill the pathogens.
3. Complement activation. Antibodies bound to a pathogen can trigger activation of the innate complement system that can enhance opsonization and in some cases directly kill bacterial cells.
4. Immune complexes. Antibodies can cross-link antigens, thereby confining them in large immune complexes that can subsequently be degraded by various mechanisms.

In contrast to the T cells, B cells can undergo somatic hypermutation for improved antigen affinity before differentiation into plasma cells. This takes place in germinal centers in lymph nodes where follicular DCs and T cells

stimulate the process by positive selection. The optimized B cells then differentiate into plasma cells and memory cells that leave the lymph node and migrate to the bone marrow.

In addition to somatic hypermutation, plasma cells may be stimulated by T cells or DCs to undergo class switching, in which they change the class of their secreted antibody. Antibodies of different classes operate in distinct places and have different effector functions.

1.2 The induction of a targeted CTL response

Cytotoxic T lymphocytes are an important part of the adaptive immune response by virtue of their capacity to kill infected cells in an antigen-specific manner. Due to their CD8 phenotype they are restricted to engage only with MHC-I complexes. The resulting TCR-pMHC-I interaction is both a critical determinant of priming of the naïve CD8β T cells, and of the subsequent activation of effector CTLs by infected cells. In the center of the interaction lies the presented peptide, being the only element providing information about the antigen within the presenting cell. The peptide has a dual role: On one side, it must associate with the MHC-I complex; on the other side, it must interact with the TCR (figure 2). In the following sections, a comprehensive description of the involved molecules, processes and interactions for the induction of a targeted cytotoxic T-cell response is given. These include the structure, polymorphisms and peptide binding properties of the MHC-I molecule (section 1.2.1); the molecular processes involved in peptide loading of the MHC-I complex (section 1.2.2); the interactions and dynamics related to priming of the naïve CD8β T cell (section 1.2.3) resulting in effector CTLs (section 1.2.4), leading to the eventual establishment of CTL memory (section 1.2.5); and finally, the various determinants of a functional epitope are discussed (section 1.2.6).

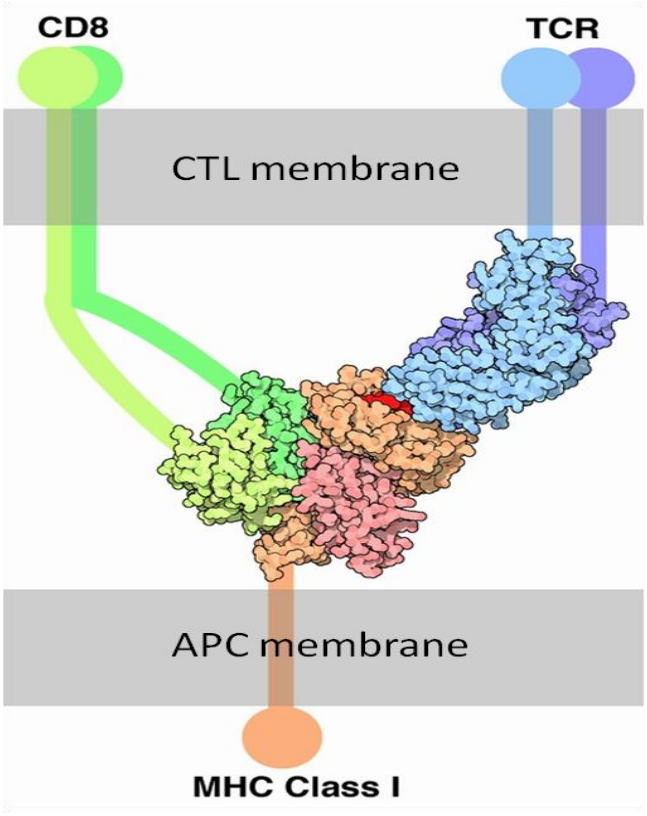

***Figure 2**: Cartoon drawings of the interaction between a pMHC-I, a TCR and a CD8 molecule. The peptide (red) is presented by the MHC-I (HC: orange, β2m: pink) on the surface of the antigen presenting cell (APC). The αβ T-cell receptor (TCR) (blue and light blue) on the surface of the cytotoxic T lymphocyte (CTL) interacts with residues of the peptide and of the peptide binding groove. The CD8 dimer (green and light green) enhances the interaction meanwhile restricting the TCR to only engage with class I MHCs. The portions anchoring the proteins to the cell membranes are shown schematically. Figure adapted from Goodsell, 2005, doi:10.2210/rcsb_pdb/mom_2005_3*

1.2.1 The MHC Class I

MHC molecules are unique in the proteome because of their extreme polymorphism, and several thousand human MHC-I alleles have been identified thus far. Currently, only 216 of the porcine equivalent, SLA-I, have been found, all of which are published in the Immune Polymorphism Database (http://www.ebi.ac.uk/ipd/mhc/group/SLA). This comparably small number is likely to be a consequence of scientific focus and limited genetic diversity within the swine industry, and the true number should be expected to be much higher.

The mature pMHC-I complex consists of 3 molecules: The heavy chain (HC), the light chain beta-2 microglobulin (β2m), and the peptide to present. The HC is comprised of three immunoglobulin domains: α1, α2 and α3. Of those, α1 and α2 together constitute two parallel alpha helices resting on a platform of beta-pleated sheet. This structure is the peptide binding groove. α3 provides a supportive structure anchoring the HC to the membrane, and β2m is a soluble immunoglobulin domain stabilizing the complex by interacting with the domains of the HC (figure 3A).

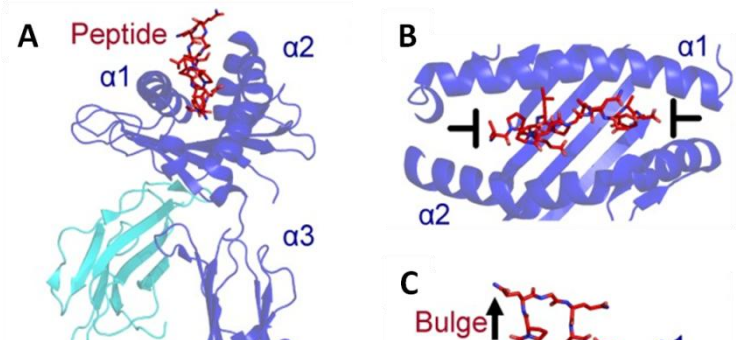

Figure 3: *Cartoon drawings of the peptide-MHC-I complex.* ***A****: MHC-I is comprised of 3 α-chain domains (α1, α2, and α3 in blue) and β2m (cyan), α1 and α2 together constitute the peptide-binding groove formed by two parallel alpha helices resting on a platform of beta-pleated sheet. α3 provides a supportive structure anchoring the HC to the membrane, and β2-microglobulin is a soluble immunoglobulin domain stabilizing the complex by interacting with the domains of the heavy chain.* ***B****: Top down view of the MHC-I binding groove demonstrating the closed conformation of the groove.* ***C****: Side view of the pMHC-I binding groove showing how the closed conformation of the groove forces the central residues of the peptide into a bulge conformation. Figure adapted from Bhati et al., 2014, doi:10.1002/pro.2412.*

The most polymorph region of the MHC is in and around the peptide binding groove. Polymorph residues on top of the alpha helices interact directly with the TCR and are responsible for the phenomenon that only self MHCs will be accepted by the T cells. Polymorph residues in the peptide binding groove change the physicochemical properties, with the effect that only peptides that conform to these properties will be presented by the given MHC allele.

The peptide binding groove is closed in each end, meaning that it can only bind relatively short peptides (8-11 residues). These are fixed by residues of the groove by hydrogen bonds and van der Waals interactions. It has been shown that most of the energy needed to bind a peptide in the peptide binding groove involves only the main-chain atoms that are common to all peptides (Fremont et al. 1992; Matsumura et al. 1992; Madden et al. 1992). The remaining small fraction of the binding energy involves the peptide side-chain atoms and takes place in the so-called

anchor positions. These are usually located in the ends of the groove, and function as determinants for the peptide-specificity of the polymorphic MHC. This exposes the middle part of the peptide to the TCR, thereby determining TCR specificity (Matsumura et al. 1992; Calis et al. 2013) (figure 3B and C).

Three functional loci of SLA-I have been found in pigs (SLA-1, SLA-2, and SLA-3), meaning that any given pig will inherit and express two alleles from each locus (one allele from each parent). Potentially, this will amount to six different alleles, while an inbred pig may only express three different alleles. Different alleles have different peptide specificities, degrees of promiscuity and even levels of expression on the cell surface. Interestingly, the two latter have recently been shown to be inversely correlated (Chappell et al. 2015). The exact reason for this is still speculative, but may likely be related to the notion that large amounts of highly promiscuous MHCs would negatively select more T cells in the thymus, and would thus pauperize the T cell repertoire (Vidović and Matzinger 1988). Alternatively, it may function as a regulatory mechanism responsible for balancing the immune response between resistance to pathogens and autoimmunity (Kaufman et al. 1995).

The high polymorphism of MHCs is a benefit to the individual animal since six different MHC alleles will present a larger fraction of the universal peptidome, than three alleles. This enhances the chances of the immune system to identify and attack intracellular pathogens. Likewise on the population level, the number of several thousand alleles enhances the chances of survival of the population as a whole. Turning this upside-down, an inbred population is more vulnerable to infection as the risk of a given pathogen to cause havoc is inversely correlated with the number of endemic alleles.

1.2.2 Peptide processing and loading of the MHC

Two major pathways are responsible for the peptide processing and loading to the MHC-I. During the cross-presentation pathway, antigen originating from outside the cell is internalized into phagosomes or macropinosomes (Norbury et al. 1995; Norbury et al. 1997; Shen et al. 1997). Subsequent processing and loading of peptide to MHC-I can occur via three different cross-presentation pathways, two of which involve proteasomal degradation in the cytosol followed by transport into membraneous compartments by Transporter associated with Antigen Processing (TAP) (Kovacsovics-Bankowski and Rock 1995; Rock and Shen 2005), whilst the third bypasses the cytosol and is independent of the proteasome and TAP (Rock and Shen 2005). Additionally, a “cross-dressing” pathway has been described where fully assembled pMHC-I complexes are transferred from one cell to another (Yewdell and Bennink 1999; Yewdell and Haeryfar 2005). During the direct presentation pathway, the antigen is synthesized within the cell and must therefore require the APC to be infected. Here, a constant synthesis and degradation of protein takes place, and as an integral part of this turn-over, samples from the degradation products are imported to the endoplasmic reticulum (ER) by TAP, after which the chaperone protein, tapasin, guides the association with nascent MHC-I complexes. These are subsequently transported in vesicles to the cell surface to present their peptides to circulating T cells, thereby informing the T cells about the intracellular processes. This direct antigen presentation pathway is constitutively being carried out by all nucleated cells (figure 4).

In addition to the MHC being the most critical determinant for pMHC complex formation by virtue of its peptide-specificities, other processes play a role in peptide selection. Obviously, the cytosolic abundance of a given protein is related to the amount of degradation products that can be derived from the protein. More than that, the proteasome is the main provider of degradation products in its capacity of exerting ubiquitin-mediated proteolysis. Different subtypes of proteasomes exist of which the standard proteasome and immunoproteasome are the best studied. Intermediate subtypes also exist, and although the distribution of subtypes have shown to be tissue specific, the general tenet is that the standard proteasome in expressed constitutively, while the immunoproteasome is induced by inflammatory mediators such as IFN-γ or oxidative stress (Heink et al. 2005; Guillaume et al. 2010). The two types of proteasomes have different substrate preferences and catalytic activities, resulting in the production of different, yet overlapping, peptide pool. The chymotrypsin-like activity of the immunoproteasome promotes the generation of peptides favored by the MHC-I binding groove (Cardozo and Kohanski 1998; Chapiro et al. 2006; Lei et al. 2010).

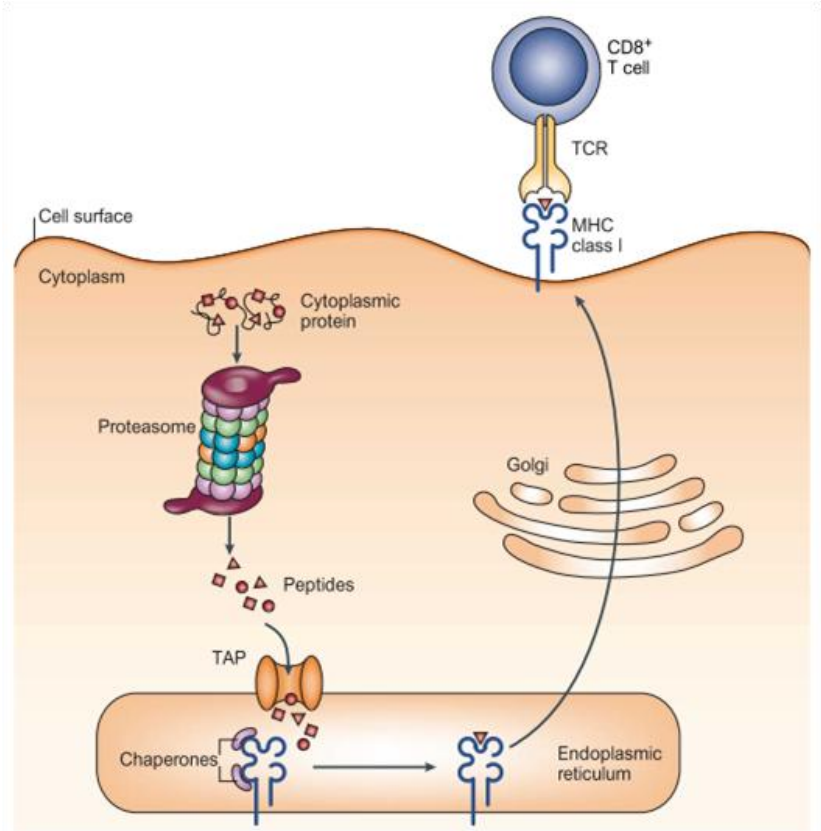

***Figure 4**: MHC-I antigen presentation: The direct antigen presentation pathway. Peptides produced by proteasomal degradation of cytosolic proteins are transported into the ER by TAP, in which they will become associated with MHC-I molecules guided by chaperones. Mature pMHC-I complexes are transported in vesicles via the Golgi Apparatus to the cell surface, for the encounter and recognition by cognate $CD8^+$ T cells. Figure adapted from Yewdell and Neefjes, 2003, doi: 10.1038/nri1250*

The following transportation of degradation fragments into the ER lumen by TAP is currently believed to be functionally indiscriminate to peptides in human. On the contrary, chicken TAP has shown peptide-translocation specificity matching the peptide-binding specificity of the dominantly expressed MHC-I molecule (Walker et al. 2011). Whether or not TAP has a discriminative role in pigs is to my best knowledge currently unknown, but since pigs diverged from humans 'only' 85 million years, while the divergence from birds dates 320 million years back, the best bet is in favor of an indiscriminate porcine TAP. However, several human studies have shown that tapasin has a capacity to skew the antigen presentation profile in favor of peptides with high binding capacities. This is done by enhancing peptide dissociation without significantly delaying the transit of MHC to the cell surface (Williams et al. 2002; Howarth et al. 2004; Dalchau et al. 2011). This observation is in compliance with another study showing that the immunogenicity of a peptide is proportionate to the stability of the peptide-MHC interaction (Harndahl et al. 2012). In addition, it provides a solution to the paradox regarding the priming of a given CD8β T cell: On the one hand, the priming of a CD8β T cell by an APC requires a certain number of TCR-pMHC-I interactions for the threshold of priming to be reached (this will be discussed in more details in section 1.2.3). On the other hand, the extensive protein metabolism constitutively taking place in a given cell results in a plethora of distinct peptides that will be available for MHC-I presentation. Together, these two dogmas represent a paradox since a peptide presenting profile of many distinct peptides of low abundance is more likely to engage but less likely to trigger a given CD8β T cell, whilst a profile of a few distinct peptides of high abundance is less likely to engage but more likely to trigger a given CD8β T cell. The capacity of tapasin thus provides a compromise by lowering the peptide diversity while at the same time increasing the quality of the nascent pMHC-I complexes.

1.2.3 CD8β T cell priming

Initial priming of a naïve CD8β T cells takes place in secondary lymphoid organs (SLO) to which DCs have migrated after being activated by antigen uptake or infection (Steinman 1991). This is an important act since the SLOs function as the main bulletin board for the exchange of antigenic information. Without this SLO-homing function the chances of encounter between an APC and a cognate T cell would be negligible. Naïve T cells exhibit a more repetitive behavior as they constantly recirculate between blood and SLOs. In humans, one cycle takes about a day of which the T cell is present in the blood for only about 30 minutes (von Andrian et al. 2000). Once having entered a SLO, the naïve T cell begins its search for antigen by crawling in an amoeboid fashion displaying large-scale random walk-like behavior (Miller et al. 2003). Upon encounter with an APC presenting the cognate antigen, the naïve CD8β T cell engages in priming. This event can be temporally divided in three phases, of which the first phase of about eight hours is characterized by short interactions between the DC and the T cell resembling brief random collisions. However, T cells are clearly activated as evidenced by their expression of the activation markers CD44 and 69. The second phase is characterized by hour-lasting interactions, during which the T cells begin secreting IL-2 and IFN-γ. In this phase the immunological synapse is formed, being a large scale molecular structure orchestrated by myosin motor proteins acting on the actin cytoskeleton (reviewed in Dustin & Cooper 2000). The synapse facilitates TCR-pMHC-I interaction by precisely aligning the opposing membranes at ~15 nm, thus solving the restraints of contact imposed by large and negatively charged glycocalyx components on the cell surfaces that would normally conflict

each other at ~50-100 nm. Microclusters of TCRs and signaling molecules form in the periphery and then migrate to the center of the synapse. These clusters are responsible for T-cell activation through engagement with cognate pMHC complexes (Yokosuka et al. 2005). The following third phase is characterized by release of partner cells, proliferation and high motility (Mempel et al. 2004; Rothoeft et al. 2006).

At the end of successful priming, an intrinsic "all-or-nothing" development program is initiated within the CD8β T cell causing it to divide at least 7 times while differentiating into effector CTLs in a manner optimized by the presence of IL-2, but independent of continual antigenic stimulation (Kaech and Ahmed 2001). This results in a dramatic expansion of up to 50.000 fold, after which the fully differentiated CTLs have the capacity to produce pro-inflammatory cytokines such as IFN-γ and TNF-α and to exert their cytotoxic effector functions at peripheral sites (Butz and Bevan 1998; Murali-Krishna et al. 1998; Doherty 1998).

The dose of antigen is strongly related to several aspects of T cell priming. In a mouse experiment in which the effects of different doses were monitored, the authors observed that the dose did not affect the expansion of the recruited CD8β T cells. Instead, the dose was proportional to the number of recruited cell, which was shown to be at least partly determined by the availability of APCs that were limited in number under low dose conditions (Kaech and Ahmed 2001). This was supported by another study adding the notion of an upper limit, beyond which larger numbers of APCs do not have a major impact (Ludewig et al. 2004). This was especially true in cases of high avidity TCRs, whereas low avidity TCRs required more and longer engagements with APCs. Similarly, increased density of antigen per APC has also been shown to lead to more efficient priming and effector differentiation (Rothoeft et al. 2006)

In summary, the density of antigen-bearing DCs in the SLOs, the level of antigen per DC, the affinity of the TCR to the antigen (TCR avidity), and the duration of antigen availability are all parameters that influence the magnitude of the resulting CTL response. Also the availability of costimulatory signals is essential. CD8β T cells express a variety of costimulatory receptors of which the most important are CTLA-4 and PD-1, who play a role in suppression of CD8β T cells reponses; and CD28 and CD137 that are important for the promotion of CD8β T cell responses. I will not go further into their mode of action but will instead refer to a recent review (Smith-Garvin et al. 2009).

1.2.4 CTL effector functions

At peripheral sites, an effector CTL will become activated upon encounter with a cell presenting the peptide to which it was initially primed. This is recognized by the TCRs of the CTL in as extremely sensitive process requiring no more than 1-50 pMHC complexes to trigger target-cell lysis (Eisen et al. 1996; Sykulev et al. 1996; Valitutti and Lanzavecchia 1997). However, a sustained TCR signaling is necessary for CTL activation, meaning that several TCRs must be engaged (Valitutti et al. 1995; Valitutti and Lanzavecchia 1997). To obtain this during low density pMHC presentation, individual pMHCs can serially engage multiple TCRs. As a prerequisite for this, the TCR-pMHC affinity must be within a narrow range; sufficiently strong to transduce a signal (McKeithan 1995), meanwhile weak enough to allow serial engagement (Lanzavecchia et al. 1999). In support of this, it has been shown that CTL activation

correlates with the half-life of the TCR-pMHC interaction (Kersh et al. 1998; Grakoui et al. 1999), and that target-cell killing is not carried out if TCR-pMHC half-life is either below or above certain threshold (Kalergis et al. 2001).

Once activated, the CTL exerts its effector function by killing the target cell through a polarized secretion of pre-made granules containing perforin and granzymes. These are released within the boundaries of an immunological synapse created by the CTL, thereby preventing collateral damage. Perforin is crucial for enabling access of granzymes into the target cell, which are involved in triggering caspase-dependent and caspase-independent cell death (de Saint Basile et al. 2010). An alternative effector function can also be exerted by CTLs, namely the induction of apoptosis of a target cell expressing the Fas receptor by engaging this with the Fas ligand on the CTL surface (Nagata and Golstein 1995).

1.2.5 CTL memory

The induction of immunological memory is usually the prime target for vaccination. The general concept of CTL memory is that about 90-95% of the effector cells initially induced during priming will undergo apoptosis once infection is resolved, while the remaining 5-10% will differentiate into memory CTLs (Kaech et al. 2002). These will be maintained at stable levels for long periods of time and can provide a rapid recall response following reexposure to the pathogen, thus enhancing protection to the host. On the basis of several mouse studies, it is now generally acknowledged that the eventual differentiation into CTL memory cells is programmed within the first 1-2 days of infection (Mercado et al. 2000; Kaech and Ahmed 2001; Prlic et al. 2006). Furthermore, the development of CTL memory has in many studies shown to be dependent on help from CD4 T cells (Bourgeois et al. 2002; Janssen et al. 2003; Shedlock and Shen 2003; Sun and Bevan 2003), despite numerous observations that a fully functional CTL response can be established without the presence of CD4 T cells during acute infections with high levels of inflammation (Buller et al. 1987; Ahmed et al. 1988; Rahemtulla et al. 1991; Reis e Sousa 2001; Iwasaki and Medzhitov 2004). In spite of their apparent importance to the induction of CTL memory, the exact mechanisms whereby CD4 T cells provide help during CD8β T cell priming remains an open question. IL-2 has initially been thought of as a critical factor produced by CD4 T cells and is still a good candidate due to its proven role in CTL expansion beyond the pre-programmed proliferation cycles (Kaech and Ahmed 2001). However, this cytokine is also secreted by the CD8β T cells during the second phase of priming (Mempel et al. 2004), meaning that the potential importance of CD4 T cells in this respect must be a matter of IL-2 quantities.

The underlying mechanisms of the maintenance and homeostasis of CTL memory are important aspects to the development of vaccination strategies. Several different subsets of memory CTLs exist, residing in different types of tissue and responds in different ways to infections. Nevertheless, a more detailed description is out of scope of this thesis, but can be found elsewhere (Williams and Bevan 2007)

1.2.6 Determinants of a functional epitope

The term immunodominance is frequently used to describe the focus of the immune system on the recognition of only a relatively small number of epitopes (Barber and Parham 1994; Fairchild and Wraith 1996). The term dominant epitope is often used to signify an epitope dominating the response in terms of recognition -magnitude or -frequency, while a subdominant epitope represents a minor component of the response observed in natural infections (Frahm et al. 2006). In the course of this thesis, however, another set of definitions inspired by Sercarz et al. (1993) will be used dividing epitopes into four categories (table 1). A dominant epitope represents a peptide recognized in the context of a natural infection. A subdominant epitope is defined as an epitope not seen in the context of natural infection, but which nevertheless can induce a T-cell response that can recognize and kill infected cells. A cryptic epitope, on the other hand, can induce a T-cell response upon peptide immunization, but is not generated by natural processes, and can hence not recognize infected cells. Lastly, a negative epitope may or may not be an MHC-I binder and/or be naturally processed and presented, but is in any case not capable of inducing a T-cell response.

Category	High affinity binder (Kd ≤ 100 nM)	Immunogenic upon peptide immunization	Naturally presented	Natural inducer of CMI
Dominant	Yes	Yes	Yes	Yes
Subdominant	Yes	Yes	Yes	No
Cryptic	Yes	Yes	No	No
Negative	Yes/No	No	Yes/No	No
Stepwise frequency	2.5%*	56%	15%	11%
Accumulative frequency**	100% (1:1)	56% (1:2)	8.4% (1:12)	0.9% (1:108)

*of all expressed 9- and 10-mers as estimated by Assarsson et al., 2014.

**of all high affinity binders

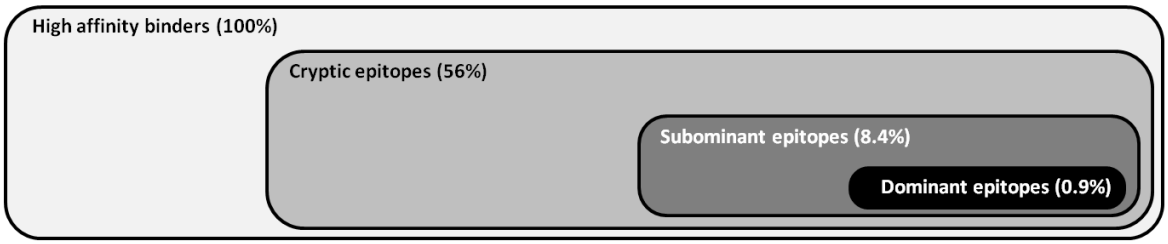

***Table 1**: The four categories of epitopes and their defining features. Each feature is characterized by a stepwise frequency related to the previous feature (the stepwise frequency of high affinity binders relates to all expressed 9- and 10-mers). An accumulative frequency was calculated based on the stepwise frequencies. The relationship between the four categories is illustrated below. Table adapted from Assarsson et al., 2014.*

To which of these four categories a given peptide belongs is of great importance to the development of an epitope-based vaccine, and by virtue of their capability to induce recognition by CTLs, only dominant and subdominant epitopes are of interest. In an attempt to quantify the impact of individual determinants involved in immunodominance, Assarsson et al. (2007) conducted an extensive study with HLA-A*0201 transgenic mice infected

with Vaccinia virus. They estimated that 2.5% of all 9- and 10-mer peptides expressed by the virus would bind to HLA-A*0201 with a high affinity of $K_d \leq 100$ nM (explained in section 2.3.1). Of these, 56% would be immunogenic upon peptide immunization, of which 15% would be processed and presented by infected cells. This last subset represents the pool of dominant and subdominant epitopes, of which an estimated 11% would be dominant. Conclusively, only 1 out of 108 high affinity binding peptides was an immunodominant epitope with respect to HLA-A*0201, while this number was estimated to be 1 out of 12 if subdominant epitopes were included.

In practice, the binding capacity is the only feature out of the four categories described in table 1 that can be tested *in vitro*. Fortunately, it is the central and most constrictive feature, and binding stability can be tested in bulk and has in many cases been estimated as a better correlate of immunogenicity than binding affinity (van der Burg et al. 1996; Slifka et al. 2003; Lazarski et al. 2005; Harndahl et al. 2012). Still, only approximately 8% of these binders will turn out capable of recognizing and killing a naturally infected cell. Potentially, this number can be raised by accounting for specificities of the circulating TCR repertoire, as well as the proteins involved in antigen processing and MHC-I loading, and prediction servers for these aspects are gaining ground. Usually, however, the functional epitopes are discovered *ex vivo* using IFN-γ enzyme-linked immunospot (ELISPOT) and cytotoxicity assays with lymphocytes from peptide immunized or virus infected animals.

1.3 The Porcine Reproductive and Respiratory Syndrome Virus

1.3.1 Discovery and taxonomy

In the late 1980s, episodes of undiagnosed reproductive failure occurred in a number of farms in North America (Keffaber 1989). A few years later, the Dutch pig industry was struck by the so-called mystery swine disease, giving rise to similar symptoms (Wensvoort et al. 1991). The etiological agents were soon discovered to be viral and were in 1992 named Porcine Reproductive and Respiratory Syndrome Virus (PRRSV). Antigenic studies (Wensvoort et al. 1992) and genomic sequence analyses (Allende et al. 1999) of the North American and European isolates revealed significant antigenic variations and a genomic difference of about 40% at the nucleotide level. Surprisingly, evidence suggested divergent evolution on the two continents from a common ancestor centuries ago (Nelsen et al. 1999; Forsberg et al. 2001; Plagemann 2003; Yoon et al. 2013), which resulted in the taxonomic division of PRRSV into two distinct genotypes, PRRSV type 1 (European) and PRRSV type 2 (North American). This has recently been updated, reclassifying the two genotypes into two distinct species: PRRSV-1 (type 1) and PRRSV-2 (type 2) (ictvonline.org). Both species belong to the *Arteriviridae* family in the only assigned genus, *Arterivirus*, together with 11 other species including lactate dehydrogenase elevating virus (LDV) and equine arteritis virus (EAV), the latter being type species for the genus. The *Arteriviridae* family is placed together with *Coronaviridae, Roniviridae,* and *Mesoniviridae* in the order *Nidovirales*.

1.3.2 Genomic organization and virion structure

The virus is a small enveloped virus containing a positive-sense single-stranded ribonucleic acid (RNA) genome of about 15 kb that encodes 11 open reading frames (ORFs): ORF1a, TF, ORF1b, ORF2a, ORF2, ORF3, ORF4, ORF5, ORF5a, ORF6 and ORF7 (Meulenberg et al. 1993; Wu et al. 2001; Johnson et al. 2011; Fang et al. 2012). The 5'-

proximal three quarters of the genome comprising ORF1a, ORF1b and ORF-TF contain two programmed ribosomal frameshifting sites (RFS) responsible for the alternating translation of four polyproteins that are co- and post-translationally cleaved into 16 nonstructural proteins (NSP) in total by four virally encoded proteinases (Fang and Snijder 2010; Fang et al. 2012). Eight structural proteins (glycoprotein (GP) 2, envelope (E), GP3, GP4, GP5, membrane (M), nucleocapsid (N) and ORF5a protein) are encoded by the ORFs in the 3'proximal quarter, ORF2a, ORF2b, ORF3-7, and ORF5a, respectively, and are expressed by a set of subgenomic RNAs (sgRNA) generated through a negative strand intermediate with the 5' untranslated region as a leader sequence (van Marle et al. 1999). Figure 5 illustrates the genomic organization and translation strategy.

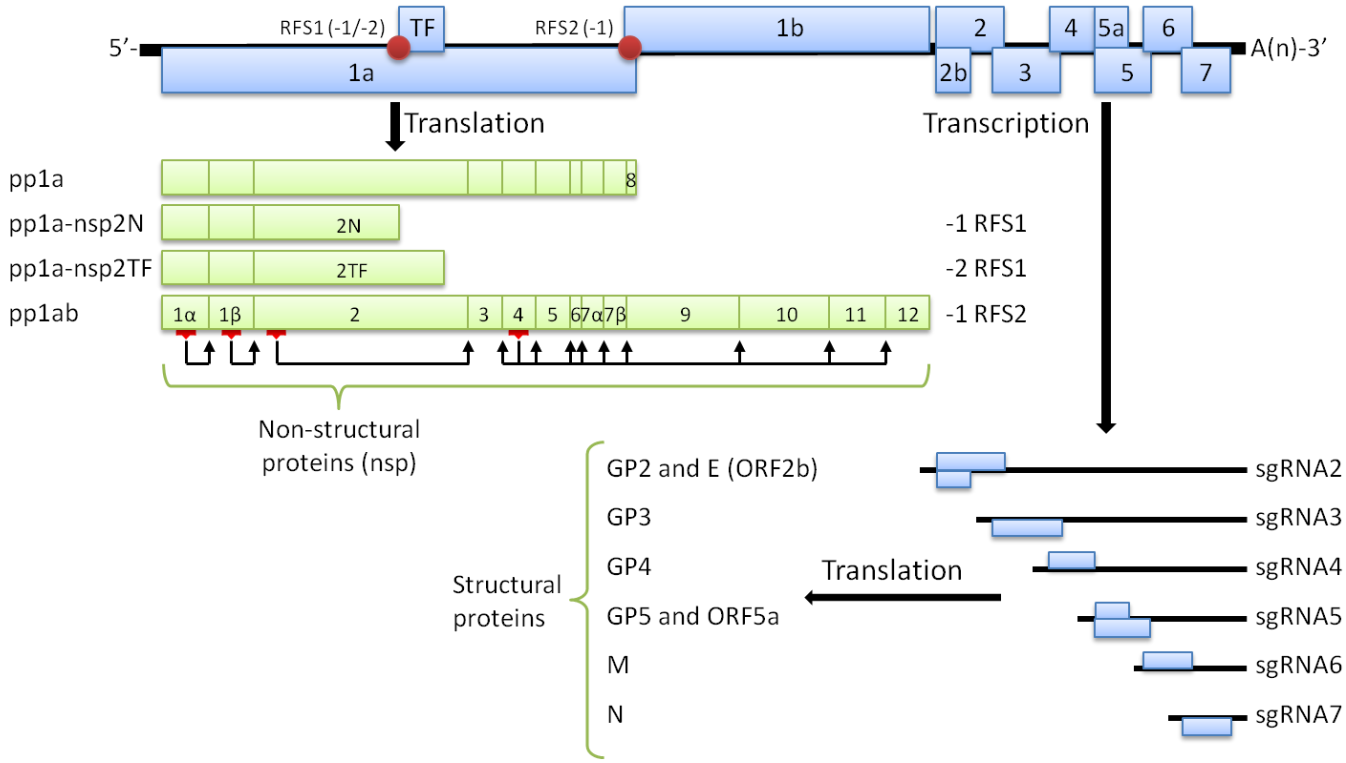

***Figure 5**: The genomic organization and translation strategy of PRRSV-2. Top panel illustrates the full genome with open reading frames (ORF) presented as blue boxes. The two ribosomal frameshifting sites (RFS) are presented as red circles and the possible offsets are given in parenthesis. The middle panel illustrates the four possible polyproteins (pp) translated from the different RFS combinations. The pps are co- and post-translationally cleaved into functional non-structural proteins as indicated by lines and the responsible proteinases are indicated with active sites (red markings) and cleavage sites (arrows). The bottom panel illustrates the six subgenomic RNAs (sgRNA) encoding the eight structural proteins, including glycoproteins (GP) 2-5, ORF5a, envelope (E), membrane (M) and nucleocapsid (N) proteins.*

The PRRSV virion is a pleomorphic particle with a size ranging from 50 to 65 nm. It has a hollow, layered core consisting of the genomic RNA bundled up by disulfide-linked homodimers of N protein. The core is covered in a lipid membrane, the envelope, in which the remaining structural proteins are embedded (figure 6) (Spilman et al. 2009). GP2, GP3, GP4 and probably also E form a complex that is necessary both for ER-to-Golgi transport before particle formation (Wissink et al. 2005) and for viral entry via interaction with the CD163 receptor on the target cell (Das et al. 2010). GP5 and M form a disulfide-linked heterodimer and constitutes the major glycoprotein complex that is vital for particle formation (Wissink et al. 2005). The exact role of the ORF5a protein is currently unknown, but it has

been shown to be required for virus viability (Sun et al. 2013). Recently, various isoforms of NSP2 has been detected in association with the viral membrane, thus raising the number of viral structural proteins from 8 to 10 or more. Although they have been shown to have membrane-modifying capacities, their exact roles are unclear (Han et al. 2010; Kappes et al. 2013; Kappes et al. 2015).

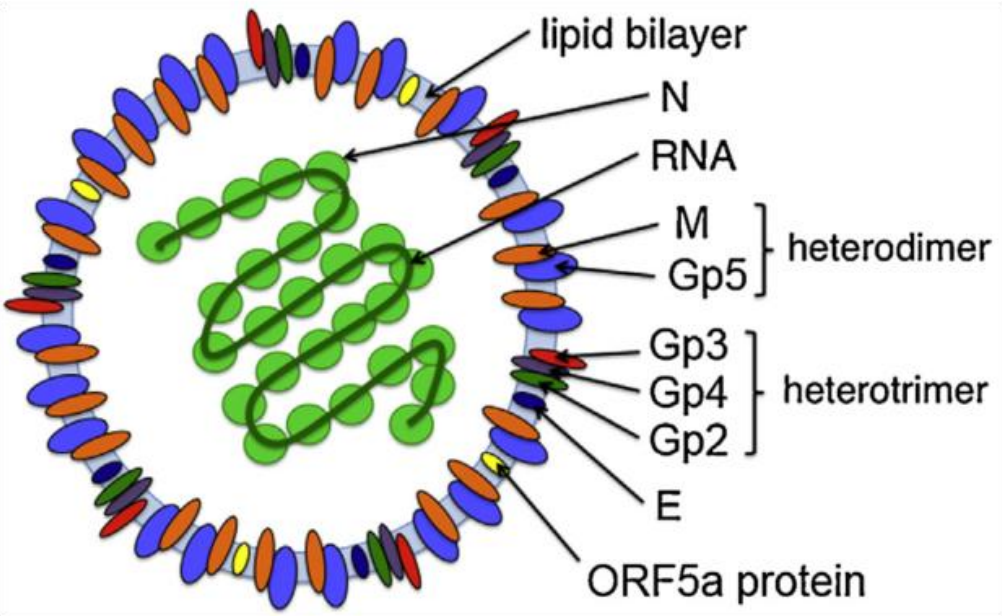

***Figure 6**: Scheme of the PRRSV particle. The membrane contains the major Gp5/M complex (blue and orange), the minor glycoprotein complex Gp2/3/4 (green, red and purple, respectively), the small hydrophobic E protein (dark blue) and the ORF5a protein (yellow). Figure adapted from Veit et al., 2014, doi:10.1016/j.virusres.2014.09.010*

1.3.3 Origin, phylogeny and diversity

The origin of PRRSV has still not been established, though it is generally assumed to have evolved from the mouse virus, LDV, based on similarities within the *Arteriviridae* family. However, LDV does not infect pigs and PRRSV does not infect mice and no intermediate species has so far been discovered. Because of this and supported by probabilistic arguments, the appearance of PRRSV is proposed to be the result of a single speciation event from which the two PRRSV species have evolved on their respective continents (Murtaugh et al. 2010). When and where this speciation event and the subsequent divergence into separate species occurred is being debated. One study suggested the speciation event to have occurred as late as in the 1980's based on molecular evolutionary analyses of the ORFs 3-6 (Hanada et al. 2005). This was challenged by Forsberg (2005), who reanalyzed the same set of data using a different methodology and concluded the divergence into separate species to have occurred 100 years earlier. A few years before, a hypothesis based on historical events and ORF5 alignments was proposed by Plagemann (2003), suggesting that the speciation event had occurred somewhere in Eastern Europe, whereafter the virus was introduced to the American continent in 1912 for isolated evolution into PRRSV-2. More recently, Yoon et al. (2013) estimated the most recent common ancestor to have existed about 790 years ago with subsequent divergence into subspecies of PRRSV-1 and PRRSV-2 to have occurred 115 and 180 years ago, respectively. The study was based on full genome sequences from 15 PRRSV-1 and 111 PRRSV-2 strains where known recombinant

strains had been excluded. Obviously, a simple model for the determination of these events cannot be made as multiple parameters and variables must be considered. Especially the frequency and impact of recombination events are hard to estimate, but since recombination is an inherent mechanism of PRRSV replication, by virtue of the generation of sgRNA and heteroclites, it must be assumed to be partly responsible for the global PRRSV diversity (Murtaugh et al. 2010). As such, phylogenetic analyses based only on a single ORF may be misleading since the full scope of recombination events will not be apparent. This was exemplified by a study in which Eurasian PRRSV-1 strains were subtyped according to both ORF5 and ORF7 (Stadejek et al. 2008). The generated phylogenetic trees were incongruent in the evolutionary relationship between Russian and Western European subtype 1. This incongruence was verified by Shi et al. (2010b), who further suggested a recombination event to be the most plausible explanation. In spite of this, it is currently accepted that PRRSV-1 can be divided into three subtypes on the basis of ORF5 and ORF7, though a fourth subtype is tentative (Stadejek et al. 2013). Of these, subtype 1 is the largest and can be further divided into 12 clades (Stadejek et al. 2008; Shi et al. 2010b). Even though the majority of its diversity is in Europe, PRRSV-1 has been introduced to 5 non-European countries, including USA, Canada, South Korea, China, and Thailand (Shi et al. 2010b).

The diversity of PRRSV-2 has likewise been divided into 9 different lineages and several sublineages based on ORF5 sequence analysis. North American strains dominate most of the lineages except for two, that are specific for Asian strains (Shi et al. 2010a). However, frequent introductions of various PRRSV-2 strains have been observed in several European and Asian countries. Especially strains of lineage 5 have been broadly introduced to more than eight countries outside of the North American continent. This lineage contains the strain used in the Ingelvac PRRS Vet vaccine that in several cases is likely to have constituted the direct route of introduction (Botner et al. 1997; Cha et al. 2006; Chen et al. 2006; An et al. 2007; Greiser-Wilke et al. 2010).

1.3.4 Virus attachment, entry, replication and release

Members of the genus *Suis* (pigs, including wild boars) are the only natural host for PRRSV, which has a tropism for cells of the monocyte lineage, especially differentiated macrophages such as porcine alveolar macrophages (PAM) that serve as the primary site of replication. This highly restricted tropism is determined by the presence of specific receptors in the target cell, which is believed to mediate infection as follows (figure 7):

Early attachment of an approaching PRRSV is aided by sticky interactions between the PRRSV M/GP5 complex and heparan molecules on the PAM surface (Delputte et al. 2002). This is followed by a gradual increase to the more stable and intimate binding between sialic acid molecules on GP5 and macrophage-restricted sialoadhesin molecules, which in turn will induce internalization by clathrin-mediated endocytosis (Vanderheijden et al. 2003; Delputte et al. 2005; Van Breedam et al. 2010). Subsequent viral uncoating and genome release is mediated by interactions between the PRRSV GP2 and GP4 proteins and the scavenger receptor, CD163, in the early endosome (Van Gorp et al. 2008; Van Gorp et al. 2009; Das et al. 2010; Tian et al. 2012).

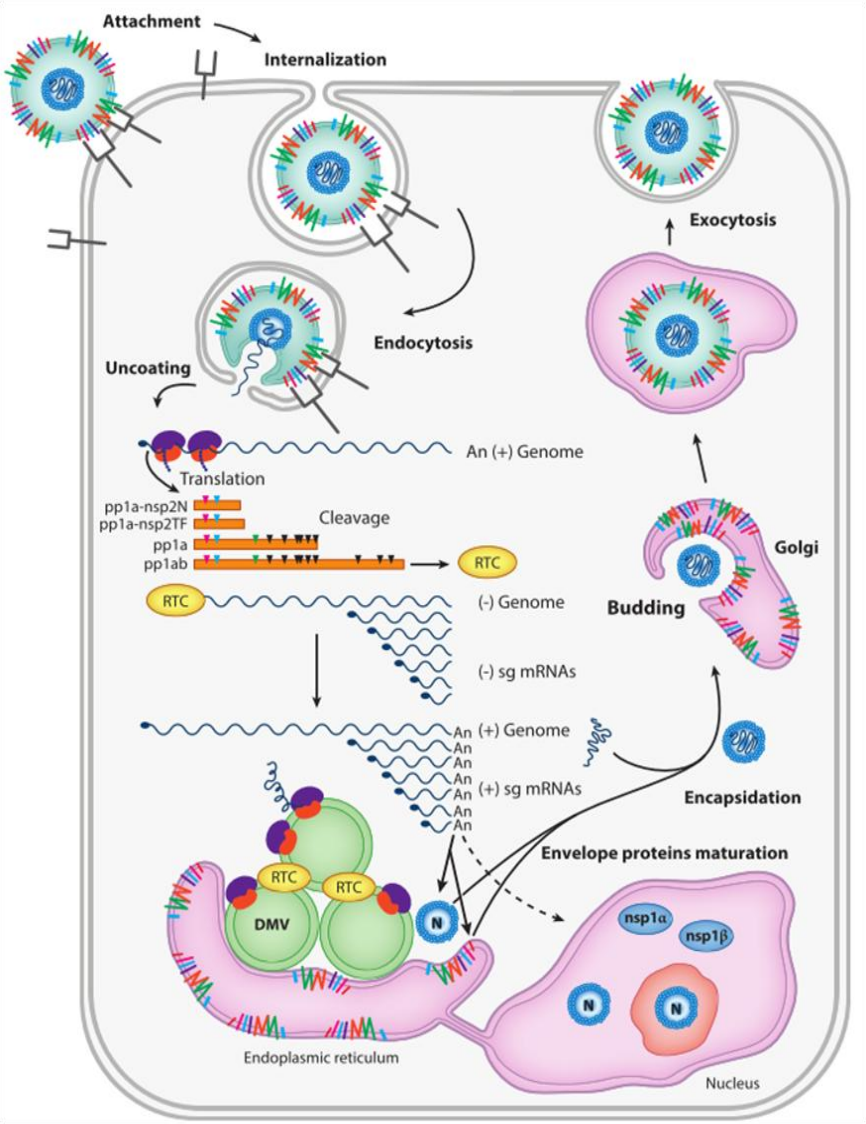

Figure 7: *PRRSV replication cycle. Following entry by receptor-mediated endocytosis and disassembly, genome translation yields the polyproteins pp1a-nsp2TF, pp1a-nsp2N, pp1a, and pp1ab that are cleaved by internal proteinases to generate at least 14 nonstructural proteins, which are assembled into a replication and transcription complex (RTC). The RTC first engages in minus-strand RNA synthesis to produce both single-strand full-length and subgenomic (sg)-length negative-strand RNAs. Subsequently, the sg mRNAs serve as templates for the synthesis of positive-strand sg mRNAs required to express the structural protein genes that reside in the 3'-proximal quarter of the genome. Newly generated RNA genomes are packaged into nucleocapsids that become enveloped by budding into intracellular compartments. The new virions are released from the cell by exocytosis. Figure adapted from Lunney et al., 2016, doi:10.1146/annurev-animal-022114-111025.*

The above model describes the main entry pathway for PRRSV into macrophages, but other pathways and permissive cells exist and with these, alternative cellular and viral molecules are involved in the entry processes of PRRSV. The African green monkey line, MA104, and its derivatives, MARC-145 and CL2621 cells, are all commonly used for virus propagation, but do not express sialoadhesin (Kim et al. 1993; Bautista et al. 1993). Another recently discovered permissive cell line, SJPL, derived from swine respiratory tract epithelial cells, neither expresses sialoadhesin nor CD163, but is permissive anyway (Provost et al. 2012). All of these alternative cell lines express the receptor, CD151, which is also expressed by PAMs. Different silencing experiments in MARC-145 cells have indeed shown that CD151 is vital for PRRSV infection, which may then also be the case for the SJPL cells (Shanmukhappa et

al. 2007). Another molecule that was shown to be important for virus entry into MARC-145 cells and interact with the nucleoprotein is vimentin (Kim et al. 2006; Song et al. 2016). Furthermore, recent experiments with genetic CD163 knock-out pigs have indicated that PRRSV-1 and PRRSV-2 may differ in their entry pathways and there may even be differences between individual strains (Wells et al. 2017).

Once the PRRSV genome has been released inside the host cell, replication begins in the cytosol, immediately translating ORF1a, ORF-TF and ORF1b for the generation of the NSPs. These quickly assemble into a membrane associated replication and translation complex (RTC) containing the two core enzymes, RNA-dependent RNA polymerase (NSP9) and RNA helicase (NSP10). Infection also triggers the formation of a large number of interconnected double membrane vesicles (DMV) derived from the ER where subunits of the RTC have been shown to co-localize (Pedersen et al. 1999; van Hemert et al. 2008). Additionally, EAV double stranded RNA has been detected within these structures, why it is believed that DMVs function as replication and translation hotspots, safely shielding the virus from the intracellular PRRs. Progeny virions are generated by budding of pre-formed nucleocapsids into the lumen of smooth intracellular membranes, after which the virions leave the cell by exocytosis, determined by the mature M/GP5 complex (Wissink et al. 2005).

1.3.5 Pathogenesis and pathology

PAMs are believed to be the primary target cells, but PRRSV has also been found in interstitial macrophages in various tissues (listed in Provost et al. 2012) and highly pathogenic strains may have expanded tropism to include various epithelial cells (Zhou and Yang 2010). PRRSV infects and replicates within macrophages and eventually kills them. The first cycle of replication occurs in the PAMs, whereupon the virus can spread to other parts of the body either by means of viremia or inside migrating macrophages. The clinical symptoms appear early after infection and the most common signs include respiratory symptoms that often leads to fever, lethargy, anorexia and pneumonia. PRRSV participates as co-factor in polymicrobial syndromes, such as Porcine Respiratory Disease Complex (PRDC) and Porcine Circovirus Associated Disease (PCAD) (Chand et al. 2012). Studies have shown that infectious PRRSV could be isolated from lymphoid tissue more than 150 days after infection even after several months of viral absence in the serum (Wills et al. 1997; Allende et al. 2000). Furthermore, viral replication has been detected for as long as 250 days after infection (Wills et al. 2003). For pregnant gilts and sows infected in late gestation the virus may infect the endometrium and placenta giving rise to sporadic late-term abortions, early farrowing and birth of litters mixed with living, stillborn and mummified fetuses (Zimmerman et al. 1997; Rossow 1998; Karniychuk and Nauwynck 2013). Viremia typically peaks after 10-15 days post infection and in most cases the level of virus in serum is below the detection limit 4 weeks after infection, but the virus may persists in some pigs (Lopez and Osorio 2004). Although the infection is not persistent *per se* it is often life-long since the average lifetime of production pigs is 180 days.

1.3.6 Virus transmission and epidemiology

Due to its bilipid envelope, PRRSV is easily inactivated by solvents, heat, drying, and is only viable within a narrow pH range between 5 and 7 (Benfield et al. 1992). Supposedly for the same reasons, outbreaks have been shown to follow a seasonal pattern in the Midwest of USA with an onset in October (Tousignant et al. 2015). Nevertheless,

PRRSV has spread to every part of the global swine industry, and in many places both genotypes have become enzootic (Shi et al. 2010). PRRSV can be transmitted by several routes that together with the age of the naïve pig are determinants of contagiousness. Infectious virus has been recovered from nasal secretions, saliva, urine, semen faeces, aerosols, milk and colostrum (reviewed in Pileri & Mateu 2016), and exposure to PRRSV occurs by the respiratory and oral routes and through the mucosae. Aerial transmission, direct contact, coitus, insemination, ingestion and inoculation can all mediate infection, in addition to fomites and vertical transmission during late gestation. Despite the absence of clinical signs, several studies have shown that transmission is possible for up to three months under natural conditions from horizontally infected pigs, and for a much longer period from vertically infected pigs (reviewed in Pileri & Mateu 2016).

Due to the above reasons, the introduction of PRRSV into a naïve herd will usually cause a clinical outbreak infecting all stages of production within 2-3 weeks. Gradual immunization will then lead to a decline in the epidemic in 1-5 months, after which the infection will typically become endemic for long periods of time depending on population size (Pileri and Mateu 2016). The routes of transmission to the herd are likewise multiple: One common way is the introduction of infected gilts or sows for which infection was not detected or the proper quarantine measures were not applied (Mortensen et al. 2002; Kwong et al. 2013; Rosendal et al. 2014). Introduction via infected semen has also been reported (Botner et al. 1997; Nathues et al. 2014), and several studies have shown that transportation vehicles, feed, boots and other equipment could transmit disease, especially during the cold season (Dee et al. 2002; Dee et al. 2003; Dee et al. 2004). Airborne transmission from farm to farm has also been evaluated, and in one study infectious virus was detected in the exhaust air 4.7 km from the infected farm (Dee et al. 2009). Other studies have shown that airborne transmission is highly dependent on the strain (Torremorell et al. 1997) and on environmental factors such as temperature, humidity, sunlight and wind (Torremorell et al. 1997; Dee et al. 2002; Dee et al. 2003; Otake et al. 2010; Dee et al. 2010).

1.3.7 Prevention and control

Preventive methods are relatively easily applied comprising purchase of animals and semen from PRRSV negative pigs, decontamination of vehicles and fomites, and filtration of inlet ventilation air. In addition, vaccination of sows and piglets is a strategy commonly used for the control of PRRSV. On the level of the individual animal, the main objective of vaccination is to reduce clinical signs and protect pregnant sows from reproductive failures. On the herd level, the objective is mainly to reduce economic losses associated with disease, to decrease antibiotic use and to increase animal welfare.

Many attempts have been made to develop an effective vaccine against PRRSV. Various virus attenuation or antigen selection strategies, adjuvants and delivery systems have been tested including killed virus (KV), modified live virus (MLV), recombinant protein based, and deoxyribonucleic acid (DNA) vaccines, and their efficacies in terms of viral clearance and relief of symptoms are diverse (reviewed in Renukaradhya et al. 2015a and Renukaradhya et al. 2015b). Most of these remained unsuccessful and commercial MLV vaccines quickly gained ground due to their

strong protection against a homologous challenge. Cross-protection against a heterologous challenge, however, has for most parts remained absent.

In one study it was shown that pigs vaccinated with a PRRSV-2 based MLV significantly reduced viral shedding in oral fluids and in the air after challenge, although the magnitude and duration of viremia was unaffected compared to unvaccinated pigs (Linhares et al. 2012). In a similar study, repeated immunization of pigs with a PRRSV-1 based MLV that were previously infected with a homologous strain both reduced the number of persistently infected pigs and viral shedding, even though complete elimination of the circulating strain could not be obtained (Cano et al. 2007). Recently, a new MLV vaccine (Fostera PRRS, Zoetis), based on the PRRSV-2 isolate, P129, showed signs of partial cross-protection after challenge with a PRRSV-1 virus by significantly reduced levels of viremia and nasal shedding, as well as a reduced severity of lung lesions (Park et al. 2015). Short after, the same lab presented results from a challenge study testing the protection against a dual challenge with both PRRSV-1 and PRRSV-2 after vaccination with either Fostera or a PRRSV-1 based MLV vaccine (Unistrain PRRS, Hipra). Again, Fostera showed significant cross-protective capacities, while this was not seen for Unistrain PRRS (Choi et al. 2016).

Despite the positive effects of MLV vaccines, a more sinister side revealed itself in 1997 when evidence appeared describing that an attenuated PRRSV-2 vaccine had reverted back to virulence and started promoting rather than preventing disease (Botner et al. 1997; Madsen et al. 1998). This marked the introduction of the type 2 PRRSV to Denmark, which subsequently spread to other parts of Europe. Similar events of MLV strains reverting to virulence have since been described for a PRRSV-1 based vaccine (Beilage et al. 2009; Frossard et al. 2012; Kvisgaard et al. 2013) and a for a vaccine based on a highly pathogenic Asian versions of a PRRSV-2 strain (Jiang et al. 2015). Furthermore, the use of MLV in pregnant animals in the last trimester increases the risk of reproductive failure.

In addition to vaccination, numerous field reports and experimental studies of circulating wild type strains provide evidence that the porcine immune system is indeed capable of mounting a response that will eventually clear the infection from the animal entirely. In one case it was observed that sows having suffered from PRRSV-induced reproductive failure could succeed in having a normal litter after rebreeding despite the apparent circulation of the virus within the herd (Stevenson et al. 1993). Expanding on this, various herd closure and farm stabilization protocols have succeeded in complete viral clearance of entire herds by selective exposure of live residing virus (Torremorell et al. 2002; Linhares et al. 2014). Investigating the protective properties of the immune response, one study showed that protection can be observed for more than 600 days after exposure of a homologous strain (Lager et al. 1997a), while another study showed that intrauterine exposure at gestation day 1 could provide protective immunity against subsequent exposure of the same strain at gestation day 90 (Lager et al. 1997b). Collectively, these cases represent a growing pile of evidence that PRRSV can indeed be controlled by correct manipulation of the immune systems of the pigs.

In Denmark, the first case of PRRSV (PRRSV-1) was diagnosed in 1992 (Bøtner et al. 1994) and a systematic monitoring of the national PRRSV status was initiated in 1996, indirectly leading to the introduction of PRRSV-2 to the Danish swine industry (Botner et al. 1997). In the period from 2010 to 2013, around 35% of all specific pathogen

free (SPF) herds were infected with PRRSV being generally less than preceding years (Kristensen et al. 2014a). A standardized herd classification system for describing the PRRSV infection status of herds has been presented by Holtkamp et al. (2011), defining four categories: 1) Positive unstable herds have positive shedding and exposure to the virus. This is also the default category for untested herds with unconfirmed exposure status. 2) Positive stable herds are without clinical signs of PRRSV in the breeding-herd population and viremia has remained undetectable for a minimum of 90 days. 3) Provisional negative herds have a negative shedding status and introduced animals must remain seronegative. However, older seropositive animals are accepted. 4) Negative herds have negative shedding and exposure status.

Depending on the severity of infection and general market demands, positive unstable herds are either completely or partially depopulated. In a complete depopulation, all animals are culled and new PRRSV-negative animals are inserted 3 weeks after the farm has been washed and disinfected. In a partial depopulation, only sections with transmission of virus are emptied, washed and disinfected (Kristensen et al. 2014b). Transmission of virus will often be seen among the weaned piglets for which reason this section can be depopulated in an action called nursery depopulation (Dee 2003). Alternatively, positive unstable herds can be stabilized by various methods, such as proper management of the gilt pool (Dee et al. 1995) and by following the 'McREBEL' guidelines (Management Changes to Reduce Exposure to Bacteria to Eliminate Losses) to limit transmission (McCaw 2003). Under Danish conditions, the MLV vaccines are used in PRRSV positive herds to stabilize the sow herd by vaccinating gilts prior to first mating, which optimally leads to avoidance of reproductive problems related to PRRSV infection and weaning of PRRSV negative piglets.

1.3.8 Immune response and immunoevasion

PRRSV has now been around for almost 30 years. In this period it has spread to all parts of the world causing wreckage in the pig industry with an estimated annual production loss in the USA worth of $664 million (Holtkamp et al. 2013). Atypical and highly pathogenic strains have evolved, such as the Belarusian type 1 subtype 3 strain, Lena (Karniychuk et al. 2010; Van Doorsselaere et al. 2012), the highly virulent MN184 strain in USA (Mengeling et al. 1998; Han et al. 2006), and the Chinese HP-PRRSV (for highly pathogenic) strains, the latter of which resulted in unparalleled outbreaks in 2006 affecting ~2 million and killing ~400,000 pigs in China (Tian et al. 2007). In addition, PRRSV has been shown to function as co-factor in disease complexes such as PRDC and PCAD (Brockmeier et al. 2002) and to be involved with a long list of other swine pathogens including *Mycoplasma Hyopneumoniae* (Thacker et al. 1999), *Bordetella Bronchiseptica* (Brockmeier et al. 2000), Porcine Circovirus-2 (Allan et al. 2000), Porcine Respiratory Coronavirus, Swine Influenza Virus and *Haemophilus Parasuis* (Van Reeth et al. 1996; Solano et al. 1997). Obviously, extensive efforts to control end eventually eradicate PRRSV have been made, and until now, this has resulted in more than 2500 scientific articles written on PRRSV. Nevertheless, eradication or even a fulfilling strategy to control the virus has not yet been achieved. The vast amount of generated scientific data, however, has shed light on several aspects of the conundrum, and it is now clear that PRRSV exhibits a multitude of immunoevasive mechanisms, manipulating both the innate and adaptive immune response on several levels. This will be briefly

reviewed in the following subsections, including the effects on the innate immune response (section 1.3.8.1), the humoral adaptive response (section 1.3.8.2) and the cell-mediated adaptive response (section 1.3.8.3).

1.3.8.1 Effects on the innate immune response

The type I IFNs (IFN-α/β) are important antiviral activators for the innate immune response and function by autocrine/paracrine signaling. Recipient cells will be triggered to express a wide variety of interferon-stimulated genes (ISG) that function to establish antiviral and immune-regulatory states in the host cells. Not surprisingly, PRRSV inhibits type I IFN signaling on several levels. PRRSV uses no less than 5 viral proteins as known IFN antagonists: NSP1, NSP2, NSP4, NSP11 and N. NSP1 and the N protein localize to the nucleus and inhibit the IFN transcription activation by targeting the interferon regulatory factor 3 (IRF-3) and the NF-κB-responsible promoter (Chen et al. 2010; Song et al. 2010; Sagong and Lee 2011). NSP2, NSP4 and NSP11 also antagonize type I IFN by inhibiting the NF-κB signaling pathway in various ways, although the antagonistic effect of NSP2 is less consistent and seems to vary with different strains (Beura et al. 2010; Sun et al. 2010; Chen et al. 2014; Sun et al. 2014; Huang et al. 2014). This inconsistency may be related to the fact that the NSP2 sequence varies most among strains. Also in recipient cells, PRRSV both suppresses the downstream signal transduction of type I IFNs by means of NSP1 (Patel et al. 2010; Wang et al. 2013), and also interferes with at least one ISG by means of NSP2 (Sun et al. 2012).

TNF-α is also a target for suppression by PRRSV by virtue of its pleiotropic functions attributed to the promotion of an antiviral state in uninfected neighboring cells, recruitment of lymphocytes to the foci of infection, selective cytolysis of virus-infected cells, and modulation of apoptosis/survival of cells (Smith et al. 1994; Natoli et al. 1998). Again, the subunits of NSP1 are responsible by modulating the activities of the transcription factors NF-κB and Sp1, respectively (Subramaniam et al. 2010). Furthermore, HP-PRRSV strains are more potent repressors of TNF-α than conventional Chinese strains, which may contribute to the pathogenesis of HP-PRRSV (Hou et al. 2012a).

On the other side of the spectrum, IL-4 and IL-10 are both upregulated in PRRSV infected cells (Genini et al. 2008; Dwivedi et al. 2012; Wongyanin et al. 2012). IL-4 is known in pigs to suppress inflammatory cytokine gene transcription in macrophages (Zhou et al. 1994), and IL-10 is an anti-inflammatory cytokine important to regulation of the immune response and can be produced by several cell types, including monocytes/macrophages, DC, T cells and B cells. It is capable of inhibiting numerous inflammatory cytokines, can counter an adaptive response, and can induce the differentiation of T cells into Tregs (Moore et al. 2001; Genini et al. 2008; Sabat et al. 2010). At least three PRRSV encoded proteins have been shown to induce IL-10, comprising NSP1 (Zhou et al. 2012), N protein (Wongyanin et al. 2012), and GP5 (Hou et al. 2012b; Song et al. 2013).

Besides manipulating expressions and responses to various cytokines, PRRSV also modulates the cells in various ways. One such way is apoptosis, which among many other roles, is a crucial innate defense mechanism to prevent viral replication and eliminate infected cells (Thomson 2001). PRRSV is able to prevent apoptosis in early stages of infection, apparently by means of GP2 (Huo et al. 2013; Pujhari et al. 2014), and to induce it in late stages by means of NSP4 (Costers et al. 2008; Ma et al. 2013). Interestingly, also neighboring cells become induced to undergo apoptosis, indicating the secretion of apoptogenic cytokines (Huo et al. 2013).

Another way to manipulate the infected cells lies in the formation of intracellular DMVs as mentioned earlier. These are likely to function as a hideout for the virus, where it can replicate freely while shielding itself from intracellular antiviral PRRs.

A third way was announced in a very recent study, in which Guo et al. (2016) presented thorough evidence that PRRSV can induce the formation of - and spread through - long membraneous nanotubes. This was done by engaging the actin cytoskeleton for structural scaffolding and the myosin motor protein for transportation of viral genetic material and proteins. The nanotubes were able to interconnect cells within a few cell widths, thereby allowing viral dissemination without the need of an extracellular phase. Viral spread by nanotubes was shown to occur in both Marc-145 and PAMs, and could transfer infection to otherwise non-receptive cells, such as HEK-293T cells. Viral spread through nanotubes was shown to be completely unaffected by neutralizing Abs, thus stressing the need for a cytotoxic response.

In addition to the mentioned manipulations, their effects progress throughout the entire immune response molding it to the benefit of the virus. The first cells affected are the NK cells that are both reduced in numbers and cytolytic activity (Shi et al. 2008; Dwivedi et al. 2012; Cao et al. 2013). This allows for unrestrained infection of the macrophages that will have their normal antiviral response suppressed by the virus. Instead, they will enter a state characterized by debris clearance and tissue repair and their foremost skill as antigen presenting cells will be battered by the reduced expressions of MHC I and II.

Besides utilizing the standard pathway for entry into the macrophage, evidence has shown that PRRSV may enter PAMs by a phenomenon known as antigen-dependent enhancement (ADE). ADE represents a mechanism in which the attachment of sub-neutralizing antibodies to the viral surface induces Fc receptor-mediated endocytosis, by which the macrophage becomes infected. Studies have shown that the yield of progeny virus increases significantly in PAMs in the presence of anti-PRRSV antisera, and that the viremic response in pigs injected with sub-neutralizing antibodies prior to infection is much more severe, than in pigs injected with normal antibodies (Mateu and Diaz 2008; Halstead et al. 2010). Further evidence suggested ADE to interfere with the innate cytokine responses, since the pretreatment of PAMs with antibodies blocking the Fc receptor responsible for ADE, FcγRIIb, resulted in increased transcription of IFN-α and TNF-α, but decreased expression of IL-10 upon PRRSV infection (Zhang et al. 2012).

DCs, being the only antigen presenting cell type superior to macrophages, constitute the main activators of the adaptive immune response. Obviously, PRRSV has found ways to manipulate these too. One rather straight forward strategy is to simply kill the infected DC by both apoptotic and necrotic mechanisms (Rodríguez-Gómez et al. 2013). Another and more sophisticated strategy involves the increased induction of IL-10, the suppression of type I IFN and the downregulation of MHC-I and -II, and the co-stimulatory molecules CD80/86 (Charerntantanakul et al. 2006; Loving et al. 2007; Wang et al. 2007; Flores-Mendoza et al. 2008; Chang et al. 2008; Liu et al. 2016).

The general result of the PRRSV-induced compromised antigen presentation is a weak and delayed onset of the adaptive immunity. T cell responses are reported to appear at 4–8 weeks post infection and $CD4^+$- and $CD8^+$-T cells remain low and constant (Bautista and Molitor 1997; López Fuertes et al. 1999; Feng et al. 2002; Xiao et al. 2004).

Additionally, infected DC have been reported to induce the differentiation of T cells into Tregs both *in vivo* and *in vitro* (Wongyanin et al. 2010; LeRoith et al. 2011; Cecere et al. 2012; Manickam et al. 2013). These immunosuppressive cells have in humans previously been associated with the suppression of antiviral immunity and in the establishment of chronic persistent HIV, hepatitis C and B viruses, cytomegalovirus and Epstein-Barr virus (Cecere et al. 2012). During PRRSV infection, Tregs may be responsible for the observation that $CD3^{+}CD8^{high}$ T cells isolated from peripheral blood mononuclear cells (PBMC) of PRRSV-infected pigs can indeed proliferate upon restimulation *in vitro*, but cannot exert cytolysis on PRRSV-infected PAMs (Costers et al. 2009).

The anti-bacterial Th17 variant of the T helper cells has also been shown to play a role in response to infection with an HP-PRRSV strain. When comparing the number of Th17 cells in infected pigs, the Th17 population was significantly suppressed in peripheral blood and in lungs of pigs infected with an HP-PRRSV strain (JXwn06), when compared to pigs infected with either mock or a low pathogenic strain. This correlated with increased bacterial loads in the lungs of HP-PRRSV infected pigs, thus suggesting a method by which PRRSV may give way for secondary infections (Zhang et al. 2016).

1.3.8.2 Effects on the humoral adaptive immune response

Humoral immunity has been regarded as the key effective component of PRRSV clearance since Osorio et al. (2002) demonstrated that passive transfer of antibodies isolated from PRRSV immunized animals could provide sterilizing immunity in pregnant sows. For many years, focus has been on GP5 as the carrier of the protective PRRSV neutralizing epitope (Ostrowski et al. 2002; Plagemann 2004a; Plagemann 2004b). By virtue of the previously mentioned role of the M/GP5 complex to mediate viral attachment and internalization through interactions with heparan sulphate and sialoadhesin, an antibody that prevents these interactions by binding to the M/GP5 complex would therefore be expected to contain neutralizing capacities. Several different vaccination platforms have been engaged in confirming the neutralizing capacities of antibodies induced either by GP5 alone or in complex with the M protein (Pirzadeh and Dea 1997; Jiang et al. 2007; Zhou et al. 2010; Vanhee et al. 2011; Xu et al. 2012; Kim et al. 2013), and it should now be assumed that the neutralizing epitope(s) on GP5 is conformational (Fan et al. 2015), and that the M protein contributes to the conformational nature of this epitope when in complex with GP5. The heterotrimer of the minor envelope glycoproteins, GP2/GP3/GP4, has also been shown to contain epitopes for neutralizing antibodies, which is in agreement with its interaction with CD163 to initiate infection. In one study, linear neutralizing epitopes were indeed identified in each of the three minor glycoproteins of the Lelystad strain using a peptide scanning technology. One epitope located on GP3 was especially potent and the corresponding epitope on strains other than Lelystad was also able to induce neutralizing antibodies. Interestingly, no linear neutralizing epitopes were found on GP5, supporting the notion of a conformational nature (Vanhee et al. 2011).

In spite of the confirmed presence of these neutralizing epitopes, the induction of a neutralizing antibody response following PRRSV infection is typically weak and delayed. Two mechanisms are generally accepted as being responsible for this immunoevasive behavior. The first is the presence of decoy epitopes luring the immune response away from the neutralizing epitope(s) (Ostrowski et al. 2002). The second is the mechanism referred to as glycan shielding by which the presence of glycan molecules attached to specific asparagines in the glycoproteins

encapsulate the neutralizing epitopes. Several reports involving site directed mutagenesis, reverse genetics and deglycosylation of the glycoproteins support the concept that glycosylation of especially GP5 renders the virus resistant to neutralization, while the other glycoproteins are less affected (Vu et al. 2011; Wei et al. 2012a; Wei et al. 2012b). One study showed that inoculation of pigs with virus stripped of GP5-bound glycans gave rise to significantly higher levels of neutralizing antibodies against the mutant as well as wild-type PRRSV, suggesting that GP5 glycans are not only relevant to the shielding but also to the immunogenicity of the virus (Ansari et al. 2006).

1.3.8.3 Effects on the cell-mediated adaptive immune response

A functional CMI during a PRRSV infection should be manifested as activated CTLs, having the ability to identify and induce apoptosis of PRRSV-infected cells. Studies have shown that CTLs are indeed present in high numbers at infected locations in the lungs of transplacentally infected animals (Tingstedt and Nielsen 2004), and that the influx of CTLs to the lungs increase during PRRSV infection (Samsom et al. 2000). Although the CTLs are present, their role in clearing the infection is unclear and controversial.

On the skeptical side, Lohse et al. (2004) showed that acute infection appeared to be unaffected by the presence of CTLs since temporary depletion of CTLs during the onset of infection with PRRSV-1 virus neither increased disease nor influenced the ability to clear virus. One study attempted to evaluate the relationship between viral persistence and the presence of CTLs in blood, tonsils, the spleen and the mediastinal lymph nodes in PRRSV-2 infected animals. Although a significant correlation between viral clearance and increased CTL counts in the spleen was observed, a delayed and impaired CMI together with low levels of CTLs were found in the tonsils and lymph nodes, allowing viral persistence in these organs (Lamontagne et al. 2003). In a last example, the cytotoxic activity of PBMCs isolated from Lelystad-infected pigs failed to show PRRSV-specific lysis of infected autologous alveolar macrophages until very late in the experiment. Even following successful expansion of $CD3^{+}CD8^{high}$ cells after a 5-day period of restimulation with virus, a PRRSV-specific cytotoxic response was not observed until day 56 post infection, suggesting a PRRSV-induced impairment of the cytotoxic activity (Costers et al. 2009).

On a more optimistic note the CMI against PRRSV-2 was first explored by Bautista (1997), who described a PRRSV-specific lymphocyte proliferation and delayed-type hypersensitivity response, thereby indicating a T cell specific memory response. Another study argued that a CMI was responsible for the protective immunity of a PRRSV-1 challenge upon vaccination with an MLV vaccine, since a virus-specific IFN-γ response was observed, while no neutralizing antibodies were present (Zuckermann et al. 2007). An *in vitro* proliferation assay of PBMCs from PRRSV-1 infected cells showed that PBMCs could be expanded upon restimulation with virus, and that the cytotoxic activity against K-562 cells increased along with this expansion (López Fuertes et al. 1999). In a more recent study, a comprehensive screening for immunogenic T-cell epitopes was performed, restimulating PBMCs from pigs immunized with either of three PRRSV-1 strains, with 15-mers covering the whole proteome of the Olot/91 strain (structural proteins) or the closely related Lelystad strain (non-structural proteins). Using IFN-γ ELISPOT as readout, the authors identified several CD8 and CD4 T-cell responses against epitopes from both structural and non-structural parts of the genome (Mokhtar et al. 2014). The same lab later expanded on this and identified dominant T-cell

responses directed against NSP5 and the M protein, with indications of both memory and cytotoxic effector functions (Mokhtar et al. 2016).

1.3.9 Upcoming innovative vaccines

By virtue of the drawbacks associated with MLV vaccines, innovative vaccination strategies have begun to appear, bringing new hope for the development of a safe vaccine with cross-protecting capacities. In one such study, pigs were immunized with seven T-cell and two B-cell epitopes, mostly derived from PRRSV-2, and adjuvanted with a truncated version of the porcine heat shock protein, Gp96. Upon challenge with the HP-PRRSV strain, JXwn06, milder clinical symptoms, lower viremia and less pathological lung lesions were observed. Long-lasting effects, however, remained absent (Chen et al. 2013). In another lab, a vaccine-challenge study was performed in which pigs were vaccinated with a DNA vaccine encoding a truncated version of the N protein. The experiment confirmed the immunomodulatory effects of the N protein as the vaccinated pigs exhibited increased numbers of PRRSV-specific activated $CD4^+CD25^+$ lymphocytes, reduced numbers of PRRSV-specific Tregs, and rapid viral clearance following infection (Suradhat et al. 2015a; Suradhat et al. 2015b). Finally, an extensive animal trial was described by a third lab, in which pigs were vaccinated intranasally with the inactivated PRRSV-2 strain, VR-2332, entrapped in poly(lactic-*co*-glycolic) acid nanoparticles adjuvanted with *Mycobacterium tuberculosis* whole-cell lysate. Subsequent challenge with the heterologous PRRSV-2 strain, MN184, showed an enhanced PRRSV-specific antibody response with neutralizing capacities, a suppressed immunosuppressive cytokine response, increased frequencies of IFN-γ secreting cells, and most importantly a complete clearance of replicating virus, and a three $\log_{10}$ reduction of viral RNA load in the blood (Binjawadagi et al. 2014a). Also in the lungs, a ten-fold reduction of viral RNA load was observed (Binjawadagi et al. 2014b).

2 GENERAL MATERIALS AND METHODS

In this chapter, I will elaborate on the materials and methods used during my studies and provide relevant information and reflections that were left out in the papers. The various methods are be listed in order of deployment and are related to epitope prediction (section 2.1); preparation and storage of the peptides (section 2.2); *in vitro* verification of the epitopes (section 2.3); SLA genotyping of pigs (section 2.4); VRP design, generation and verification (section 2.5); titration of VRPs and PRRSV (section 2.6); applied diagnostic methods (section 2.7); and the enzyme-linked immunospot assay (ELISPOT) (section 2.8).

2.1 Epitope prediction

As previously mentioned, the capacity of a peptide to bind to an MHC-I complex is the most critical determinant of a functional epitope. Because of this, a rational identification and selection of potential epitopes was a central milestone in the development of the final vaccine and occupied most of my first year as a PhD student.

PRRSV has a genome of about 15 kilobases encoding for several thousands of 9- and 10-mer peptides, so testing them all in the lab would not only be extremely laborious, but would also pose a risk of the final verified epitopes of being specific for only a few strains. Instead, a bioinformatic approach was established, providing a strict filtering of potential epitopes, requiring that successful candidates would be conserved among PRRSV-2 strains, and would be predicted binders to at least one of five SLA alleles. The bioinformatic pipeline is described in more details in paper 1 and includes the following steps:

1. Selecting, curating and preparing all 9- and 10-mer peptides derived from available PRRSV-2 sequences for epitope prediction (section 2.1.1).
2. Selecting the relevant SLAs to be applied for epitope prediction (section 2.1.2).
3. Performing epitope prediction of the peptides by combining the two prediction methods, NetMHCpan (section 2.1.3), and positional scanning combinatorial peptide library (PSCPL) (section 2.1.4). For the latter, I designed a program that is mentioned in section 2.1.5.
4. Prioritizing the predicted strong binders according to conservation among strains and SLA coverage using the PopCover algorithm (section 2.1.6).

Several tools for epitope prediction exist for both epitope affinity and stability but most of these are not applicable to porcine MHCs. In this study, I combined the prediction outputs of the affinity prediction server, NetMHCpan, and the matrix based method, PSCPL. The output of both methods, given in the form of a percentile rank score, were combined by calculating the harmonic mean. Peptide candidates with a combined percentile rank score ≤ 2 for at least one of the selected SLAs, were subsequently passed on for prioritization by the PopCover algorithm.

2.1.1 Selection, curation and preparation of PRRSV sequences

Initially, it was undecided which of the two PRRSV species should provide the basis of the epitopes. Thus, both PRRSV-1 and PRRSV-2 strains were curated and prepared for epitope prediction. The procedure was cumbersome and involved several steps. First, all available full genome sequences were collected and their associated references were scrutinized in order to verify that each sequence was derived from a wild type strain. Secondly, the sequences were aligned in two global alignments, one for each species, and were subsequently partitioned in minor alignments representing each of the virus encoded protein products. This step was complicated further by the presence of two RFSs resulting in four protein products (pp1a, pp1a-NSP2-N, pp1a-NSP2-TF and pp1ab) translated from the three ORFs (ORF1a, ORF-TF and ORF1b) in the 5'-terminal three quarters of the genome (figure 5, page 29). Thirdly, all alignments were split up in individual nucleotide sequences that were then translated *in silico* and verified to all start with methionine and to not contain non-sense stop codons. Strains encoding protein products that did not comply with these criteria were excluded. At this point it was decided to proceed with PRRSV-2 as only 25 PRRSV-1 sequences had passed the test, while this number was 104 for PRRSV-2. Finally, all protein products were cleaved according to naturally occurring post-translational cleavage sites before being used as template for the *in silico* generation of 9- and 10-mer peptides. Conclusively, 43.634 unique 9-mers and 47.305 unique 10-mers verified to be a natural part of the wildtype PRRSV-2 panproteome were passed on for epitope prediction.

The curation and preparation of sequences was executed using CLC workbench aided by several small Python scripts written for bulk handling and processing of sequences.

2.1.2 Selecting the SLAs

Five SLA alleles (SLA-1*0401, SLA-1*0702, SLA-2*0401, SLA-2*0502, and SLA-3*0401) were used for epitope prediction. These SLAs were chosen since most of them had previously been shown to be common in Danish pigs (Pedersen et al. 2014) and were all readily accessible for *in vitro* analysis as recombinant biotinylated HC. Furthermore, PSCPL matrices were available for all five. Unfortunately, however, a general misconception had led to the belief that SLA-2*0502 were in fact SLA-2*0501. This meant that all prediction analyses were executed with SLA-2*0501 as it was believed that the subsequent *in vitro* analyses should be performed with this allele. The PSCPL analysis, on the contrary, had unknowingly been performed with the correct allele, since the PSCPL matrix was based on *in vitro* experiments with this very same recombinant HC. Conclusively, huge disagreements appeared between the two prediction methods that probably might have alerted an experienced person. This, however, I was not and when the misconception was finally acknowledged, the peptides had already been purchased.

2.1.3 Prediction using NetMHCpan

NetMHCpan (Hoof et al. 2009) is a publicly available epitope affinity prediction server based on artificial neural networks. The version used in this study (version 2.8) has been trained on >150,000 quantitative binding data covering >150 different MHC-I alleles. NetMHCpan not only accounts for the peptide sequence in relation to a fixed MHC-I allele, but also for the pseudosequence being the sequence of polymorphic residues in the peptide binding

groove responsible for interacting with the peptide. Consequently, predictions can be performed for virtually all species of interest given that the pseudosequence is provided. In case of the five SLAs relevant to the current study, providing the pseudosequences was not needed as these were already integrated in the prediction server. The output of NetMHCpan is given as a percentile rank score being calculated from a standard curve of 200,000 random natural peptides.

The performance of NetMHCpan was recently benchmarked against three other publicly available MHC-I prediction servers, of which NetMHCpan performed the best (Trolle et al. 2015). It was developed at the Technical University of Denmark, Center for Biological Sequence Analysis (DTU-CBS), by Morten Nielsen, who is also co-author of paper 1. He advised me to use NetMHCpan, and further advised me to combine the outputs of both NetMHCpan and PSCPL, in compliance with previous studies that had shown a better performance for swine MHCs using the combined method than either method alone (Pandya et al. 2015; Pedersen et al. 2016). This was further confirmed by our own analyses in paper 1.

NetMHCpan was, together with PSCPL and PopCover, accessed and executed on the DTU-CBS (Technical University of Denmark, Center for Biological Sequence Analysis) server using UNIX scripts via secure shell client on my laptop computer.

2.1.4 Prediction using PSCPL

PSCPL is a prediction method that, in contrast to NetMHCpan, is based on binding data obtained from a rationally selected set of artificially generated peptide libraries. The method was first described in details by Stryhn et al. (1996) and has since been applied to porcine immunology by Pedersen et al. (2011), who analyzed the binding affinity of 9x20+1=181 peptide libraries. Each library represented a pool of 9-mer peptides where a specific position was occupied by a specific amino acid, while the remaining 8 positions contained random out of 19 amino acids (cystein excluded). As such, the first set of 20 libraries had a fixed amino acid at position one, the second set was fixed at position two, and so forth to the ninth set fixed at position nine (table 2). An additional library designated X_9 contained completely random peptides (cystein excluded) with no fixed position.

Position 1	Position 2	...	Position 9
AXXXXXXXX	XAXXXXXXX	...	XXXXXXXA
CXXXXXXXX	XCXXXXXXX	...	XXXXXXXC
...	...	...	...
YXXXXXXXX	XYXXXXXXX	...	XXXXXXXY

***Table 2**: Positional scanning combinatorial peptide libraries. A total of 9x20+1=181 libraries represent all possible 9-mer peptides, in addition to a single library of completely random 9-mer peptides (cystein excluded). Twenty libraries were synthesized to address each of the 20 naturally occurring amino acids in each of the 9 positions of an 9-mer peptide. The first column indicates the 20 libraries describing the first position, the second column indicates the 20 libraries describing the second position, etc. to the last column indicating the 20 libraries describing the ninth position. X = a mixture of 19 amino acids (cystein excluded). Underscored amino acids are indicated by their one-letter code. Table adapted from Stryhn et al., 1996.*

The authors subsequently measured the binding affinity of all 181 peptide libraries to SLA-1*0401 using peptide affinity enxyme-linked immunosorbent assay (ELISA) as described in section 2.3.1. Based on these measurements, a matrix was generated representing the relative binding factor (RB) of each individual amino acid (a) at each specific position (p), defined as $RB_{ap} = IC_{50}(X_9)/IC_{50}(library_{ap})$ normalized so that $\sum_{a=1}^{20} RB_{ap} = 20$, IC_{50} being the peptide concentration needed to obtain half-saturation of the SLA (table 3). RB values >2 were considered to represent a position where the given amino acid was in favor of binding (large and bold), while RB values <0.5 were considered to represent positions where the given amino acid was detrimental to binding (small and italic) (thresholds representing 95% confidence intervals). An anchor position (AnP) value was also calculated for each position as $AnP_p = \sum_{a=1}^{20}(RB_{ap} - 1)^2$. In the present example, AnP-values >15 identified anchor positions at p9, p3 and p2 in order of importance. Biologically, an anchor position is defined as a restrictive site in the peptide binding groove that rejects most and strongly favors only a few amino acids, thus constituting the basis for MHC-specificity. This is quite well reflected in the strongest anchor of SLA-1*0401, p9, that almost exclusively accepts large and bulky aromatic amino acids such as tyrosine (Y), tryptophane (W) and phenylalanine (F).

Once the laborious *in vitro* experiments have been performed and a PSCPL matrix has been established for a given MHC, the binding capacity of any given peptide can be calculated from this matrix by simply multiplying the RB values for the corresponding peptide. The product can then be converted to a percentile rank score by the use of a standard curve, thereby enabling comparison with other prediction servers such as NetMHCpan.

The theory behind the PSCPL method rests on the assumption that MHC-I specificity is the result of an array of largely independent subspecificities acting in a combinatorial mode. This assumption is probably not completely correct since it is known that peptide-MHC-I interaction result in conformational changes in the HC that would undoubtedly affect the pockets of the peptide binding groove (Bhati et al. 2014). Nevertheless, the method has shown to identify strong binders in cases where other prediction servers have failed.

SLA-1*0401	Amino acid position in peptide								
	1	2	3	4	5	6	7	8	9
A	1,7	0,8	1,6	1,1	0,8	*0,4*	1,7	0,7	*0,0*
C	0,8	*0,2*	*0,4*	**2,7**	1,1	1,0	0,7	1,7	*0,0*
D	*0,4*	0,7	**7,7**	**2,1**	0,8	*0,1*	0,5	1,8	*0,0*
E	1,6	*0,0*	**2,8**	0,6	1,0	1,4	0,9	0,9	*0,2*
F	*0,4*	*0,2*	0,8	*0,0*	1,0	1,1	1,1	1,1	**5,8**
G	0,5	*0,3*	*0,1*	1,5	1,1	1,4	*0,0*	1,0	*0,0*
H	0,5	*0,2*	*0,1*	*0,1*	1,3	**2,4**	0,5	0,7	*0,4*
I	0,7	**3,4**	*0,3*	0,8	0,8	0,9	0,7	0,9	*0,3*
K	1,1	*0,2*	*0,1*	*0,4*	*0,4*	1,2	*0,4*	0,9	*0,0*
L	0,6	**2,1**	*0,2*	0,6	1,0	1,7	1,0	1,2	0,6
M	1,7	1,9	1,0	1,2	1,4	1,4	1,2	1,4	0,7
N	1,4	0,5	0,6	1,4	1,9	0,7	1,0	1,9	*0,0*
P	*0,0*	*0,0*	*0,1*	1,6	0,5	1,1	1,9	1,2	1,1
Q	1,0	0,9	*0,2*	1,0	0,5	*0,4*	0,8	0,7	*0,0*
R	**2,3**	*0,0*	*0,1*	0,6	**2,4**	0,9	1,0	0,5	*0,2*
S	1,8	**2,4**	1,8	1,1	0,8	1,5	1,6	0,7	*0,0*
T	1,4	**2,5**	1,6	0,7	0,9	0,5	2,0	0,7	*0,0*
V	1,1	**3,7**	*0,3*	0,5	0,7	0,8	0,9	0,6	0,8
W	*0,3*	*0,0*	*0,2*	0,6	1,0	0,8	0,6	1,4	**5,6**
Y	0,6	*0,0*	*0,5*	1,3	0,6	*0,2*	1,6	*0,3*	**4,3**
Sum	20	20	20	20	20	20	20	20	20
AnP-value	7	28	57	8	4	6	5	4	67

***Table 3**: PSCPL matrix based on binding affinity data of SLA-1*0401 providing the relative binding factor (RB) of each natural amino acid corresponding to each position of a 9-mer peptide. Bold and enlarged numbers represent amino acids that in the indicated positions, lead to enhanced binding (RB > 2) while italized and small numbers represent amino acids that in the indicated position lead to reduced binding (RB < 0.5). Anchor position (AnP) values are represented on the bottom line, identifying p9, p3 and p2 as anchor position in order of importance. Table adapted from Pedersen et al., 2011.*

2.1.5 "The Program!" - Python-based program for PSCPL analysis

During the bioinformatics period of my PhD, I attended an introductory course for various bioinformatic tools and programming languages. To my own great surprise, I discovered that the hitherto black box of computer programming was actually quite exiting (and I even had a flair for it). I immediately started writing a program in Python-language that in the end was able to chop up a polypeptide of any given length into 9- and 10-mers, calculate their rank scores on basis of available PSCPL matrices, and identify relevant anchor positions. I was quite content with my work, my wife was quite jealous at my computer, and when I eventually presented "The Program!" to Morten Nielsen, my bioinformatics guru, he gave me a comforting smile and said that he had already developed a program capable of all that and much more. So I never used it for anything relevant other than having a great time learning how to code. And for this, it deserved a place in the appendix (appendix A, page 129).

2.1.6 PopCover - prioritizing the epitope candidates

The PopCover algorithm provides a rational epitope selection strategy that accounts for both pathogen variation and the diversity of the host MHC polymorphisms. The input parameters are the peptides of interest, together with information about which genomes encode the given peptides, and to what SLAs they can bind. PopCover then iteratively scores each peptide giving the highest score to the most conserved peptide with the broadest SLA allelic coverage. Subsequent peptides are scored similarly while also accounting for gabs left by previously prioritized peptides in relation to both genomic conservation and SLA coverage. Coefficients of impact can be applied to the included genomes and the relevant SLAs, if needed (Lundegaard et al. 2010).

In my case, the input was 6,140 top candidates with a combined percentile rank score ≤ 2 for at least one of the selected SLAs, as determined by the combined epitope predictions. Appendix B (page 134) shows the 53 peptides selected for subsequent *in vitro* binding assays based on the PopCover output illustrated with PopCover rank, assigned ID, peptide sequence, locus, SLA coverage and strain coverage. Peptide ID 14 (PopCover rank 14) was originally also ordered from GenScript, but could not be synthesized and was thus excluded from the list. Among peptides with PopCover ranks 1-50, four peptides were further excluded as they represented 9-mers nested within included 10-mers. Peptides with assigned ID 47-49 were included for more representatives of NSP2 and ORF6, and peptides with assigned ID 50-54 were included as previous studies had provided evidence of their immunogenicity. Note that SLA-2*0501 was included in the analysis to illustrate that the analysis was performed on the flawed notion that this was the correct allele.

The outcome of the PopCover analysis was the advent of 142 pSLA combinations to be verified in the lab. 30 for SLA-1*0401, 26 for SLA-1*0702, 36 for SLA-2*0401, 24 for SLA-2*0501 and 26 for SLA-3*0401.

2.2 Preparation and storage of the peptides

The 53 peptides were delivered from GenScript with purities ranging from 85.6% to 99.9% and masses ranging from 1.6 mg to 4.9 mg. Based on their molecular weights, they were dissolved to concentrations of 500 µM. Dissolution of

peptides were mostly done in MilliQ water although in some cases other solvents (N-metrhyl-2-pyrrolidone (NMP), dimethylsulphoxide (DMSO) and 3% NH_3) were added in small amounts as recommended by the manufacturer. Dissolved peptides were aliquoted in screw cap stock vials (830 µl) and working vials (40 µl), and were stored at -20 °C.

2.3 *In vitro* verification of selected epitopes

True binders among the predicted 142 pSLA combinations were verified by peptide affinity ELISA (section 2.3.1) and scintillation proximity assay (SPA) (section 2.3.2), measuring the affinity and stability, respectively, using recombinant biotinylated HCs of the five SLAs. It should be noted here, that no functional assay could be generated to test SLA-3*401 *in vitro*, why it was excluded from the project after *in vitro* verification had ended.

2.3.1 Peptide-SLA affinity determination by peptide affinity ELISA

The affinity of a pMHC interaction is indicative of how likely a binding is to occur and is represented by the equilibrium dissociation constant K_d = [peptide][MHC]/[pMHC]. This can be approximated by the peptide concentration needed to half-saturate a significantly lower concentration of MHC molecules. In my studies, this was measured using a modified sandwich ELISA (Sylvester-Hvid et al. 2002; Pedersen et al. 2011), employing the principle that the dissociation of β_2m from pMHC-I complexes provide an indirect measurement of peptide dissociation (Parker et al. 1992). Briefly, a series of samples containing incremental concentrations of the target peptide, a fixed concentration of the target denatured biotin conjugated HC, and a fixed excess of β_2m were set to obtain binding equilibrium before being transferred to a streptavidin coated ELISA plate. Subsequent removal of unbound peptide and β_2m allowed for quantitative analysis of bound complexes using anti-β_2m antibodies. The measured data points representing the concentrations of formed pMHC complexes as a function of peptide concentrations were fitted using a sigmoidal regression curve. From this, the K_d-value was read and normalized using a standard curve based on the prefolded biotinylated FLPSDYFPSV/HLA-A*0201 (Kast et al. 1994) (figure 8).

During my time in the lab, I conducted several of these plates. Many were for refining the protocol and adjusting the parameters but mostly for determining the binding affinities of the predicted pMHC combinations. Most of the time, reproducibility was obtained, but for some pSLA combinations a markedly strong affinity was observed once, after which no affinity at all could be measured. The protocol was quite strict and detailed, and especially the HCs and β_2m were intrinsically vulnerable and should not be exposed to freeze-thaw cycles and vortexing. Besides, several steps in the protocol required many logs of dilution, transferring between plates, and changing of pipet tips. Precautionary measures were of course taken such as aliquoting the sensible reagents and making sure that incubations were kept safe and untouched, but other things were out of my control, such as seasonal temperature changes affecting incubation temperatures, available pipets, and the fact that other personel were also using the reagents and equipment. In summary, many things could go wrong, and some mistakes were inevitable despite my effort to avoid them.

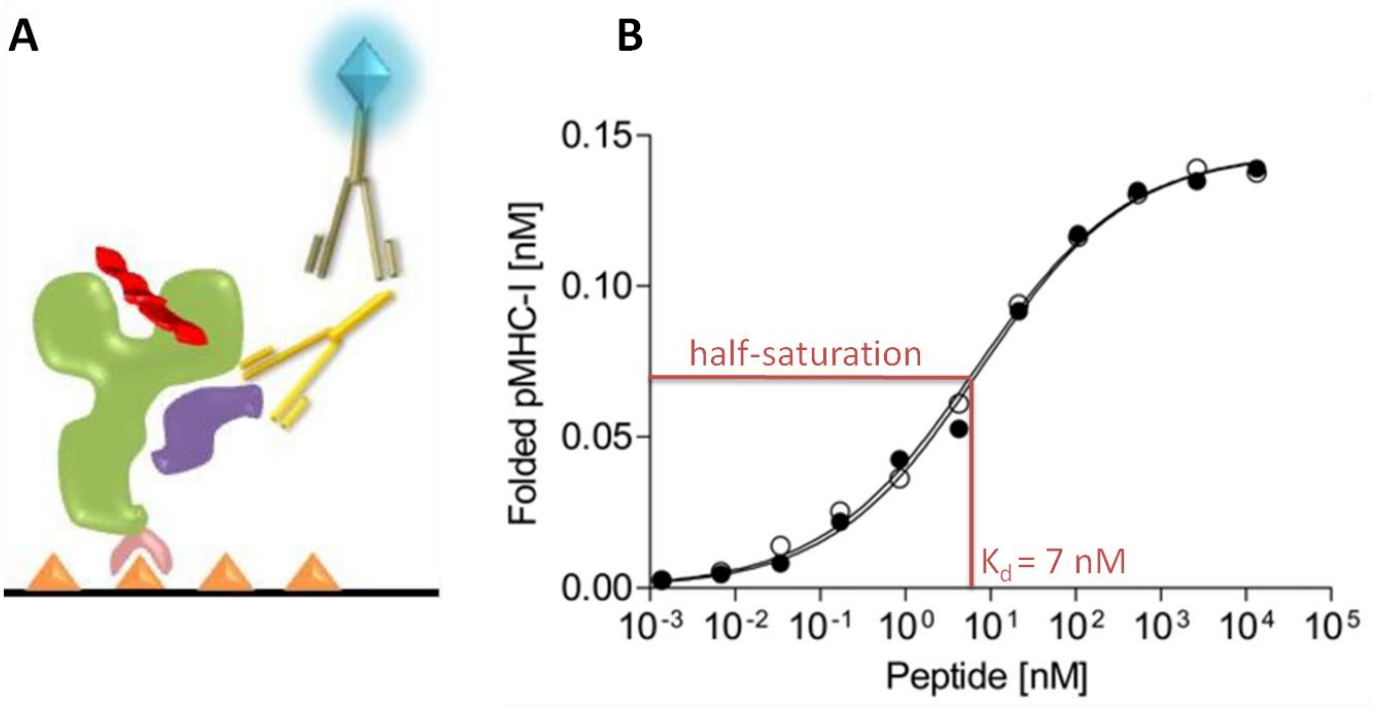

***Figure 8**: Peptide affinity ELISA. **A**: Setup: Heavy chain (green) in complex with peptide (red) and β$_2$m (purple) attached by biotin (pink) to streptavidin molecules (orange) in the well. Bound complexes are detected by a quantitative enzymatic color reaction (glowing blue) upon binding of primary anti-β$_2$m antibodies (yellow) and secondary enzyme conjugated antibodies (grey). Figure adapted from the PhD thesis by Lasse Eggers Pedersen, 2012. **B**: Sigmoidal curve fitting: Two peptides (white and black circle) exhibiting similar binding affinity with K_d=7. Figure adapted from Harndahl et al., 2012.*

2.3.2 Peptide-SLA stability determination by scintillation proximity assay

The stability of a pMHC interaction is indicative of how long a binding will persist once it has been established. This is represented by the binding half-life ($t_{½}$) that can be measured using SPA, which basically employs the same principle as in the affinity assay, namely that β$_2$m will dissociate from the complex when the peptide falls off. The assay design is simple, yet brilliant, and relies on the detection of light signals emitted by the scintillation plate upon absorption of Auger electrons emitted by ^{125}I-radiolabeled β$_2$m in close proximity. In practice, the target peptide and denatured biotin conjugated recombinant MHC HC is set to incubate in the streptavidin coated scintillation plate together with ^{125}I-radiolabeled β$_2$m. Upon steady-state, unlabeled β$_2$m is added and the dissociation rate is monitored by consecutive measurements resulting in a decay curve from which $t_{½}$ can be read (Harndahl et al. 2011) (figure 9).

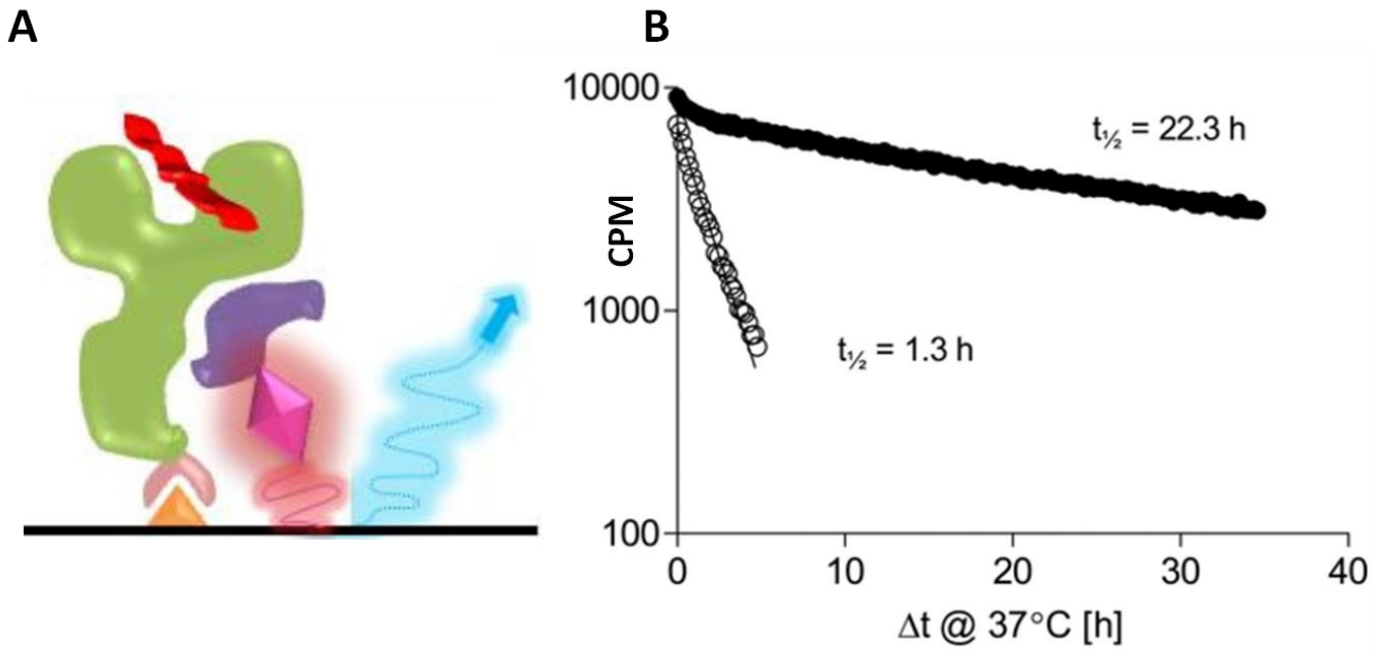

***Figure 9**: Scintillation proximity assay. **A**: Setup: Heavy chain (green) in complex with peptide (red) and ^{125}I-radiolabeled β_2m (purple) attached by biotin (pink) to streptavidin molecules (orange) in the well. Auger electrons (glowing pink) emitted by ^{125}I trigger the emission of light (glowing blue) from the scintillation plate. Figure adapted from the PhD thesis by Lasse Eggers Pedersen, 2012. **B**: Decay curve fitting: Two peptides (white and black circle) exhibiting different dissociation rates. CPM: counts per minute. Figure adapted from Harndahl et al., 2012.*

In relation to my studies, the SPA analysis was performed by Michael Rasmussen at the University of Copenhagen, the Laboratory of Experimental Immunology. I was politely advised not to show up, as my presence would be inexpedient as only trained personnel should prepare the plates and handle the machine. So I don't have any hands-on experience with this method. Instead I put my trust in that Michael did a great job.

2.4 SLA genotyping of pigs

Given that the final epitopes were predicted and verified as binders to a limited number of SLAs, it was of course relevant to know the SLA profiles of animals used in various experiments. Two methods were applied for this including a DNA based SLA genotyping (section 2.4.1) and a Next-generation sequencing (NGS) based SLA genotyping using messenger RNA (mRNA) (section 2.4.2).

2.4.1 DNA-based SLA genotyping

This method was originally adapted for swine MHC-I by Martens et al. (2003) and subsequently optimized to comprise a set of 47 sequence specific primer pairs based on the polymorphisms in exons 1, 2 and 3 of published SLA-I DNA sequences available at that time (Ho et al. 2006; Ho et al. 2009). All primer pairs (listed in Ho et al. 2009) were designed with similar melting and annealing temperatures enabling a simple polymerase chain reaction (PCR) setup, where all reactions could be executed simultaneously on genomic DNA from the target animal. This provided a low resolution SLA genotyping, of which the presence or absence of specific SLA groups could be confirmed by gel electrophoresis. High resolution typing could subsequently be performed by PCR using more specific primers (table 4), followed by amplicon sequencing and single nucleotide polymorphism (SNP) analysis comparing the obtained sequences with the sequences of known alleles.

Primer name	Direction	Sequence (5' - 3')	Product size (bp)
SLA-1*04 105-123	Forward	GCCTGACCGCGGGGACTCT	641
SLA-1*04 519-499	Reverse	CTCATCGGCCGCCTCCCACTT	
SLA-1*07 331-353	Forward	GCCGGGTCTCACACCATCCAGAT	220
SLA-1*07 550-528	Reverse	GGCCCTGCAGGTAGCTCCTCAAT	
SLA-2*04 294-314	Forward	CCGAGGGAACCTGCGCACAGC	316
SLA-2*04 383-362	Reverse	CCCACGTCGCAGCCGTACATGA	
SLA-2*05 295-318	Forward	CGAGTGAACCTGCGCACAGCTCTT	544
SLA-2*05 612-589	Reverse	CTGCAGCGTGTCCTTCCCCATCTC	
SLA-3*04 116-135	Forward	GGAAGCCCCGTTTCATCGAA	192
SLA-3*04 307-284	Reverse	GCAGGTTTTTCAGGTTCACTCGGA	

***Table 4**: Primers used for the generation of amplicons for high resolution SLA genotyping*.

2.4.2 Next-generation sequencing-based SLA genotyping

This method was recently developed in Gregers Jungersen's lab and in contrast to the previous method that can only provide information about the presence or absence of specific SLA-I genes, this method provides quantitative information on the expression of these genes by applying NGS of copy DNA (cDNA)-based amplicons. PCR was performed on cDNA reverse transcribed from SLA-I mRNA using barcoded primers specific for conserved regions in exon 2 and 3 of all known SLA-I genes. Sequences of the barcoded amplicons obtained by NGS were de-multiplexed, pair mate joined, quality checked and sorted into clusters showing the expression levels of each allele. The method is described by Ilsøe et al., (manuscript in preparation) and was applied by Overgaard et al. (2015), the latter of which I participated as co-author.

In relation to my own studies, this method was applied once, but did unfortunately not provide any useful data due to NGS difficulties (data not shown).

2.5 VRP design, generation and verification

In the following subsections I will describe some basic characteristics of the VRP used as a template for the vaccines (section 2.5.1). I created a program for the design of the inserted polyepitopes, which is described in section 2.5.2. Following this, I describe how the final VRPs were rescued and storaged (section 2.5.3). Finally, the resulting VRPs were verified using flow cytometry (section 2.5.4) and western blot (section 2.5.5) analyses.

2.5.1 The virus replicon particle

From the very beginning, it was intended for the verified epitopes to at some point be integrated in VRPs serving as platform for the final vaccine. This idea emanated from the collaboration between my supervisors and Nicolas Ruggli and Artur Summerfield from the Institute of Virology and Immunology (IVI) in Switzerland, who had previously shown promising results with VRPs based on the Classical Swine Fever Virus (CSFV) (Suter et al. 2011).
In the wild, CSFV is prone to infect cDC where they will prevent maturation and suppress type-I IFN by targeting the IRF-3 pathway by means of the structural protein, N^{pro} (Bauhofer et al. 2007), which is necessary for type-I IFN production (Bauhofer et al. 2005). Also pDCs are susceptible, which on the other hand give rise to strong type-I IFN responses due to their high levels of IRF-7, the master regulator of type-I IFN (Liu 2005; Honda et al. 2005), that is not targeted by CSFV (Carrasco et al. 2004; Bauhofer et al. 2005).
In the present study, the bicistronic plasmid, pA187-N^{pro}-IRES-C-delE^{rns}, was selected as an appropriate vaccine platform due to its tropism for DCs and to its previously demonstrated capacity to express transgenic proteins with measurable activities (Suter et al. 2011). The previously mentioned suppression of type-I IFN was abrogated by a single amino acid substitution in the C-terminal part of N^{pro}, thereby eliminating the zinc-binding domain responsible for the suppression.

2.5.2 "Juncitope" - Python-based program for neoepitope removal between epitopes in a polyepitope

In the process of concatenating adjoining epitopes to a polyepitope, artificial sequences spanning residues of neighboring epitopes will appear. By chance, some of these sequences may exhibit SLA binding capacities and are in such cases referred to as neoepitopes. Neoepitopes with strong SLA binding capacities have the potential to misdirect the immune response by overruling real epitopes competing to bind to the same SLA molecules, or by priming otherwise anergic self-recognizing T cells, thus triggering autoimmunity. In order to avoid this, I used my new-found programming skills to create a program named Juncitope with the purpose of minimizing the impact of emerging neoepitopes. This was done by alternately identifying the neoepitope with NetMHCpan version 2.8 and subsequently nullifying these by adding/deleting/replacing junctional spacer amino acids and/or by changing the succession of the true epitopes.

The program was designed to be flexible with regards to defining neoepitopes in terms of length and rank score, number and impact of relevant SLA alleles, and length and composition of the spacers used for nullification. In addition, it was designed to be compatible with other prediction tools available at the DTU-CBS servers. In the settings used for the generation of the polyepitopes relevant to this study, a neoepitope was defined as a peptide

with a predicted binding affinity to a given SLA leading to a rank score ≤ 1 for 8-mers, ≤ 4 for 9- and 10-mers, or ≤ 2 for 11-mers. Optimally, the algorithm should have been adjusted to account only for SLAs expressed by the animals ultimately receiving the vaccine, but since the herd from which the experimental animals would come was undecided when purchase of the polyepitopes was needed, the prevalent SLAs could not be determined. Hence, 19 SLA alleles were included in the analysis as these were estimated to represent a broad diversity of peptide specificities. These are seen in the output file associated with the generation of the VRP 1 polyepitope, together with other relevant parameters including input epitopes, initial and final neoepitope distribution, and the final polyepitope sequence (appendix C, page 135). The program code was written in Python and integrated with a downloaded version 2.8 of NetMHCpan running in Ubuntu on my laptop. The program code is seen in appendix D (page 140).

2.5.3 Rescue and storage of the VRPs

All cloning, amplification in XL-1 blue competent *E. Coli* and transfection of plasmid with subsequent rescue of VRPs from cells of the E^{rns} complemented cell line, SK6-E^{rns}, was performed in the lab of Nicolas Ruggli at IVI by Simea Werder, Marcus Gerber and Matthias Liniger. Occasionally, I was involved in this process, mostly offering a helping hand while learning the techniques. These are described in more detail in paper 2. The plasmid-transfected cells yielded the first batch (p0) of VRPs. These were used to infect SK6-E^{rns} cells for the rescue of the next batch, p1, which again were used for the rescue of the p2 batch that was ultimately used in the vaccines. The p1 and p2 batches were harvested by me. For p0 and p1, the cell lysates containing the VRPs were immediately aliquoted and stored at -80 °C. During the last day of my 2½ month stay at IVI, I harvested the p2 VRPs and sealed them in 50 ml falkon tubes for storage at -80 °C. Once back in Denmark, I had them sent by courier to the biosafety level 3 agriculture (BSL3-ag) facility at Lindholm, which was the only place they were allowed to be opened due to the risk of FMDV contamination from IVI. Here, they were thawed, aliquoted and stored at -80 °C until later use in the vaccines. Titration was performed on these aliquots as described in section 2.6.

2.5.4 Flow cytometry

The forerunner of today's flow cytometers, the cell sorter, was invented by Fulwyler (1965). Nowadays, the flow cytometry is a powerful and widely used technique for the rapid analysis and/or sorting of single cells in a heterogenous mixture by means of light-scattering and fluorescence measurements. It is composed of three main components: a fluidics, an optics and an electronics component (figure 10). The fluidics component is composed of a flow chamber that separates and aligns particles, such as cells, by injecting the cells into a flowing stream of sheath fluid that is stretched by gradual acceleration. The cells then enter the optics component in which they pass by a laser. Directly opposite to the laser is a photodiode detecting the decrease in light intensity as a cell passes by. This is referred to as forward scatter (FSC) and is proportional to the size of the cell. Other parts of the light will be scattered in large angles. This will be detected by the side scatter (SSC) photomultiplier tube (PMT) and is caused by the granularity and structural complexity inside the cell. Together, the characteristics of FSC and SSC can be used to identify cell types that differ in size and granularity. For more sophisticated differentiation of cell types, antibodies

conjugated with different fluorochromes and with specificities against various intracellular or surface antigens can be applied. Light from the laser(s) will then excite the fluorochromes that will result in the emission of light of defined wavelengths. By redirecting this light through a series of lenses, dichroic mirrors and filters, a dedicated array of PMTs can result in the detection of up to 14 parameters in a single sample. The electronics component enables the attribution of relevant parameters to the individual cells and facilitates analysis by a wide range of gating options and visualizations (Rowley 2012).

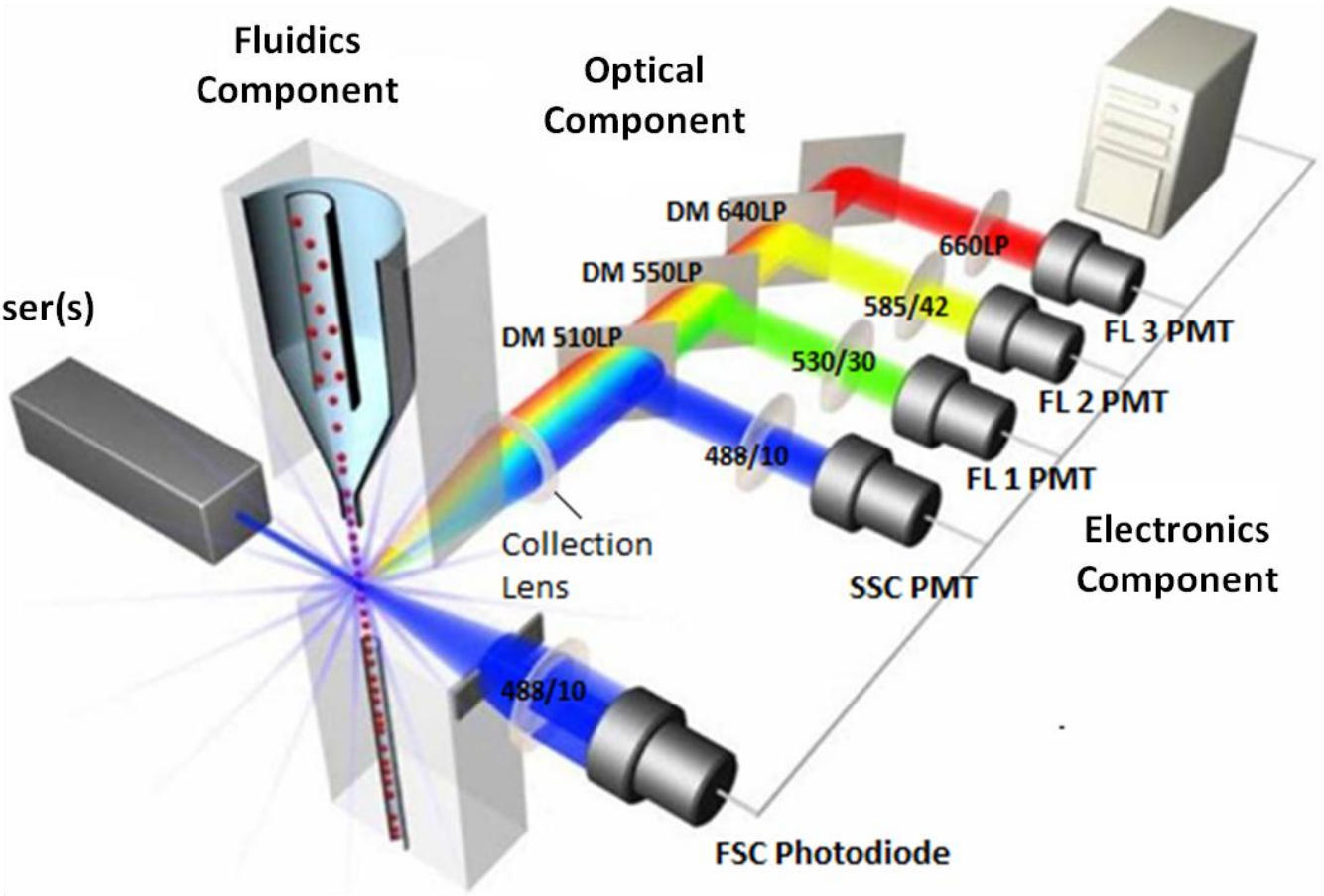

***Figure 10**: Schematic diagram of a flow cytometer, showing focusing of the fluid sheath, laser(s), optics, photomultiplier tubes (PMTs), and analysis workstation. Dichroic mirrors (DM) only reflect light of wavelengths lower than the specified long pass (LP) wavelength (i.e. DM 510LP reflects light of wavelengths below 510 while letting light of higher wavelengths pass). Filters (FL) only allows transmission of the wavelength specified before the dash and with a transmission band of the size specified after the dash (i.e. 530/30 allows transmission of light within the wavelengths 515-545 nm). PMT: photomultiplier tube. Figure adapted from Rowley, 2012, doi:10.13070/mm.en.2.125*.

In the current study, flow cytometry was used to verify infectivity and capacity of the rescued VRPs (p1 batch) to induce polyepitope expression in infected SK6 cells using intracellular antibodies against the CSFV E2 structural protein (infectivity) and against the FLAG tag expressed immediately downstream of the polyepitope site. Parallel samples treated with and without the proteasome inhibitor, epoximicin, were conducted in order to verify the targeted proteasomal degradation of the polyepitopes. The analysis was conducted at IVI with the help and guidance from Sylvie Python and Carmen-Alexandra Sautter.

2.5.5 Western blot

Western blot (WB) is a widely used analytical technique to detect specific proteins in a sample. The stepwise procedure is as follows:

1. Separation of sample proteins using gel electrophoresis.
2. Transfer of proteins from the gel and onto a membrane made of nitrocellulose or polyvinylidene difluoride (PVDF). Transfer was originally done by simple capillary action but is now mostly done by electroblotting in which an electric current pulls the proteins from the gel and onto the membrane.
3. Blocking of the membrane in order to avoid unspecific binding of antibodies. This is typically done with non-fat dry milk.
4. Incubation with antibodies specific for the protein of interest that will either directly or indirectly provide detection by colorimetry of fluorescence.

In this project, WB was applied twice for the detection of VRP-induced polyepitope expression. The first attempt was performed by Simea Werder at IVI after I had returned to Denmark. Briefly, 12 samples were prepared using 5E5 SK6-E^{rns} cells pr sample infected with VRPs at a multiplicity of infection (MOI) of 2. The ten generated VRPs from the p1 batch were used (VRP 0-9), in addition to two negative controls comprising mock infected cells and cells infected with the VRP rescued from the original plasmid, pA187-N^{pro}-IRES-C-delE^{rns}, being devoid of FLAG-tag and haemagglutinin (HA)-tag. Another setup was conducted in parallel, in which cells after 2 days of infection were treated with the proteasome inhibitors epoximicin (Sigma, E3652) and MG132 (Sigma, C2211) at final concentration of 100 nM and 500 nM, respectively. For both setups, infected cells were incubated for 3 days at 37 °C, 5% CO_2, after which lysates were extracted and subjected to gel electrophoresis. Subsequent transfer to a nitrocellulose membrane was verified by coomassie staining and bands were developed using primary antibodies specific for both FLAG-tag (Sigma, F3165) and HA-tag (Roche, 12CA5), and goat anti-mouse IRDye 800CW (Licor, 926-32210) as the secondary antibody. Bands were read using an Odyssey Scanner (Licor) at 800 nm.

The output of the above was discouraging since no bands were detected (data not shown). The absence of bands was believed to be due to low concentrations of the target protein. Hence, a second attempt was performed in which the lysates were extracted from cells infected with a recombinant vaccinia virus, vTF7-3 (Fuerst et al. 1986), and transfected with the original plasmids encoding the VRPs. This approach should boost T7 promoter based transcription of the plasmids by the T7 polymerase expressed by the vaccinia virus, which in turn should result in higher protein yields due to the increased amount of mRNA (Fuerst et al. 1986; Belsham et al. 2008). This was conducted by me in Graham Belshams lab at Lindholm. Briefly, 2 µg per plasmid were transfected using 3 µl FuGene6 (Promega, E2691) into baby hamster kidney (BHK) cells at 80-90% confluency previously infected with the vaccinia virus. Plasmids encoding for the 10 VRPs (VRP 0-9) were used for transfection in addition to two negative controls comprising the parental plasmid, pA187-N^{pro}-IRES-C-delE^{rns}, and a sample with only water. After four hours of incubation at 37 °C, 5% CO_2, 2 ml modified Eagles medium (MEM) was added to each well of the 6-well cell culture plates. Similar to the setup at IVI, an additional 12 samples were run in parallel in which 500 nM epoximicin

(ApexBio, A2606) was added together with the 2 ml of MEM. After an additional 24 hours of incubation at 37 °C, 5% CO_2, lysates were extracted from all 24 samples and subjected to WB. Briefly, protein bands separated by gel electrophoresis were transferred to PVDF membranes and developed using a primary antibody specific for FLAG-tag (ThermoFisher, MA1-91878), and horseradish peroxidase (HRP)-conjugated goat-anti mouse (DAKO) and a chemiluminescence detection kit (ECL Prime, Amersham) with a Chemi-Doc XRS system (Bio-Rad).

Also in this setup no bands were seen and WB was not pursued further.

2.6 Titration of VRPs and PRRSV

A standard method for virus quantification is the end point dilution assay for calculation of the 50% tissue culture infective dose ($TCID_{50}$). This is usually performed in microtiter plates with a monolayer of receptive cells coating the bottom of the wells. A serial 10-fold dilution of the target virus is made and a small volume (typically 50 µl) of each dilution step is used to infect multiple wells (4-8 wells/dilution step). The plate is then incubated for a period of time allowing a clear development of cytopathology for cytopathic viruses or until sufficient viral growth can be detected by immunohistochemistry. Next, the wells are scored for being either positive (infected) or negative (uninfected) and the scores are then used to tabulate a cumulative infectivity from which a percent infectivity can be calculated (table 5). From this, the 50% endpoint is calculated by the following formula as this gives the proportional distance between dilutions spanning the 50% endpoint:

$$\frac{(\%\ infectivity\ at\ dilution\ next\ \ above\ 50\%) - \ 50\%}{(\%\ infectivity\ at\ dilution\ next\ above\ 50\%) - (\%\ infectivity\ at\ dilution\ next\ below)} = \frac{78-50}{78-10} = 0.41$$

For data in table 5, this value is 0.41, which is then subtracted from the potency of the dilution next above 50% infectivity: $10^{-5-0.41}=10^{-5.41}$. This number represents the dilution of the original virus stock needed to give one $TCID_{50}$/50µl (test volume). Divided by 20, this is the dilution needed for one $TCID_{50}$/ml, and calculating the reciprocal of this yields the titer of the virus stock: 5 x 10^6 $TCID_{50}$/ml (Barthold et al. 2011).

Virus Dilution	Positives	Negatives	Cumulative Positives	Cumulative Negatives	Infectivity Ratio	Percent Infectivity
10^{-3}	8	0	23	0	23:23	100
10^{-4}	8	0	15	0	15:15	100
10^{-5}	6	2	7	2	7:9	78
10^{-6}	1	7	1	9	1:10	10
10^{-7}	0	8	0	17	0:17	0

***Table 5**: Table for calculating the endpoint dilution using a serial 10-fold dilution with 8 replicates per dilution step. Cumulative positive are calculated starting from the highest dilution. Cumulative negatives are calculated starting from the lowest dilution. Infectivity ratio is calculated for each dilution step taking the cumulative positives divided by the sum of cumulative positives and cumulative negatives. This ratio converted to percent yields the percent infectivity from which the 50% endpoint and ultimatively the virus titer can be calculated.*

The titer of the PRRSV-2 strain used for inoculum in paper 2 was determined by Lise Kirstine Kvisgaard in Lars E. Larsen's lab. The titers of the VRP batches, p0 and p1, were determined by Simea Werder in Nicolas Ruggli's lab at IVI using SK5-E^{rns} cells for optimal detection of endpoint dilution wells since cell-to-cell propagation of VRPs could only occur in this cell line. In contrast, the VRPs of the p2 batch had to be titrated in the BSL3-ag facility at Lindholm, since no traces of this batch had remained at IVI. This was regrettable as a stable setup for VRP titration was established at IVI, while in Denmark I neither had the experience, nor the SK5-E^{rns}. I attempted to titrate on PK-15 cells. After all, the exact titers were not that important, whereas the relative titers were important for adjusting the amounts of individual VRPs in the final vaccines. Titration on PK-15 cells went well. Infected cells were easily identified although it required some searching in the endpoint dilution wells. Also, the calculated titers were within the expected range having the titers of the parental p1 stocks in mind. Based on these titers, I decided on a final titer of 1E7 $TCID_{50}$/ml in the vaccines, as this was the lowest common denominator.

At the day of the third vaccination, I had planned to titrate on both the PRRSV-containing and the PRRSV-empty vaccines directly after preparation, and had prepared an extra of each vaccine type to titrate upon after they had been in the stables (details of the experimental setup is given in paper 2). My original plan was to titrate this time on SK6-E^{rns} cells that I had received from IVI for the purpose. However, the cells grew slower than anticipated, so I ended up titrating on PK-15 cells once again. For the sake of reproducibility, I also titrated on the individual VRPs. The obtained titers from these experiments were far from the initially determined titers, which obviously caused a lot of confusion as the samples were theoretically identical. Few days later, I had grown sufficient SK6-E^{rns} cells to titrate all VRPs upon, but again the outcomes were highly questionable. Colored cells were present in several samples, but only in wells infected with VRP 6 a pattern indicative of cell-to-cell propagation was observed. This caused me to speculate that maybe only this VRP was able to reproduce although I could not find a reason why. After all, the VRPs of the p1 stock had all worked fine. Alternatively, something in the titration setup caused the problem. Nevertheless, I had lots of other things to be concerned about, and decided that I would await the anti-E2 ELISA (section 2.7.1 and paper 2) to verify if VRP replication had occurred in the animals. This, it had with no marked differences in anti-E2 responses among animal. The measured titers of the VRPs are presented in table 6. I would have preferred to show some pictures of my attempts, but unfortunately the camera inside the BSL3-ag facility was broken and no one wanted to sacrifice theirs, so this could not be done.

	p0 (SK6-Erns)	**p1** (SK6-Erns)	**p2** (PK-15)	**p2*** (PK-15)	**p2**** (SK6-Erns)
VRP 0	7,94E+06	1,26E+07	1,00E+07	7,50E+06	2,37E+09
VRP 1	1,26E+06	1,26E+07	1,00E+08	2,37E+09	1,33E+07
VRP 2	3,16E+06	1,26E+07	1,59E+07	2,37E+09	1,33E+08
VRP 3	7,94E+05	1,26E+07	2,52E+07	2,37E+09	1,33E+08
VRP 4	7,94E+05	1,26E+07	1,59E+07	2,37E+08	7,50E+04
VRP 5	7,94E+05	2,00E+07	1,59E+07	7,50E+06	2,37E+05
VRP 6	2,00E+06	2,00E+07	1,00E+07	4,22E+09	4,22E+09
VRP 7	1,26E+06	3,16E+07	1,00E+07	4,22E+09	4,22E+09
VRP 8	7,94E+05	5,01E+07	2,52E+07	4,22E+09	4,22E+09
VRP 9	2,00E+07	5,01E+07	1,59E+08	4,22E+09	4,22E+09
PRRSV-positive vaccine before stables				4,22E+09	
PRRSV-positive vaccine after stables				4,22E+09	
PRRSV-negative vaccine (VRP 0) after stables				4,22E+09	

Table 6: *Calculated titers of VRPs throughout the experiment. Titers of p0 and p1 were determined by Simea Werder at IVI. Titers of p2 were determined by the author at Lindholm, DTU. Titers are given in $TCID_{50}$/ml. *Measurements performed at day of third vaccination. **Measurements performed 4 days after third vaccination.*

2.7 Diagnostic methods

Two diagnostic methods were applied during the studies. These are ELISA (section 2.7.1) and quantitative reverse transcription polymerase chain reaction (qRT-PCR) (section 2.7.2).

2.7.1 ELISA

ELISA is a central biochemical method for a quantitative or qualitative detection of an analyte in solution. The basic principle relies on the immobilization of the analyte to the well of an ELISA plate with subsequent detection using analyte-specific immunochromotography. The color intensity that is proportional to the amount of immobilized analyte can then be read using a spectrophotometer. This yields an optical density value that can be converted to analyte concentration by the use of a standard curve.

The ELISA principle embraces numerous types, variation and applications, and more details of this can be found in Crowther (2000). In the current thesis, different ELISA-based methods have been applied serving several purposes. These include the verification of pSLA affinity using peptide affinity ELISA (described in section 2.3.1); the verification of a PRRSV-negative herd from which the animals used in the VRP-challenge experiment came (this analysis was performed by others); the detection of E2 antibodies in pigs following VRP infection; and the detection of PRRSV antibodies in pigs following PRRSV challenge. The two latter are described in paper 2.

2.7.2 qRT-PCR

PCR provides a fundamental tool for anyone working with nucleic acids. By this simple and easily conducted method, specific sequences of DNA can be amplified as desired. The basic principle exploits the capacity of the polymerase complex to synthesize a complementary DNA sequence on the basis of a template sequence. As such, a pair of primers is used to target a specific site of the template for PCR amplification.

Quantitative reverse transcription PCR (qRT-PCR) is a modified version of PCR in which mRNA (in this case viral RNA) is reverse transcribed to cDNA, providing the template for subsequent quantitative PCR (qPCR). During qPCR, fluorescent DNA probes will become activated as PCR proceeds, thus gradually increasing the intensity. This can be detected in real time, and after a certain number of PCR cycles the fluorescence intensity will reach a given threshold (cycle threshold, ct). The number of PCR cycles needed for this to happen can be used to calculate the original amount a template RNA, thus quantifying the original copy number of virus particles.

2.8 ELISPOT

The principle of the ELISPOT assay relies on the general notion that specific cell types in a particular state will secrete specific molecules under specific stimulations. Briefly, the cells are incubated with the specific stimulation (typically the presence of an antigen) in the wells of an ELISPOT plate previously coated with capturing antibodies specific for the secreted molecules. In case of productive stimulation, secretion will occur that will be captured by the immobilized antibodies in the immediate vicinity of the secreting cells. Subsequent washing and addition of

detection antibodies capable of mediating a color reaction will form microscopic spots, each representing a secreting cell.

During the course of my PhD, I used the ELISPOT assay to detect peptide-specific IFN-γ secreting cells by restimulation PBMC from previously immunized animals with selected peptides verified as SLA binders. This was performed in PVDF-backed ELISPOT plates using secondary antibodies conjugated with either HRP or alkaline phosphatase (AP) for developing the spots with 3-amino-9-ethylcarbazole (AEC) or 5-bromo-4-chloro-3'-indolyphosphate p-toluidine / nitro-blue tetrazolium chloride (BCIP/NBT), respectively. The theoretical basis was that increased spot counts would reflect the presence and numbers of activated peptide-specific CTLs, thus proving that immunization had induced a CMI response, and that the verified epitopes were in fact immunogenic.

The ELISPOT assay was first described by Sedgwick and Holt (1983), who developed the assay for the detection of idiotype- and isotype-specific antibody-secreting cells. Since then, it has been widely applied in several fields of immunology for the quantification of a wide range of cell types secreting various molecules including antibodies and cytokines (Meier et al. 2005; Streeck et al. 2009; Saletti et al. 2013; Ewer et al. 2013). The broad versatility with respect to different types of cells, stimulations, and readouts has earned the method a high status. Especially the strong sensitivity with detection levels as low as one cell in 100,000/1,000,000 has been decisive, since antigen-specific T cells typically occur in low frequencies *in vivo* (Zhang et al. 2009).

However, despite the simplicity of the assay design, both assay execution and interpretation are not at all straight forward. About a decade ago, results from proficiency panels revealed drastic differences in reported results from panelists testing the same samples using their own protocols for IFN-γ ELISPOT (Cox et al. 2005; Britten et al. 2008; Janetzki et al. 2008). Subsequent rounds of extensive analysis, evaluations and retesting revealed multiple critical protocol parameters impacting the assay outcome, including medium/serum combinations used, resting status of cells, assessment of viable cells, training status of executive person, and most profoundly the evaluation of plates. These findings were summarized and recommended to the field as ELISPOT harmonization guidelines (Janetzki et al. 2008), after which marked improvements in ELISPOT performance, comparability and reproducibility were observed (Janetzki and Britten 2012). Recently, a protocol for ELISPOT plate evaluation was presented implementing recommendations obtained from an international ELISPOT plate reading panel comprising >100 scientists from various immunological backgrounds (Janetzki et al. 2015). Here, the non-parametric distribution free resampling (DFR(eq)) method is recommended and was thus applied to my analyses (Moodie et al. 2006). In addition to this, I also applied a method referred to as ratio-2, in which positive calls were identified as being twice the magnitude of the pig-specific background.

3 EXPERIMENTAL DESIGNS

In this section, I will give a brief overall description of the courses of experiments conducted during my studies, including challenges and reflections along the way. The first study described, is the VRP vaccine-challenge animal experiment (section 3.1), while the second is a preliminary infection study conducted in order to calibrate the ELISPOT setup prior to being applied in the vaccine-challenge study (section 3.2).

3.1 The VRP vaccine-challenge animal experiment

The VRP vaccine-challenge animal experiment was the conclusive test of everything that I had been working on during the whole period of my PhD. Preceding this, 53 conserved PRRSV-2 epitopes had been predicted and tested *in vitro* for their binding capacities to selected SLA-I alleles (described in paper 1), and 33 epitopes had been implemented as polyepitopes in VRPs, designed to induce a CMI in pigs of matching SLA-profiles. VRP infectivity and polyepitope expression in infected cells had been verified in cell culture (this, and the final version of the animal experiment is described in paper 2). From this point on, the experimental plan was to vaccinate pigs of matching SLA-profiles with the VRPs and subsequently challenge these with a wild type PRRSV-2 strain. Pre challenge, the CMI induced by the vaccines should be monitored with IFN-γ ELISPOT screening for immunogenic peptides. Positive immunogens should be characterized further using tetramer-stained flow cytometry for identifying peptide specific T cell subsets. Plans for executing cytotoxicity assays for verifying peptide-specific CTL activity was also in the pipeline. Post challenge, the potential protective functions of the found CTLs should be investigated using the above immunological assays as well as qRT-PCR for the monitoring of viral load in serum. Upon euthanasia, viral loads in lungs should be characterized with qRT-PCR and peptide-specific cells in the lymph node draining the site of vaccination should be identified with ELISPOT.

Originally, the plan was to conduct the animal trial at IVI, where the VRPs had been generated. IVI provided optimal conditions for this with every needed assay and equipments available and several clever people to provide a helping hand and to discuss scientific matters with *ad hoc*. Then, SLA-typing of the Swiss pigs showed that none of the relevant alleles were present. We considered the possibilities of importing pigs from Danish herds where the relevant SLAs were predominant, but the idea was rejected. Besides, my wife had announced that she was pregnant with delivery of our second son in March 2016, so the whole plan had to be reevaluated. At this point it was clear, that the animal trial could no longer be performed at IVI, and my stay was scheduled to only last for 2½ months. Instead I started seeking opportunities for conducting the experiment in Denmark. Due to the fact that the VRPs were based on Classical Swine Fever Virus (CSFV) and had been generated in a BSL3-ag facility where live Foot and Mouth Disease virus (FMDV) was handled routinely, the only possible place was in the BSL3-ag facility at Lindholm. Thus, after several months of heavy planning and negotiation with the Danish Veterinary and Food Administration, the Danish Working Environment Authorities, and the Coordination Committee for Animal Experiments at DTU, I was permitted to conduct the experiment at Lindholm in the period from primo April to medio July 2016.

These were of course fantastic news to me, but resulted nonetheless in several challenges based on three main aspects: First of all, Lindholm was sparsely populated and especially within the BSL3-ag facility only one person, Jani Christiansen, had her daily routine. Jani helped me a lot with various equipments and practicalities and without her help I would have been lost. At days of PBMC purification and ELISPOT setup, I was favored with the help from the lab technician, Katrine Fog Thomsen, who often helped me till the late hours. Secondly, due to the sparsely utilized state of the facility only reagents and equipment relevant to a few tasks were available, mainly related to the surveillance of FMDV. Thirdly, the facility was located two hours of transport from my front door.

Combined, these aspects meant that I did a lot of careful planning. Partly, in order to be as efficient as possible when I was there, and partly in order to not forget important materials relevant to my experiments. This however happened anyway at a single occasion with the result that the first purification of PBMCs the day before first vaccination went awry due to heavy contamination of erythrocytes afflicting the ELISPOT readouts and leaving no cells for backup cryopreservation. Furthermore, equipment central to my analyses, such as a flow cytometer and an ELISPOT reader, were not available inside the facility, so I had to figure out how to circumvent these challenges.

Flow cytometry (FCM) was planned to be applied for the identification of peptide-specific CTLs using relevant cell surface antibodies and tetramers on PBMCs isolated from the vaccinated animals. Thus, live cells should be exported from the facility, which for obvious reasons posed a risk of releasing FMDV to the environment. This represented the first problem with respect to FCM but was however solved with the following work-around: Inside the BSL3-ag facility, PBMCs stained with antibodies were spun down and resuspended in 4% parafomaldehyde in water in sealed vials. The vials were fully submerged in 1% VirkonS for 20 minutes in an airlock used for showering out people. Meanwhile, I showered out, transferred the vials to a sealed box and brought this with me to the BSL2 lab where a flow cytometer was available. This led to the second problem imposed by the fact that the flow cytometer was not maintained and had not had service for more than two years. As a consequence, the fluidics system was silted up with dried out solvents and the support for the sample injection tube crunched when moved. Furthermore, only two of the lasers were functional thus limiting the assortment of usable fluorochromes. I spent a lot of time trying to get it up and running, strongly compromised by my own limited experience with regards to FCM troubleshooting and by the absence of available experts. Also, service was not an option due to budget restrictions. Nevertheless, I managed to do a few successful pilot trials although the computer crashed at occasions forcing me to abandon the full scope of my trials in order to catch the last ferry away from the island. In any case, I never applied FCM on real samples, which was mostly due to the lack of positive results from my pre-challenge ELISPOT analyses.

The challenge imposed by the absence of an ELISPOT reader was also a profound source of frustration. As will be described in more details below, ELISPOT interpretation relies on the counting of microscopic spot on the bottom of a membrane-backed microtiter plate. Counting these spots using a microscope inside the BSL3-ag facility would be highly disadvantageous because of the unavoidable introduction of man-made counting bias, and because of the multitude of ELISPOT plates generated during the experiment that in itself would take weeks behind a microscope to count. Consequently, a work-around was made: After the development of spot by immunochromotography, the

plates were directly and fully submerged in 1% VirkonS for 30 minutes before being exported from the facility. On the outside, the plates were washed and dried in the dark until being read on an ELISPOT reader at DTU, Frederiksberg. Although this protocol was relatively easily applied, the quality of the wells and spots were compromised in terms of raised and uneven levels of background and contamination with debris from the VirkonS. As a consequence, all wells had to be carefully curated post reading, thus introducing a bias anyhow.

In the end, the experiment was executed as planned, although without conducting flow cytometric analyses and cytotoxicity assays.

3.2 *Ex vivo* analysis of pigs vaccinated with Ingelvac PRRS Vet (unpublished)

In an attempt to screen for dominant epitopes and at the same time and to test the effects of various ways of treating the PBMCs prior to ELISPOT analysis, such expansion with IL-2 and treatment with IL-18, six contingency pigs were vaccinated with Ingelvac PRRS Vet and PBMCs were harvested and cryopreserved at post vaccination day (dpv) -1, 7, 14, 21, 28, 35 and 42. The experiment is described in more details in appendix E (page 153), including materials and methods, results and discussion.

As discussed in appendix E, more analyses should have been performed in order to verify the presence of immunodominant epitopes. Unfortunately, I ran out of time and had to move on with more urgent matters, and eventually a student forgot to lock the rack containing my PBMCs leading them to fall out of the box and into the liquid nitrogen where the labels fell off. However, even though the experiment was not confirmatory with respect to the presence of immunodominant epitopes, it was not rejecting it either. The observation that no strong signal would appear without a combination of expansion and IL-18 treatment prior to analysis was of course a little unsettling, as this would not be practically applicable in the large setup of the vaccination-challenge experiment. I appeased myself with the assumption that vaccinating with VRPs would induce a stronger priming of CD8β T cells by virtue of the VRP characteristics including self-adjuvanting properties, the designed introduction of the polyepitopes into the MHC-I association pathway, and the lack of immunoevasive mechanisms.

In addition to the described setup, several other setups using the frozen PBMCs were designed and executed to optimize the signal-to-noise ratio (SEB- vs non-stimulated cells) with respect to various parameters including different way of resting thawed cells, media, and antibody concentrations (data not shown). Based on these experiments, I concluded that resting did not significantly change the outcomes to the better, that AIM-V and RPMI-1640\10%FBS gave the same results and were both superior to Dulbecco's modified eagle medium, and that the antibody concentrations should be as described in paper 2.

4 GENERAL DISCUSSION AND PERSPECTIVES

In the following, I will discuss the results obtained from my studies and set them into perspective with regards to available literature. It should be noted that none of the papers have currently been accepted, why it is likely that some parts may be changed later on. Additionally, parts of the following discussion may be written into the papers. The discussion is divided in three sections. In section 4.1, I discuss the results obtained from my studies; in section 4.2, I evaluate the general approach and suggest how this could be improved; in section 4.3, I provide a summary and conclusion of the general discussion.

4.1 Discussion of the obtained results

The general objective of this thesis was to develop a vaccine capable of inducing a CMI against PRRSV-2. The applied platform was an ensemble of CSFV-based VRPs modified to encode for a series of PRRSV-2 derived conserved epitopes with verified binding to selected SLA-I alleles. The working hypothesis was that DCs of vaccinated SLA-matched pigs would be manipulated into presenting the VRP-encoded epitopes, hence priming cognate CD8β T cells for subsequent effector and memory functions upon challenge with a wild-type strain encoding for the same epitopes (an overview is illustrated in figure 1, page 12). The identification and *in vitro* verification of the epitopes used in the final VRP-vaccine are described in paper 1. The design, generation and verification of the VRPs and the following vaccine-challenge animal experiment are described in paper 2. The progression steps of the epitopes from the point where they are incorporated into the VRPs and on, are summarized in table 7 together with the tests applied at the individual steps and their outcomes.

Step	Description	Applied test	Outcome
1	**33 epitopes cloned into plasmids**	Sequencing of midipreps	Positive
2	**Expression of polyepitopes in VRP-infected cells**	Flow cytometry Western blot	Positive Negative
3	**Presentation of epitopes on the surface of VRP-infected cells**	Not tested	
4	**Replication of VRPs in vaccinated animals**	Seroconversion for E2	Positive
5	**Epitopes from VRPs recognized by PBMCs**	Pre-challenge ELISPOT	Test failed
6	**Epitopes from VRPs/PRRSV recognized by PBMCs**	Post-challenge ELISPOT	Positive
7	**Epitopes capable of inducing protection**	qRT-PCR of serum qRT-PCR of lung	Negative Positive

***Table 7**: The progression steps of the epitopes from the point where they are incorporated into the VRPs and until the point where a protective effect of these are identified.*

In light of the general objective, the outcome was not as successful as I had hoped, but included nonetheless evidence of a peptide-specific CMI and of lowered virus loads in lungs of PRRSV-VRP vaccinated compared to control-VRP vaccinated pigs. In the following, I will discuss the different aspects that could be contributing to this outcome. This includes a discussion of the suitability of the selected epitopes (section 4.1.1); of different conditions related to CD8β T cell priming that might have been suboptimal (section 4.1.2); and of the effects of an established CTL response against a natural infection (section 4.1.3).

4.1.1 Suitability of the selected epitopes

The selection of epitopes was based partly on their degree of conservation across PRRSV-2 strains, and partly on their predicted binding capacities to the selected SLAs. Subsequent *in vitro* determination of their binding affinity and stability measures were supposed to provide the basis for their inclusion in the VRPs. Accordingly, peptides for inclusion should have either a $t_{½} \geq 0.5$ decimal hours (30 minutes) or a $K_d \leq 500$ nM. At the time of inclusion, however, these analyses had only been partially completed, why the inclusion of some peptides cannot be fully justified on basis of these measurements (table 8). Also, the applied thresholds were rather tolerant compared to other studies. Thus, Harndahl et al. (2012) suggested a minimum stability threshold for immunogenic epitopes of $t_{½} \geq$ 1 hour. This was based on the measured binding stability of known immunogenic and nonimmunogenic epitopes for which $t_{½} = 1$ was the lowest common denominator of the immunogenic epitopes. Applying this threshold to the peptides included in the VPRs, the SLA-1*0401 and SLA-1*0702 VRPs would contain 4 compliant peptides each and the SLA-2*0401 VRPs would contain 6 peptides (table 8). In the study performed by Assarsson et al. (2007), the authors set their threshold for inclusion at $K_d \leq 100$ nM to the analysis of immunodominant epitopes recognized in mice transfected with the human MHC-I, HLA-A*0401, and infected with Vaccinia virus. In addition, the authors observed that 56% of such high affinity binders were capable of inducing a T-cell response upon peptide immunization (table 1, page 27). For the peptides included in the PRRSV VRPs, a threshold at $K_d \leq 100$ nM would reduce the numbers of peptides to 6 for SLA-1*0401, 18 for SLA-1*0702 and 6 for SLA-2*0401 (table 8). Assuming that immunization with VRPs would be equally effective as immunizing with peptides in inducing T-cell responses, 3.4, 10 and 3.4 (56% of 6, 18 and 6, respectively) of the VRP-encoded peptides should be expected to induce T-cell responses specific for the three SLAs, respectively. Regarding the animals used in the present vaccine-challenge experiment, each pig expressed either the SLA-1*0702 or the SLA-2*0401 allele in addition to the SLA-1*0401 that was expressed by all pigs. As such, the VRP-vaccinated SLA-1*0702 pigs would be expected to present an average of 13.4 VRP-encoded peptides (3.4 + 10), while this number would be 6.8 for the SLA-2*0401 pigs (3.4 + 3.4). Regardless, this forecast was quite poorly reflected in the ELISPOT analysis of PBMCs isolated from VRP vaccinated animals at 7 and 20 days post PRRSV challenge (dpc). Here, 14 peptides were used for restimulation of which 2 complied with either the Harndahl or the Assarsson thresholds, while the remaining 12 complied with both. The group of pigs from the test group with an SLA-1*0702 profile exhibited the broadest diversity of peptide responses, especially when positive responses were defined by the ratio-2 method. Even then, this group exhibited an average number of distinct responding peptides per pig of 2.7, which was five-fold less than the expected 13.4 (figure 11).

ID	Sequence	Locus	SLA-1*0401		SLA-1*0702		SLA-2*0401		In compliance with thresholds			Post-challenge ELISPOT
			stab. (h)	aff. (nM)	stab. (h)	aff. (nM)	stab. (h)	aff. (nM)	t½ ≥ 0.5 or Kd ≤ 500 nM*	t½ ≥ 1**	Kd ≤ 100 nM***	
2	YAQHMVLSY	nsp9	-	-	● 0.9	4	● 1.1	60	Yes	Partly	Yes	√
4	YSFPGPPFF	nsp9	0.2	37†	● 0.2	18,708	-	-	No	No	No	
5	RALPFTLSNY	ORF2a			● 0.3	12	0.1	-	Yes	No	Yes	
7	QVYERGCRWY	nsp1a	● 0.3	682	● 4.5	168	● 0.7	209†	Partly	Partly	No	√
9	IVYSDDLVLY	nsp9	-	-	● 0.5	13	-	-	Yes	No	Yes	
10	KVAHNLGFYF	nsp11	● 0.3	122	● 0.3	99			Yes	No	Partly	
11	TRARHAIFVY	nsp10			● 0.3	60	0.2	-	Yes	No	Yes	
12	LSFSYTAQF	ORF3					● 1.3	73	Yes	Yes	Yes	√
13	FTWYQLASY	nsp12	0.1	92†	● 0.2	62	● 9.1	2	Yes	Partly	Yes	√
17	RTAIGTPVY	ORF4	● 0.5	57	● 0.2	1,852	● -	385†	Partly	No	Partly	
18	YTAQFHPEIF	ORF3	-	-	● 0.2	24,378	● 0.4	-	No	No	No	
19	LSDSGRISY	ORF7	● 1.1	10	● 0.2	383	0.2	4,182†	Yes	Partly	Partly	√
21	KVAHNLGFY	nsp11	● 1.5	4	● 2.8	11	-	-	Yes	Yes	Yes	√
22	KIFRFGSHKW	nsp1b	● 0.2	98			0.1	9†	Yes	No	Yes	
23	NISAVFQTYY	ORF3	● 0.1	413	● 0.9	6	● -	862	Partly	No	Partly	√
24	RTAPNEIAF	nsp2	● 2.1	4			0.1	-	Yes	Yes	Yes	√
25	ASDWFAPRY	ORF2a	● 4.9	2	● 0.2	71	-	-	Yes	Partly	Yes	√
27	RPFFSSWLV	ORF3			● 37.4	1			Yes	Yes	Yes	√
28	FVLSWLTPW	nsp5	-	-	● 0.2	1,372	● 13.7	3	Partly	Partly	Partly	√
29	MVNTTRVTY	nsp10	0.1	206†	● 0.2	47	-	-	Yes	No	Yes	
30	CVFFLLWRM	nsp5			● 0.2	283			Yes	No	No	
33	ITANVTDENY	ORF4	0.1	-	● 0.3	69	-	-	Yes	No	Yes	
34	SSEGHLTSVY	ORF3	-	-	● 0.2	12,701†	0.1	1,692†	No	No	No	
36	LTAALNRNRW	nsp5	-	-			● 3.6	40	Yes	Yes	Yes	√
38	LSASSQTEY	nsp2	0.1	91†	● 0.2	479	0.2	-	Yes	No	No	
39	VRWFAANLLY	nsp9			● 2.7	44			Yes	Yes	Yes	√
43	TTMPSGFELY	nsp9	● -	576	● 0.8	6	0.2	1,838†	Partly	No	Partly	
44	MSWRYSCTRY	ORF5	-	-	● 0.5	87	● 1.5	15	Yes	Partly	Yes	√
46	ALATAPDGTY	nsp3	-	607†	● 0.1	2,736			No	No	No	
48	WGVYSAIETW	ORF6					● 0.2	21,433	No	No	No	
49	FLNCAFTFGY	ORF6	-	-	● 0.3	20	● 0.3	2,069	Partly	No	Partly	
50	NSFLDEAAY	nsp10			● 0.1	43	-	-	Yes	No	Yes	
53	MPNYHWWVEH	nsp9			● 0.6	32			Yes	No	Yes	
# Included in VRPs			10		28		12					
# t½ ≥ 0.5 or Kd ≤ 500 nM*			8		22		8					
# t½ ≥ 1**			4		4		6					
# Kd ≤ 100 nM***			6		18		6					

***Table 8**: Overview of the 33 PRRSV epitopes included in the respective VRPs used for vaccination. The top left side section provides the basic peptide characteristics: ID, sequence and locus. Note that the peptide 21 is nested within the peptide 10. The top left-middle section presents the determined binding data for the three SLAs. Left-side columns represent measured binding stability (average dissociation half-life (t½) in decimal hour (h)), right-side columns represent measured binding affinity (average equilibrium dissociation constant (Kd in nM)). The top right-middle side section illustrates whether the included pSLA combinations are in compliance with the inclusion thresholds set my *me; by **Harndahl et al. (2012); and by ***Assarsson et al. (2007). The booleans used in this section (Yes, No and Partly) only apply to the pSLA combinations included in the respective VRPs (●). The right section indicates which epitopes were included in the post-challenge ELISPOT. The bottom section sums the numbers of peptides included in the individual VRPs, as well as the number of included peptides complying with the three different thresholds. †: only one successful affinity measurement could be obtained. Hyphen (-): no successful measurements could be obtained (stability or affinity). Empty field: Not tested.*

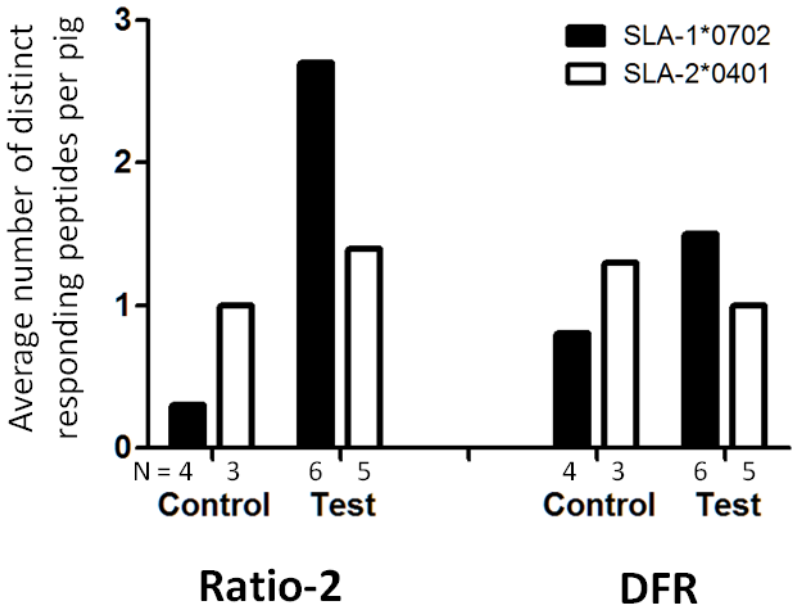

Figure 11*: Response diversity according to SLA profile. Columns represent the average number of distinct responding peptides per pig of a given group and SLA profile. This is based on the pooled response diversity extracted from the IFN-γ ELISPOT analysis of PBMCs isolated at 7 and 20 days after challenge (paper 2). Responding peptides are define by either the ratio-2 or DFR method.*

Despite this, the ELISPOT observations did provide evidence of a few epitopes induced by the VRPs that could be recalled upon peptide restimulation. Firstly, in agreement with the calculations above the SLA-1*0702 pigs of the test group exhibited a broader diversity of peptide responses compare to the SLA-2*0401 test pigs; secondly, the VRP-immunized pigs of the test group were in general more responsive than pigs of the control group; and thirdly was is observed that peptide responses at dpc 7 were as frequent as at dpc 20, despite the fact that PRRSV-specific CTLs are usually not detected within the first 4 weeks after challenge (Bautista and Molitor 1997; López Fuertes et al. 1999; Feng et al. 2002; Xiao et al. 2004). In further support of a VRP-induced CMI was the observation that Toby responded to peptide 44 (MSWRY**S**CTRY), being different from the homologous sequence encoded by the PRRSV challenge strain (MSWRY**A**CTRY). It is unlikely that the peptide-specific response was induced by the challenge strains, since in that case the A6S polymorphism would introduce a hydroxylic group of Serine in the TCR-binding middle part of the peptide. This substitution would supposedly be detrimental to the binding of a TCR induced by the flat and aliphatic Alanin-containing challenge version, thus indicating that the response originated from the VRP encoded peptide. Furthermore, the response was observed already at dpc 7, and was hence unlikely to be induced by the challenge. For Tyra, a difference between recall peptide and challenge homologue was also detected in the form of a V7I polymorphism with respect to peptide 24 at dpc 20 (challenge: RTAPNE**V**AF; peptide 24: RTAPNE**I**AF). Since both polymorphic residues are aliphatic and of similar size, a challenge-induced CTL could also be expected to recognize peptide 24 and convincing arguments for a VRP-induced response can thus not be given in this case.

In conclusion, the VRPs partly fulfilled their purpose of inducing a CMI via encoded PRRSV-2 polyepitopes. According to the ratio-2 method, responses towards all 14 peptides included in the post-challenge ELISPOT were observed. As

such, these peptides can be assumed to be cryptic epitopes as a minimum and in this regard, the selection of these epitopes was appropriate. Additionally, it can be seen that these epitopes are widely spread across the whole genome, which is in accordance with similar observations of the PRRSV-1 genome (Mokhtar et al. 2014). This justifies that I did not favor specific ORFs for the initial selection of epitopes although differences in their degree of expression have been estimated as a result of the RFSs (Kappes and Faaberg 2015). On that note, I will proceed to the next section for the discussion of the conditions related to CD8β T cell priming, as I believe this to be responsible for the five-fold reduction of the expected response diversity.

4.1.2 Compromised CD8β T cell priming

Several processes are involved in the VRP-induced priming of CD8β T cells for their differentiation into effector CTLs. The translation, processing and loading of epitopes to SLAs within infected DCs are evident prerequisites (section 1.2.2), but also the activation of infected DCs leading to their migration to lymph nodes where priming takes place is important (section 1.2.3). By virtue of the VRP's natural tropism for DCs in addition to the conclusions of the previous section, it must be assumed that the VRPs are capable of both infecting DC and expressing the polyepitopes. In support of this, the intradermal route of administration used in the present study has previously been shown superior to intranasal administration with regards to the induction of both humoral and cell mediated responses (Frey et al. 2006). Supposedly, the problem of a low response is more of a quantitative nature than of a qualitative one, why focus should be on 1) the number of APCs during priming (section 4.1.2.1) and 2) the abundance of expressed and presented epitopes (section 4.1.2.2). The effects of the two are not easily separated with the obtained data but I will try anyway to elaborate them individually in the following subsections.

4.1.2.1 Density of APCs

Initially, the difficulties with the determination of VRP titers led to speculations that the injected VRPs had been inert. The observations of a slight increases in rectal temperatures following second and third vaccination and the observed seroconversion against the VRP-specific E2 protein before the third vaccination, indeed confirmed the induction of an inflammatory response and that the VRPs had replicated within cells, both of which are prerequisites for T cell priming. It can therefore be assumed that at least some on the infected cells were DCs that subsequently migrated to the SLOs. On this note it should be mentioned that three pigs contained PRRSV-specific IFN-γ secreting cells in the lymph node draining the area of vaccination. Since all three were test pigs, it is tempting to interpret this as an effect of vaccination, although it remains unclear whether these cells have remained in the lymph node since vaccination or were randomly passing through at time of excision.

However, the data obtained from the flow cytometry analysis of SK-6 cells infected with VRPs (figure 3 in paper 2, page 110; and supplementary data 2, page 128), indicated that only a fraction of the successfully infected cells expressed the polyepitopes. Accounting for the titer adjustments of the individual VRPs administered in the final vaccine, only about 10% of cells successfully infected by the vaccine could be expected to express the polyepitopes. The remaining 90% would still contribute to temperature rise and seroconversion, however, and would also give rise

to DC migration to the SLOs where they would dilute the density of PRRSV-presenting APCs. This provides a reasonable explanation for the low diversity of responsive peptides per pig as described in the section 4.1.1..

4.1.2.2 Density of presented epitopes

The abundance of translated polyepitope within the cytosol of a VRP-infected cell must be presumed to be proportional to the density of individually presented epitopes on the surface. In turn, this density has shown to be proportional to the probability of T cell recognition and the duration needed for T cell priming (section 1.2.3). In the light of this, the results obtained from the flow cytometry analysis of SK-6 cells infected with VRPs were reassuring. Not only did VRP-infected cells express the FLAG tag downstream of the polyepitope, but this was also detected only in the presence of proteasome inhibitor, indicating that the polyepitopes were degraded as planned. However, the distinction between FLAG-positive and FLAG-negative populations was blurred and was only detected as a common density reaching across the threshold set for FLAG-detection (figure 3 in paper 2, page 110; and supplementary data 2, page 128). How to interpret this in terms of expressed amounts is difficult as it can either represent varying levels of expression or residual proteasomal activity. Besides, no positive FLAG reference with known level of expression was included.

The subsequent absence of bands in the two attempted western blots was further unsettling as this confirmed the suspicion of very low expression levels. Due to time restraints, however, and to the fact that the outcome wouldn't influence the course of the ongoing experiment, further analyses for the quantification of polyepitope expression was not conducted.

The conversion efficiency of translated polyepitope to presented individual epitopes must also be assumed to be substantially less than 100%, although an exact estimate is hard to give. This is due to the many intracellular processes involved in polyepitope degradation and peptide loading as described in section 1.2.2. In conclusion, the density of presented epitopes on the surface of VRP-infected APCs can in general be thought of as low, being the cumulative result of low polyepitope expression and low conversion efficiency to presented epitopes. This has supposedly contributed to the low response and efficiency of the vaccine.

4.1.3 Effects of an established CTL response against a natural infection

The results from the qRT-PCR revealed that no effect of vaccination was seen in the viral load in serum, while slight indications of an effect were seen in the viral load in the lungs (figure 4 in paper 2, page 112). On this note it should be mentioned that viral load in serum was measured at dpc 5 and 13, while the lungs were excised upon euthanasia at dpc 26/27. This could indicate that the effects of vaccination were present but nevertheless delayed until several weeks after challenge. This is in accordance with the established literature on the subject, describing a delayed adaptive response as a result of modulations of the innate response (section 1.3.8). Specific causes of this may include the PRRSV-induced suppression of TNF-α normally aiding in the recruitment of lymphocytes to the site of infection; the upregulation of IL-4 in infected macrophages suppressing the inflammatory cytokine response; and the downregulation of MHC-I on infected cells. Additionally, PRRSV has been shown to induce the differentiation of T

cells into Tregs that are capable of suppressing the cytolytic activities of CTLs otherwise responsive to restimulation *in vitro*. In concert, these PRRSV-induced modulations of the immune response in addition to other modulations described in section 1.3.8 may explain the low effects of vaccination, even though a proper priming of CD8β cells may have occurred in the first place.

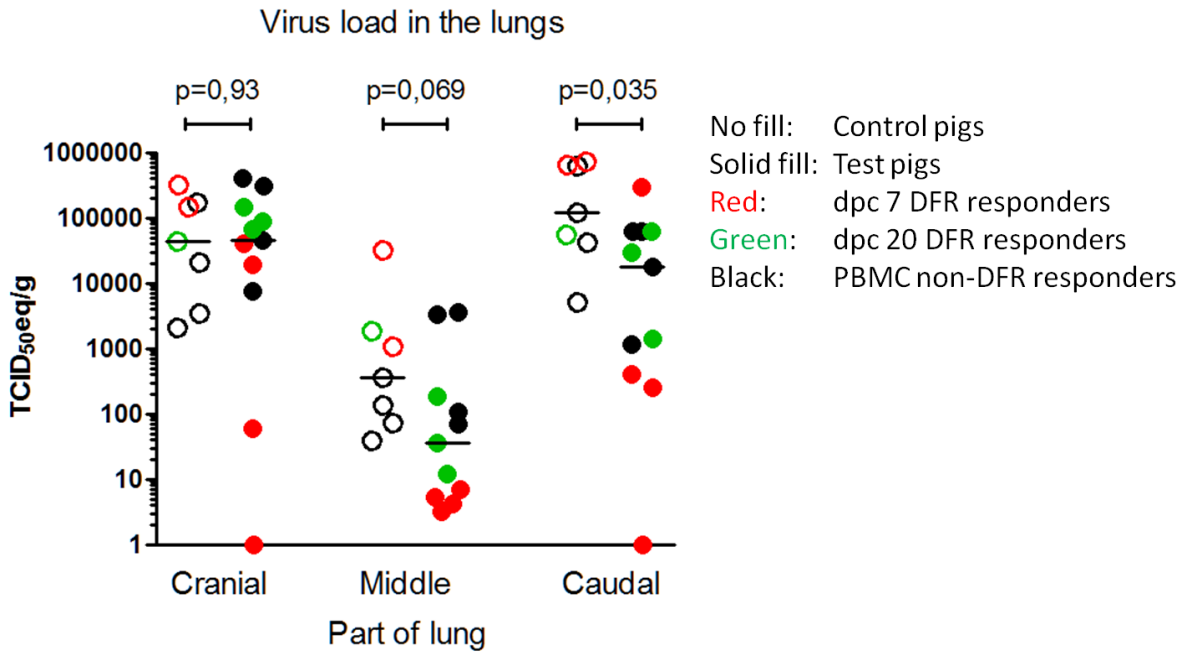

***Figure 12**: Virus load in the lung tissue from cranial, middle and caudal parts of the lung prepared from cutouts of 0.2-0.4 gram and normalized to TCID50 equivalents to 1 gram of tissue. Color codes indicate pigs with DFR-interpreted ELISPOT responses at dpc 7 (red) and dpc 20 (green). Among test animals a trend is apparent since dpc 7 responders are more represented below the median, indicating an effect of vaccination in these pigs. P-values are calculated using Mann-Whitney. All measurements were performed in duplicates and were converted from ct values using a standard curve based on a purified 10-fold dilution series of the challenge isolate. Group medians are indicated with a line.*

Interestingly, however, a weak correlation was seen for pigs of the test group exhibiting peptide responses at dpc 7 with their viral loads in lungs (figure 12). Here, test pigs who responded to peptides in ELISPOT at dpc 7 according to the DFR method (Toby, Trisha, Thomas and Tina colored red in figure 12) (see figure 7 in paper 2, page 115 for further details), all had titers below the median in all parts of the lungs (except for Tina, who was above the median in the caudal part). For test pigs responding to peptides at dpc 20 (Tyra, Tania and Tyson colored green in figure 12), no such trend could be observed. As previously mentioned, a CTL response induced by challenge would not be detectable already at dpc 7, why the observation of this indicates that the response was induced by the vaccine. As such, the notion that this coincides with a noticeably lowered viral load could indicate that the vaccine actually had a significant effect in these four animals, while the remaining animals were unaffected by the vaccine. On this note it should be mentioned that these four pigs came from four different litters and were equally represented with regards to day of euthanasia/box number. A potential confounder could however be that all had the SLA-1*0702 profile,

except for Tina who had the SLA-2*0401 profile and were the only of the four that was not consistently below median in all lung parts.

4.2 Discussion of the applied approach

Obviously, several things have happened differently than originally planned, or haven't happened at all. That's just part of doing research in general, and for a PhD in particular a relatively broad margin of deviation must be expected. Having worked my way through the whole process, I now realize that several things could or should have been done differently. This, I will elaborate on in the following sections with regards to the processes related to the curation and selection of PRRSV sequences (section 4.2.1); the preparation of strains prior to epitope prediction (section 4.2.2); the process of selecting and identifying the epitopes (section 4.2.3); the vaccine platform (section 4.2.4); the experimental conditions (section 4.2.5); the challenge strain (section 4.2.6); and the readouts (section 4.2.7).

4.2.1 Curation and selection of PRRSV sequences

I spend an enormous amount of time curating the strains prior to epitope prediction. The main purpose for this was to ensure that the actual diversity of PRRSV-2 in the field was reflected in the degree of conservation of the final epitopes. To obtain this, I only accepted wild type strains. In principle, I think this was a reasonable approach, but in effect I failed to acknowledge that the actual field diversity of PRRSV was not reflected in the publicly available wild type sequences either. As such, the curation of strains was mostly a waste of time. A better estimate of conservation could probably be obtained by a simple whole-proteome phylogenetic analysis including all strains indiscriminately. From this, strains being too similar would be easy to identify and could thus be excluded accordingly. Eventually, the outcome of this would represent truly conserved areas in which epitopes could be sought.

4.2.2 Prerapation of selected strains prior to epitope prediction

In parallel with the curation of strains, these were prepared for epitope prediction by generating all naturally occurring 9- and 10-mer peptides as described in section 2.1.1. This was a relatively daunting process and had to be executed in bulk since the procedure was based on alignments to which new sequences could not be easily added. Meanwhile doing so, I considered developing a bioinformatic pipeline that could do it automatically on the basis of full genome nucleotide sequences. In spite of the numerous epitope prediction servers available, I have not found a single service capable of doing this. I think it could be a very useful tool for the development of epitope vaccines in general, and could probably quite easily be applied to several other vira in which RFSs and post-translational cleavage sites are present. However, I never pursued this idea but focused instead on developing "The Program", which turned out to be completely redundant.

4.2.3 Identification and selection of epitopes

The identification and selection of epitopes is the most central part of developing a vaccine for inducing a CTL response. Several approaches for this exist with varying significance of outcome. These will be described in the following and are summarized in table 9. A good place to start is to take advantage of the multiple available services for the prediction of several relevant aspects related to epitope presentation. Alone on the DTU-CBS server, prediction services are available for proteasomal cleavage (NetChop); pMHC-I binding affinity combined with proteasomal C terminal cleavage and TAP transport efficiency (NetCTLpan); pMHC-I binding affinity (NetMHCpan and PickPocket); and pMHC-I binding stability (NetMHCstabpan). These services are based on either artificial neural networks (ANN), position specific weight matrices (PSWM), or a combination of the two. Most of them are based on human binding data, but some can be applied to the prediction of porcine MHCs. A prediction service also exists for the prediction of immunogenicity (Immunogenicity predictor). This is based on the observation that large, aromatic and acidic residues are more frequently represented in the central 4-6 positions of peptides with known immunogenicity than in non-immunogenic peptides. On this, a PSWM has been established from which the immunogenicity of natural peptides can be predicted with a significant accuracy (Calis et al. 2013).

Even though predictors can significantly refine the pool of potential epitopes, no predictor is completely accurate, why some sort of verification is needed. This can be done in several ways depending on timeframe, budget and information demands. The simplest of these are based on molecular assays and provide information on the binding strength of a pMHC. In addition to the two methods used in the present study (peptide affinity ELISA and SPA), a third method for determining pMHC affinity should also be mentioned. This is called Luminescent oxygen channeling immunoassay (LOCI) and is based on the principle of a donor bead that produces singlet oxygen upon illumination at 680 nm, and an acceptor bead that emits light at 520-620 nm

Name	Platform	Method	Species	MHC binding	MHC ID	Antigen processing	Immuno-genicity	Cyto-toxicit	Workload	Resources	Reference	Online
NetChop	prediction server	ANN	human	no	no	proteasome	no	no	mild	free	find online	[1]
NetCTLpan	prediction server	ANN, PSWM	mostly human	affinity	yes	proteasome, TAP	no	no	mild	free	find online	[1]
NetMHCpan	prediction server	ANN	mammalian	affinity	yes	no	no	no	mild	free	find online	[1]
NetMHCstabpan	prediction server	ANN	human	stability	yes	no	no	no	mild	free	find online	[1]
PickPocket	prediction server	PSWM	mammalian	affinity	yes	no	no	no	mild	free	find online	[1]
PSCPL	prediction	PSWM	human, pig	affinity/stability	yes	no	no	no	mild	free	Pedersen et al. 2011	
Immunogenicity predictor	prediction server	PSWM	mammalian	no	no	no	yes	no	mild	free	Calis et al. 2013	[2]
Affinity ELISA	ELISA based	molecular assay	available MHCs	affinity	yes	no	no	no	moderate	moderate	Pedersen et al. 2011	
SPA	ELISA based	molecular assay	available MHCs	stability	yes	no	no	no	mild	moderate	Pedersen et al. 2016	
LOCI	ELISA based	molecular assay	available MHCs	affinity	yes	no	no	no	mild	moderate	Harndahl et al. 2009	
Mass spectrometry	Infected cells	Mass spectrometry	all	yes	partly	yes	no	no	heavy	expensive	Reinhold et al. 2010	
Immunogenicity assay	ELISPOT	Restimulated PBMCs	all	yes	partly	yes	yes	no	heavy	expensive	Zhang et al. 2009	
Multimer staining	Flow cytometry	Restimulated PBMCs	available MHCs	yes	yes	yes	yes	no	heavy	expensive	Bentzen et al. 2016	
Cytotoxicity assay	in/ex vivo	cytotoxicity assay	all	yes	partly	yes	yes	yes	heavy	expensive	Stanke et al. 2010	

Table 9: *Methods for selection and identification of epitopes. PSCPL: position scanning combinatorial peptide library. ELISA: enzyme-linked immunosorbant assay. SPA: scintillation proximity assay. LOCI: Luminescent oxygen channeling immunoassay. ELISPOT: enzyme-linked immunospot assay. ANN: artificial neural network. PSWM: position specific weight matrix. PBMC: peripheral blood mononuclear cell. MHC: major histocompatibility complex. TAP: transporter associated with antigen presentation. [1]: www.cbs.dtu.dk/services. [2]: tools.iedb.org/immunogenicity/*

upon activation by the singlet oxygen that will decay to its ground state within 4 µs. As such, the affinity of a pMHC complex conjugated to a donor bead can be determined, since a specific antibody conjugated to the acceptor bead will only recognize correctly folded, hence peptide-bound, pMHC. This method is superior to the peptide affinity ELISA with regards to speed, sensitivity and hands-on time needed (Harndahl et al. 2009).

An interesting technology was described by Reinhold et al. (2010), who infected culture cells with Influenza virus, harvested the presented pMHC complexes and subsequently identified and quantified the presented peptides using mass spectrometry (MS). This technology has the advantage that only presented epitopes will be identified, thus accounting for the intracellular processes regarding protein abundance, degradation, ER import and MHC binding and loading. However, in order for detection to be possible, the MS spectrum for the given peptide must be determined in advance.

Verification of the immunogenicity of potential epitopes can unfortunately not be performed without the identification of an epitope-specific CMI, which again requires immunization of living animals. ELISPOT represents a widely used method for this and can be adapted in several ways as explained in section 2.8. This method does however not provide information on the MHC alleles on which the epitopes are presented although it can be narrowed down to the limited number of MHCs expressed by the animal by genotyping this. A different approach for the verification of cognate CD8 T cells is by the use of flow cytometry in combination with multimer staining. For this, multimers of a specific pMHC-I combination are conjugated with an identifier tag and incubated with PBMC or purified CD8 T cells from immunized animals. The multimers will thus associate with the TCRs of a cognate CD8 T cells and can subsequently be identified by flow cytometry. The avidity of these multimers is determined by the number of monomers, but a widely used multimer is the tetramer in which biotin-conjugated monomers are linked together by fluorescently labeled streptavidin molecules. Using this setup, the availability of fluorochromes, filters and lasers of the machine limits the screening to distinguish 10-100 distinct TCR specificities. Recently, however, a novel technology was developed at DTU-Vet in which >1000 peptide specificities could be distinguished in a single sample by combining flow cytometric cell sorting with subsequent amplification and sequencing of DNA-based barcode tags specific for the individual pMHC complexes (Bentzen et al. 2016). This significantly increases the applicability of multimer staining. In addition to the identification of peptide-specific T cells, indicators of cell effector functions could also be applied when using flow cytometry. This could be done by the simultaneous staining against intracellular IFN-γ, perforin or CD107a, the latter being presented on the cell surface only following the release of cytotoxic granules.

Despite having identified epitopes as immunogenic, the cognate CD8 T cells may not necessarily be cytotoxic, which for instance could be due to a state of anergy induced by present Tregs. Conclusively, this can only be determined using a cytotoxicity assay. The general principle for this is to evaluate the rate of killing executed by effector CTLs on target cells presenting the peptide in question on a relevant MHC allele. The target cells can either be pulsed with the peptide or be infected with the pathogen encoding the peptide. The former will only provide information about epitope-specific CTL cytotoxicity, while the latter will also provide evidence that epitope-specific killing will indeed be

possible of naturally infected cells. As a control, the killing of non-pulsed/non-infected target cells should also be assessed.

Different versions of cytotoxicity assays exist. The classical assay is the ^{51}Chromium (Cr) release assay, in which the target cells expressing the epitope of interest are labeled with ^{51}Cr. During *in vitro* incubation with effector CTLs, ^{51}Cr is released from the target cells when killed. The amount of supernatant ^{51}Cr can subsequently be measured by liquid scintillation from which the rate of killing can be calculated. The drawbacks of this assay are the use of radioactive material, spontaneous release of the isotope and the fact that only fresh cells can be used.

A different approach to measure cytotoxicity has been developed for flow cytometry in which peptide-positive target cells are stained with carboxyfluoroscein succinimidyl ester (CFSE), while peptide-negative target cells are stained with Far Red. Both peptide-positive and -negative cells are then incubated with CTLs and are subsequently analyzed by flow cytometry gating for CFSE and Far Red. The rate of killing can then be determined from the ratio between CFSE and Far Red stained cells (Stanke et al. 2010). This method has several advantages as it is highly sensitive, easily executed and does not contain radioactive material.

Approaches for determining the *in vivo* cytotoxicity have also been developed in which the peptide-positive and -negative cells are transferred into immunized animals. By analyzing blood extracted at different time points after transfer, the in vivo cytotoxic rate can be determined accordingly (Regoes et al. 2007). This method has the obvious advantage of not being bias by *in vitro* conditions. A pilot study for this was recently performed in pigs in Gregers Jungersens lab at DTU-Vet, showing promising results.

In summary, several methods are available for the identification and selection of functional epitopes with required workloads spanning widely. If I was to redo my selection of epitopes, I would still combine NetMHCpan and PSCPL, since this provided a better prediction than either of the methods alone. Preferably, I would use the NetMHCstabpan but this service is currently not applicable to porcine MHCs. I used a threshold of a combined percentile ranks score ≤ 2 for selecting peptides for PopCover analysis, since this was considered a good compromise between having enough epitope and still having a relatively broad allelic coverage. In the light of two of the five SLAs being excluded for various reasons, a lower threshold could have been applied. It would have been interesting to include results from the immunogenicity predictor prior to PopCover analysis, since this represents the TCR-pMHC interaction, which is otherwise not represented in the predictions. Supposedly, this would have changed the final ensemble of epitopes considerably. Finally, I would not conduct the peptide affinity ELISA, since this was rather cumbersome and moreover inferior to the SPA stability assay with respect to predicting immunogenicity.

4.2.4 The vaccine platform

Ever since I read the initial project description for the present PhD, my mind was set on a future in which the final vaccine product was applied in the field. I envisioned a library of VRPs, each encoding conserved epitopes specific for a given SLA allele, from which a customized vaccine could be made to any given swine population by mixing VRPs

representing predominant alleles. The VRPs generated in this study should hence provide the cornerstones of the library, and for this reason, I designed three VRP-families representing the three SLAs.

In reality, however, the present study only provides a proof-of-concept that VRPs can be applied as a platform for the induction of a CTL response through expression of polyepitopes. Yet, the final aim of presenting a mature technology still lies far ahead. Besides, the present VRPs would never be authorized for being released in the field, since they are only one structural protein short of encoding for a fully virulent CSFV.

So instead of designing three VRP-families, I should have designed just one VRP-family encoding for all epitopes. After all, each test pig was administered with the same VRP mix regardless of SLA profile. As such, I would have had only three PRRSV-encoding VRPs instead of nine, which would obviously have saved me a lot of time and resources. This would apply to polyepitope design; cloning; VRP rescue; titration; batch generation; verification; aliquoting; storage; and vaccine mixing. Besides, I didn't even live up to my own vision since the epitopes were selected based on the PopCover output, which by definition prioritized epitopes on the basis of several SLAs. Had I been true to my vision, the PopCover output should have been completely disregarded, and the SLA-specific VRPs should have contained epitopes prioritized according to binding characteristics specific for the given SLA, exclusively.

The VRP as a platform for the induced expression of epitopes must be regarded as functional. Nevertheless, several improvements could be made for improved T cell priming. First of all, it should be a more potent inducer of polyepitope expression. Not least to ensure that a larger fragment of infected cells would also express the polyepitope, but the general level of expression should also be higher. Secondly, a means for targeting the VRPs to the DCs would also aid in the potency of the vaccine. In this regard it is important to mention that the DCs must be infected in order for intracellular translation to occur. This excludes the use of DC-specific antibodies conjugated to the VRP surface, since this would induce opsonization and cross-presentation, after which only preformed structural proteins - and not encoded peptides - would be presented. Recently, a study using the same delE^{rns} replicon framework as applied in this PhD, showed that different chitosan-based nanoparticulate vehicles were able to deliver the replicating RNA to DCs both *in vitro* and *in vivo*, in which cytosolic translation could be confirmed for a period of 96 hours (McCullough et al. 2014). This plasform would be an obvious alternative to VRPs as it is independent of a packaging cell line.

4.2.5 The experimental conditions

Despite feeling really happy and privileged that I was able to conduct the animal trial, I still think that the conditions were worse than anticipated as explained in section 3.1 and that this lowered the general standard of the outcome. This especially relates to the lack of easily available reagents and equipment, the long distance from my home, and the limited presence of people with immunological experience that I could discuss matters with *ad hoc*. Furthermore, the large number of animals resulted in extensive workloads in the lab, which limited my focus on the big picture. A smaller setup could for instance have prevented the lack of attention on the unresponsive pre-challenge ELISPOT, why this could have been rectified in due time. I am not saying this in an attempt to evade

responsibility but more for the acknowledgement of my own limitations. I think that the general outcome would have been better, had it been conducted at IVI. Alternatively, it should have been conducted at a lower biosafety level, preferably at Frederiksberg campus where the relevant equipment and expertise was readily available. At some point it was considered to export the original plasmids from IVI and then rescue the VRPs in Denmark, but at that point there was not enough time to establish the needed SK6-E^{rns} cell line, rescue and titrate the VRPs. Besides, it would probably still require some level of biosafety due to nature of the VRPs with regards to gene manipulation and CSFV origin.

4.2.6 The challenge strain

In the present setup, the challenge strain used to inoculate the pigs did not result in any clinical symptoms. While this was a good thing for the pigs, it concealed a potential effect of the vaccine in lowering clinical signs. As such, this still remains unknown and it could be argued to use a strain of higher pathogenicity in future studies.

4.2.7 The readouts

The immunological effects of the vaccine were almost exclusively monitored with IFN-γ ELISPOT. Originally, it was planned to use ELISPOT only for the narrowing down of responsive epitopes. The combination of 18 pigs that should be screened for 33 peptides was an extensive task to perform and as a compromise, the pre-challenge setup described in paper 2 was established. This was simply too deficient as only 300,000 cells/well were used and each sample was only analyzed in doublicates. In addition, the stimulations were pools of 6 peptides. Looking back, I really cannot grasp that I didn't recognize the weakness of this setup to begin with but I guess that's just how it feels getting wiser. In any case, I never came to the point as planned where I should characterize the responsive epitopes further with tetramer staining and cytotoxicity assays.

Tetramer staining of all pSLA combinations was considered, but the idea was dismissed since it would be too daunting, especially because of the general problems with the available flow cytometer, the numerous samples required to include all pSLA combinations, and the procedure for exporting samples out of the BSL3-ag facility.

4.3 Summary and conclusions

During the course of this PhD, I have identified and verified SLA-I epitopes conserved across PRRSV-2 strains; incorporated these into VRPs and used these to vaccinate pigs of matching SLA profiles. The pigs were subsequently challenged with a Danish PRRSV-2 field strain and the effects of vaccination were monitored in terms of IFN-γ recall ELISPOT and changes in viral load. On this basis, I have discussed aspects including the suitability of the selected epitopes; the components involved in priming of CD8β T cells; the limitations imposed by low expression of polyepitopes; the induction of a CTL response; and the effects of the applied vaccine in context of challenge.

From that I conclude that at least the 14 epitopes analyzed in post-challenge ELISPOT were suitably selected; that a CTL response was established although not as strongly as anticipated, which is supposedly related to poor

polyepitope expression in VRP-infected cells; and that an effect of vaccination was seen in viral load after challenge, although this was only weak and limited to just a few of the test pigs.

The VRP as a platform for epitope vaccination can be concluded as functional although advancements must be made for an increased polyepitope expression, and a means of targeting it to DCs would be an advantage. However, its natural adjuvanting effect in addition to its continuous expression of polyepitope, promotes the VRP to yield a highly suitable platform for vaccination.

Apart from the presence of an elegant connecting thread of the general approach, many loops and leaps were also present that should preferably have been straightened out in due time. These encompass the inclusion of peptides in the VRPs despite their lack of confirmed binding; the below-detection of expressed polyepitope in VRP-infected cells; and the difficulties with determining the VRP titers. While these all represent matters that were rushed forward without the confirmatory data being at hand, other things were done with exquisite attention to detail meanwhile completely ignoring the big picture. This, for instant, led to the development of two bioinformatic programs of which the first, “The Program”, was completely redundant, while the second “Juncitope” for the riddance of neoepitopes within the polyepitopes was indeed applied, although its biological significance in context of the vaccine is highly dubious. However, I really learned a great deal from this and was pleasantly entertained. Finally, I founded the central immunological monitoring on a blatantly bad setup.

In light of it all, I regard the present PhD in general as being a great success.

EPILOGUE

Ever since I began this project I was intrigued by the innovative and rational approach of it. How cool was it not to deliberately design a vaccine from scratch assembling it piece by piece including only functional epitopes. I was convinced that it would work.

When I received the qRT-PCR data, however, it hit me that none of this had worked. This was embarrassing and depressing, but nonetheless it was results were worth publishing. With this set of mind I started writing paper 2, which also has a rather humble/pessimistic sound to it. However, during the process of writing the thesis, I delved deeper into the analyses and this led to a kind of revelation that my data maybe wasn't that bad after all. As a matter of fact, I ended up concluding that it *had* worked, although not as profoundly as I had hoped for. But who was I anyway to expect that I could revolutionize 25+ years of hardcore scientific dissection of PRRSV.

The whole period of my PhD has been a fantastic journey with extraordinary experiences and lots of exciting learnings. I have presented my work at international conferences and have studied abroad. I have received scholarships and have been corresponding with the Danish authorities. I have been locked up with some of the most dangerous animal viruses and have showered enough for a lifetime. I have gotten to know so many great and interesting people and I have even learned a new language, Python. I have grown with the project and have acknowledged my own not so few limitations in respect to the huge complexity of the PRRS virus, the porcine immune system, and the interaction of the two. All of which I have developed a profound interest of. I have been taken really good care of by my supervisors, who have supported me and guided my training as a scientist. I have now become a scientist.

It is therefore with both sadness and joy that I will now end this wondrous time. I am deeply grateful.

PUBLICATIONS

In addition to the two accompanying papers presented in the following with me as a first author, I have contributed as co-author on one paper:

Overgaard NH, Frøsig TM, Welner S, Rasmussen M, Ilsøe M, Sørensen MR, Andersen MH, Buus S, Jungersen G. (2015) Establishing the pig as a large animal model for vaccine development against human cancer. Front Genet. 6:286. doi: 10.3389/fgene.2015.00286.

PAPER 1

Submitted to Immunogenetics

PREDICTION AND IN VITRO VERIFICATION OF CONSERVED PRRSV-2 CTL EPITOPES

ABSTRACT

Porcine Reproductive and Respiratory Syndrome Virus (PRRSV) is the causative agent of one of the most important porcine diseases with a high impact on animal health, welfare and production economy. PRRSV exhibits a multitude of immunoevasive strategies that in combination with a very high mutation rate, has hampered the development of safe and broadly protective vaccines.

Aiming at a vaccine inducing an effective cytotoxic T cell response, a bioinformatics approach was taken to identify common PRRSV epitopes predicted to react broadly with common swine leukocyte antigen (SLA) class I alleles. Briefly, all possible 9- and 10-mer peptides were generated from 104 complete PRRSV type 2 genomes of confirmed high quality, and peptides with high binding affinity to five common SLAs were identified combining the NetMHCpan and Positional Scanning Combinatorial Peptide Libraries binding predictions. Predicted binders were prioritized according to genomic conservation and SLA coverage using the PopCover algorithm. From this, 53 peptides were acquired for further analysis. Binding affinity and stability of a subset of 101 peptide-SLA combinations were validated *in vitro* for 4 of the 5 SLAs. Eventually, 23% of the predicted peptide-SLA combinations showed to form complexes with a dissociation half-life ≥ 30 minutes. Additionally, combining the two prediction methods proved to be more robust across alleles than either method used alone in terms of predicted-to-observed correlations. In summary, our approach represents a finely tuned epitope identification pipeline providing a rationally selected ensemble of peptides for future *in vivo* experiments with pigs expressing the included SLAs.

AUTHORS

Simon Welner: Email: siwel@vet.dtu.dk, Institutional address: Section of Virology, National Veterinary Institute, Technical University of Denmark, Bülowsvej 27, 1870 Frederiksberg C, Denmark.

Morten Nielsen (Corresponding author): Email: mniel@cbs.dtu.dk, telephone: +45 45 25 24 77, fax: +45 45 93 15 85, Institutional address #1: Center for Biological Sequence Analysis, Department of Bio and Health Informatics, Technical University of Denmark, Kemitorvet, building 208, 2800 Lyngby, Denmark. Institutional address #2: Instituto de Investigaciones Biotecnológicas, Universidad Nacional de San Martín, Av. 25 de Mayo y Francia, 1650 San Martín, Cdad. Autónoma de Buenos Aires, Argentina.

Michael Rasmussen: Email: michaelrasmussen1978@gmail.com, Institutional address: Laboratory of Experimental Immunology, University of Copenhagen, Blegdamsvej 3B, 2200 Copenhagen N, Denmark.

Søren Buus: Email: sbuus@sund.ku.dk, Institutional address: Laboratory of Experimental Immunology, University of Copenhagen, Blegdamsvej 3B, 2200 Copenhagen N, Denmark.

Gregers Jungersen: Email: grju@vet.dtu.dk, Institutional address: Section of Immunology and Vaccinology, National Veterinary Institute, Technical University of Denmark, Bülowsvej 27, 1870 Frederiksberg C, Denmark.

Lars Erik Larsen: Email: Lael@vet.dtu.dk, Institutional address: Section of Virology, National Veterinary Institute, Technical University of Denmark, Bülowsvej 27, 1870 Frederiksberg C, Denmark.

INTRODUCTION

Porcine Reproductive and Respiratory Syndrome (PRRS) is one of the most important porcine diseases in all swine-producing countries and has a high impact on animal health, welfare and production economy (Nieuwenhuis et al. 2012; Holtkamp et al. 2013). The causative agent, the PRRS virus (PRRSV), is a member of the Arteriviridae family, Rodartevirus genera together with lactate dehydrogenase elevating virus (Kuhn et al. 2016). The clinical signs of infected pigs vary from subclinical to fever, lethargy, anorexia and pneumonia. For pregnant gilts and sows the virus may infect the endometrium and placenta giving rise to late-term abortions, early farrowing, return to oestrus and birth of litters mixed with living and stillborn piglets (Karniychuk and Nauwynck 2013).

Many attempts have been made to develop an effective vaccine against PRRSV. Various virus attenuation or antigen selection strategies, adjuvants and delivery systems have been tested including killed virus, modified live virus (MLV), recombinant protein based, and DNA vaccines, and their efficacies in terms of viral clearance and relief of symptoms are diverse (reviewed in Renukaradhya et al. 2015a and Renukaradhya et al. 2015b). In broad terms, they all succeed to amend the immune response by raising the levels of virus-specific antibodies and/or increasing the cell-mediated immune response (CMI). Commercial MLV vaccines provide moderate to strong protection against a homologous challenge, but none of them seem to be capable of providing cross-protection against heterologous challenges with a sustained protective effect. In addition, the use of MLVs has an immense disadvantage that the attenuated vaccine strain may revert to virulence and start promoting rather than preventing viral infection (Botner et al. 1997; Madsen et al. 1998; Beilage et al. 2009; Jiang et al. 2015). Furthermore, the use of MLV in pregnant animals in the last trimester increases the risk of reproductive failure.

Ideally, a vaccine against PRRSV should induce neutralizing antibodies capable of clearing the virus in its extracellular phase, while a CMI should eliminate infected cells as fast as possible to reduce tissue damage and viral transmission. A key effector cell for this latter task is the cytotoxic T lymphocyte (CTL), having the ability to identify and induce apoptosis of PRRSV-infected cells. Studies have shown that CTLs are indeed present in high numbers at infected locations in the lungs of transplacentally infected animals (Tingstedt and Nielsen 2004), and that the influx of CTLs to the lungs increase during PRRSV infection (Samsom et al. 2000). Although the CTLs are present, their role in clearing the infection is unclear and controversial.

On the skeptical side, Lohse et al. (2004) showed that acute infection appeared to be unaffected by the presence of CTLs since temporary depletion of CTLs during the onset of infection with PRRSV-1 (PRRSV type 1) virus neither increased disease nor influenced the ability to clear virus. One study attempted to evaluate the relationship between viral persistence and the presence of CTLs in blood, tonsils, the spleen and the mediastinal lymph nodes in PRRSV-2 (PRRSV type 2) infected animals. Although a significant correlation between viral clearance and increased CTL counts in the spleen was observed, a delayed and impaired CMI together with a low level of CTLs was found in the tonsils and lymph nodes, allowing viral persistence in these organs (Lamontagne et al. 2003). In a last example, the cytotoxic activity of peripheral blood mononuclear cells (PBMCs) isolated from Lelystad-infected pigs failed to show

PRRSV-specific lysis of infected autologous alveolar macrophages until very late in the experiment. Even following successful expansion of $CD3^{+}CD8^{high}$ cells after a 5-day period of restimulation with virus, a PRRSV-specific cytotoxic response was not observed until day 56 post infection, suggesting a PRRSV-induced impairment of the cytotoxic activity (Costers et al. 2009).

On a more optimistic note the CMI against PRRSV-2 was first explored by Bautista (1997), who described a PRRSV-specific lymphocyte proliferation and delayed-type hypersensitivity response, thereby indicating a T cell specific memory response. Another study argued that a CMI was responsible for the protective immunity of a PRRSV-1 challenge upon vaccination with an MLV vaccine, since a virus-specific interferon-gamma (IFN-γ) response was observed, while no neutralizing antibodies were present (Zuckermann et al. 2007). An *in vitro* proliferation assay of PBMCs from PRRSV-1 infected cells, showed that PBMCs could be expanded upon restimulation with virus, and that the cytotoxic activity against K-562 cells increased along with this expansion (López Fuertes et al. 1999).

The observations and conclusions put forward in the literature of CMI responses in relation to PRRSV are thus in many cases contradictory, and it is obvious that more knowledge is needed for a better understanding of the importance of CMI against PRRSV. In this study, a rational approach has been taken to identify major histocompatibility complex (MHC) class I restricted epitopes that are conserved among PRRSV-2 strains. Potential epitopes restricted by five swine leukocyte antigen (SLA) class I alleles, SLA-1*0401, SLA-1*0702, SLA-2*0401, SLA-2*0502 and SLA-3*0401, were identified using bioinformatics tools, and subsequently verified *in vitro* as SLA-binders by affinity and stability assays.

MATERIALS AND METHODS

Sequences

Verification of genomic data

All available full genome sequences (access date: September 24th, 2014) of PRRSV-2 were evaluated and excluded if they failed the criteria of 1) being a wild type strain, 2) being published, 3) having methionine begin all protein products, and 4) being without non-sense stop codons.

Phylogenetic tree

A phylogenetic tree was created in order to illustrate the diversity of the strains used for the prediction. Briefly, for each strain, all naturally occurring protein products (nsp1a, nsp1b, nsp2, nsp2TF, nsp3-6, nsp7a, nsp7b, nsp8-12, ORF2a, ORF2b, ORF3, ORF4, ORF5a, ORF5, ORF6 and ORF7) were concatenated and aligned in CLC (workbench v7.0). The tree was subsequently generated in CLC using the integrated neighbor joining algorithm with a bootstrap of 1000 replicates.

Peptide generation

For each verified strain, all possible 9- and 10-mer peptides were generated *in silico* from all naturally occurring protein products, excluding peptides spanning post-translational cleavage sites.

Swine Leukocyte Antigen

Five SLA class I alleles were used: SLA-1*0401, SLA-1*0702, SLA-2*0401, SLA-2*0502 and SLA-3*0401. Most of these alleles have been shown to be common in Danish pigs (Pedersen et al. 2014) and were readily accessible for *in vitro* analysis as recombinant biotinylated heavy chains as previously described (Pedersen et al. 2011).

Epitope Bioinformatics

NetMHCpan

NetMHCpan (Hoof et al. 2009) version 2.8 was used to predict the binding affinity of the peptides against the five SLA alleles. Version 2.8 has been trained on more than 150,000 quantitative binding data covering more than 150 different MHC-I molecules. The output, being a measure of the binding affinity of a given peptide to a given SLA allele, was converted to a percentile rank score, using SLA-specific standard curves based on the prediction of 200,000 random natural peptides, e.g. a percentile rank score of 2% indicated that the given peptide was among the top 2% best binders to the given SLA out of the 200,000 random natural peptides used for the standard curve.

Positional Scanning Combinatorial Peptide Library

The Positional Scanning Combinatorial Peptide Library (PSCPL) method was first described in details by Stryhn et al. (1996) and has since been applied to porcine immunology by Pedersen et al. (2011). Briefly, an SLA specific scoring matrix providing the average contribution on binding of any amino acid at each position in a 9-mer peptide is used to calculate the overall binding score of a given peptide. The PSCPL experiments providing the scoring matrices for the five SLAs have been performed previously (SLA-1*0401: Pedersen et al. 2011, SLA-2*0401: Pedersen et al. 2013, SLA-3*0401: Pedersen et al. 2014, SLA-1*0702 and SLA-2*0502: Lasse Eggers Pedersen – personal communication, April 2014). The matrices for SLA-1*0401, SLA-2*0401 and SLA-3*0401 were based on affinity measurements, while the matrices for SLA-1*0702 and SLA-2*0502 were based on stability measurements (shown to give very similar outcomes by Rasmussen et al. (2014)). Since the matrices are based on the binding of 9-mers only, an extrapolation was performed to obtain estimates of 10-mers as described by Lundegaard et al. (2008). The output was converted to a percentile rank score, similar to the above.

Combining the methods

Due to the limited amount of porcine MHCs binding data available for training of NetMHCpan, the two methods, NetMHCpan and PSCPL, were combined as this has been shown previously to provide more exact predictions than either method alone (Pandya et al. 2015; Pedersen et al. 2016). A combined rank score was determined for each individual peptide-SLA (pSLA) pair by calculating the harmonic mean of the two method-specific percentile rank scores. Only peptides with a combined rank score ≤ 2% for at least one of the five SLAs were selected as epitope candidates.

Prioritizing the epitope candidates

The PopCover algorithm was used to rank the epitope candidates by iteratively prioritizing the peptides with the broadest SLA allele and strain coverage, while covering the gaps left by previously chosen peptides (Lundegaard et al. 2010; Buggert et al. 2012).

In vitro verification of predicted epitopes

Based on the bioinformatics described above, 53 peptides (purity > 85%, GenScript) were acquired for *in vitro* verification. Stability and affinity assays were performed on each pSLA with a predicted combined rank score ≤ 2% using recombinant biotinylated heavy chains of the five SLAs.

Stability assays

The stability of the pSLA complexes was determined *in vitro* using a scintillation proximity assay (SPA) employing the principle of ^{125}I-radiolabeled β_2m dissociation as a measure of pSLA complex stability (Harndahl et al. 2011; Parker et al. 1992). Briefly, denatured biotinylated recombinant SLA heavy chains were refolded with ^{125}I-radiolabeled β_2m and the peptide to be tested in streptavidin coated scintillation 384-well FlashPlate PLUS microplates (SMP410A001PK, Perkin Elmer). In case of a binding peptide, a scintillation signal was observed and the off-rate was subsequently determined by the addition of excessive amounts of unlabeled β_2m while monitoring the scintillation signal in a liquid microplate scintillation plate reader (Topcount NXT, Perkin Elmer). The off-rate is equivalent to the peptide-specific dissociation rate and serves as a good measure for pSLA complex stability. The stability values reported are the averages of duplicates in half-life (t½) decimal hours.

Affinity assays

Binding affinity of pSLA complexes was determined *in vitro* using a modified enzyme-linked immunosorbent assay (ELISA) (Sylvester-Hvid et al. 2002; Pedersen et al. 2011). Briefly, 1-2 nM denatured biotinylated recombinant SLA heavy chains were refolded with 15 nM human β_2m (hβ_2m) and eight 5-fold incremental concentrations of the peptide to be tested spanning from 0-13 µM. Following obtained equilibrium after two nights of incubation at RT the samples were transferred to a streptavidin coated 96-well capture plate (436014, Thermo Scientific) for 1½ hour of incubation. Mouse-anti-hβ_2m, BBM1, and horseradish peroxidase-conjugated goat-anti-mouse IgG (A9917, Sigma Aldrich) were used as primary and secondary detection antibodies, respectively. Washing steps were performed with 0.05% Tween 20 in PBS. The color reaction of TMB Plus2 (4395A, Kem-En-Tec Diagnostics) was stopped with equivalent amounts of H_2SO_4 (0.5 M, cat 30144.294, VWR International) and the plates were read at 450-650 nm using a Multiskan EX ELISA reader (Thermo). OD values were converted to measures of affinity (equilibrium dissociation constant, K_D) using the prefolded biotinylated FLPSDYFPSV/HLA-A*0201 as standard (Kast et al. 1994), and were again converted to percentile rank scores by the same SLA specific standard curves that are integrated in NetMHCpan. A minimum of two reliable measurements were aspired for each pSLA combination, and in most cases this was obtained. The results are presented as the range between the minimum and maximum measurements converted to rank scores.

RESULTS AND DISCUSSION

Sequence selection and Epitope Bioinformatics

Initially, 334 PRRSV-2 full genome (~15.1 kb) sequences were included. Of these, 104 sequences were accepted in accordance with the described verification criteria. Figure 1 illustrates their evolutionary relatedness, while Table 1 shows the year and country of isolation. Out of the 104 accepted strains, 90,939 unique 9- or 10-mer peptides were generated *in silico*. Binding of each peptide to each of the five SLAs was predicted using the two methods, NetMHCpan and PSCPL. By excluding peptides with a combined rank score $>$ 2% with all of the SLAs, the number of unique peptides was reduced to 6,140 that were subsequently prioritized using PopCover.

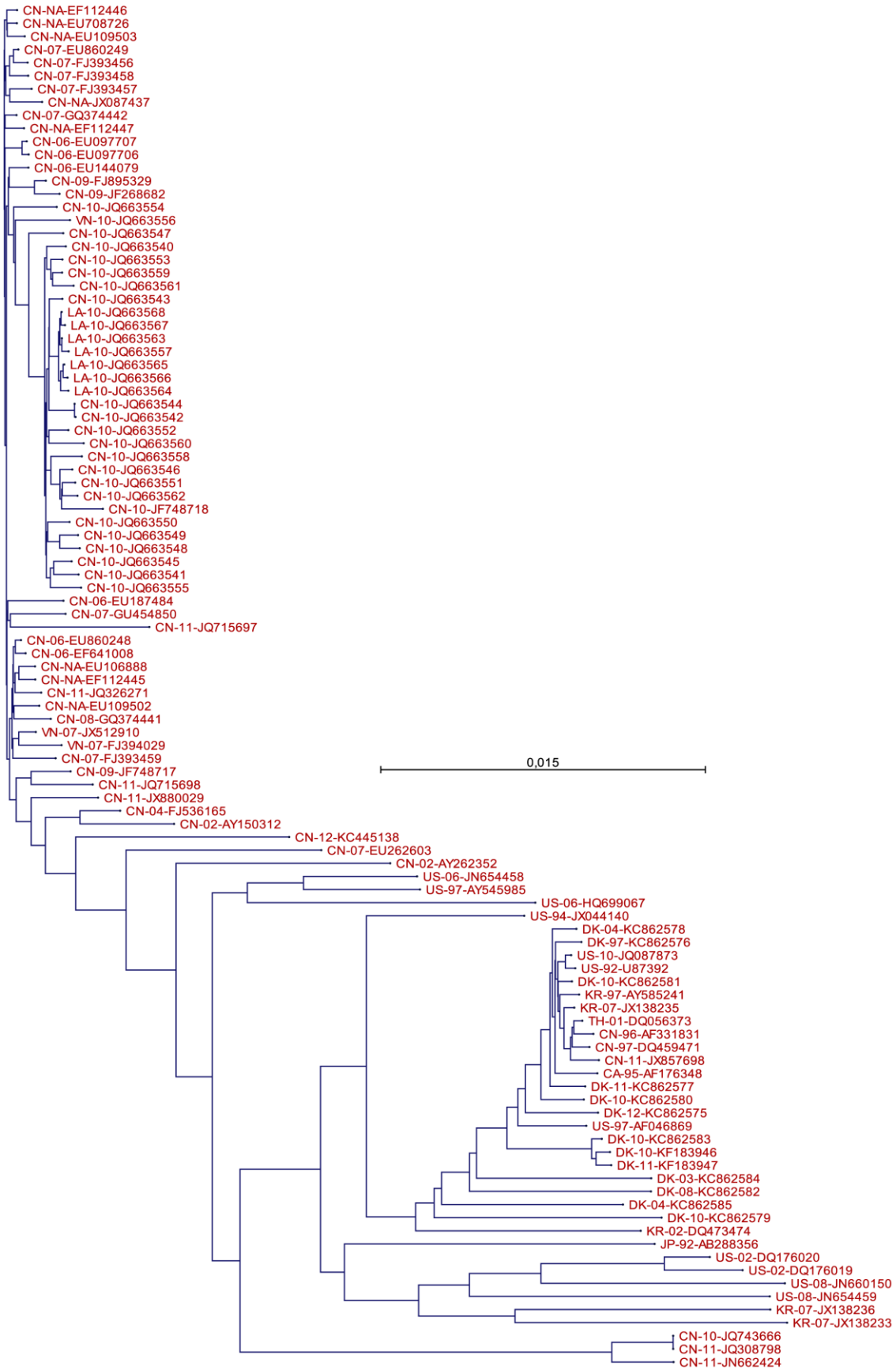

***Figure 1**: Phylogenetic tree of the 104 strains based on their full proteome. Isolation data (country and year) and accession number is indicated in the legend for each strain, country as a two-letter ISO country code, and year as the last two digits. NA: no information about isolation year available. Scale bar indicates the number of amino acid substitutions per site.*

Country of isolation		Year of isolation																	
		NA	'92	'94	'95	'96	'97	'01	'02	'03	'04	'06	'07	'08	'09	'10	'11	'12	%
Canada	**CA**				1														1
China	**CN**	8				1	1		2		1	6	8	1	3	23	7	1	60
Denmark	**DK**						1			1	2			1		5	2	1	13
Japan	**JP**		1																1
Laos	**LA**															7			6,7
South Korea	**KR**						1		1				3						4,8
Thailand	**TH**							1											1
USA	**US**		1	1		1	2		2			1		2		1			11
Vietnam	**VN**												2			1			2,9
	%	7,7	1,9	1	1	1,9	4,8	1	4,8	1	2,9	6,7	13	3,8	2,9	36	8,7	1,9	100

***Table 1**: Distribution of the 104 strains according to isolation year and country. NA: not available*

Among the top-50 on the PopCover output, four 9-mer peptides nested within top-50 10-mer peptides were excluded, and three peptides further down the list (top-70) were included to give a more even distribution along the genome. In addition, six peptides were included as they have previously been described in the literature in various restimulation studies of PBMCs from pigs immunized with live or attenuated PRRSV-2 virus: Four 17-mers containing the peptides ID43 (TTMPSGFELY), ID50 (NSFLDEAAY), ID53 (MPNYHWWVEH) and ID54 (EVALSAQII), respectively, were found to induce both T-cell proliferation and IFN-γ secretion in a screening study of NSP9 and NSP10 (Parida et al. 2012); 15-mers containing peptide ID51 (RGRLLGLLHL) and ID52 (LYRWRSPVI) were found to induce spots in IFN-γ ELISPOT assays when screening GP5 (Vashisht et al. 2008) and the M protein (Wang et al. 2011), respectively. Furthermore, the same ID52 containing 15-mer as above, was included in a peptide-based vaccine with the N-terminal part of the heat chock protein Gp96 as adjuvant. Restimulation with this peptide of PBMCs from the immunized animals was shown to induce lymphocyte proliferation with a Th1-type cytokine bias, and the immunized piglets exhibited milder clinical symptoms, lower viremia and less pathogenic lesions than non-immunized piglets upon challenge with a highly pathogenic PRRSV strain (Chen et al. 2013). Unfortunately, none of these studies had a clear phenotypic description of the responding cells, nor had their test animals been haplotyped.

In total, 54 peptides were ordered from Genscript, but only 53 were received as peptide ID14 could not be synthesized (table 2).

ID	Sequence	Locus	Cons.	SLA-1*0401					SLA-1*0702					SLA-2*0401					SLA-2*0502				
			104 strains (%)	stab. (h)	aff. (nM)	PSCPL (rank)	NMP (rank)	comb. (rank)	stab. (h)	aff. (nM)	PSCPL (rank)	NMP (rank)	comb. (rank)	stab. (h)	aff. (nM)	PSCPL (rank)	NMP (rank)	comb. (rank)	stab. (h)	aff. (nM)	PSCPL (rank)	NMP (rank)	comb. (rank)
1	RTILGTNNF	nsp9	98	0.1	1,030†	3	1.5	2			32	6	10.1	0.1	-	1.5	1.5	1.5			50	4	7.4
2	YAQHMVLSY	nsp9	100	-	-	32	0.4	0.8	0.9	4	1.5	0.03	0.1	1.1	60	15	1	1.9			50	4	7.4
3	RSTPAIVRWF	nsp9	97	0.1	-	0.25	3	0.5			50	32	39	-	-	0.8	4	1.3			50	10	16.7
4	YSFPGPPFF	nsp9	71	0.2	37†	0.8	0.5	0.6	0.2	18,708	8	1	1.8	-	-	0.5	1.5	0.8	0.1	-	50	0.17	0.3
5	RALPFTLSNY	ORF2a	96			9	1.5	2.6	0.3	12	2	1.5	1.7	0.1	-	1.5	1.5	1.5			50	15	23.1
6	KSGHPHGLLF	nsp9	95	0.1	-	50	1	2			50	7	12.3			7	3	4.2			50	32	39
7	QVYERGCRWY	nsp1a	100	0.3	682	2	2	2	4.5	168	5	0.8	1.4	0.7	209†	4	0.17	0.3			50	32	39
8	GGNWFHLEW	ORF3	99			10	5	6.7			50	4	7.4	0.2	16,627	1.5	3	2			50	15	23.1
9	IVYSDDLVLY	nsp9	99	-	-	6	0.8	1.4	0.5	13	0.5	0.1	0.2	-	-	1.5	1	1.2			50	9	15.3
10	KVAHNLGFYF	nsp11	95	0.3	122	15	0.4	0.8			2	4	2.7			10	4	5.7			50	4	7.4
11	TRARHAIFVY	nsp10	95			50	15	23.1	0.3	60	0.25	1.5	0.4	0.2	-	7	0.8	1.4			50	50	50
12	LSFSYTAQF	ORF3	99			5	3	3.8			32	1.5	2.9	1.3	73	3	0.3	0.5	-	-	50	0.8	1.6
13	FTWYQLASY	nsp12	97	0.1	92†	8	0.8	1.5	0.2	62	4	0.15	0.3	9.1	2	0.025	0.25	0.0			50	7	12.3
15	TLSNYRRSY	ORF2a	97	-	-	1.5	1.5	1.5	0.3	29,504	1	1.5	1.2	-	-	15	1	1.9			32	50	39
16	SGHPHGLLF	nsp9	96			10	4	5.7			9	4	5.5	-	-	15	0.8	1.5			50	15	23.1
17	RTAIGTPVY	ORF4	96	0.5	57	1	0.25	0.4	0.2	1,852	4	1	1.6	-	385†	1	0.8	0.9			50	10	16.7
18	YTAQFHPEIF	ORF3	98	-	-	3	1	1.5			9	2	3.3	0.4	-	0.1	2	0.2	0.2	555†	32	0.5	1
19	LSDSGRISY	ORF7	95	1.1	10	0.8	0.12	0.2	0.2	383	15	0.3	0.6	0.2	4,182†	1	1.5	1.2			50	15	23.1
20	ASYVWVPLTW	nsp3	88			4	3	3.4			50	4	7.4	0.1	17,142	2	0.5	0.8			50	3	5.7
21	KVAHNLGFY	nsp11	95	1.5	4	50	0.2	0.4	2.8	11	0.5	1.5	0.8	-	-	6	0.5	0.9			50	16	24.2
22	KIFRFGSHKW	nsp1b	88			5	2	2.9			50	4	7.4	0.1	9†	15	1	1.9			50	6	10.7
23	NISAVFQTYY	ORF3	93	0.1	413	2	1.5	1.7	0.9	6	50	0.3	0.6	-	862	1.5	2	1.7			50	15	23.1
24	RTAPNEIAF	nsp2	66	2.1	4	0.125	0.4	0.2			9	6	7.2	0.1	-	0.8	4	1.3			32	4	7.1
25	ASDWFAPRY	ORF2a	92	4.9	2	0.8	0.05	0.1	0.2	71	9	0.17	0.3	-	-	3	0.8	1.3			50	32	39
26	RMMGHAWTPL	nsp5	99			5	2	2.9			32	15	20.4			50	4	7.4			15	3	5
27	RPFFSSWLV	ORF3	100			50	50	50	37.4	1	0.15	5	0.3			50	32	39			32	3	5.5
28	FVLSWLTPW	nsp5	90	-	-	3	1.5	2			32	2	3.8	13.7	3	3	0.8	1.3	-	-	50	0.4	0.8
29	MVNTTRVTY	nsp10	91	0.1	206†	3	0.8	1.3	0.2	47	1.5	0.17	0.3	-	-	4	1	1.6			32	9	14
30	CVFFLLWRM	nsp5	100			50	15	23.1	0.2	283	0.8	5	1.4			50	8	13.8			15	7	9.5
31	ATQEWLSRMW	nsp2	85	-	-	3	0.8	1.3			50	6	10.7	0.1	50,000†	5	1	1.7			50	2	3.8
32	VAHNLGFYF	nsp11	95			16	4	6.4			3	3	3			50	4	7.4			50	2	3.8
33	ITANVTDENY	ORF4	89	0.1	-	5	0.8	1.4	0.3	69	7	0.8	1.4	-	-	0.4	0.8	0.5			50	6	10.7
34	SSEGHLTSVY	ORF3	88	-	-	0.25	0.12	0.2	0.2	12,701†	32	0.8	1.6	0.1	1,692†	2	0.05	0.1			50	15	23.1
35	RTILGTNNFI	nsp9	94			15	4	6.3			50	32	39			15	4	6.3	0.3	60	5	0.4	0.7
36	LTAALNRNRW	nsp5	85	-	-	2	1.5	1.7			50	3	5.7	3.6	40	0.8	1	0.9	-	-	50	0.5	1
37	RTMLFTPSQL	nsp3	93			15	1.5	2.7			50	15	23.1			6	4	4.8	-	-	32	0.8	1.6
38	LSASSQTEY	nsp2	79	0.1	91†	3	0.5	0.9	0.2	479	50	0.5	1	0.2	-	0.5	1	0.7			50	6	10.7
39	VRWFAANLLY	nsp9	93			50	16	24.2	2.7	44	0.8	1	0.9			7	3	4.2			50	50	50
40	RMTSGNLNF	nsp1a	100	-	-	0.25	0.8	0.4			15	4	6.3			9	8	8.5			50	7	12.3
41	AGACWLSAIF	nsp1a	99	-	-	0.8	6	1.4			32	15	20.4			7	3	4.2			50	15	23.1
42	SAIPFRAPFF	nsp2	68			8	3	4.4			4	3	3.4	-	-	3	0.8	1.3			32	1.5	2.9
43	TTMPSGFELY	nsp9	75	-	576	0.8	0.25	0.4	0.8	6	0.5	0.05	0.1	0.2	1,838†	0.4	0.2	0.3	-	-	50	0.25	0.5
44	MSWRYSCTRY	ORF5	74	-	-	7	0.8	1.4	0.5	87	8	0.1	0.2	1.5	15	0.8	0.05	0.1			50	4	7.4
45	SSAFFLRYF	nsp5	66			50	2	3.8			15	5	7.5	0.1	-	0.8	0.5	0.6			50	4	7.4
46	ALATAPDGTY	nsp3	100	-	607†	50	0.5	1	0.1	2,736	0.8	1.5	1			7	3	4.2			50	32	39
47	RVRMGVFGCW	nsp2	99			32	7	11.5			50	16	24.2	-	-	1.5	3	2			50	32	39
48	WGVYSAIETW	ORF6	97			32	32	32			50	10	16.7	0.2	21,433	0.5	5	0.9			50	7	12.3
49	FLNCAFTFGY	ORF6	97	-	-	4	0.8	1.3	0.3	20	1	0.25	0.4			2	3	2.4			50	15	23.1
50	NSFLDEAAY	nsp10	96			2	3	2.4	0.1	43	9	0.5	0.9	-	-	5	0.4	0.7			50	15	23.1
51	RGRLLGLLHL	ORF6	100			32	50	39			50	50	50			32	15	20.4			50	50	50
52	LYRWRSPVI	ORF5	94			50	50	50			50	50	50			50	32	39			15	50	23.1
53	MPNYHWWVEH	nsp9	100			50	50	50	0.6	32	0.5	3	0.9			10	32	15.2			50	32	39
54	EVALSAQII	nsp9	89			15	32	20.4			32	32	32			15	15	15	18.3	2	0.5	1.5	0.8

***Table 2**: Overview of the results obtained from the in vitro studies. Left section lists the individual peptides represented by ID, sequence, locus of origin, and percent conservation among the 104 ancestry strains. Right section presents the measured and predicted values for the respective peptide-SLA combinations. Only combination predicted to have a combined rank score ≤ 2% were measured. From left to right the columns represent measured stability (average dissociation half-life in decimal hour (h)), measured affinity (average equilibrium dissociation constant (nM)), predicted binding by PSCPL (rank), predicted binding by NetMHCpan (rank), and combined predicted binding by calculating the harmonic mean of PSCPL and NetMHCpan (rank). †: only one successful affinity measurement could be obtained. Hyphen (-): no successful measurement (stability or affinity) could be obtained. Empty field: Not tested due to a predicted combined rank score > 2% for the given peptide-SLA combination.*

Due to internal errors, the NetMHCpan prediction was performed on SLA-2*0501 instead of the correct SLA-2*0502. Even though the two alleles are genetically very similar, their peptide binding specificities are only partly overlapping. Unfortunately, the mistake was not discovered before the peptides were purchased and as a consequence, only 9 out of the 53 peptides were predicted as binders to SLA-2*0502 while this number was formerly believed to be 24. For obvious reasons, this insight would have resulted in a different PopCover output and hence a different choice of peptides for purchase.

Experimental verification of predicted pSLA complexes

For each of the 53 peptides, each pSLA combination that was predicted to have a combined rank score ≤ 2% was tested *in vitro* for their individual binding characteristics in terms of affinity and stability. The results are presented in table 2. Note that only SLA-1*0401, SLA-1*0702, SLA-2*0401 and SLA-2*0502 were included in this experimental validation, as no functional assay could be generated for SLA-3*0401.

While the affinity represents the strength of a peptide-MHC (pMHC) interaction, the stability represents the longevity of this interaction once established. The two properties are mechanistically interrelated but are not mutually redundant, meaning that a peptide having a strong affinity will not necessarily form a highly stable complex, and vice versa. Obviously, the probability of a pMHC complex on the surface of a given cell to encounter and be recognized by an extremely rare circulating CTL with a cognate receptor is proportionate to how long this peptide is being displayed on the cell surface - the stability. Likewise, this probability is also proportionate to the number of successfully formed pMHC molecules in the first place - the affinity. Factors other than affinity and stability may also play a role, such as the level of protein being expressed in the cytosol from which the peptide is derived, and the rate at which the MHC molecule is internalized after peptide presentation on the cell surface.

In the earliest works of characterizing the pMHC interaction, both affinity and stability was given considerable focus (Buus et al. 1987; Parker et al. 1992). Regardless, the vast majority of available pMHC binding data is in the form of affinity data since the acquisition of stability data has previously been cumbersome and laborious. Recently, the SPA method used in this study, being a high-throughput one-step method for measuring pMHC stability was developed by Harndahl et al. (2011), and shortly after, Harndahl et al. (2012) showed that immunogenic peptides tend to be more stably bound to MHC-I molecules than non-immunogenic peptides, suggesting to focus on stability rather than affinity as a determinant for peptide immunogenicity. In the wake of this, the NetMHCstab and NetMHCstabpan servers were recently established (Jørgensen et al. 2014; Rasmussen et al. 2016). Unfortunately, these servers have so far only been trained with human data, and could therefore not be implemented in this study.

In the light of the indicated proportionality between immunogenicity and stability, it has become convenient to define a threshold separating binders from non-binders. While the NetMHCstab server defines the thresholds for weakly and strongly stable pMHC complexes to be a t½ ≥ 2 hours and t½ ≥ 6 hours, respectively, other studies have been less strict and included pMHCs with t½ ≥ 30 minutes. Out of the 101 pMHC complexes tested in this study, 23 of these exhibited a t½ ≥ 30 minutes (5/30 pSLA-1*0401, 10/26 pSLA-1*0702, 7/36 pSLA-2*0401 and 1/9 pSLA-2*0502). 10 of these had a t½ ≥ 2 hours, and 4 had a t½ ≥ 6 hours. Interestingly, peptide ID54 (EVALSAQII), that was included due to its previous mention in the literature was measured to bind very stably to SLA-2*0502 (t½ = 18.3 h), hinting that the responsive animals used by Parida et al. (2012) could have expressed this particular allele.

Correlations between predicted and measured values

To quantify the performance of the three prediction strategies employed for peptide selection, a correlation analysis between the predicted rank score and the measured binding affinity and binding stability values was performed. The

analysis was limited to the molecules SLA-1*0401, SLA-1*0702, SLA-2*0401, and SLA-2*0502, and the results are displayed in figure 2. From this analysis, it is apparent that none of the two methods, NetMHCpan and PSCPL, consistently outperformed the other.

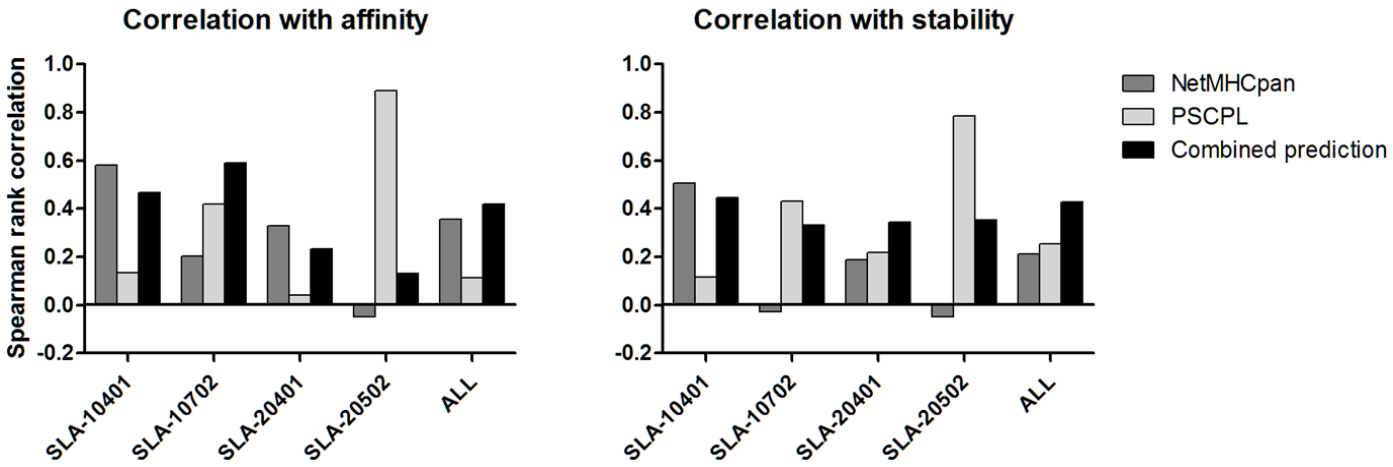

***Figure 2**: Correlation analysis between measured binding affinity/stability and predicted rank values for the three methods NetMHCpan, PSCPL, and combined prediction. Correlations were quantified in term of Spearman rank correlation. ALL gives the correlation values for the combined data set of the four SLA molecules.*

The PSCPL method achieved the highest performance of the two methods for 50% of the SLA alleles on the binding affinity data and for 75% of the alleles in the stability data. Each method performed very poorly with close to zero or negative correlations in at least one case each. In contrast to this, the performance of the combined method was consistently high across all 4 SLA alleles, thus achieving the highest performance of the three methods on both the affinity and stability data when evaluated on the data set combined of all SLA measurements. This finding thereby confirmed the earlier finding that combining prediction of NetMHCpan and PSCPL leads to a superior performance for identifying peptide binders to MHC molecules characterized by limited or no binding data (Rasmussen et al. 2014; Hansen et al. 2014).

We next extended this analysis to include an evaluation of the sensitivity (true positive rate) and specificity (true negative rate) of the respective methods. Due to the inconsistencies between the SLA allele used to selected peptides and the allele actually used in the study for the SLA-2*0501/02, the SLA-2*0501 allele was excluded from this analysis, which was hence limited to SLA-1*0401, SLA-1*0702 and SLA-2*0401. The results are given in figure 3, depicting the sensitivity and specificity as a function of the prediction rank threshold for the three respective methods for the three different SLA molecules.

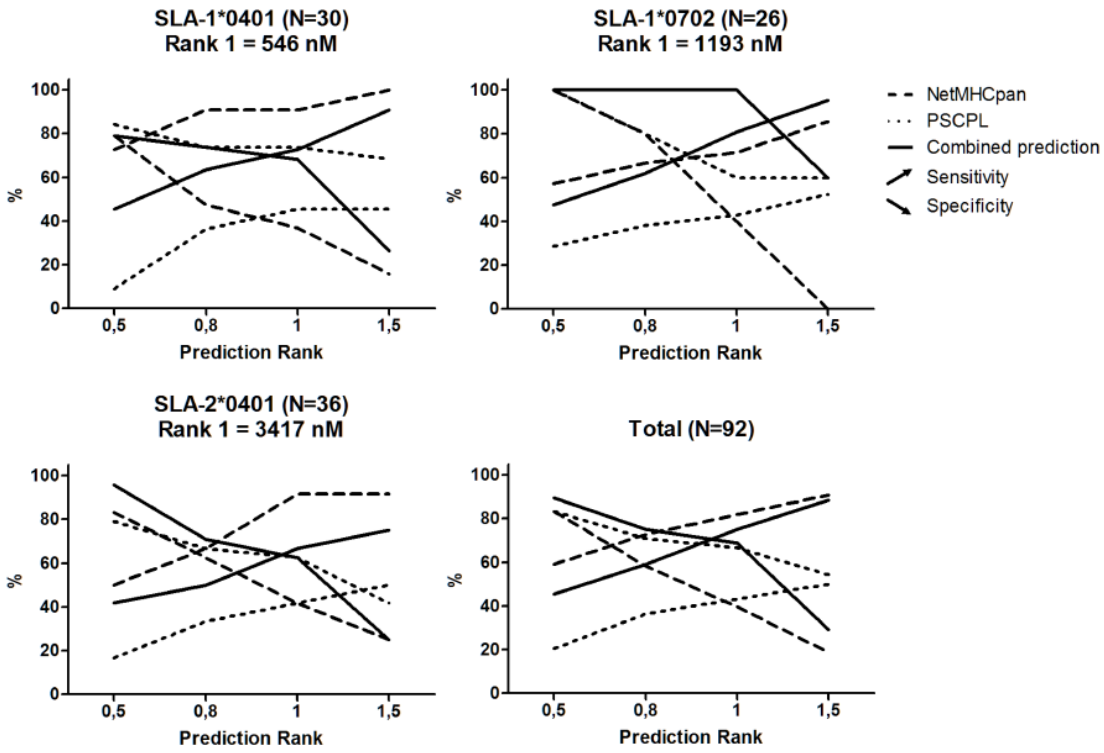

***Figure 3**: Analysis of sensitivity and specificity of the three methods with relation to the three alleles: SLA-1*0401, SLA-1*0702 and SLA-2*0401. Values of sensitivity and specificity were calculated based on four different values of prediction rank against a constant observed rank of 1. kD values in nM corresponding to rank=1 are stated for each allele.*

Due to the fact different MHC molecules display very different binding potential when it comes to both affinity (Paul et al. 2013; Nielsen and Andreatta 2016) and stability (Rasmussen et al. 2016), an allele specific affinity threshold was identified to define peptide binders. This threshold was defined from the 1% percentile affinity score obtained by predicting binding to 200,000 random natural peptides using NetMHCpan (version 2.9).We are aware that using this approach might introduce a bias in favor of the NetMHCpan prediction. Nevertheless, we regarded this as a better estimate and representative of the individual alleles, than the hitherto general definition of a uniform threshold at 500 nM that does not account for any allele specific-variation (Yewdell and Bennink 1999). As expected, the obtained affinity thresholds demonstrated substantial variations with values spanning 546 nM for SLA-1*0401 to 3415 nM for SLA-2*0401.

In general, a high performance method should have a point on the graphs with high sensitivity and specificity values. Given this, the value corresponding to the cross-point of the sensitivity and specificity curves can be taken as a measure of predictive performance of a given method. Using this performance measure, NetMHCpan demonstrates a general very high performance, with cross-point values for the three SLA molecules in the range 0.64 – 0.75, meaning that on average 70% of the binding peptides are captured at a false positive rate of 30% (figure 3). For the PSCPL method these values are substantially lower and in two of the three cases no cross-point is identified in the rank score range included in the analysis, suggesting a low sensitivity of this approach. However, even in this situation, the combination of the two approaches leads to an overall improved performance, with a substantially improved cross-point (0.86 compared to 0.68) value for SLA-1*0702. These findings thus consolidate the earlier

conclusion that integrating PSCPL and NetMHCpan predictions lead to overall superior performance compared to any of the individual methods alone.

Perspectives of an epitope based vaccine strategy

The central concept of vaccinology is defined by the proper presentation of antigen to the immune system. For a vaccine to induce a CMI, more specifically, the antigen is presented on a MHC-I molecule as an 8-10-mer epitope for subsequent recognition by a cognate cytotoxic T cell. Applying this to a real life vaccine trial, this concept splits up into three cardinal points that should be considered during the development of an epitope-based vaccine: 1) *Pathogen diversity*. While it would be very unlikely to identify a single immunogenic epitope expressed by all circulating strains of the target pathogen, the epitopes included in the vaccine should reflect the diversity of the circulating target pathogen. Choosing conserved epitopes must be regarded as the only rational approach, as this would not only ensure the highest degree of pathogen coverage attained by the lowest number of epitopes, but would also exclude epitopes that are dispensable for the pathogen. It is likely, however, that a higher selection pressure on conserved epitopes may lead to the employment of mechanisms to prevent these epitopes from being immunogenic. Such mechanisms could result in a level of surface display sufficiently low to avoid CTL priming and activation. If this is the case, one could speculate that an artificially raised level of display in terms of a vaccine could activate cognate CTLs to such an extent that they would recognize and kill cells displaying an otherwise negligible level of epitopes, i.e. cells infected with wild type virus. 2) *Herd diversity*. Currently, 216 SLA class I alleles are known, including 62 SLA-1, 61 SLA-2, and 32 SLA-3 alleles. The majority of the SLA alleles are published in the Immune Polymorphism Database (http://www.ebi.ac.uk/ipd/mhc/sla/). This number is relatively small compared to the known human MHC-I diversity counting several thousand proteins and is likely to be a consequence of scientific focus and limited genetic diversity within the swine industry. Although their peptide specificities overlap to some extent, the limited number of epitopes included in a vaccine should be selected to match the allelic diversity of a target population. 3) *Epitope immunogenicity*. While the notion of being immunogenic is not synonymous with providing protection, it is definitely a prerequisite. Beyond epitope abundance, the underlying mechanisms of epitope immunogenicity involve six steps: i) cleavage of a cytosolic protein into smaller fragments by the immuno- or conventional proteasome; ii) transportation of these fragments into the endoplasmic reticulum by TAP; iii) N-terminal trimming of the fragments by aminopeptidases (Serwold et al. 2002) iv) association of the peptide to the MHC-I molecule; v) vesicular transportation of the pMHC complex to the cell surface; and vi) recognition of the pMHC by a CTL with a cognate T cell receptor. The steps i-iii relate to the preprocessing of the peptides, and even though information can be gained from the specificities of the involved enzymes and transporters, this information has no impact on the NetMHCpan predictions used in this study (Peters et al. 2003; Nielsen et al. 2005). Consequently, it was decided not to take this into account. The steps iv and vi, however, represent the most selective steps in the MHC-I presentation pathway and recognition by circulating T cells, respectively.

In this study, we have defined and characterized an ensemble of conserved PRRSV-2 CTL epitopes for the future development of an epitope-based vaccine. The abovementioned three cardinal points have been met by 1) deriving all 9-10 mer peptides from a database of 104 wild type strains; 2) designing an ensemble of 53 epitope candidates predicted for an optimal representation of antigen to a fictive target population expressing the five SLAs in question. This was done by the use of bioinformatics tools for epitope prediction (NetMHCpan and PSCPL) and subsequent ranking of epitope candidates (PopCover); and 3) verification of MHC binding of the 53 selected epitopes candidates to the five SLAs using *in vitro* pMHC stability and affinity assays. In addition to this, the correlation between predicted and observed binding data was analyzed for NetMHCpan, PSCPL and the combination of the two. In accordance with earlier studies, none of the individual methods consistently outperformed the other, and the combination of the two performed a robust prediction across all SLA with a relatively high correlation.

CONCLUDING REMARKS

In order to obtain an ensemble of epitopes that can provide protection to a population of diverse haplotypes, the ensemble must consist of epitopes that collectively will bind to the majority of haplotypes present in the population. The PopCover algorithm was employed in this study to prioritize between the peptides based on both their degree of conservation and their 'promiscuity' with regards to SLA binding. While these two factors are central in the definition of a peptide ensemble, weight coefficients could be adjusted in relation to the individual strains, peptides, and SLA alleles, in order to fine-tune the definition of the ensemble. Weight coefficients related to the individual strains should be set to compensate for a bias induced by an overrepresentation of similar strains in cases where this would reflect an intensely sequenced incidence of disease rather than reflecting the actual diversity of the strains. As an example, this study includes 7 viruses isolated in Laos in 2010. As seen in figure 1, these strains are very closely related and do most likely represent 7 variants of the same strain rather than 7 different strains. Consequently, the weight coefficients of these should be adjusted to make them have a collective impact corresponding to a single strain. For the individual peptides, weight coefficients should be given to reflect their relative levels of expression. In case of PRRSV, the expression levels differ substantially between loci, strongly influenced by the programmed ribosomal frameshifting sites. According to Fang et al. (2012) only about 15% of the translation initiated at the beginning of ORF1a will proceed to ORF1b. As a result, peptides derived from ORF1b will be much less abundant compared to peptides derived from ORF1a, and should be reflected accordingly by their weight coefficients. Also for the MHC alleles a weight coefficient could be implemented to reflect their relative levels of expression. On that node, we have observed that the average level of cDNA derived from SLA-3 mRNA was less than 10% of the overall SLA cDNA. The remaining 90% were more or less evenly distributed between SLA-1 and SLA-2 derived cDNA (unpublished data). This may, however, stand in contrast to the abundance of a given MHC allele in the herd in general, which in case of SLA-3 was indeed found to be quite abundant in some populations (Pedersen et al. 2014). Thus, two weight coefficients could be given for the MHCs, reflecting both the relative levels of expression in the individuals, and levels of abundance in the population.

It is obvious that the definition of an optimal epitope ensemble for the induction of an immune response against a pathogen on the population level is not straight forward. In the current study, none of the abovementioned weight coefficients have been used to balance the epitope candidates. Because of this, and because of confusion regarding SLA-2*0501 and SLA2*0502, the presented ensemble of 53 peptides is most probably different from how it would be composed otherwise. Nonetheless, 53 conserved peptides have been analyzed *in vitro* for their binding capacities to five different SLAs. The biological significance of these results are yet to be tested, and may ultimately aid in the development of a CTL-activating vaccine against PRRSV.

AUTHOR'S CONTRIBUTIONS

LL and GJ conceived the study. MR performed the *in vitro* stability measurements. SB provided the recombinant proteins for the affinity and stability studies, in addition to lab equipment for the latter. SW analyzed the sequences and performed the *in vitro* affinity measurements. SW and MN performed the bioinformatics analyses and wrote the manuscript. All authors read and approved the final manuscript.

REFERENCES

Bautista E, Molitor T (1997) Cell-mediated immunity to porcine reproductive and respiratory syndrome virus in swine. Viral Immunol 10:83–94.

Beilage E, Nathues H, Meemken D, et al (2009) Frequency of PRRS live vaccine virus (European and North American genotype) in vaccinated and non-vaccinated pigs submitted for respiratory tract diagnostics in North-Western Germany. Prev.Vet.Med. 92:31–37.

Botner A, Strandbygaard B, Sorensen KJ, et al (1997) Appearance of acute PRRS-like symptoms in sow herds after vaccination with a modified live PRRS vaccine. Vet.Rec. 141:497–499.

Buggert M, Norström MM, Czarnecki C, et al (2012) Characterization of HIV-specific CD4+ T cell responses against peptides selected with broad population and pathogen coverage. PLoS One 7:e39874. doi: 10.1371/journal.pone.0039874

Buus S, Sette A, Colon SM, et al (1987) The relation between major histocompatibility complex (MHC) restriction and the capacity of Ia to bind immunogenic peptides. Science 235:1353–8.

Chen C, Li J, Bi Y, et al (2013) Synthetic B- and T-cell epitope peptides of porcine reproductive and respiratory syndrome virus with Gp96 as adjuvant induced humoral and cell-mediated immunity. Vaccine 31:1838–47. doi: 10.1016/j.vaccine.2013.01.049

Costers S, Lefebvre DJ, Goddeeris B, et al (2009) Functional impairment of PRRSV-specific peripheral CD3+CD8high cells. Vet Res 40:46. doi: 10.1051/vetres/2009029

Fang Y, Treffers EE, Li Y, et al (2012) Efficient -2 frameshifting by mammalian ribosomes to synthesize an additional arterivirus protein. Proc Natl Acad Sci U S A 109:E2920-8. doi: 10.1073/pnas.1211145109

Hansen AM, Rasmussen M, Svitek N, et al (2014) Characterization of binding specificities of bovine leucocyte class I molecules: impacts for rational epitope discovery. Immunogenetics 66:705–18. doi: 10.1007/s00251-014-0802-5

Harndahl M, Rasmussen M, Roder G, et al (2012) Peptide-MHC class I stability is a better predictor than peptide affinity of CTL immunogenicity. Eur J Immunol 42:1405–16. doi: 10.1002/eji.201141774

Harndahl M, Rasmussen M, Roder G, Buus S (2011) Real-time, high-throughput measurements of peptide-MHC-I dissociation using a scintillation proximity assay. J Immunol Methods 374:5–12. doi: 10.1016/j.jim.2010.10.012

Holtkamp DJ, Kliebenstein JB, Neumann EJ, et al (2013) Assessment of the economic impact of porcine reproductive and respiratory syndrome virus on United States pork producers. J Swine Heal Prod 21:72–84.

Hoof I, Peters B, Sidney J, et al (2009) NetMHCpan, a method for MHC class I binding prediction beyond humans. Immunogenetics 61:1–13. doi: 10.1007/s00251-008-0341-z

Jiang Y, Xia T, Zhou Y, et al (2015) Characterization of three porcine reproductive and respiratory syndrome virus isolates from a single swine farm bearing strong homology to a vaccine strain. Vet Microbiol 179:242–249. doi: 10.1016/j.vetmic.2015.06.015

Jørgensen KW, Rasmussen M, Buus S, Nielsen M (2014) NetMHCstab - predicting stability of peptide-MHC-I complexes; impacts for cytotoxic T lymphocyte epitope discovery. Immunology 141:18–26. doi: 10.1111/imm.12160

Karniychuk UU, Nauwynck HJ (2013) Pathogenesis and prevention of placental and transplacental porcine reproductive and respiratory syndrome virus infection. Vet Res 44:95. doi: 10.1186/1297-9716-44-95

Kast WM, Brandt RM, Sidney J, et al (1994) Role of HLA-A motifs in identification of potential CTL epitopes in human papillomavirus type 16 E6 and E7 proteins. J Immunol 152:3904–12.

Kuhn JH, Lauck M, Bailey AL, et al (2016) Reorganization and expansion of the nidoviral family Arteriviridae. Arch Virol 161:755–768. doi: 10.1007/s00705-015-2672-z

Lamontagne L, Pagé C, Larochelle R, Magar R (2003) Porcine reproductive and respiratory syndrome virus persistence in blood, spleen, lymph nodes, and tonsils of experimentally infected pigs depends on the level of CD8high T cells. Viral Immunol 16:395–406. doi: 10.1089/088282403322396181

Lohse L, Nielsen J, Eriksen L (2004) Temporary CD8+ T-cell depletion in pigs does not exacerbate infection with porcine reproductive and respiratory syndrome virus (PRRSV). Viral Immunol 17:594–603. doi: 10.1089/vim.2004.17.594

López Fuertes L, Doménech N, Alvarez B, et al (1999) Analysis of cellular immune response in pigs recovered from porcine respiratory and reproductive syndrome infection. Virus Res 64:33–42.

Lundegaard C, Karlsson A, Perez C, et al (2010) PopCover: A method for selecting of peptides with optimal Population and Pathogen Coverage. BCB '10 Proc First ACM Int Conf Bioinforma Comput Biol 658–659.

Lundegaard C, Lund O, Nielsen M (2008) Accurate approximation method for prediction of class I MHC affinities for peptides of length 8, 10 and 11 using prediction tools trained on 9mers. Bioinformatics 24:1397–8. doi: 10.1093/bioinformatics/btn128

Madsen KG, Hansen CM, Madsen ES, et al (1998) Sequence analysis of porcine reproductive and respiratory syndrome virus of the American type collected from Danish swine herds. Arch.Virol. 143:1683–1700.

Nielsen M, Lundegaard C, Lund O, Keşmir C (2005) The role of the proteasome in generating cytotoxic T-cell epitopes: insights obtained from improved predictions of proteasomal cleavage. Immunogenetics 57:33–41. doi: 10.1007/s00251-005-0781-7

Nielsen M, Andreatta M (2016) NetMHCpan-3.0; improved prediction of binding to MHC class I molecules integrating information from multiple receptor and peptide length datasets. Genome Med 8:33. doi: 10.1186/s13073-016-0288-x

Nieuwenhuis N, Duinhof TF, van Nes A (2012) Economic analysis of outbreaks of porcine reproductive and respiratory syndrome virus in nine sow herds. Vet Rec 170:225. doi: 10.1136/vr.100101

Pandya M, Rasmussen M, Hansen A, et al (2015) A modern approach for epitope prediction: identification of foot-and-mouth disease virus peptides binding bovine leukocyte antigen (BoLA) class I molecules. Immunogenetics 67:691–703. doi: 10.1007/s00251-015-0877-7

Parida R, Choi I-SS, Peterson DA, et al (2012) Location of T-cell epitopes in nonstructural proteins 9 and 10 of type-II porcine reproductive and respiratory syndrome virus. Virus Res 169:13–21. doi: 10.1016/j.virusres.2012.06.024

Parker KC, Bednarek MA, Hull LK, et al (1992a) Sequence motifs important for peptide binding to the human MHC class I molecule, HLA-A2. J Immunol 149:3580–7.

Parker KC, DiBrino M, Hull L, Coligan JE (1992b) The beta 2-microglobulin dissociation rate is an accurate measure of the stability of MHC class I heterotrimers and depends on which peptide is bound. J Immunol 149:1896–904.

Paul S, Weiskopf D, Angelo MA, et al (2013) HLA class I alleles are associated with peptide-binding repertoires of different size, affinity, and immunogenicity. J Immunol 191:5831–9. doi: 10.4049/jimmunol.1302101

Pedersen LE, Harndahl M, Nielsen M, et al (2012) Identification of peptides from foot-and-mouth disease virus structural proteins bound by class I swine leukocyte antigen (SLA) alleles, SLA-1*0401 and SLA-2*0401. Anim Genet 44:251–8. doi: 10.1111/j.1365-2052.2012.02400.x

Pedersen LE, Harndahl M, Rasmussen M, et al (2011) Porcine major histocompatibility complex (MHC) class I molecules and analysis of their peptide-binding specificities. Immunogenetics 63:821–34. doi: 10.1007/s00251-011-0555-3

Pedersen LE, Jungersen G, Sorensen MR, et al (2014a) Swine Leukocyte Antigen (SLA) class I allele typing of Danish swine herds and identification of commonly occurring haplotypes using sequence specific low and high resolution primers. Vet Immunol Immunopathol 162:108–16. doi: 10.1016/j.vetimm.2014.10.007

Pedersen LE, Rasmussen M, Harndahl M, et al (2014b) An analysis of affinity and stability in the identification of peptides bound by Swine Leukocyte Antigens (SLA) combining matrix- and NetMHCpan based peptide selection.

Pedersen LE, Rasmussen M, Harndahl M, et al (2016) A combined prediction strategy increases identification of peptides bound with high affinity and stability to porcine MHC class I molecules SLA-1*04:01, SLA-2*04:01, and SLA-3*04:01. Immunogenetics 68:157–165. doi: 10.1007/s00251-015-0883-9

Peters B, Bulik S, Tampe R, et al (2003) Identifying MHC Class I Epitopes by Predicting the TAP Transport Efficiency of Epitope Precursors. J Immunol 171:1741–1749. doi: 10.4049/jimmunol.171.4.1741

Rasmussen M, Fenoy E, Harndahl M, et al (2016) Pan-Specific Prediction of Peptide-MHC Class I Complex Stability, a Correlate of T Cell Immunogenicity. J Immunol 197:1517–24. doi: 10.4049/jimmunol.1600582

Rasmussen M, Harndahl M, Stryhn A, et al (2014) Uncovering the peptide-binding specificities of HLA-C: a general strategy to determine the specificity of any MHC class I molecule. J Immunol 193:4790–802. doi: 10.4049/jimmunol.1401689

Renukaradhya GJ, Meng X-J, Calvert JG, et al (2015a) Inactivated and subunit vaccines against porcine reproductive and respiratory syndrome: Current status and future direction. Vaccine 33:3065–72. doi: 10.1016/j.vaccine.2015.04.102

Renukaradhya GJ, Meng X-J, Calvert JG, et al (2015b) Live porcine reproductive and respiratory syndrome virus vaccines: Current status and future direction. Vaccine 33:4069–80. doi: 10.1016/j.vaccine.2015.06.092

Samsom JN, de Bruin TG, Voermans JJ, et al (2000) Changes of leukocyte phenotype and function in the broncho-alveolar lavage fluid of pigs infected with porcine reproductive and respiratory syndrome virus: a role for CD8(+) cells. J Gen Virol 81:497–505. doi: 10.1099/0022-1317-81-2-497

Serwold T, Gonzalez F, Kim J, et al (2002) ERAAP customizes peptides for MHC class I molecules in the endoplasmic reticulum. Nature 419:480–483. doi: 10.1038/nature01074

Stryhn A, Pedersen LO, Romme T, et al (1996) Peptide binding specificity of major histocompatibility complex class I resolved into an array of apparently independent subspecificities: quantitation by peptide libraries and improved prediction of binding. EurJImmunol 26:1911–1918. doi: 10.1002/eji.1830260836

Sylvester-Hvid C, Kristensen N, Blicher T, et al (2002) Establishment of a quantitative ELISA capable of determining peptide - MHC class I interaction. Tissue Antigens 59:251–8.

Tingstedt J-E, Nielsen J (2004) Cellular immune responses in the lungs of pigs infected in utero with PRRSV: an immunohistochemical study. Viral Immunol 17:558–64. doi: 10.1089/vim.2004.17.558

Vashisht K, Goldberg TL, Husmann RJ, et al (2008) Identification of immunodominant T-cell epitopes present in glycoprotein 5 of the North American genotype of porcine reproductive and respiratory syndrome virus. Vaccine 26:4747–53. doi: 10.1016/j.vaccine.2008.06.047

Wang Y-X, Zhou Y-J, Li G-X, et al (2011) Identification of immunodominant T-cell epitopes in membrane protein of highly pathogenic porcine reproductive and respiratory syndrome virus. Virus Res 158:108–15. doi: 10.1016/j.virusres.2011.03.018

Yewdell JW, Bennink JR (1999) Immunodominance in major histocompatibility complex class I-restricted T lymphocyte responses. Annu Rev Immunol 17:51–88. doi: 10.1146/annurev.immunol.17.1.51

Zuckermann FA, Garcia EA, Luque ID, et al (2007) Assessment of the efficacy of commercial porcine reproductive and respiratory syndrome virus (PRRSV) vaccines based on measurement of serologic response, frequency of

gamma-IFN-producing cells and virological parameters of protection upon challenge. Vet Microbiol 123:69–85. doi: 10.1016/j.vetmic.2007.02.009

PAPER 2

Manuscript in preparation

CHALLENGE STUDY OF PIGS IMMUNIZED WITH VIRUS REPLICON PARTICLES FOR THE INDUCED EXPRESSION OF CONSERVED PRRSV-2 CTL EPITOPES

ABSTRACT

Porcine Reproductive and Respiratory Syndrome Virus (PRRSV) is the causative agent of respiratory distress and reproductive failure in swine, can act as a co-factor in multiple bacterial and viral diseases, and has resulted in devastating outbreaks of highly pathogenic strains. Despite numerous attempts to develop a vaccine capable of inducing persistent protection against heterologous PRRSV infection, none have so far succeeded. Here we describe the generation of virus replicon particles (VRP) using a defective classical swine fever virus genome incapable of producing infectious progeny and designed to express conserved PRRSV-2 epitopes. These epitopes were selected from previous experiments in which they were defined as binders to selected swine leukocyte antigens (SLA) class I alleles. VRP Infectivity and induced epitope expression was verified *in vitro* before the VRPs were used to vaccinate or sham vaccinate 18 SLA-matched pigs divided in a test group and a control group, respectively, followed by PRRSV challenge. Clinical, virological, serological and immunological analysis of the pigs was performed throughout the experiment, to monitor VRP replication and PRRSV infection and the immunological responses after both. A decrease in virus load in the test group was significant in one out of three analyzed lung parts. However, no significant difference of challenge virus load was observed in the serum, when compared to the control group. The number of PBMCs secreting IFN-γ upon peptide stimulation was higher and was triggered by more peptides in the test group than in the control group. However, the same IFN-γ secretion profiles could not be obtained with PBMCs isolated 2 weeks later. The current study provides indications of a shapeable PRRSV-specific cell-mediated immune response with protective capacities, and may inspire to future study designs.

AUTHORS

Simon Welner: Email: Simon@Welner.dk, Institutional address: Section of Virology, National Veterinary Institute, Technical University of Denmark, Bülowsvej 27, 1870 Frederiksberg C, Denmark.

Simea Werder: Email: SimeaWerder@gmail.com, institutional address: Institute of Virology and Immunology IVI, Sensemattstrasse 293, 3147 Mittelhäusern, Switzerland.

Markus Gerber: Email: Markus.Gerber@ivi.admin.ch, institutional address: Institute of Virology and Immunology IVI, Sensemattstrasse 293, 3147 Mittelhäusern, Switzerland.

Matthias Liniger: Email: Matthias.Liniger@ivi.admin.ch, institutional address: Institute of Virology and Immunology IVI, Sensemattstrasse 293, 3147 Mittelhäusern, Switzerland.

Artur Summerfeld: Email: Artur.Summerfield@ivi.admin.ch, institutional address: Institute of Virology and Immunology IVI, Sensemattstrasse 293, 3147 Mittelhäusern, Switzerland.

Nicolas Ruggli: Email: Nicolas.Ruggli@ivi.admin.ch, institutional address: Institute of Virology and Immunology IVI, Sensemattstrasse 293, 3147 Mittelhäusern, Switzerland.

Gregers Jungersen: Email: grju@vet.dtu.dk, Institutional address: Section of Immunology and Vaccinology, National Veterinary Institute, Technical University of Denmark, Bülowsvej 27, 1870 Frederiksberg C, Denmark.

Lars Erik Larsen: Email: lael@vet.dtu.dk, Institutional address: Section of Virology, National Veterinary Institute, Technical University of Denmark, Bülowsvej 27, 1870 Frederiksberg C, Denmark.

INTRODUCTION

Porcine Reproductive and Respiratory Syndrome Virus (PRRSV) is a small enveloped virus with a single-stranded positive-sense RNA genome belonging to the *Arteriviridae* family. It is the causative agent of reproductive failure in late gestation sows (Karniychuk and Nauwynck 2013) and respiratory distress, particularly in young pigs (Rossow 1998). PRRSV infections continue to cause tremendous economic losses in pig producing countries around the world, in particular outbreaks with virulent strains such as 'Porcine High Fever Disease' in South-East Asia (Tian et al. 2007) and the highly virulent MN184 strains in the US (Han et al. 2006).

The virus was originally divided into two genotypes, type 1 and type 2, representing the European and North American/Asian genotypes, respectively. Recent restructuring of the *Arteriviridae* taxonomy, however, has reclassified the two genotypes into two distinct species: PRRSV-1 (type 1) and PRRSV-2 (type 2) (ictvonline.org). Both species are enzootic in most swine producing countries (Chen et al. 2011; Kvisgaard et al. 2013; Nilubol et al. 2013)

The most common method to control the virus is by the use of vaccination. The strongest protective response is obtained using species-specific modified live virus (MLV) vaccines. The use of MLV vaccines, however, is connected to a number of unwanted effects: 1) there is an inherent and documented risk that the attenuated strain spreads to naïve animals within the herd and by that promote reversion to virulence and subsequent viral transmission and disease (Botner et al. 1997; Madsen et al. 1998; Beilage et al. 2009; Jiang et al. 2015); 2) Vaccination of pregnant sows in the last trimester may results in reproductive failures, birth of stillborn and/or persistently infected piglets (Rowland et al.); 3) The MLV persist in the herds for months or even years making the vaccines difficult to use as a tool to eradicate the virus from the herd without production stop; 4) Impaired effect of the some of the MLV vaccines against heterologous field strains. Thus, there is a need for development of PRRSV vaccines that can circumvent some or all of the limitation of the existing vaccines as described above.

Multiple strategies for antigen selection, virus attenuation, adjuvants and delivery systems have been tested including killed virus (KV), 2nd generation MLV, and vaccines based on recombinant protein and DNA. The performance of these new vaccine entities in terms of effect on viral clearance and relief of symptoms are diverse (reviewed in Renukaradhya et al. 2015a and Renukaradhya et al. 2015b). Although they all succeed to induce some degree of an immune response – characterized as virus-specific antibodies or an increased cell-mediated immune response (CMI) – none of them seem capable of providing a sustained protective response against a heterologous challenge.

Both CMI and especially humoral immunity have been intensely investigated in response to PRRSV infection. The results of these studies are often contradictive and the conclusions about the importance of a CMI in the protective immune response against PRRSV are vague. It appears that many unknowns are present, resulting in different observations among strains and among pigs. Nonetheless, the theoretical framework is unambiguously suggesting that a legion of activated CTLs primed against specific PRRSV epitopes, should be able to identify and kill PRRSV infected cells (briefly reviewed in paper 1).

Virus replicon particles (VRP) represent a platform that – similar to virus vectors – can induce both a humoral and a cell mediated immune response through the continuous replication and translation of viral genes and transgenes. In comparison to virus vectors though, VRPs are safer and easier to control, as they cannot package into progeny virions unless a key structural protein is provided *in trans*. This means that once a cell has been infected with VRP, genes encoded by the VRP will be continuously translated and presented to circulating immune cells without any risk of cell-to-cell propagation. Nonetheless, the similarity of replicon RNA to a natural pathogen, can trigger multiple immune pathways and can therefore be regarded as self-adjuvanting (McCullough et al. 2014).
The replicon technology has been known for many decades and several replicon-based vaccines have been tested in both human and animal trials, some of which have been licensed as commercial vaccines (replicon vaccines reviewed in Hikke & Pijlman 2017; Lundstrom 2016). A very recent experiment described the vaccination with a recombinant vesicular stomatitis virus VRP expressing the PRRSV structural proteins, GP2-5, M and the nucleocapsid protein, N (Eck et al. 2016). Although no reduction in viremia was observed following challenge with PRRSV, antibodies against the N protein was detected prior to challenge, and a 2 weeks earlier antibody response against GP3/GP4/GP5 was observed after challenge compared with the pigs vaccinated with the empty control VRP.
A majority of studies describe replicons that express whole proteins or larger antigenic fragments, but recent advances in custom DNA synthesis and next-generation sequencing technologies have accelerated replicon development and facilitated the integration of specifically designed transgenes. Several examples exist of replicon- or viral vector-based vaccines expressing transgenic single epitopes or polyepitopes for the induction of a cytotoxic T-cell response and in many cases protective immunity upon challenge have been successfully established (Blomquist et al. 2002; Herd et al. 2004; Wang et al. 2012; De Baets et al. 2013). To the best of our knowledge, no vaccination studies with replicons for the induction of a CMI against PRRSV have been reported.

In the present study, we describe the development of a VRP-based vaccine targeting the induction of a sustained and cross-reactive CMI against PRRSV-2 by the expression of conserved epitopes previously verified as binders to relevant swine leukocyte antigens (SLA), SLA-1*0401, SLA-1*0702, and SLA-2*0401 (paper 1). We further describe the execution of a subsequent vaccination-challenge experiment and the concurrent measuring of relevant serological, virological, clinical and immunological parameters.

MATERIALS AND METHODS

Plasmid design and cloning

The bicistronic plasmid pA187-N^{pro}-IRES-C-delE^{rns} encoding a CSFV replicon was described previously (Suter et al. 2011). It was derived from the full-length cDNA clone pA187-1 (Ruggli et al. 1996) by deleting the E^{rns} gene and introducing an internal ribosome entry site (IRES) between the N^{pro} and C genes. In the present study, a synthetic gene cassette codon-optimized for porcine tRNA and encoding the C-terminal part of N^{pro} with a $C_{138}A$ substitution, a porcine ubiquitin monomer (Ub, Acc: NP_001098779), a hemagglutinin tag (HA), a KasI restriction site, the SIINFEKL

epitope, a MluI restriction site, a FLAG tag, and a stop codon was obtained from GenScript (Piscataway) and used to replace the ClaI-to-NotI fragment of pA187-N^{pro}-IRES-C-delE^{rns}. The C-terminal glycine of Ub was mutated to a valine ($G_{76}V$) in order to prevent cell-mediated cleavage of Ub from the downstream HA-tagged polyepitope, ensuring poly-ubiquitination and proteasomal degradation of the Ub-polyepitope chimera, thereby favoring MHC-I-mediated peptide presentation (Bazhan et al. 2010). The $C_{138}A$ substitution in N^{pro} prevents N^{pro}-mediated inhibition of type I IFN induction (Szymanski et al. 2009). This plasmid was termed pA187-N^{pro}-epi-IRES-C-delE^{rns} and served as a backbone for the nine different PRRSV-2 polyepitopes (figure 1) by replacing the SIINFEKL epitope with the polyepitope sequence of interest using the restriction sites KasI and MluI. For each of the three SLAs, three polyepitopes were designed containing the same individual PRRSV epitopes, but in a different order to compensate for potential translation and/or degradation artifacts related to primary structures (supplementary data 1, page 123). The individual epitopes (table 1, black dots) were selected based on *in vitro* binding data obtained from a previous study (paper 1). A Python-based program was developed to minimize the number of neoepitopes in the regions spanning two neighboring PRRSV epitopes. This software was used to design the polyepitopes that were subsequently reverse translated to cDNA. Synthetic codon-optimized gene cassettes of the cDNA sequences were purchased from GenScript (Piscataway) and inserted between the KasI and MluI restriction sites of. All constructs were verified by nucleotide sequencing.

ID	Sequence	Locus	SLA-1*0401		SLA-1*0702		SLA-2*0401		Challenge strain	ELISPOT
			stab. (h)	aff. (nM)	stab. (h)	aff. (nM)	stab. (h)	aff. (nM)		
2	YAQHMVLSY	nsp9	-	-	● 0.9	4	● 1.1	60	√	√
4	YSFPGPPFF	nsp9	0.2	37†	● 0.2	18,708	-	-		
5	RALPFTLSNY	ORF2a			● 0.3	12	0.1	-	√	
7	QVYERGCRWY	nsp1a	● 0.3	682	● 4.5	168	● 0.7	209†	√	√
9	IVYSDDLVLY	nsp9	-	-	● 0.5	13	-	-	√	
10	KVAHNLGFYF	nsp11	● 0.3	122	● 0.3	99			√	
11	TRARHAIFVY	nsp10			● 0.3	60	0.2	-	√	
12	LSFSYTAQF	ORF3					● 1.3	73	√	√
13	FTWYQLASY	nsp12	0.1	92†	● 0.2	62	● 9.1	2	√	√
17	RTAIGTPVY	ORF4	● 0.5	57	● 0.2	1,852	● -	385†	√	
18	YTAQFHPEIF	ORF3	-	-	● 0.2	24,378	● 0.4	-	√	
19	LSDSGRISY	ORF7	● 1.1	10	● 0.2	383	0.2	4,182†	√	√
21	KVAHNLGFY	nsp11	● 1.5	4	● 2.8	11	-	-	√	√
22	KIFRFGSHKW	nsp1b	● 0.2	98			0.1	9†	√	
23	NISAVFQTYY	ORF3	● 0.1	413	● 0.9	6	● -	862	√	√
24	RTAPNEIAF	nsp2	● 2.1	4			0.1	-		√
25	ASDWFAPRY	ORF2a	● 4.9	2	● 0.2	71	-	-	√	√
27	RPFFSSWLV	ORF3			● 37.4	1			√	√
28	FVLSWLTPW	nsp5	-	-	● 0.2	1,372	● 13.7	3	√	√
29	MVNTTRVTY	nsp10	0.1	206†	● 0.2	47	-	-	√	
30	CVFFLLWRM	nsp5			● 0.2	283			√	
33	ITANVTDENY	ORF4	0.1	-	● 0.3	69	-	-	√	
34	SSEGHLTSVY	ORF3	-	-	● 0.2	12,701†	0.1	1,692†	√	
36	LTAALNRNRW	nsp5	-	-			● 3.6	40	√	√
38	LSASSQTEY	nsp2	0.1	91†	● 0.2	479	0.2	-	√	
39	VRWFAANLLY	nsp9			● 2.7	44			√	√
43	TTMPSGFELY	nsp9	● -	576	● 0.8	6	0.2	1,838†		
44	MSWRYSCTRY	ORF5	-	-	● 0.5	87	● 1.5	15		√
46	ALATAPDGTY	nsp3	-	607†	● 0.1	2,736			√	
48	WGVYSAIETW	ORF6					● 0.2	21,433	√	
49	FLNCAFTFGY	ORF6	-	-	● 0.3	20	● 0.3	2,069	√	
50	NSFLDEAAY	nsp10			● 0.1	43	-	-	√	
53	MPNYHWWVEH	nsp9			● 0.6	32			√	

Table 1*: Overview of the 33 PRRSV epitopes included in the respective VRPs used for vaccination. The left side section provides the basic peptide characteristics: ID, sequence and locus. Note that the peptide 21 is nested within the peptide 10. The middle section presents the previously determined binding data for the three SLAs Left-side columns represent measured binding stability (average dissociation half-life in decimal hour (h)), right-side columns represent measured binding affinity (average equilibrium dissociation constant (nM)). †: only one successful affinity measurement could be obtained. Hyphen (-): no successful measurements could be obtained (stability or affinity). Empty field: Not tested. ●: Peptide included in the VRPs for the respective SLAs; SLA-1*0401 (VRP 1-3), SLA-1*0702 (VRP 4-6), and SLA-2*0401 (VRP 7-9). The right side section provides information on the peptides being encoded by the challenge strain, and on the peptides included in the post challenge ELISPOT analysis.*

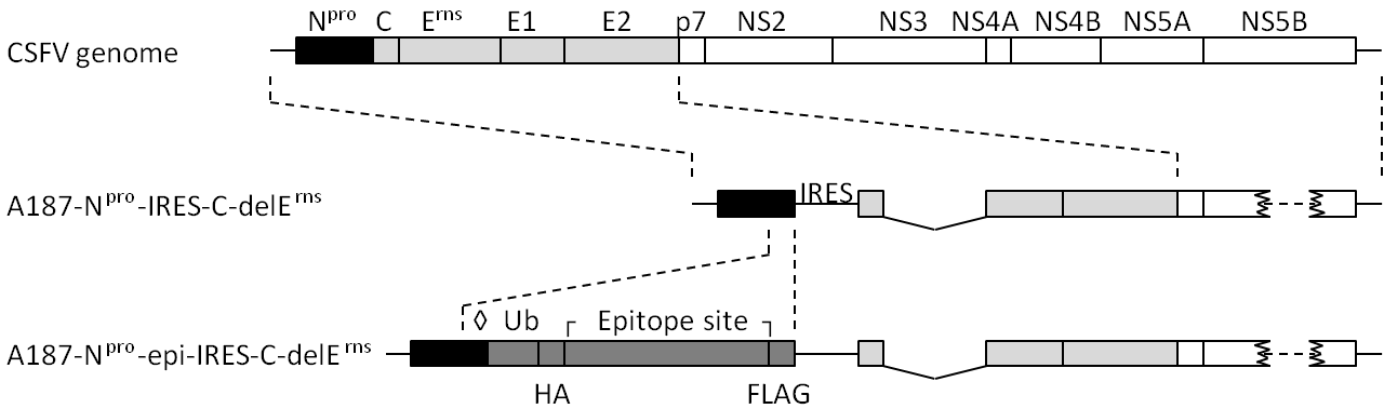

***Figure 1**: Construction of the template plasmid, A187-N^{pro}-epi-IRES-C-delE^{rns}. The plasmid constructs used in this study are represented schematically, with the N^{pro} gene shown in black, the structural proteins in light gray, and the non-structural proteins in white. The inserted genes are shown in dark gray, representing a non-cleavable ubiquitin (Ub), a haemaglutinin tag (HA), an epitope site, and a FLAG tag. Additionally, a C138A mutation was introduces in the N^{pro} gene (◊), and the epitope site containing the preliminary SIINFEKL epitope was flanked by an upstream KasI restriction site (┌) and a downstream MluI restriction site (┐) for subsequent replacement of SIINFEKL with PRRSV polyepitopes.*

Plasmid amplification and VRP rescue

The backbone plasmid pA187-N^{pro}-epi-IRES-C-delE^{rns} and the nine plasmids containing PRRSV-2 polyepitopes were used for the rescue VRP0 to VRP9 (supplementary data 1, page 123) as described elsewhere (Suter et al. 2011). Briefly, plasmids were linearized with the restriction endonuclease SrfI and RNA run-off transcription was performed using the MEGAscript T7 kit (Ambion). One µg RNA was then used to electroporate 8x10^6 SK6-E^{rns} cells maintained in Eagle's minimum essential medium (EMEM) supplemented with 7% horse serum (Håtunalab) and 0.25 mg/ml G418 (Calbiochem). After three days of incubation at 37˚C, the VRPs were harvested by two freeze-thaw cycles and the lysates were clarified by centrifugation (p0 stocks). The VRPs were further propagated in SK6-E^{rns} cells by infection at a multiplicity of infection (MOI) of 0.1 and 72 hours of culture to generate p1 and p2 stocks. Mock consisted of SK6-E^{rns} lysate obtained in parallel to the VRP stocks.

Titration of VRPs and PRRSV

The VRP were titrated in SK6-E^{rns} cells by end point dilution and immunoperoxidase staining using the anti-E2 monoclonal antibody (mAb) HC/TC26 (Greiser-Wilke et al. 1990) kindly provided by I. Greiser-Wilke (Hannover Veterinary School, Hannover, Germany) and a horseradish peroxidase (HRP)-conjugated rabbit anti-mouse IgG (Dako). Alternatively, the VRP were titrated in PK-15 cells using the mAb WH211 (AHVLA, RAE0242) and a HRP-conjugated polyclonal goat anti-mouse serum (Jackson ImmunoResearch Laboratories). Titration of the PRRSV-2 strain used for challenge was performed in MARC-145 cells using the monoclonal antibody, SDOW17-A (RTI LLC) and HRP-conjugated rabbit anti-mouse serum (Dako). The SK6-E^{rns} cells were maintained as described above, and the PK-15 and MARC-145 cells were cultured in EMEM supplemented with 5% fetal bovine serum (FBS).

Flow cytometry

Flow cytometry (FCM) was applied to VRP infected cells for the detection of the FLAG-tagged epitope expression. Briefly, 10^5 SK6 cells were infected with the VRPs 0-9 from the p1 stock or mock infected. In addition, VRP rescued from the original backbone replicon vector pA187-N^{pro}-IRES-C-delE^{rns} were included as a negative sample control as this replicon does not encode a FLAG tag. All infections were performed with a MOI of 5 in the presence of 100 nM of the proteasome inhibitor epoxomicin (Sigma) or of an equivalent amount of DMSO as solvent control added 28 h post infection, in order to take the expected proteasomal degradation of the poly-ubiquitinylated epitopes into account. After another 18 hours, the cells were detached by trypsin treatment, fixed with 4% paraformaldehyde in PBS, and permeabilized with 0.1% saponin in PBS. Infection was confirmed by the detection of the CSFV E2 protein with the mAb HC/TC26 and AlexaFluor647-conjugated goat anti-mouse IgG2b (ThermoFisher). Polyepitope expression was confirmed by FLAG tag detection with the F3165 mAb (Sigma), and the PE conjugated goat anti-mouse IgG1 (BioConcept). All antibodies were diluted in PBS/0.3% saponin. The cells were washed with Cell Wash (BD Biosciences) after each treatment and subjected to FCM (FACSCanto II, BD Biosciences).

SLA genotyping

Sequence-specific SLA genotyping was performed by PCR on genomic DNA extracted from EDTA-stabilized whole blood from potential experimental animals using primers specific for the supertypes SLA-1*04 (forward: 5'-GCCTGACCGCGGGGACTCT-3', reverse: 5'-CTCATCGGCCGCCTCCCACTT-3'), SLA-1*07 (forward: 5'-GCCGGGTCTCACACCATCCAGAT-3', reverse: 5'-GGCCCTGCAGGTAGCTCCTCAAT-3') and SLA-2*04 (forward: 5'-CCGAGGGAACCTGCGCACAGC-3', reverse: 5'-CCCACGTCGCAGCCGTACATGA-3'). Amplicons were sequenced by commercial Sanger sequencing (LGC Genomics) and identification of the alleles, SLA-1*0401, SLA-1*0702 and SLA-2*0401 was performed by SNP analysis using CLC Main workbench 7.0.

Selection, grouping and maintenance of experimental animals

Since the epitopes included in the VRPs have previously been verified *in vitro* to bind to at least one of the three SLAs (SLA-1*0401, SLA-1*0702, and SLA-2*0401) (paper 1), we were only interested in using animals expressing these alleles. Initially, 13 sows that had been inseminated for a farrowing date 5 weeks before the first vaccination were genotyped for the presence of the three SLA alleles as described in the previous section. This resulted in 4 sows of interest from which all 45 newborn piglets were genotyped. Correspondingly, 18 piglets were selected as experimental animals and were divided into a test group (N=11) and a control group (N=7) stratified to an even distribution of SLA-profile, litter of origin and initial bodyweight. The piglets were purchased from a Danish herd assumed to be PRRSV-negative due to the absence of PRRSV-specific antibodies in 19 randomly sampled weaners, analyzed by ELISA (results not shown). The 4-week old pigs were all housed in the same section of the BSL-3ag animal isolation facility at the National Veterinary Institute, Lindholm. After seven weeks the pigs were separated in

two boxes with an even distribution of test pigs and control pigs in each box. Pig data regarding group distribution, pig ID, SLA profile, bodyweight, litter and box can be found in table 2. Throughout the whole experiment the pigs had free access to water and were fed on a daily basis with zink substituted fodder purchased together with the pigs (first two weeks) or Porkido 10,5 Ideal AU (DLG) (rest of period).

Group	Pig	SLA-1*0401	SLA-1*0702	SLA-2*0401	Weight (kg)	Litter	Box
Control	Calvin	●	●		8	2	2
	Casper	●	●		9,6	2	1
	Chloe	●	●		11,7	3	2
	Charlotte	●	●		5,7	4	2
	Charlie	●		●	8,5	1	1
	Connor	●		●	7,1	1	1
	Cameron	●		●	8,5	3	1
Test	Toby	●	●		8,9	1	1
	Tracy	●	●		8,1	2	2
	Trisha	●	●		9,2	2	1
	Tyra	●	●		10,3	2	1
	Tristan	●	●		6,1	3	2
	Thomas	●	●		7,8	4	2
	Tania	●		●	7,4	1	2
	Tara	●		●	6,7	1	1
	Tia	●		●	5,7	1	1
	Tyson	●		●	10,2	1	2
	Tina	●		●	10,8	3	2

Table 2: *Presentation of the 18 pigs included in the vaccine-challenge experiment. Pigs were distributed between the control group (N=7) and test group (N=11) for an even distribution of SLA profile, body weight and litter of origin. All pigs were kept in the same box in the first 7 weeks after which they were split in two neighboring boxes due to space constraints*.

In vivo study experimental setup

A week after arrival, at day 0 post first vaccination (dpv 0), all pigs were vaccinated. Subsequent identical booster vaccinations were administered at dpv 28 and 51. The pigs in the test group were vaccinated with a titer adjusted mix of the PRRSV epitope containing VRPs (VRPs 1-9), while the pigs in the control group received the PRRSV-empty VRP (VRP 0). Vaccinations were administered as intradermal injections (27G needle) of 0.5 ml 1E7 $TCID_{50}$/ml VRP from the p2 stock applied as five spots of 0.1 ml each in the dermis of the right-side neck region. At dpv 64, all pigs were challenged intranasally, day post challenge (dpc) 0, with 2E6 $TCID_{50}$/animal of the low pathogenic Danish PRRSV-2 isolate, DK-1997-19407B (acc. KC862576), by spraying 2 ml virus solution into each nostril using a syringe. The pigs in box 1 were euthanized at dpc 26 and the pigs in box 2 were euthanized at dpc 27. Euthanasia was performed by captive bolt stunning followed by exsanguination by cutting *vena* and *arteria axillaris*. The assignment of the pigs to vaccine of control group remained unknown to the caretakers throughout the whole experiment. All procedures of animal handling and experimentation were in compliance with the Danish biosafety regulations and approved by the Danish Animal Experiments Inspectorate (2015-15-0201-00789). An overview of the experimental timeline is given in figure 2.

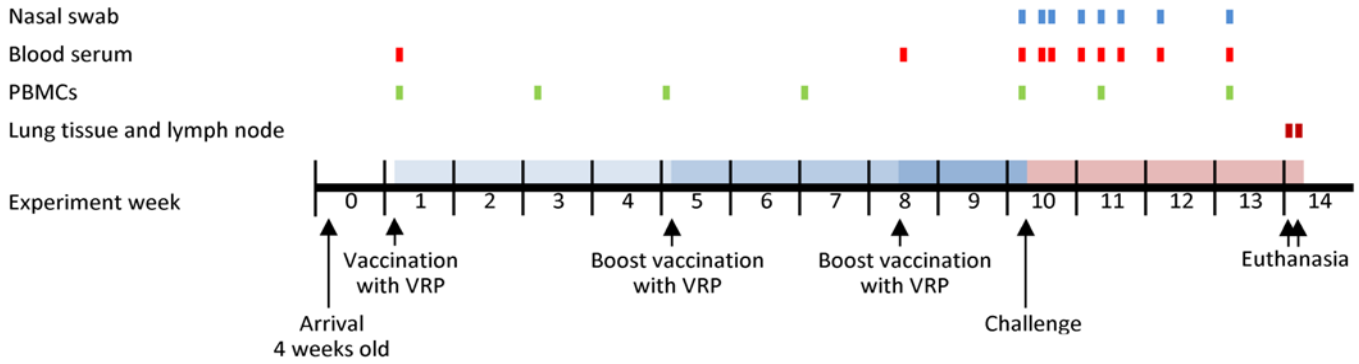

***Figure 2**: Timeline of the vaccine-challenge experiment indicating the major interventions.*

Clinical observations

The pigs were observed twice daily and any deviant clinical observations with respect to the general well-being, respiration, eye disorder, and appetite were recorded. Body weight was measured at dpv -1, dpc -1, and at necropsy. Rectal temperatures were measured in relation to the three vaccinations and to the challenge inoculation, respectively, at dpv -1, 1, 2, 3; and 28, 29, 30, 31; and 51, 52, 53, 54; and 63, 65, 66, 67, 69, 71, 72, 73, 77, 84.

Blood and nasal swab sampling

Blood samples were collected from the jugular vein of all pigs at dpv 0, 14, 21, 41, 51; and dpc -1, 1, 2, 5, 7, 9, 13, and 20 for the recovery of serum and/or PBMCs. The samples at dpv 0 were collected prior to vaccination. Serum was recovered from non-stabilized tubes after coagulation overnight at 4 ˚C by centrifugation at 3500 rpm for 10 minutes at 4 ˚C and stored at -80 ˚C for subsequent analysis. Porcine peripheral blood mononucleated cells (PBMCs) were isolated from heparin-stabilized tubes by density centrifugation on Lymphoprep (Stemcell) in 50 ml SepMate tubes (Stemcell) at 1200 g for 10 min at room temperature (RT). Contaminating erythrocytes were lysed with lysis buffer (77 mM NH_4Cl, 5 mM $KHCO_3$, 63 µM EDTA in water) for 3 minutes at RT and washed with PBS+2% FBS. PBMCs were used the same day for immunological examination by IFN-γ ELISPOT after being counted on a microscope. Nasal swabs were collected from all pigs at dpc -1, 1, 2, 5, 7, 9, 13, and 20 and placed in cryotubes containing 1 ml PBS and stored at -80 ˚C for subsequent analysis.

Tissue sampling

Upon euthanasia, a macroscopic inspection of the lungs of all pigs was performed, and three samples of approximately 1 cm^3 of lung tissue (left cranial, medial and caudal) were collected and kept at -80 degree for subsequent analysis. Additionally, the lymph node draining the vaccination site, *cervicales superficiales dorsales*, was excised from all pigs and cells were extracted manually, separated from debris through a 100 µm cell strainer and washed with PBS+2% FBS. The cells were used the same day for immunological examination by IFN-γ ELISPOT after being counted on a microscope.

Serology

The detection of serum antibodies against the CSFV E2 glycoprotein was performed on serum from dpv -1 and 51 using a classical swine fever E2 competition ELISA kit (CSFE2C-5P, ID-vet) following the manufacturer's instructions and reading the plates at 450 nm using a BioTek ELx808 absorbance microplate reader (Fisher Scientific). The detection of serum antibodies against PRRSV was performed on serum from dpc -1, 7, 9, 13, and 20 using an IDEXX PRRS X3 Ab Test (99-40959, IDEXX) following the manufacturer's instructions with the sole modification that the TMB color reaction was stopped with equivalent amounts of 1M H_2SO_4 (in house), after which the plate was read at 450-630 nm using the BioTek ELx808 absorbance microplate reader. Positive and negative controls were measured in duplicates, while samples were performed in single measurements.

Quantification of viral RNA

Viral RNA was purified from the challenge inoculum, serum samples, nasal swabs and lung tissue homogenate. The samples were clarified by centrifugation and RNA extracted using the MagNA Pure LC Total Nucleic Acid Isolation Kit (03 038 505 001, Roche) on a MagNA Pure LS Instrument (Roche). Quantitative PCR was performed using the Qiagen OneStep RT-PCR Kit (210210, Qiagen) on an MX3005P QPCR System (Agilent) with the following primers: forward: 5'-ATRATGRGCTGGCATTC-3', reverse: 5'-ACACGGTCGCCCTAATTG-3'. The probe was modified from the TEX-containing version to contain HEX instead: 5'-(HEX)-TGTGGTGAATGGCACTGATTGACA-(BHQ2)-3' (Kleiboeker et al. 2005; Wernike et al. 2012). Ct values were converted to equivalents of 50% tissue culture infective dose (TCID50eq) using a standard curve based on a purified 10-fold dilution series of the challenge isolate. Quantitative reverse transcription PCR was performed in duplicates for all samples. Prior to purification, lung tissue homogenate was prepared from cutouts of approximately 0.2-0.4 g of tissue homogenized in 1 ml Eagle's EMEM using lysing matrix D (MP bio) in a FastPrep FP120 cell homogenizer (Thermo Savant) for 60 seconds at speed 5.

IFN-γ enzyme-linked immunospot (ELISPOT) assay

MultiScreen IP filter 96-well plates (Millipore, MSIPS4510) were treated with 35% EtOH for <60 seconds and coated with 250 ng/well mouse anti-porcine IFN-γ monoclonal antibody (clone P2F6, ThermoFisher) in PBS at 4 ˚C overnight. Plates were washed three times in PBS and blocked with AIM-V albuMAX (31035025, ThermoFisher) at 37 ˚C, 5% CO_2 for at least 1 h after which freshly isolated cells were seeded in presence of stimuli as described below. Following 2 days of incubation at 37 ˚C, 5% CO_2, the plates were emptied and the cells were lysed by two times washing with MilliQ, then three times with washing buffer (PBS\0.01% Tween 20). Plates were incubated with 100 ng/well biotinylated mouse anti-porcine IFN-γ mAb (clone P2C11, BD Biosciences) in reaction buffer (PBS\0.01% Tween 20\0.1% bovine serum albumin) on a shaker at RT for 1 h. The plates were washed four times and incubated with 50 mU/well streptavidin-AP-conjugate (11089161001, Sigma-Aldrich) in reaction buffer on a shaker at RT for 1 h. Plates were washed three times with washing buffer followed by two times with PBS. Spots were developed using 100

µl/well BCIP/NBT tablets (B5655, Sigma-Aldrich) dissolved in 10 ml/tablet MilliQ in the dark at RT for 5 min, and the development was stopped under running tab water while the underdrain was removed. Still wet, the plates were completely submerged in 1% VirkonS for 30 min for exporting them from the BSL-3Ag facility in compliance with the biosafety regulations. The plates were washed under running tab water and left to dry in the dark. Ultimately, the spots were counted on an AID iSpot Reader Spectrum (Autoimmun diagnostika GmbH).

Pre challenge ELISPOT

ELISPOT assays using PBMCs isolated at dpv 0, 14, 27, 41, and 63 were designed to screen for reactive peptides included in the VRPs pre challenge. Twelve peptide-pools were used for restimulation of the PBMCs representing a 2-dimensional matrix with 6 pools in each dimension containing 5 to 6 peptides each. Together, each of the 33 PRRSV peptides included in the VRPs was represented by exactly one pool in each dimension. Stimulations with the VRP mixture used for vaccination and the PRRSV strain used for challenge were also included together with their respective mocks. Peptide stimulations were done with partial concentrations of 2 µM/peptide, while virus and VRP stimulations were done with an MOI of 0.1. Unstimulated wells were included as baseline, and wells stimulated with 1 µg/ml staphylococcal enterotoxin B (SEB) (S4881, Sigma-Aldrich) were included as positive controls. All stimulations were seeded in duplicates with 300,000 cells/well.

Post challenge ELISPOT

ELISPOT assays using PBMCs isolated at dpv 71 and 84 dpv (dpc 7 and 20, respectively) were designed to identify individual reactive peptides among 14 peptides chosen from the 33 vaccine peptides. Stimulations were done with individual peptides in concentrations of 5 µM. Unstimulated wells were included as baseline, and wells stimulated with 1 µg/ml SEB were included as positive controls. All stimulations were seeded in quadruplicates with 500,000 cells/well. This setup was also used for the ELISPOT assays using cells extracted from the lymph nodes, although only with 300,000 cells/well.

Statistics

Positive signals upon restimulations in the ELISPOT data were identified by two criteria, using the online (http://www.scharp.org/zoe/runDFR/) non-parametric distribution free resampling (DFR) tool as described by (Moodie et al. 2006) and by defining responders when number of spots were more than twice the background with a minimum number of spots at 8 (ratio-2 method). This method furthermore allowed for a quantitative analysis of the response magnitudes. P-values for the differences in lung tissue virus load between groups were calculated using Mann-Whitney. A paired, two-tailed T test was used to test for significant peaks in rectal temperature within the

groups pre challenge. An unpaired, two-tailed T test was used to test for significant difference between the groups post challenge.

RESULTS

Verification of VRP infectivity and epitope expression

FCM was used for the verification of VRP infection and polyepitope expression, by staining infected SK6 cells for E2 and FLAG tag, respectively. The results are summarized in figure 3A with a representative example of the FCM gating setup for VRP 6 in figure 3B. Figures of the individual gatings are seen in supplementary data 2 (page 128). The threshold for infectivity (E2) was defined based on the epoxomicin treated mock infected sample, and the threshold for FLAG tag detection was defined based on the epoxomicin treated sample infected with the FLAG-negative VRP rescued from the original plasmid, pA187-N^{pro}-IRES-C-delE^{rns}. For all samples, a clear division of infected and non-infected cells was not seen. Rather, a smooth transition was observed in shape of an oblong density. Comparing the DMSO treated samples with their respective epoxomicin treated samples, a characteristic 'tilt of the head' was observed, shifting the population in a more FLAG-positive direction.

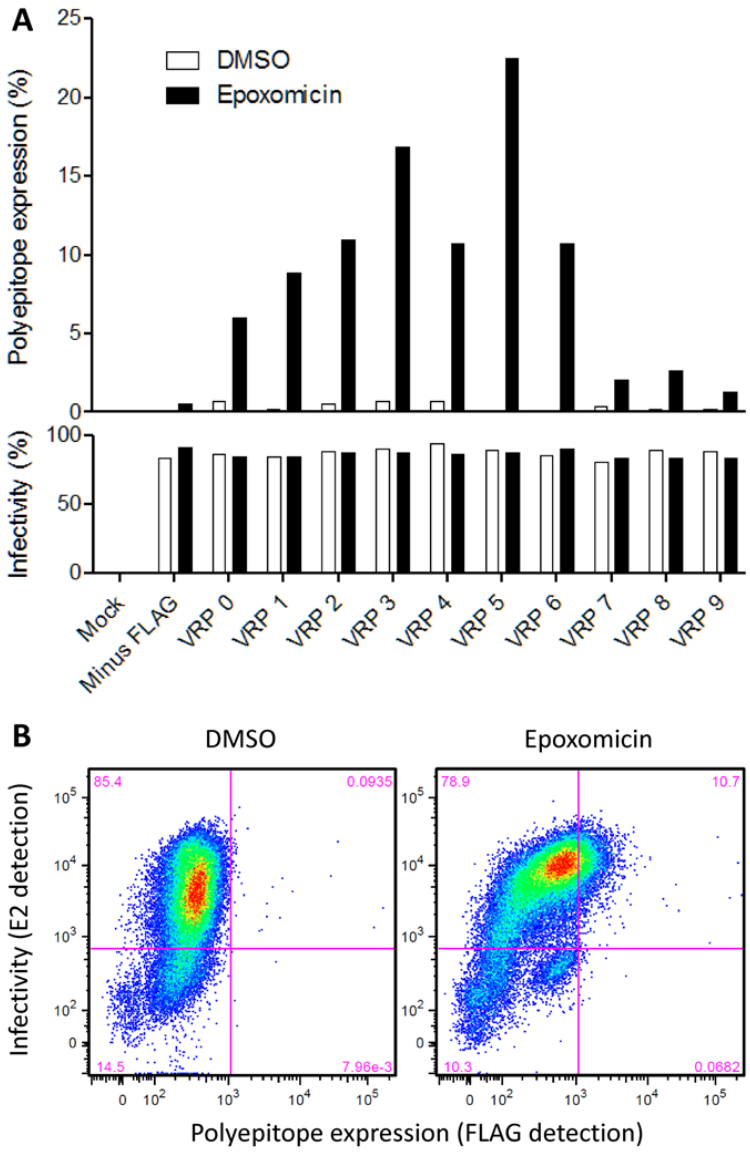

***Figure 3**: Verification of VRP infectivity and induced polyepitope expression in SK6 cells. **A**: 1E5 cells were infected at a MOI of 5 with VRPs 0-9 or the VRP lacking FLAG (A187-N^{pro}-IRES-C-delE^{rns}) or mock-infected as control. 28 h post infection cells were treated with epoxomicin (100 nM) or DMSO. After and additional 18 hours, the percentage of cells expressing the polyepitope (top panel) and the percentage of infected cells (bottom panel) were determined by FCM using anti-FLAG and anti-E2 antibodies, respectively. At least 36,000 events were acquired for each sample. **B**: The FCM plots of VRP 6-infected cells under DMSO versus epoxomicin treatment are shown as an example.*

This shift was also seen in the sample infected with the FLAG-negative VRP, and even the mock seemed to be affected, indicating that the right shifting induced by the epoxomicin had an unspecific component. Nonetheless, the shift was least pronounced in the sample infected with the FLAG-negative VRP, making this sample a compelling reference. The observation that only the E2-positive fraction was reaching into the FLAG-positive quadrant was further reassuring. The shift of the samples infected with VRPs 7-9 was remarkably weaker than all of the other VRPs, except for the FLAG-negative sample. This was an interesting observation as these VRPs collectively represent all of the SLA-2*0401 specific polyepitopes. While no other deviations, such as lower infectivity or poor cloning, are were characteristic for these VRPs, the weak FLAG detection could be the result of either ribosomal arrest or spatial hindrance of the anti-FLAG antibodies. In any case, since a noticeable FLAG detection was observed in all of the other FLAG-encoding VRPs, the weak detection of FLAG in the SLA-2*0401 VRPs were not pursued any further.

Antibody responses to the VRP vaccinations

Confirmation that the CSFV-based VRPs replicated within the vaccinated animals was obtained by strong seroconversion against the E2 protein of all tested pigs at dpv 51 (mistakenly no serum was collected from Tara) as previously demonstrated (Suter et al. 2011). All pigs were E2 seronegative at dpv 0 (data not shown).

Antibody response against PRRSV

The kinetics of a humoral response against PRRSV after challenge was investigated using the semiquantitative IDEXX PRRS X3 Ab Test kit on serum from dpc -1, 7, 9, 13, and 20. The results showed that all animals mounted a strong antibody response against PRRSV with no difference between the groups (data not shown).

Virus load in serum, lung tissue and nasal swabs

Serum samples isolated at dpc 5 and 13 and lung tissue samples from the cranial, middle and caudal parts of the lungs were analyzed for virus load using real-time RT-PCR (figure 4). While no differences between the groups were seen in the serum (figure 4A), differences were seen in the middle and caudal parts of the lungs of which the difference in the caudal part was significant (figure 4B). In order to trace the individual animals across lung parts, the animal-specific measurements were connected with lines in figure 4C. In addition, nasal swabs collected at dpc 5, 9, and 13 were also analyzed. Prior to purification and real-time RT-PCR, they were pooled according to groups in order to provide quick indications of an interesting response. Very low level of virus was detected with no apparent trend between groups (data not shown).

Clinical signs

Apart from minor unrelated infirmities, no clinical signs were seen in any of the pigs during the experimental period and all pigs had normal weight gains (data not shown). Variations in rectal temperature, however, did reflect the second and third vaccination events by a moderate increase (up to 40.6 °C) in rectal temperature.
Similarly, following challenge, no difference in rectal temperature between the two groups was observed (figure 5).

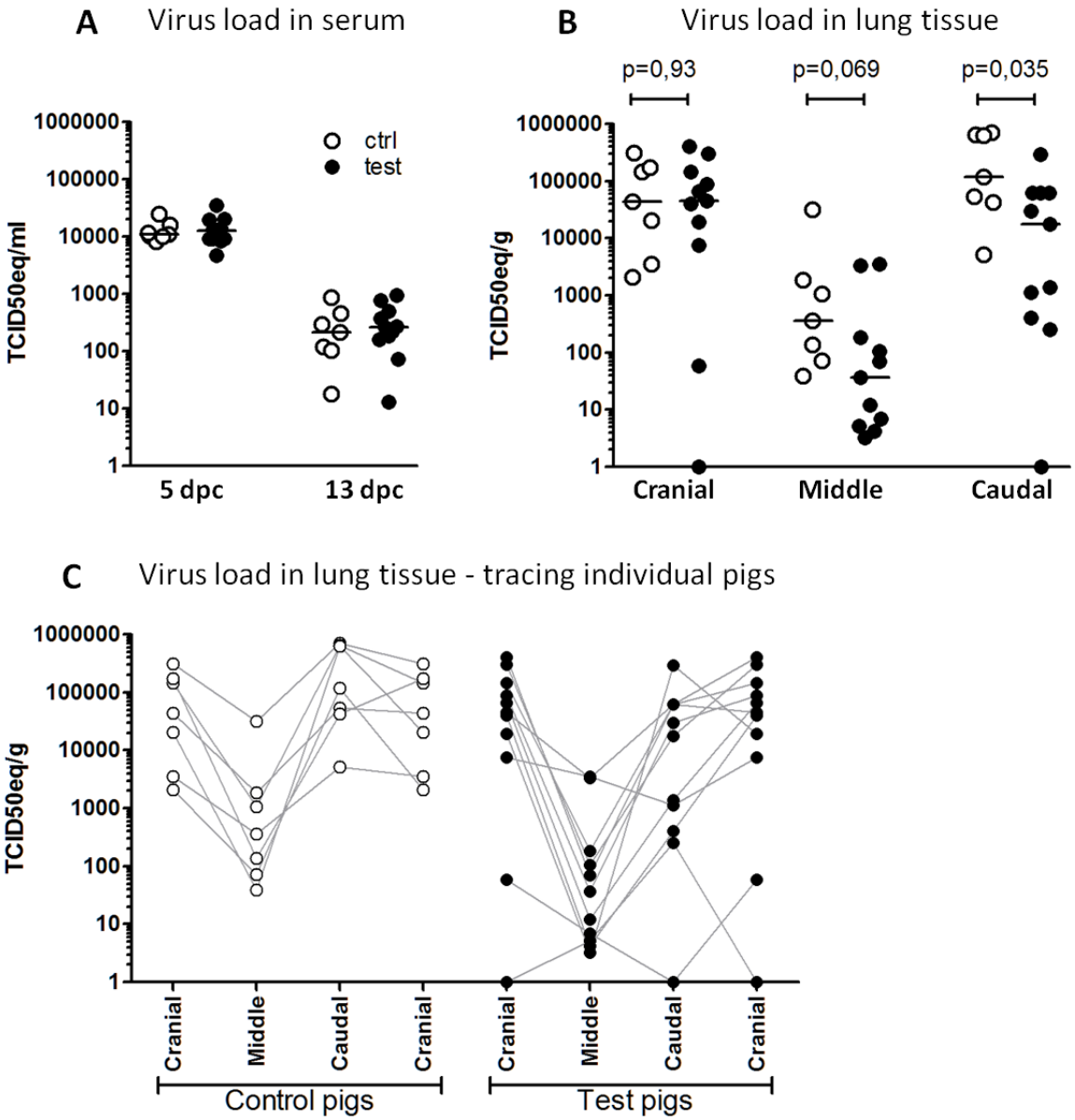

***Figure 4**: Virus load in serum and lung tissue analyzed by qPCR. **A**: Virus load in the serum at dpc 5 and 13 given in TCID50 equivalents per ml serum. **B**: Virus load in the lung tissue from cranial, middle and caudal parts of the lung prepared from cutouts of 0.2-0.4 gram and normalized to TCID50 equivalents to 1 gram of tissue. P-values are calculated using Mann-Whitney. **C**: Virus load in lung tissue presented for the tracing of the individual animals across lung parts. All measurements were performed in duplicates and were converted from ct values using a standard curve based on a purified 10-fold dilution series of the challenge isolate. Group medians are indicated with a line in A and B.*

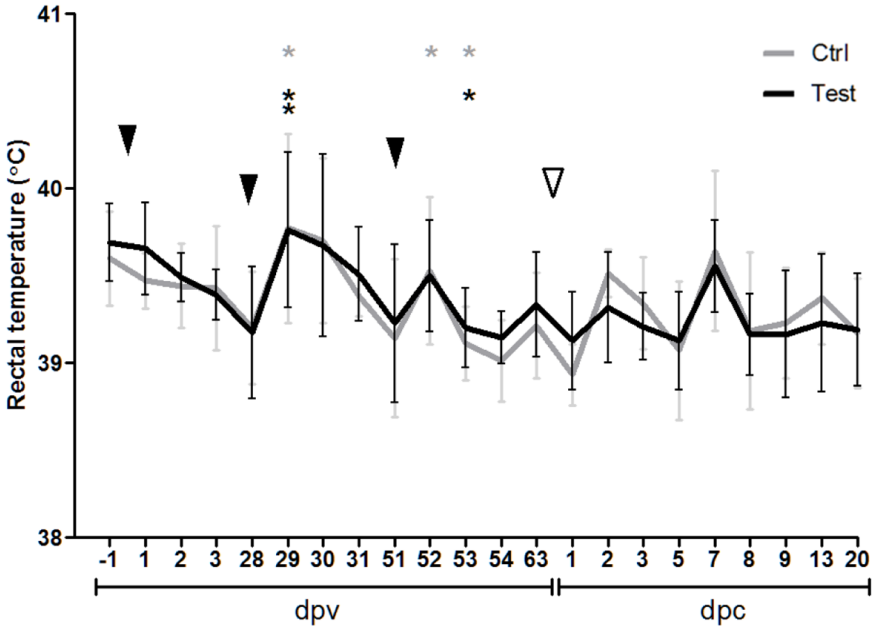

***Figure 5**: Rectal temperature measurements throughout the course of experiment. Black and grey lines represent the group averages of the test group and the control group, respectively. Error bars indicate the standard deviations. Black arrowheads indicate vaccination events. White arrowhead indicates PRRSV challenge. Before challenge, asterisks indicate group-wise temperature peaks that are significantly different from the previous day calculated using a two-tailed paired Student's T-test. After challenge, asterisks indicate significant differences between the two groups calculated using a two-tailed unpaired Student's T-test (no significant differences). *: 0.05 ≥ P > 0.01; **: 0.01 ≥ P > 0.001.*

ELISPOT

The pre challenge ELISPOT plates were dominated by non-specific spots in all wells including non-stimulated controls making it impossible to identify peptide-specific signals in a rational and uniform manner and could thus not be analyzed (data not shown).

An improved IFN-γ ELISPOT setup was performed at day 7 and 20 after challenge (71 and 84 dpv), providing a higher resolution by increasing the number of cells/well and relicates while restimulating with a higher concentration of peptide. In addition, individual peptides were used as stimuli instead of peptide pools with the consequence that only 14 peptides could be included in the assay. These were chosen based on their *in vitro* binding capacities and have the IDs: 2, 7, 12, 13, 19, 21, 23, 24, 25, 27, 28, 36, 39 and 44 (with reference to table 1, page 103). The same stimulations were used for the analysis of the lymph node derived cells. The results from the post challenge ELISPOT have been summarized in Figure 6 depicting the distribution of positive responses according to day, group and peptide. From this, it can be seen that pigs of the test group exhibit have a higher response frequency and magnitude than pigs of the control group.

Results of the individual animals are presented in figure 7 with the cell count for the lymph node cells normalized to spots per 500.000 cells for better comparison.

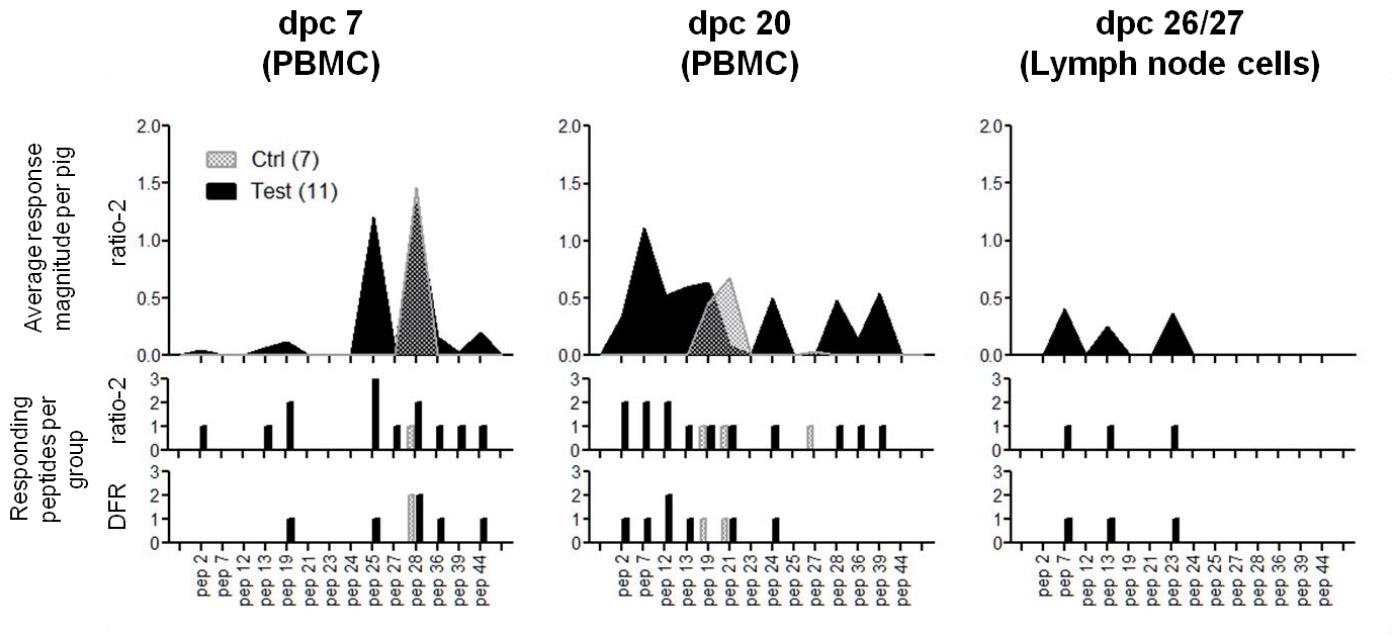

Figure 6*: Cell mediated immune responses to peptides post challenge - summary. The top panel represents the average magnitude of positive responses per pig according to the ratio-2 method. The middle panel represents the numbers of positively responding peptides per group according to the ratio-2 method, and the bottom panel represents the numbers of positively responding peptides per group according to the DFR method. With relevance to the middle and bottom panel, it should be noticed that the number of pigs in two groups are not the same. Gray fill: control group (N=7); black fill: test group (N=11)*

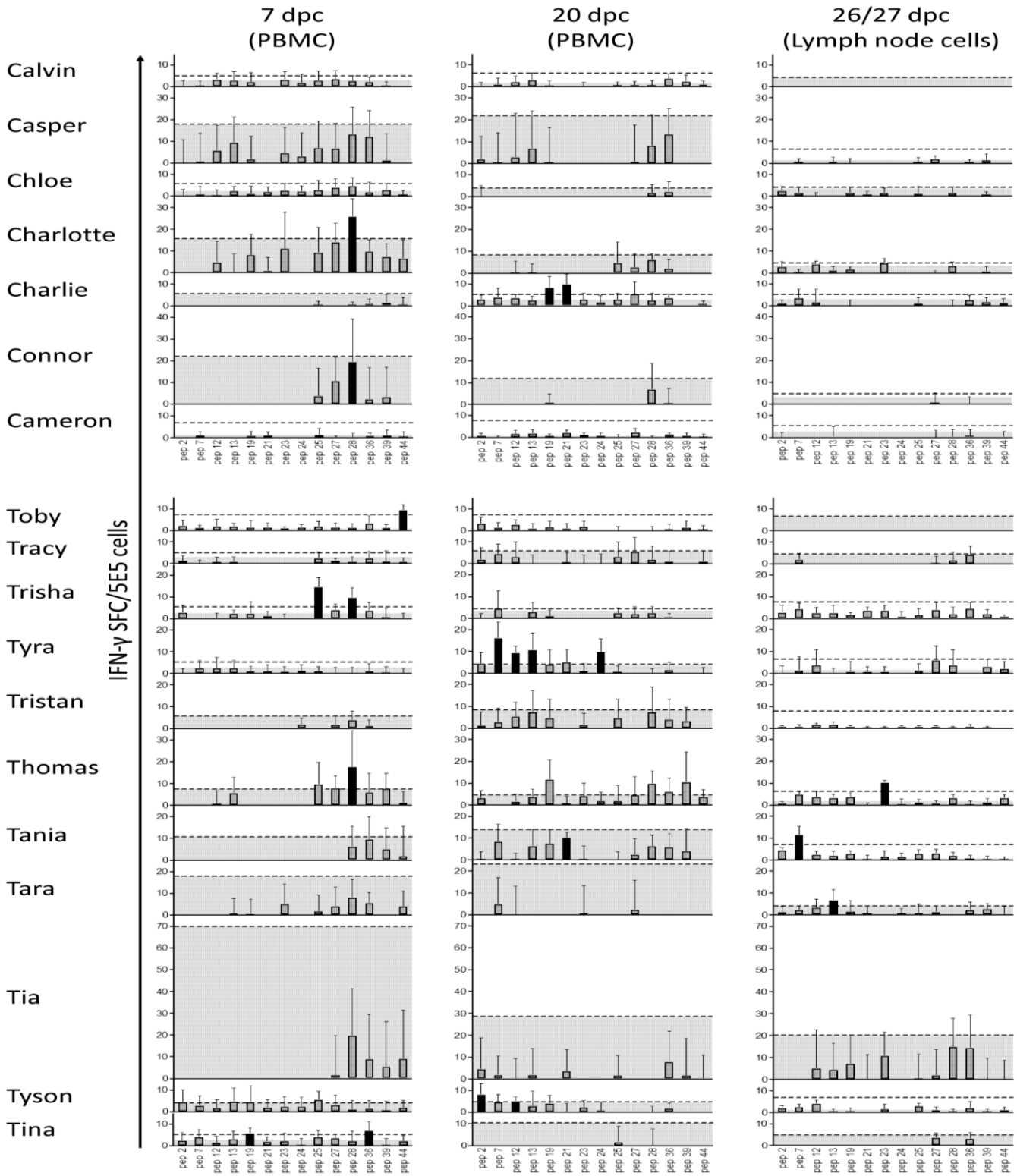

Figure 7*: Cell mediated immune responses to peptides post challenge - Overview. At dpc 7 and 20, 5E5 freshly purified PBMCs were restimulated separately with 14 selected peptides and with media as a background control. upon euthanasia (dpc 26/26), 3E5 cells derived from the lymph node were treated the same way and output was adjusted to 5E5 cells/well for comparison. Response to restimulation is presented here as columns indicating the average number of IFN-γ spot forming cells (SFC) in response to restimulation with peptide (signal) minus the average number of SFC in response to restimulation with media (background). Error bars represent the corresponding standard deviations. Upper edges of the gray area represent the retracted average backgrounds for reference. Dashed lines indicate ratio-2 thresholds, defined as 2 x background, minimum a limit of detection of 8. Black columns represent positive calls according to the DFR(eq) method.*

DISCUSSION

The bicistronic CSFV-based VRP used as vaccine backbone in this study, has previously been shown to induce expression and activity of transgenic luciferase and granulocyte macrophage colony-stimulating factor in infected SK6 cells (Suter et al. 2011). In the current study, polyepitopes of SLA class I restricted conserved PRRSV-2 epitopes were inserted in the same transgenic site. Both VRP infectivity, expression of the transgene and subsequent proteasomal degradation of the protein product, was confirmed *in vitro* by flow cytometry of infected SK6 cells treated with proteasome inhibitor and stained for E2 and FLAG tag expression. In response to vaccinations, infectivity and replication of VRPs within vaccinated animals was confirmed by the detection of a progressive anti-E2 response, and clinical reactions to the vaccinations were observed for the two booster vaccinations as increased rectal temperatures without inducing fever.

Evaluating the results of the viral load in serum, it was obvious that no overall difference was seen between the two groups, why analysis of serum samples from the remaining dates was cancelled.

The viral loads in lung tissue, however, revealed a significant difference between groups in favor of the vaccine in tissue from the caudal part of the lung. Subsequently, test of virus loads of individual pigs revealed that a pig with high titers in one part of the lung did not necessarily have higher loads in other parts of the lung (figure 4C, page 112). Consequently, this inconsistency undermines the link between the measured values and the actual biological virus load.

Following challenge, a fluctuation in rectal temperature was observed at dpc 2, which was largest for the control group, hinting that this group was more affected by the PRRSV challenge than the test group. At dpc 7 another peak was observed with similar strength for both groups that could reflect a response to the first wave of viremia. This is in line with the current observation that the response to challenge in rectal temperature is delayed by two days, combined with a previous observation that viremia peaks at day 5 dpc (Larsen et al. unpublished data). In general, the average rectal temperatures of the two groups were more or identical with only minor variations. Although none of the measure effect parameters were statistically significant, there were trends that the vaccinated animals had less rise in temperature and less virus load, and it is tempting to speculate if these differences would have increased if a more virulent strain had been used for challenge.

Regrettably, the quantification of the CMI in response to VRP immunization was hampered by the poor quality of the pre-challenge ELISPOT. The post challenge ELISPOT data was however more reliable, revealing a trend pointing in the direction of a weak, yet present, peptide-specific CMI response. This is most clearly seen in figure 6 (page 114) summing up the post challenge ELISPOT data interpreted using the ratio-2 and DFR methods. The two methods are mostly overlapping, but while the DFR method might be the most statistically correct method, the ratio-2 method allows for a qualitative analysis as seen in the top panel in figure 6. Regardless of the method, more frequent and stronger responses were clearly seen in animals of the test group compared to the animals of the control group. Although this is in line with the expected of a functional vaccination, the conviction fades upon examination of the

individual animals, since no animal responded to the same peptide twice according to the DFR method, and only one animal ("Thomas", peptide 28) did so according to the ratio-2 method. This indicates that peptide-specific responses were not dominated by single clones but covered several peptides with low response levels. Comparing responses from the PBMC with responses from lymph node cells, the latter showed to be generally much less responsive than the PBMC with only three responding pigs out of all 18 pigs. Although all three pigs belonged to the test group, the responsible peptides did not induce any positive responses in the PBMCs of the same animals.

The polyepitope VRP vaccine was designed to specifically induce strong peptide-specific CTL responses, so the very low response level measured by ELISPOT was a clear disappointment and does not support this vaccine platform as an effectice means of inducing CTL responses to designed polyepitope strings
Searching for correlations between readouts on the scale of individual animals, neither revealing any clear patterns (data not shown), although two animals from the test group (Thomas and Toby) could be regarded as outliers in terms of both lung tissue viral load and ELISPOT responses. Thomas had the lowest virus load of all pigs in serum at dpc 13 and in the caudal lung part, the second lowest in the cranial lung and the fourth lowest in the middle lung (figure 4, page 112). In addition, the pig was the only pig whose PBMCs responded to the same peptide twice (peptide 28, dpc 7 and 20, ratio-2 method) (figure 7, page 115). Interestingly, peptide 28 was measured to have no binding and only very weak binding capacity to SLA-1*0401 and SLA-1*0702, respectively (table 1, page 103), being the two alleles expressed by Thomas (table 2, table 106). However, it cannot be ruled out that Thomas expressed other and undiscovered alleles that were responsible for the signal. Toby had the lowest virus load of all pigs in the cranial lung, the second lowest in the caudal lung and the third lowest in the middle lung (figure 4). This CMI was generally absent with the exception of a clear response to peptide 44 at dpc 7 (figure 7, page 115). This response was interesting, since peptide 44 was not expressed by the challenge strain (table 1, page 103), meaning that the response, if not an artifact, could only be induced by the vaccination. This is in accordance with the SLA profile of Toby expressing SLA-1*0401 and SLA-1*0702 (table 2, page 106) of which binding of peptide 44 was determined to have a high affinity for the latter (table 1).

In summary, readouts from virus load, rectal temperature and ELISPOT, all give weak indications of a positive effect of the vaccine and convincing results supporting a strong CMI against PRRSV following vaccination with VRPs were lacking, leading to the overall conclusion that the effects of vaccination given in the current setup were, if at all present, either too weak or too difficult to detect with the applied methods.

The reasons for a weak effect of vaccination may originate from an unsuccessful VRP-induced priming of the CTLs. The chain of events from vaccination to CTL priming is long and involves several steps subjected to potential erroneous processing that may ultimately result in unsuccessful priming. An important first step is the activation of dendritic cells (DC) for subsequent migration to, and antigen presentation in, the lymph nodes. This step is unlikely to be the cause of unsuccessful priming for several reasons. First of all, CSFV has a tropism for both conventional DCs (cDC) and plasmacytoid DCs (pDC) that are both early targets for the virus (Jamin et al. 2008). Secondly, both N^{pro}

and E^{rns} have been shown to possess type I IFN antagonistic activities, respectively, by targeting IRF7 (Szymanski et al. 2009) and by degrading viral RNA to prevent triggering of IRF7 (Python et al. 2013). In the current study these activities have both been abolished by point mutation (N^{pro}) and deletion (E^{rns}). Thirdly, a previous study testing the immune response in pigs vaccinated intradermally with a related VRP, pA187-del E^{rns} showed a clear CMI response to a single vaccination by an increase of IFN-γ (Frey et al. 2006). In a study attempting to determine the source of CSFV-induce IFN-γ, it was demonstrated that $CD3^{+}CD4^{-}CD8\alpha^{high}$ were the initial source of CSFV-specific IFN-γ producing cells upon challenge of animals vaccinated with an attenuated CSFV C-strain. In contrast, no T cell IFN-γ was detectable upon challenge of unvaccinated animals who developed clinical signs of disease (Franzoni et al. 2013).

Assuming that infection and activation of antigen presenting cells was not the issue, failures in intracellular processes related to polyepitope expression and processing may be responsible. In this context, epitope abundance and insufficient peptide-MHC complex stability are relevant candidates. Attempts with western blot of lysate of epoxomicin treated VRP-infected cells failed twice to show visible bands (data not shown). Regardless, the experiment was continued as intended, since data from the sequencing of midipreps and flow cytometric analyses of VRP-infected SK6 cells both pointed in the direction of correct transgene insertion and expression. The absence of bands was hence assumed to be the result of protein levels below the limit of detection, which in turn was not considered a hindrance to CTL priming. Following transgene translation the amount of individual epitopes would have decreased further upon proteasomal degradation and N-terminal trimming by aminopeptidases, processes that undoubtedly would chop up a fraction of the intended epitopes. One study indicated that the sets of peptides produced by either the conventional or the immunoproteasome differ more than expected. This is highly relevant due to the fact that activated DCs mainly contain the latter (Chapiro et al. 2006). Ultimately, the peptide-MHC complex stability of the selected epitopes may for some of the peptides not have been sufficiently high to maintain complex formation long enough for T cell encounter and recognition to occur. In effect, these aspects combined most likely have resulted in a very low rate of pMHC-TCR encounters on the surfaces of infected cells, with a pauper priming to follow.

Alternatively or additionally, the primed CTL response was there in full force before challenge, but was inhibited by the PRRSV infection. Again, the poor quality of the pre-challenge ELISPOT data is highly regrettable, as this could have cleared out this uncertainty. Nevertheless, PRRSV is notoriously known for its multiple immunoevasive mechanisms (reviewed in Huang et al. 2014) among many others are the downregulation of SLA-I molecules on the surface of infected cells (Du et al. 2015); the increased secretion of interleukin-10 (IL-10), and the activation of regulatory T cells, that could put primed CTLs into quiescence. These mechanisms could explain at least part of the low IFN-γ responses and the weak effect on virus load.

In this study, a rational approach for the induction of a PRRSV-specific CMI was attempted through vaccination with VRPs expressing conserved PRRSV-2 epitopes. Although convincing results remained absent, indications of vaccine

induced modifications of the immune responses were present, and may aid to inspire in new and better experiments in the quest for an effective vaccine against PRRSV.

AUTHOR'S CONTRIBUTIONS

LL and GJ conceived the study. LL, GJ, SWelner, AS and NR designed and planned the experiment. NR, TL and SWelner designed the VRPs. TL, MG and SWerder cloned the plasmids, sequenced the midipreps, rescued the VRPs, and titrated on p0 and p1. SWelner perfomed most of the analyses, and wrote the manuscript. All authors read, corrected and approved the final manuscript.

REFERENCES

Bazhan SI, Karpenko LI, Ilyicheva TN, et al (2010) Rational design based synthetic polyepitope DNA vaccine for eliciting HIV-specific CD8+ T cell responses. Mol Immunol 47:1507–15. doi: 10.1016/j.molimm.2010.01.020

Beilage E, Nathues H, Meemken D, et al (2009) Frequency of PRRS live vaccine virus (European and North American genotype) in vaccinated and non-vaccinated pigs submitted for respiratory tract diagnostics in North-Western Germany. Prev.Vet.Med. 92:31–37.

Blomquist DV, Green P, Laidlaw SM, et al (2002) Induction of a Strong HIV-Specific CD8 + T Cell Response in Mice Using a Fowlpox Virus Vector Expressing an HIV-1 Multi-CTL-Epitope Polypeptide. Viral Immunol 15:337–356. doi: 10.1089/08828240260066260

Botner A, Strandbygaard B, Sorensen KJ, et al (1997) Appearance of acute PRRS-like symptoms in sow herds after vaccination with a modified live PRRS vaccine. Vet.Rec. 141:497–499.

Chapiro J, Claverol S, Piette F, et al (2006) Destructive cleavage of antigenic peptides either by the immunoproteasome or by the standard proteasome results in differential antigen presentation. J Immunol 176:1053–61.

Chen N, Cao Z, Yu X, et al (2011) Emergence of novel European genotype porcine reproductive and respiratory syndrome virus in mainland China. J Gen Virol 92:880–892. doi: 10.1099/vir.0.027995-0

De Baets S, Schepens B, Sedeyn K, et al (2013) Recombinant influenza virus carrying the respiratory syncytial virus (RSV) F85-93 CTL epitope reduces RSV replication in mice. J Virol 87:3314–23. doi: 10.1128/JVI.03019-12

Du J, Ge X, Liu Y, et al (2015) Targeting Swine Leukocyte Antigen Class I Molecules for Proteasomal Degradation by the nsp1α Replicase Protein of the Chinese Highly Pathogenic Porcine Reproductive and Respiratory Syndrome Virus Strain JXwn06. J Virol 90:682–93. doi: 10.1128/JVI.02307-15

Eck M, Durán MG, Ricklin ME, et al (2016) Virus replicon particles expressing porcine reproductive and respiratory syndrome virus proteins elicit immune priming but do not confer protection from viremia in pigs. Vet Res 47:33. doi: 10.1186/s13567-016-0318-0

Franzoni G, Kurkure N V., Edgar DS, et al (2013) Assessment of the Phenotype and Functionality of Porcine CD8 T Cell Responses following Vaccination with Live Attenuated Classical Swine Fever Virus (CSFV) and Virulent CSFV Challenge. Clin Vaccine Immunol 20:1604–1616. doi: 10.1128/CVI.00415-13

Frey CF, Bauhofer O, Ruggli N, et al (2006) Classical swine fever virus replicon particles lacking the Erns gene: a potential marker vaccine for intradermal application. Vet Res 37:655–70. doi: 10.1051/vetres:2006028

Greiser-Wilke I, Moennig V, Coulibaly CO, et al (1990) Identification of conserved epitopes on a hog cholera virus protein. Arch Virol 111:213–25.

Han J, Wang Y, Faaberg KS (2006) Complete genome analysis of RFLP 184 isolates of porcine reproductive and respiratory syndrome virus.

Herd KA, Harvey T, Khromykh AA, Tindle RW (2004) Recombinant Kunjin virus replicon vaccines induce protective T-cell immunity against human papillomavirus 16 E7-expressing tumour. Virology 319:237–248. doi: 10.1016/j.virol.2003.10.032

Hikke MC, Pijlman GP (2017) Veterinary Replicon Vaccines. Annu Rev Anim Biosci 5:annurev-animal-031716-032328. doi: 10.1146/annurev-animal-031716-032328

Huang C, Zhang Q, Feng W-H (2014) Regulation and evasion of antiviral immune responses by porcine reproductive and respiratory syndrome virus. Virus Res. doi: 10.1016/j.virusres.2014.12.014

Jamin A, Gorin S, Cariolet R, et al (2008) Classical swine fever virus induces activation of plasmacytoid and conventional dendritic cells in tonsil, blood, and spleen of infected pigs. Vet Res 39:7. doi: 10.1051/vetres:2007045

Jiang Y, Xia T, Zhou Y, et al (2015) Characterization of three porcine reproductive and respiratory syndrome virus isolates from a single swine farm bearing strong homology to a vaccine strain. Vet Microbiol 179:242–249. doi: 10.1016/j.vetmic.2015.06.015

Karniychuk UU, Nauwynck HJ (2013) Pathogenesis and prevention of placental and transplacental porcine reproductive and respiratory syndrome virus infection. Vet Res 44:95. doi: 10.1186/1297-9716-44-95

Kleiboeker SB, Schommer SK, Lee S-M, et al (2005) Simultaneous Detection of North American and European Porcine Reproductive and Respiratory Syndrome Virus Using Real-Time Quantitative Reverse Transcriptase–PCR. J Vet Diagnostic Investig 17:165–170. doi: 10.1177/104063870501700211

Kvisgaard LK, Hjulsager CK, Kristensen CS, et al (2013) Genetic and antigenic characterization of complete genomes of Type 1 Porcine Reproductive and Respiratory Syndrome viruses (PRRSV) isolated in Denmark over a period of 10 years. Virus Res 178:197–205. doi: 10.1016/j.virusres.2013.10.009

Lundstrom K (2016) Replicon RNA Viral Vectors as Vaccines. Vaccines 4:39. doi: 10.3390/vaccines4040039

Madsen KG, Hansen CM, Madsen ES, et al (1998) Sequence analysis of porcine reproductive and respiratory syndrome virus of the American type collected from Danish swine herds. Arch.Virol. 143:1683–1700.

McCullough K, Milona P, Thomann-Harwood L, et al (2014) Self-Amplifying Replicon RNA Vaccine Delivery to Dendritic Cells by Synthetic Nanoparticles. Vaccines 2:735–754. doi: 10.3390/vaccines2040735

Moodie Z, Huang Y, Gu L, et al (2006) Statistical positivity criteria for the analysis of ELISpot assay data in HIV-1 vaccine trials. J Immunol Methods 315:121–32. doi: 10.1016/j.jim.2006.07.015

Nilubol D, Tripipat T, Hoonsuwan T, et al (2013) Genetic diversity of the ORF5 gene of porcine reproductive and respiratory syndrome virus (PRRSV) genotypes I and II in Thailand. Arch Virol 158:943–953. doi: 10.1007/s00705-012-1573-7

Python S, Gerber M, Suter R, et al (2013) Efficient sensing of infected cells in absence of virus particles by plasmacytoid dendritic cells is blocked by the viral ribonuclease E(rns.). PLoS Pathog 9:e1003412. doi: 10.1371/journal.ppat.1003412

Renukaradhya GJ, Meng X-J, Calvert JG, et al (2015a) Inactivated and subunit vaccines against porcine reproductive and respiratory syndrome: Current status and future direction. Vaccine 33:3065–72. doi: 10.1016/j.vaccine.2015.04.102

Renukaradhya GJ, Meng X-J, Calvert JG, et al (2015b) Live porcine reproductive and respiratory syndrome virus vaccines: Current status and future direction. Vaccine 33:4069–80. doi: 10.1016/j.vaccine.2015.06.092

Rossow KD (1998) Porcine Reproductive and Respiratory Syndrome. Vet Pathol l:1–20.

Rowland RR, Lawson S, Rossow K, Benfield DA Lymphoid tissue tropism of porcine reproductive and respiratory syndrome virus replication during persistent infection of pigs originally exposed to virus in utero. Vet.Microbiol. 96:219–235.

Ruggli N, Tratschin JD, Mittelholzer C, Hofmann MA (1996) Nucleotide sequence of classical swine fever virus strain Alfort/187 and transcription of infectious RNA from stably cloned full-length cDNA. J Virol 70:3478–87.

Suter R, Summerfield A, Thomann-Harwood LJ, et al (2011) Immunogenic and replicative properties of classical swine fever virus replicon particles modified to induce IFN-α/β and carry foreign genes. Vaccine 29:1491–503. doi: 10.1016/j.vaccine.2010.12.026

Szymanski MR, Fiebach AR, Tratschin J-D, et al (2009) Zinc binding in pestivirus N(pro) is required for interferon regulatory factor 3 interaction and degradation. J Mol Biol 391:438–49. doi: 10.1016/j.jmb.2009.06.040

Tian K, Yu X, Zhao T, et al (2007) Emergence of fatal PRRSV variants: unparalleled outbreaks of atypical PRRS in China and molecular dissection of the unique hallmark. PLoS One 2:e526. doi: 10.1371/journal.pone.0000526

Wang F, Feng X, Zheng Q, et al (2012) Multiple linear epitopes (B-cell, CTL and Th) of JEV expressed in recombinant MVA as multiple epitope vaccine induces a protective immune response. Virol J 9:204. doi: 10.1186/1743-422X-9-204

Wernike K, Bonilauri P, Dauber M, et al (2012) Porcine reproductive and respiratory syndrome virus: interlaboratory ring trial to evaluate real-time reverse transcription polymerase chain reaction detection methods. J.Vet.Diagn.Invest 24:855–866.

PAPER 2 - SUPPLEMENTARY DATA 1:

NUCLEOTIDE AND AMINO ACID SEQUENCES OF CASSETTES INSERTED IN THE VRPS

VRP name	SLA specificity	Epitope succession in polyepitope*	#aa of polyepitope
VRP 0	[not relevant]	[not relevant]	8
VRP 1	SLA-1*0401	19-23-43-25-24-17-7-22-10	130
VRP 2	SLA-1*0401	23-7-22-10-25-24-43-19-17	130
VRP 3	SLA-1*0401	19-17-7-22-10-43-25-24-23	143
VRP 4	SLA-1*0702	34-33-10-5-18-17-13-29-46-43-2-50-28-39-19-30-11-25-23-4-49-53-7-27-44-38-9	395
VRP 5	SLA-1*0702	13-18-38-27-23-11-25-19-7-53-46-2-17-4-33-49-9-39-5-28-10-29-44-30-34-50-43	397
VRP 6	SLA-1*0702	2-13-34-33-18-23-50-53-5-28-39-7-29-46-17-9-49-25-4-30-27-43-11-19-44-38-10	395
VRP 7	SLA-2*0401	23-13-44-7-2-48-28-12-18-36-17-49	180
VRP 8	SLA-2*0401	2-12-23-44-7-18-13-48-36-17-49-28	176
VRP 9	SLA-2*0401	13-12-28-2-44-7-48-36-17-18-23-49	179

*Overview of the nine cassettes and their characteristics in terms of SLA specificity, epitopes, epitope succession, and length of polyepitopes. *with reference to the epitope IDs in table 1 (page 103)*

Color codes:

restriction sites (ClaI: cATCGATg, KasI: GGCGCC, MluI: ggACGCGTg, NotI: GCGGCCGC)
C-terminal part of CSFV N^{pro}
spacer
porcine UbV_{76}
HA tag
Flag tag
Stop codon
(Poly)epitope
mutations

Backbone cassette (VRP 0)

Aa sequence (*NproC138A-UbV-HA-SIINFEKL-Flag):

GAILLKLAKRGEPRTLKWIRNFTDCPLWVTSCSGMQIFVKTLTGKTITLEVEPSDTIENVKAKIQDKEGIPPDQQRLIF
AGKQLEDGRTLSDYNIQKESTLHLVLRLRGVYPYDVPDYAGASIINFEKLGRVSGDYKDDDDK*

Reverse translated and modified with flanking restriction sites:

CATCGATGGTGCCATACTGCTGAAGCTAGCCAAGAGGGGCGAGCCAAGAACCCTGAAGTGGATTAGAAATTTCACCGAC
TGTCCATTGTGGGTTACCAGTTGCAGCGGAATGCAGATTTTTGTCAAGACCCTCACCGGGAAGACCATTACACTGGAAG
TGGAGCCAAGCGATACCATCGAGAATGTCAAGGCCAAGATCCAGGACAAGGAGGGCATCCCCCCAGACCAGCAGAGGCT
GATCTTCGCTGGCAAGCAGCTGGAGGACGGACGCACCCTGTCCGACTACAACATCCAGAAGGAGAGCACCCTGCACCTG
GTGCTGAGGCTGAGGGGCGTGTACCCATACGACGTGCCAGACTACGCTGGCGCCTCCATCATTAACTTTGAGAAACTCG
GACGCGTGTCAGGAGACTACAAGGACGACGACGATAAATGAAGCGGCCGCT

VRP 1

Aa sequence of designed polyepitope (epitopes are underlined):

LSDSGRISYGDKKDPNISAVFQTYYNEQDQPTTMPSGFELYEDDQKDASDWFAPRYGDNPRTAPNEIAFGDKKDPRTAI
GTPVYEEEDDQVYERGCRWYDQEEDGKIFRFGSHKWNDENPKVAHNLGFYF

Reverse translated and modified with flanking restrictions sites:

GCAGGCGCCCTCAGCGACTCTGGCAGGATTTCTTATGGGGACAAAAAGGACCCTAATATCTCCGCCGTGTTTCAGACCT
ACTACAACGAGCAGGACCAGCCCACCACCATGCCATCCGGCTTCGAGCTGTACGAGGACGACCAGAAGGACGCCAGCGA
CTGGTTCGCTCCAAGATACGGCGACAACCCCAGAACCGCCCCAAACGAGATCGCCTTCGGCGACAAGAAGGACCCAAGG
ACCGCTATCGGAACCCCAGTGTACGAGGAGGAGGACGACCAGGTGTACGAGAGGGGATGCAGGTGGTACGACCAGGAGG
AGGACGGCAAGATCTTCAGGTTCGGCTCCCACAAATGGAACGATGAAAACCCCAAGGTCGCCCACAATCTCGGATTCTA
CTTCGGACGCGTGA

VRP 2

Aa sequence of designed polyepitope (epitopes are underlined):

NISAVFQTYYEQGEDGQVYERGCRWYDKPKKKKIFRFGSHKWGNGDGPKVAHNLGFYFNDDDDDASDWFAPRYPNEGDP
RTAPNEIAFEDPPTTMPSGFELYNDDDDDLSDSGRISYNKKPRTAIGTPVY

Reverse translated and modified with flanking restrictions sites:

GCAGGCGCCAATATTTCAGCCGTGTTCCAGACCTACTATGAGCAGGGGGAGGATGGGCAGGTGTATGAGAGGGGATGTC
GGTGGTATGATAAACCCAAGAAGAAGAAGATCTTCCGCTTCGGATCCCACAAGTGGGGAAACGGCGACGGACCAAAGGT
GGCTCACAACCTGGGCTTCTACTTCAACGACGACGACGACGACGCCAGCGACTGGTTCGCTCCAAGGTACCCAAACGAG
GGCGACCCAAGGACCGCCCCAAACGAGATCGCCTTCGAGGACCCCCCAACCACCATGCCATCCGGCTTCGAGCTGTATA
ATGACGACGACGACGACCTGAGCGACAGCGGAAGAATCTCCTACAATAAGAAACCAAGAACAGCCATCGGCACCCCAGT
CTATGGACGCGTGA

VRP 3

Aa sequence of designed polyepitope (epitopes are underlined):

LSDSGRISYADDGKDPRTAIGTPVYEDGKNEDDQVYERGCRWYEEEDKDEKIFRFGSHKWGNPPQPKVAHNLGFYFDKD
DADPPTTMPSGFELYEEGEDPKDASDWFAPRYGNPPQPRTAPNEIAFGEPPDPPNISAVFQTYY

Reverse translated and modified with flanking restrictions sites:

GCAGGCGCCCTCTCCGACTCAGGACGAATCTCTTATGCTGACGACGGGAAGGACCCTAGAACCGCTATTGGAACCCCAG
TGTACGAGGATGGAAAAAACGAGGACGACCAGGTGTACGAGAGGGGATGCAGGTGGTACGAGGAGGAGGACAAGGACGA
GAAGATCTTCCGCTTCGGCTCCCACAAGTGGGGAAACCCACCACAGCCAAAGGTGGCTCACAACCTGGGCTTCTACTTC
GACAAGGACGACGCTGACCCACCAACCACCATGCCATCCGGCTTCGAGCTGTACGAGGAGGGAGAGGACCCAAAGGACG
CCAGCGACTGGTTCGCTCCAAGATACGGCAATCCACCACAGCCAAGAACCGCCCCAAACGAGATCGCCTTCGGGGAACC
ACCAGACCCACCCAATATCTCAGCCGTGTTTCAGACATACTACGGACGCGTGA

VRP 4

Aa sequence of designed polyepitope (epitopes are underlined):

SSEGHLTSVYDDEKPGITANVTDENYEDPQPKVAHNLGFYFDPGDKDRALPFTLSNYDDNEEDYTAQFHPEIFNGPRTA
IGTPVYDPGDKDFTWYQLASYQPCDDMVNTTRVTYEGALATAPDGTYNDDDTTMPSGFELYNDDDYAQHMVLSYDDNEE
DNSFLDEAAYDPGDKDFVLSWLTPWDPGDKDVRWFAANLLYDGDDLSDSGRISYKPPDGKCVFFLLWRMQQPPPTRARH
AIFVYDPGDKDASDWFAPRYKDPKPNISAVFQTYYENVPHSKKDYSFPGPPFFDGDDFLNCAFTFGYPEDPGMPNYHWW
VEHDDNEEDQVYERGCRWYNEDDERPFFSSWLVKDPKPMSWRYSCTRYDDEKPGLSASSQTEYDPGDKDIVYSDDLVLY

Reverse translated and modified with flanking restrictions sites:

GCAGGCGCCTCATCCGAAGGCCACCTCACCTCCGTGTACGACGACGAGAAGCCAGGCATCACCGCTAATGTCACCGACG
AGAACTACGAAGACCCCCAGCCCAAGGTGGCCCACAACCTGGGCTTCTACTTCGACCCAGGCGACAAGGACCGCGCCCT
GCCATTCACCCTGTCCAACTACGACGACAACGAGGAGGACTACACCGCCCAGTTCCACCCCGAGATCTTCAACGGACCA
AGGACCGCTATCGGAACCCCCGTGTACGATCCCGGCGACAAGGACTTCACCTGGTACCAGCTGGCCTCCTACCAGCCCT
GCGACGACATGGTGAACACCACCCGCGTGACCTACGAGGGAGCCCTGGCTACCGCCCCCGACGGAACCTACAACGACGA
CGACACCACCATGCCAAGCGGCTTCGAGCTGTACAACGACGACGACTACGCCCAGCACATGGTGCTGTCTTATGATGAT
AACGAGGAGGACAACAGCTTCCTGGACGAGGCTGCTTATGATCCAGGCGACAAGGACTTCGTGCTGTCCTGGCTGACCC
CATGGGATCCTGGCGACAAAGACGTGAGGTGGTTCGCCGCCAACCTGCTGTACGACGGCGACGACCTGTCCGACAGCGG
AAGGATCAGCTACAAGCCCCCAGACGGCAAGTGCGTGTTCTTCCTGCTGTGGAGAATGCAGCAGCCACCACCAACCCGC
GCTAGGCACGCTATCTTCGTGTACGATCCTGGCGACAAGGACGCCTCCGACTGGTTCGCCCCAAGATACAAGGACCCAA
AGCCCAACATCAGCGCCGTGTTCCAGACCTACTACGAGAACGTGCCCCACTCCAAGAAGGACTACAGCTTCCCAGGCCC
ACCCTTCTTCGACGGCGACGACTTCCTGAACTGCGCCTTCACCTTCGGCTACCCAGAGGACCCCGGCATGCCAAACTAC
CACTGGTGGGTGGAGCATGATGACAACGAGGAGGACCAGGTGTACGAGAGGGGCTGCAGATGGTACAACGAGGACGACG
AGCGGCCCTTCTTCTCCAGCTGGCTGGTGAAGGACCCAAAGCCCATGTCCTGGCGCTACAGCTGCACCCGGTATGATGA
CGAGAAGCCAGGCCTGAGCGCCTCCAGCCAGACCGAATATGACCCAGGGGATAAAGACATCGTGTACTCAGATGACCTC
GTGCTCTACGGACGCGTGA

VRP 5:

Aa sequence of designed polyepitope (epitopes are underlined):

FTWYQLASYEPDDKPYTAQFHPEIFDNDKDLSASSQTEYDDADPERPFFSSWLVEPDDKPNISAVFQTYYNQPDDPTRA
RHAIFVYDNDKDASDWFAPRYDNDKDLSDSGRISYPPPGNGQVYERGCRWYPDEPGMPNYHWWVEHNQPDDPALATAPD
GTYNPKDYAQHMVLSYNPQQPPRTAIGTPVYQEDYSFPGPPFFPPPGNGITANVTDENYDNDKDFLNCAFTFGYPPPQG
DIVYSDDLVLYDDADPEVRWFAANLLYNQPDDPRALPFTLSNYDNDKDFVLSWLTPWEPDDKPKVAHNLGFYFDDMVNT
TRVTYEPDDKPMSWRYSCTRYDNDKDCVFFLLWRMDNDKDSSEGHLTSVYNPQQPPNSFLDEAAYNQPDDPTTMPSGFE
LY

Reverse translated and modified with flanking restrictions sites:

GCAGGCGCCTTTACATGGTATCAGCTCGCCTCCTATGAGCCAGACGACAAGCCCTACACCGCCCAGTTTCACCCAGAGA
TTTTCGACAATGACAAGGACCTGTCCGCCTCCAGCCAGACCGAGTACGACGACGCTGACCCAGAGAGGCCCTTCTTCTC
CAGCTGGCTGGTGGAGCCCGACGACAAGCCAAACATCAGCGCCGTGTTCCAGACCTATTATAACCAGCCAGACGACCCA
ACCCGCGCTAGGCACGCTATCTTCGTGTACGACAACGACAAGGACGCCTCCGACTGGTTCGCCCCCAGATATGATAACG
ACAAGGACCTGTCCGACAGCGGCAGAATCAGCTACCCACCACCAGGAAACGGACAGGTGTACGAGAGGGGATGCAGATG
GTACCCAGACGAGCCCGGCATGCCAAACTACCACTGGTGGGTGGAGCATAATCAGCCCGACGACCCAGCCCTGGCTACC
GCCCCCGACGGCACCTACAACCCAAAGGACTACGCCCAGCACATGGTGCTGTCCTACAACCCACAGCAGCCACCAAGGA
CCGCTATCGGAACCCCCGTGTACCAGGAGGACTACAGCTTCCCAGGACCACCCTTCTTCCCACCACCAGGCAACGGCAT
CACCGCCAACGTGACCGACGAGAACTATGATAATGACAAGGACTTCCTGAACTGCGCCTTCACCTTCGGCTACCCACCA
CCACAGGGCGACATCGTGTACTCCGACGACCTGGTGCTGTATGATGACGCTGACCCAGAGGTGCGCTGGTTCGCTGCCA
ACCTGCTGTACAATCAGCCCGATGACCCACGGGCCCTGCCATTCACCCTGTCCAACTATGATAACGATAAGGACTTCGT
GCTGAGCTGGCTGACCCCATGGGAACCCGACGACAAGCCCAAGGTGGCCCACAACCTGGGCTTCTACTTCGACGACATG
GTGAACACCACCAGGGTGACCTACGAACCTGACGACAAGCCAATGTCCTGGCGCTACAGCTGCACCCGGTATGATAATG
ATAAAGACTGCGTGTTCTTCCTGCTGTGGAGAATGGACAACGACAAGGACTCCAGCGAGGGCCACCTGACCTCCGTGTA
CAACCCCCAGCAGCCACCCAACAGCTTCCTGGACGAAGCCGCCTACAACCAGCCAGACGACCCCACCACAATGCCATCA
GGATTTGAACTCTATGGACGCGTGA

VRP 6:

Aa sequence of designed polyepitope (epitopes are underlined):

YAQHMVLSYDDEKPGFTWYQLASYGEDSSEGHLTSVYGGDKNGITANVTDENYDDNEEDYTAQFHPEIFGPDDKPNISA
VFQTYYGPDDKPNSFLDEAAYPEDPGMPNYHWWVEHGPDDKPRALPFTLSNYDPGDKDFVLSWLTPWDDADPEVRWFAA
NLLYGPDDKPQVYERGCRWYEDDDMVNTTRVTYDDGALATAPDGTYGGPRTAIGTPVYDPGDKDIVYSDDLVLYNDPKD
FLNCAFTFGYDQEEPASDWFAPRYEDDDYSFPGPPFFDDEKPGCVFFLLWRMPGNEKPRPFFSSWLVQGEPPTTMPSGF
ELYPEPPTRARHAIFVYQPDPDDLSDSGRISYGPDDKPMSWRYSCTRYQPDPDDLSASSQTEYGPDDKPKVAHNLGFYF

Reverse translated and modified with flanking restrictions sites:

GCAGGCGCCTATGCCCAGCACATGGTCCTGTCCTACGACGATGAGAAGCCCGGATTCACATGGTATCAGCTCGCCAGCT
ACGGAGAAGATTCCAGCGAGGGACACCTGACCTCCGTGTACGGAGGCGACAAGAACGGCATCACCGCCAACGTGACCGA
CGAGAACTACGACGACAACGAGGAGGACTACACCGCCCAGTTCCACCCCGAGATCTTCGGCCCAGACGACAAGCCCAAC
ATCTCCGCCGTGTTCCAGACCTACTATGGACCCGATGACAAGCCCAACAGCTTCCTGGACGAGGCTGCTTACCCAGAGG
ACCCAGGCATGCCCAACTACCACTGGTGGGTGGAGCACGGACCAGACGACAAGCCAAGGGCCCTGCCATTCACCCTGTC
CAACTACGACCCCGGCGACAAGGACTTCGTGCTGAGCTGGCTGACCCCATGGGACGACGCTGACCCAGAGGTGAGATGG
TTCGCTGCTAACCTGCTGTATGGCCCAGACGACAAGCCACAGGTGTACGAGAGGGGCTGCAGATGGTACGAGGACGACG
ACATGGTGAACACCACCCGCGTGACCTACGACGACGGAGCCCTGGCTACCGCCCCCGACGGCACCTACGGCGGCCCAAG
GACCGCTATCGGAACCCCCGTGTACGACCCAGGCGACAAGGACATCGTGTACTCCGACGACCTGGTGCTGTACAACGAC
CCCAAGGACTTCCTGAACTGCGCCTTCACCTTCGGCTACGACCAGGAGGAGCCAGCTTCCGACTGGTTCGCTCCACGCT
ACGAGGACGACGACTACAGCTTCCCAGGACCACCATTCTTCGACGACGAGAAGCCAGGCTGCGTGTTCTTCCTGCTGTG
GAGGATGCCCGGCAACGAGAAGCCCAGACCATTCTTCTCCAGCTGGCTGGTGCAGGGAGAGCCACCAACCACCATGCCA
AGCGGCTTCGAGCTGTACCCAGAGCCACCAACCCGCGCTAGGCACGCTATCTTCGTGTACCAGCCAGACCCAGACGACC
TGTCCGACAGCGGAAGGATCTCCTATGGGCCAGACGACAAGCCAATGTCCTGGAGGTACAGCTGCACCCGGTATCAGCC
CGACCCAGACGACCTGAGCGCCTCCAGCCAGACAGAGTATGGACCTGACGATAAACCTAAAGTCGCCCACAACCTCGGA
TTCTATTTCGGACGCGTGA

VRP 7:

Aa sequence of designed polyepitope (epitopes are underlined):

NISAVFQTYYNEEDKDFTWYQLASYNEEDKDMSWRYSCTRYGPEDPDQVYERGCRWYGPEDPDYAQHMVLSYDDEKPGW
GVYSAIETWNEEDKDFVLSWLTPWPPQKPPLSFSYTAQFNEEDKDYTAQFHPEIFPPQKPPLTAALNRNRWDEGPPRTA
IGTPVYNEEDKDFLNCAFTFGY

Reverse translated and modified with flanking restrictions sites:

GCAGGCGCCAACATTTCCGCCGTGTTTCAGACCTACTACAACGAGGAGGACAAGGACTTTACATGGTATCAGCTGGCTT
CATACAACGAGGAGGACAAGGACATGTCCTGGAGGTACAGCTGCACCAGGTACGGACCAGAGGACCCAGACCAGGTGTA
CGAGAGGGGATGCAGATGGTATGGCCCAGAGGACCCAGACTACGCTCAGCACATGGTGCTGTCCTACGACGACGAGAAG
CCAGGATGGGGCGTGTACAGCGCCATCGAGACCTGGAATGAAGAGGACAAGGACTTCGTGCTGTCCTGGCTGACCCCAT
GGCCACCACAGAAGCCACCACTGTCCTTCAGCTACACCGCCCAGTTCAACGAAGAAGACAAGGACTACACCGCCCAGTT
CCACCCCGAGATCTTCCCCCCCCAGAAGCCACCACTGACCGCCGCCCTGAACCGCAACCGGTGGGACGAGGGCCCCCA
CGCACCGCCATCGGCACCCCTGTCTACAACGAGGAGGATAAGGATTTTCTGAACTGTGCTTTTACATTTGGATACGGAC
GCGTGA

VRP 8:

Aa sequence of designed polyepitope (epitopes are underlined):

YAQHMVLSYDPPDEDLSFSYTAQFPPEDPNISAVFQTYYDPPDEDMSWRYSCTRYEPDEGQVYERGCRWYQEDEDDYTA
QFHPEIFDGPKDFTWYQLASYEEKKDGWGVYSAIETWPPEEKNLTAALNRNRWDEEEPRTAIGTPVYPPEDPFLNCAFT
FGYDPPDEDFVLSWLTPW

Reverse translated and modified with flanking restrictions sites:

GCAGGCGCCTATGCCCAGCACATGGTCCTCTCCTATGATCCCCCCGACGAAGACCTCTCCTTTTCCTACACCGCTCAGT
TTCCTCCAGAAGACCCTAACATCTCCGCCGTGTTCCAGACCTACTACGACCCCCCAGACGAGGACATGTCCTGGCGCTA
CAGCTGCACCAGGTACGAGCCAGACGAGGGCCAGGTGTACGAGAGGGGCTGCAGATGGTACCAGGAGGACGAGGACGAC
TACACCGCCCAGTTCCACCCCGAGATCTTCGACGGCCCAAAGGACTTCACCTGGTACCAGCTGGCCTCCTACGAGGAGA
AGAAGGACGGCTGGGGCGTGTACAGCGCCATCGAGACCTGGCCCCCAGAGGAGAAGAACCTGACCGCCGCCCTGAACAG
GAACAGATGGGACGAGGAGGAGCCAAGGACCGCTATCGGAACCCCAGTGTACCCACCAGAGGACCCCTTCCTGAACTGC
GCCTTTACATTTGGATACGACCCACCCGATGAGGACTTTGTGCTGTCTTGGCTGACCCCTTGGGGACGCGTGA

VRP 9:

Aa sequence of designed polyepitope (epitopes are underlined):

FTWYQLASYKDEEEDLSFSYTAQFPEDDEKFVLSWLTPWQNGDPDYAQHMVLSYDDDPEPMSWRYSCTRYGPPPGGQVY
ERGCRWYPPPKDGWGVYSAIETWGPPPGGLTAALNRNRWDDDPEPRTAIGTPVYGGAKDDYTAQFHPEIFDNKKPNISA
VFQTYYDEKKDFLNCAFTFGY

Reverse translated and modified with flanking restrictions sites:

GCAGGCGCCTTCACATGGTATCAGCTGGCTTCATACAAGGACGAGGAGGAGGATCTGTCATTCTCATACACCGCTCAGT
TTCCCGAGGACGACGAAAAGTTCGTGCTGTCCTGGCTGACCCCATGGCAGAACGGCGACCCAGACTACGCTCAGCACAT
GGTGCTGAGCTACGACGACGACCCAGAGCCCATGTCCTGGAGGTACAGCTGCACCAGGTACGGACCACCACCAGGAGGA
CAGGTGTACGAGAGGGGCTGCAGATGGTACCCACCACCAAAGGACGGATGGGGCGTGTACTCCGCCATCGAGACCTGGG
GCCCCCCACCAGGAGGACTGACCGCCGCCCTGAACCGCAACCGGTGGGACGACGACCCAGAGCCAAGGACCGCTATCGG
AACCCCCGTGTACGGAGGAGCCAAGGACGACTACACCGCCCAGTTCCACCCAGAGATCTTCGACAACAAGAAGCCCAAC
ATCAGCGCCGTGTTCCAGACCTACTATGACGAGAAGAAGGATTTCCTGAACTGTGCTTTTACATTTGGCTATGGACGCG
TGA

PAPER 2 - SUPPLEMENTARY DATA 2:

VERIFICATION OF VRP INFECTIVITY AND POLYEPITOPE EXPRESSION AND DEGRADATION

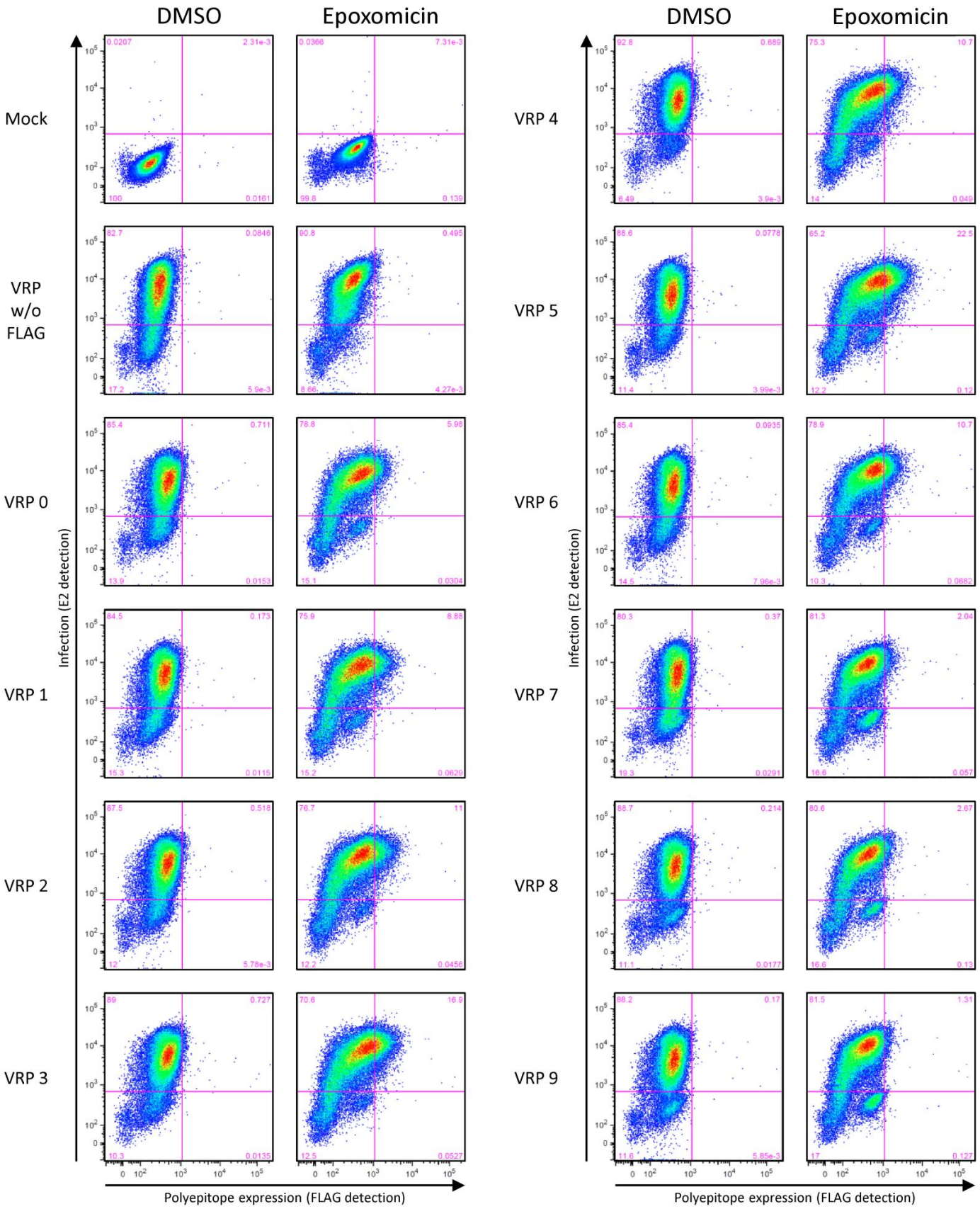

APPENDICES

Appendix A - “The Program” - code

```
### INPUT FILE(S) ###
sbx = "C:\\Users\\Siwel\\Desktop\\test\\"
gt2_consensus = "I:\\BACKUP\\Siwel\\Bioinformatic\\Sequences\\gt2\\Protein\\Consensus\\As FASTA\\"

input_path = gt2_consensus
multiple_files = 0 # Test multiple files yes/no from input_path (1/0)
overview = 1 # Only relevant if multiple_files == 1
ORF = "ORF1a"
criteria = "" # Test files only if criteria is in filename
inputfile = "A2 - ORF1a - majority - Consensus.fa" # Not relevant if testing multiple files

### MATRICES ###
# Turn matrices on/off (1/0)
IO = {"SLA1-0401": 1,
      "SLA1-0702": 1,
      "SLA2-0401": 1,
      "SLA2-0501": 0,
      "SLA3-0401": 0}
matrix_path = "I:\\Documents\\Bioinformatic\\PSCPL Matrices\\"


### MODULE DISPLAY ###
# Choose modules and module order (0 leaves out module)
nine_mer_bind_score = 0
nine_mer_anchor     = 0
matrix_rank_score   = 1
ten_mer_bind_score  = 2
ten_mer_anchor      = 0


### PARAMETERS ###
RB_limit = 2 # Relative binding
MRS_threshold = 25 # Matrix rank score


### OUTPUT ###
print_seqFile = 0
print_overview = 0
overwrite = 1
outputPath = "C:\\Users\\Siwel\\Desktop\\test\\out\\"
```

--(new block)--

```
### VARIOUS FUNCTIONS ETC

OV_go = 0
if overview == 1 and multiple_files == 1:
    if input_path != sbx and ORF != "":
        OV_go = 1
    else:
        print "change overview parameters"

PSCPL_content = {"SLA1-0401": {"P": range(1,3), "AA": range(3), "Anchors": ["P2", "P3", "P9"], "AnchorValues": ["P2: 28", "P3: 57", "P9: 67"]},
                 "SLA1-0702": {"P": range(1,2), "AA": range(2), "Anchors": ["P2", "P9"], "AnchorValues": ["P2: 16", "P9: 25"]},
                 "SLA2-0401": {"P": range(1,2), "AA": range(2), "Anchors": ["P2", "P7", "P9"], "AnchorValues": ["P2: 77", "P7: 19", "P9: 132"]},
                 "SLA2-0501": {"P": range(0), "AA": range(0), "Anchors": ["P9"], "AnchorValues": ["P9: 61"]},
                 "SLA3-0401": {"P": range(1,2), "AA": range(2), "Anchors": ["P2"], "AnchorValues": ["P2: 27"]}}

### MATRIX LIST CALCULATOR
mat_list = ["SLA1-0401", "SLA1-0702", "SLA2-0401", "SLA2-0501", "SLA3-0401" ]
Matrix = []
for mat in range(len(mat_list)):
    if IO[mat_list[mat]] == 1:
        Matrix.append(mat_list[mat])

### PRESENTATION ORDER OF MODULES CALCULATOR
comp_order = []
newOrder = [nine_mer_bind_score, nine_mer_anchor, matrix_rank_score, ten_mer_bind_score, ten_mer_anchor]
modOrder = [0,1,2,3,4]
points = zip(newOrder, modOrder)
sorted_points = sorted(points)
for point in sorted_points:
    if point[0] > 0:
        comp_order.append(point[1]) # for point in sorted_points)

Anchor_conv = {"P1": 1, "P2": 2, "P3": 3, "P4": 4, "P5": 5, "P6": 6, "P7": 7, "P8": 8, "P9": 9}
conservation = ["majority", "50%", "60%", "70%", "80%", "90%", "100"]


fragment_size = 10

def addtoheader(sublist,count,string0, string1):
    if current == 0:
        if sublist == 0:
            if count == 0:
                header[sublist][module].append(string0)
```

```
            else: #elif count > 1:
                header[sublist][module].append("")
        elif sublist == 1:
            header[sublist][module].append(string1)
        elif sublist == 2:
            for a in range(sublist):
                if a == 0:
                    if count == 0:
                        header[a][module].append(string0)
                    else: #elif count > 1:
                        header[a][module].append("")
                else:
                    header[a][module].append(string1)

def module_iter():
    global module_counter
    global module
    global output
    module_counter += 1
    module = module_counter -1
    output.append([])
    if OV_go == 1:
        if current == 0:
            OV[seqs][M].append([])
        OV[seqs][M][module].append([])
    if current == 0:
        for n in range(2):
            header[n].append([])

def spacer_add():
    if comp_order[0] == module:
        addtoheader(2,0,SLAbreak,SLAbreak)
        output[module].append(SLAbreak)
    else:
        addtoheader(2,0,spacer,spacer)
        output[module].append(spacer)
```

--(new block)--

```
# Testing ALL fasta files in testfile_path
# Multiple PSCPLs
# Fragment length = 10 incl 9

from Bio import SeqIO
import os
import fnmatch
from numpy import prod
import sys

STOP = 0
testfile = []
inputlist = []
if multiple_files == 1:
    if OV_go == 1:
        OV = []
        Perm_out = []
        OV_out = []
        for root, dir, files in os.walk(input_path):
            for num in range(len(conservation)):
                for item in fnmatch.filter(files, "*.fa"):
                    if (ORF+" ") in item and conservation[num] in item:
                        inputlist.append(item)
        for seqs in range(len(inputlist)):
            if not len(SeqIO.read(input_path+inputlist[seqs],"fasta").seq)-len(SeqIO.read(input_path+inputlist[0],"fasta").seq) == 0:
                STOP = 1
                print "Seqs have different length"
            else:
                print "Seqs have same lenght"
    else:
        for root, dir, files in os.walk(input_path):
            for item in fnmatch.filter(files, "*.fa"):
                if criteria in item:
                    inputlist.append(item)
else:
    inputlist.append(inputfile)

if not STOP == 1:
    for seqs in range(len(inputlist)):
        if OV_go == 1:
            OV.append([])
        M_out = []
        top_head = []
        bottom_head = []
        outputString_data = ""
        top_header = ""
        bottom_header = ""

        spacer = "|"
        SLAbreak = "|//\\\\\|"

        ### IMPORT SEQUENCE ###
        with open(input_path + inputlist[seqs], "r") as handle:
            record = "-"+str(SeqIO.read(handle,"fasta").seq)
            print "req len", len(record)

        for M in range(len(Matrix)):
            PSCPL = Matrix[M]
            if OV_go == 1:
                OV[seqs].append([])

            ### IMPORT MATRIX ###
            with open(matrix_path + "%s.csv" % PSCPL, "r") as handle:
```

```
                SLA_lib = []
                content = [line.strip().split(";") for line in handle.readlines()[2:22]]
                for p in range(9):
                    SLA_lib.append({}) # Danner 9 tomme dictionaries - én for hver 'lomme' (P) i MHC'en
                    for line in range(len(content)): # len(content) = 20, da der er en linje for hver amino syre.
                        lineList = content[line]
                        SLA_lib[p][lineList[0]] = float(lineList[p+1].replace(",","."))

            ### ITERATING THROUGH SEQUENCE ###
            current = 0
            while True:

                ### LOOP BREAK ###
                if current+fragment_size-1 == len(record):
                    if M == 0:
                        outputString_break = "Break after:        \t"+ str(current+fragment_size-1)
                    break

                ### LISTS ###
                output = []
                if current == 0:
                    header = [[],[]]
                if M == 0:
                    M_out.append([])

                module_counter = 0

                ### PERMANENT MODULE  ###
                # List of fragments
                frag = record[current:current+fragment_size]
                if M == 0:
                    M_out[current] = [(str( current+1 ).zfill(3)), ("("+frag[0]+")"+frag[1:10])] # laver en liste over lister. Hver underliste
indholder PSCPL scores for det pågældende fragment
                    if "majority" in inputlist[seqs] and OV_go == 1:
                        Perm_out.append([])
                        for line in M_out[current]:
                            Perm_out[current].append(line)
                        Perm_out[current].append(SLAbreak)
                    if not "X" in frag[3:9]:
                        M_out[current].append("cons")
                    else:
                        M_out[current].append("")
                    if current == 0:
                        top_head = ["","  Seq      ", ""]
                        bottom_head = ["Start", "(0)123456789", "CONS"]

                    ### MODULE
                    # Standard binding (9-mers) - Raw data input
                    module_iter()
                    spacer_add()
                    std_list = []
                    if OV_go ==1:
                        OV_std_list = []
                    for i in range(fragment_size-1):
                        if frag[i+1] in SLA_lib[i]:
                            val = SLA_lib[i][frag[i+1]] # angiver værdien i PSCPL matricen for position i, aminosyre i
                        else:
                            val = "NA"
                        output[module].append(val) # tilføjer denne værdi til underlisten for det aktuelle fragment
                        addtoheader(2,i,PSCPL[-6:],"aa"+str(i+1)+"/P"+str(i+1))

                    if not "NA" in output[module]:
                        MRS = str(round(prod(output[module][1:]),1)).rjust(5)
                    else:
                        MRS = "  NA"

                    for j in range(len(PSCPL_content[PSCPL]["Anchors"])):
                        if output[module][Anchor_conv[PSCPL_content[PSCPL]["Anchors"][j]]] >= RB_limit and
output[module][Anchor_conv[PSCPL_content[PSCPL]["Anchors"][j]]] != "NA":
                            std_list.append("aa"+str(Anchor_conv[PSCPL_content[PSCPL]["Anchors"][j]])+"/"+PSCPL_content[PSCPL]["Anchors"][j])
                            if OV_go ==1:

OV_std_list.append(str(Anchor_conv[PSCPL_content[PSCPL]["Anchors"][j]])+str(Anchor_conv[PSCPL_content[PSCPL]["Anchors"][j]]))
                        elif output[module][Anchor_conv[PSCPL_content[PSCPL]["Anchors"][j]]] == "NA":
                            std_list.append("  --")
                            if OV_go ==1:
                                OV_std_list.append("--")
                        else:
                            std_list.append("")
                            if OV_go ==1:
                                OV_std_list.append("  ")

                    ### MODULE
                    # Standard binding (9-mers) - Anchor highlight
                    module_iter()
                    spacer_add()
                    for j in range(len(std_list)):
                        output[module].append(std_list[j])
                        addtoheader(2,j, PSCPL[-6:],"Std AP")
                    if OV_go == 1:
                        stdString = ""
                        for j in range(len(OV_std_list)-1):
                            stdString += str(OV_std_list[j])+"-"
                        stdString += str(OV_std_list[len(OV_std_list)-1])
                        OV[seqs][M][module][current].append(stdString)

                    ### MODULE
                    # Matrix Rank Score (MRS)
                    module_iter()
                    spacer_add()
                    output[module].append(MRS)
                    if OV_go == 1:
                        if "majority" in inputlist[seqs]:
                            OV[seqs][M][module][current].append(MRS)
                    if MRS != "  NA":
                        if float(MRS) >= MRS_threshold:
                            output[module].append(">"+str(MRS_threshold))
                            if OV_go ==1:
                                OV[seqs][M][module][current].append(">"+str(MRS_threshold))
```

```
                        else:
                            output[module].append("")
                            if OV_go ==1:
                                OV[seqs][M][module][current].append("")
                    else:
                        output[module].append("--")
                        if OV_go ==1:
                            OV[seqs][M][module][current].append("--")

                    addtoheader(2,0,PSCPL[-6:], "MRS")
                    addtoheader(2,0,"", ">"+str(MRS_threshold))

                    ### MODULE
                    # Alternative binding (10-mers) - Raw data input
                    module_iter()
                    spacer_add()
                    alt_list = []
                    if OV_go ==1:
                        OV_alt_list = []
                    for p in PSCPL_content[PSCPL]["P"]:
                        for aa in PSCPL_content[PSCPL]["AA"]:
                            if aa < p+1:
                                if frag[aa] in SLA_lib[p]:
                                    val = SLA_lib[p][frag[aa]] # angiver værdien i PSCPL matricen for position 2, hhv aminosyre 1 og 2
                                else:
                                    val = "NA"
                                output[module].append(val) # tilføjer denne værdi til underlisten for det aktuelle fragment, hvis dette ikke er
en aminosyre

                                if val >= RB_limit and val != "NA":
                                    alt_list.append("aa"+str(aa)+"/P"+str(p+1))
                                    if OV_go ==1:
                                        OV_alt_list.append(str(aa)+str(p+1))
                                elif val == "NA":
                                    alt_list.append("  --")
                                    if OV_go ==1:
                                        OV_alt_list.append("--")
                                else:
                                    alt_list.append("")
                                    if OV_go ==1:
                                        OV_alt_list.append("  ")

                                addtoheader(1,0,"","aa"+str(aa)+"/P"+str(p+1))
                    for i in range(len(output[module])-1):
                        addtoheader(0,i,PSCPL[-6:],"")

                    ### MODULE
                    # Alternative binding (10-mers) - Anchor highlight
                    module_iter()
                    spacer_add()
                    for j in range(len(alt_list)):
                        output[module].append(alt_list[j])
                        addtoheader(2,j, PSCPL[-6:],"Alt AP")
                    if OV_go == 1:
                        altString = ""
                        for j in range(len(OV_alt_list)-1):
                            altString += str(OV_alt_list[j])+"-"
                        altString += str(OV_alt_list[len(OV_alt_list)-1])
                        OV[seqs][M][module][current].append(altString)
                        OV[seqs][M][module][current].append(spacer)

                    ### COLLECT MODULE DATA / HEADINGS
                    for modules in comp_order:
                        if len(output[modules]) > 1:
                            for values in range(len(output[modules])): # table data
                                M_out[current].append(output[modules][values])
                            if current == 0:
                                for values in range(len(header[0][modules])): # table headings
                                    top_head.append(header[0][modules][values])
                                for values in range(len(header[1][modules])):
                                    bottom_head.append(header[1][modules][values])


                    current += 1
        if 1==0:
            ### ADD MODULE DATA TO OUTPUT STRING
            for line in range(len(M_out)):
                for value in range(len(M_out[line])):
                    outputString_data += str(M_out[line][value]).replace('.', ',') + "\t"
                outputString_data += "\n"

            ### ADD MODULE HEADINGS TO OUTPUT STRING
            for top_headings in range(len(top_head)):
                top_header += str(top_head[top_headings]) + "\t"
            for bottom_headings in range(len(bottom_head)):
                bottom_header += str(bottom_head[bottom_headings]) + "\t"

            ### COMPILE OUTPUT STRING
            outputString = "Sequence:         \t"+ inputlist[ORFgroup][seqs] + "\n"
            outputString += "Length:              \t"+ str(len(record))+" amino acids\n"
            outputString += outputString_break+"\n"
            outputString += "Fragment Length:\t"+ str(fragment_size)+"\n"
            outputString += "Relative binding:\tThreshold = "+ str(RB_limit)+"\n"
            outputString += "Matrix rank score:\tThreshold = "+ str(MRS_threshold) + "\n"
            for n in range(len(Matrix)):
                outputString += "PSCPL:                \t"+ Matrix[n]+ " - "+str(PSCPL_content[Matrix[n]]["AnchorValues"])+"\n"
            outputString += "\n"+top_header + "\n"
            outputString += bottom_header + "\n"
            outputString += outputString_data

            ### CREATE .TXT FILE
            outputFile = outputPath + "PSCPL - " + str(fragment_size) + " aa - RT"+str(RB_limit)+" @ " + inputlist[ORFgroup][seqs][:-3] + ".txt"
            if print_seqFile == 1:
                if os.path.exists(outputFile) and overwrite == 1 or not os.path.exists(outputFile):
                    file = open(outputFile, "w")
                    file.write(str(outputString))
                    file.flush()
                    print "file created: " + outputFile
```

```
            else:
                print "could not overwrite: " + outputFile
        else:
            print "Not allowed to print seqfiles"


### COLLECT OVERVIEW DATA
if OV_go == 1:
    OVstring = ""
    for M in range(len(Matrix)):
        for seqs in range(len(inputlist)):
            for module in [2, 1, 4]:
                for current in range(len(OV[seqs][M][module])):
                    for values in range(len(OV[seqs][M][module][current])):
                        Perm_out[current].append(OV[seqs][M][module][current][values])
        Perm_out[current].append(SLAbreak)

    for line in range(len(Perm_out)):
        for val in range(len(Perm_out[line])):
            OVstring += str(Perm_out[line][val]) + "\t"
        OVstring += "\n"

    OVoutput = outputPath + "OVtest.txt"
    if os.path.exists(OVoutput):
                file = open(OVoutput, "w")
                file.write(str(OVstring))
                file.flush()
                print "file created: " + OVoutput
```

Appendix B - PopCover output

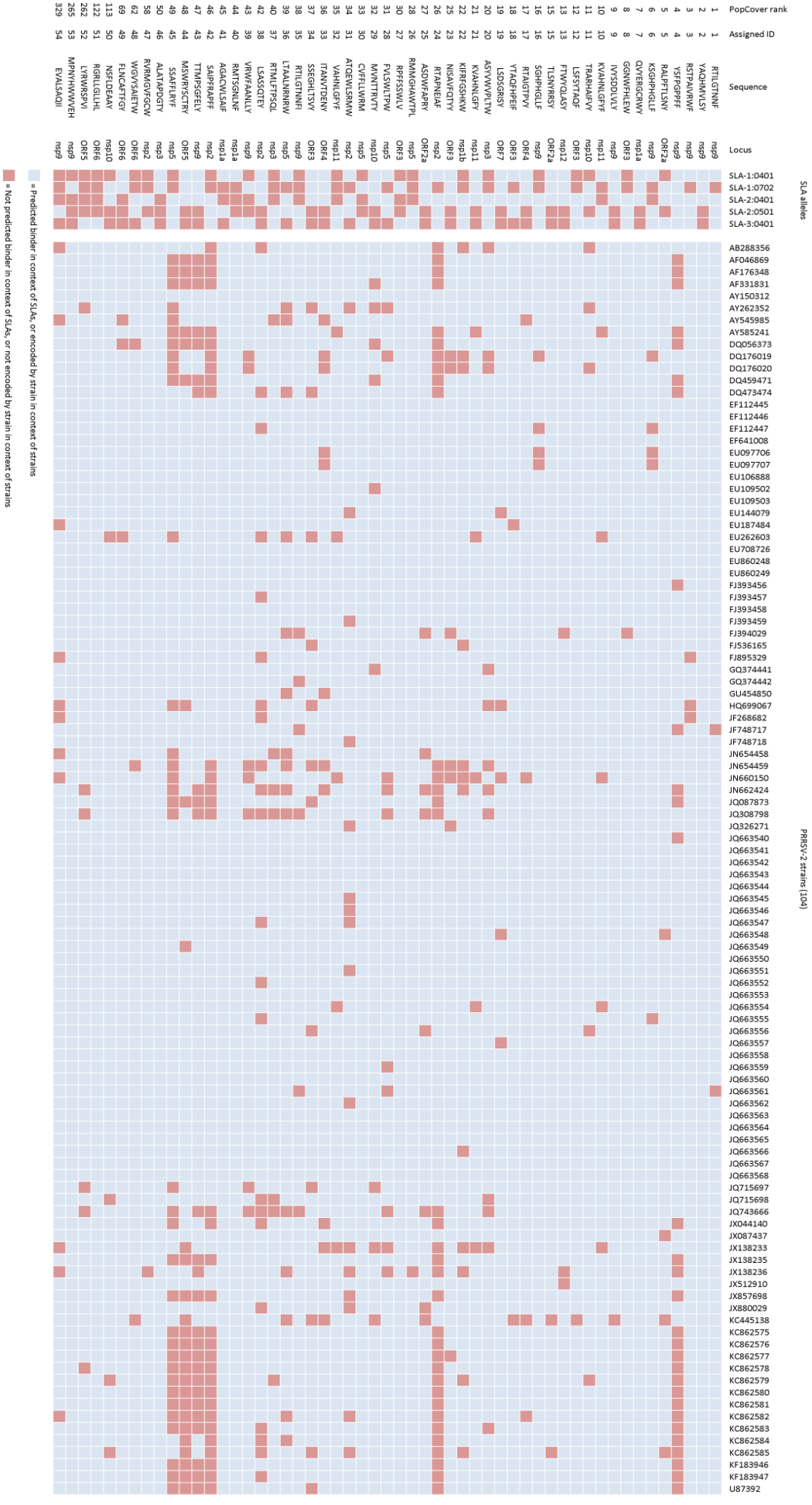

Appendix C - "Juncitope" output - VRP1

```
PROCESSING ID:
              User:                       Simon
              Start time:                 28-Jul-2015, 09:40:55
              End time:                   29-Jul-2015, 15:03:13
              Processing time:            05:22:17
              Inputfile:                  /home/siwel/Documents/SLA-10401.txt


SETTINGS:
              Rank threshold:             4
              Neotope weight:             8-mer:                      25%
                                          9-mer:                      100%
                                          10-mer:                     100%
                                          11-mer:                     50%

              MHC weight:                 SLA-1*0401:   100%
                                          SLA-1*0501:   100%
                                          SLA-1*0702:   100%
                                          SLA-1*0801:   100%
                                          SLA-1*1101:   100%
                                          SLA-1*1201:   100%
                                          SLA-2*0202:   100%
                                          SLA-2*0301:   100%
                                          SLA-2*0401:   100%
                                          SLA-2*0502:   100%
                                          SLA-2*0601:   100%
                                          SLA-2*0701:   100%
                                          SLA-2*1001:   100%
                                          SLA-2*1101:   100%
                                          SLA-3*0101:   100%
                                          SLA-3*0302:   100%
                                          SLA-3*0401:   100%
                                          SLA-3*0502:   100%
                                          SLA-6*0101:   100%

              Spacer aa's:                ADEGKNPQ
              Spacer length:              0-7 aa's
              Spacers per iteration:      Maximum allowed
              Iterations:                 5

PRE PROCESSING:
              Neotopes:                   179
              Junctions:                  8

              Neoepitope Distrib:         8-mer         9-mer         10-mer        11-mer
              SLA-1*0401:                   0             0             2             1
              SLA-1*0501:                   0             3             5             6
              SLA-1*0702:                   0             2             6             4
              SLA-1*0801:                   0             1             3             1
              SLA-1*1101:                   1             1             4             2
              SLA-1*1201:                   0             2             6             6
              SLA-2*0202:                   0             2             2             2
              SLA-2*0301:                   1             2             2             1
              SLA-2*0401:                   0             2             7             5
              SLA-2*0502:                   0             1             4             3
              SLA-2*0601:                   1             4             4             0
              SLA-2*0701:                   1             2             3             2
              SLA-2*1001:                   0             1             3             0
              SLA-2*1101:                   0             2             2             0
              SLA-3*0101:                   1             6             6             0
              SLA-3*0302:                   0             6             9             2
              SLA-3*0401:                   0             5             6             3
              SLA-3*0502:                   0             4             3             1
              SLA-6*0101:                   0             3             7             2

CURRENT PROCESSING SUMMARY:
              Neotopes left:              3 real, 4 false
              Junctions:                  3

              Neoepitope Distrib:         8-mer         9-mer         10-mer        11-mer
              SLA-1*0401:                   0             0             0             0
              SLA-1*0501:                   0             0             0             0
              SLA-1*0702:                   0             1             1             0
              SLA-1*0801:                   0             0             0             0
              SLA-1*1101:                   0             0             0             0
              SLA-1*1201:                   0             1             0             0
```

```
            SLA-2*0202:                 0           0           0           0
            SLA-2*0301:                 0           0           0           0
            SLA-2*0401:                 0           0           2           0
            SLA-2*0502:                 0           0           0           0
            SLA-2*0601:                 0           0           0           0
            SLA-2*0701:                 0           0           0           0
            SLA-2*1001:                 0           0           0           0
            SLA-2*1101:                 0           1           0           1
            SLA-3*0101:                 0           0           0           0
            SLA-3*0302:                 0           0           0           0
            SLA-3*0401:                 0           0           0           0
            SLA-3*0502:                 0           0           0           0
            SLA-6*0101:                 0           0           0           0

            End reason:               No more combinations
            Random spacers tried:     1624
            Combinations tried:       4

INPUT:
            Epitopes      ID
            QVYERGCRWY    ID7-V1-S+
            KVAHNLGFYF    ID10-V1-S+
            KIFRFGSHKW    ID22-V1-S+
            NISAVFQTYY    ID23-V1-S+
            TTMPSGFELY    ID43-V0-S+
            RTAIGTPVY     ID17-V1-S++
            LSDSGRISY     ID19-V1-S++
            RTAPNEIAF     ID24-V0-S++
            ASDWFAPRY     ID25-V1-S++

            Excluded
            KVAHNLGFY nested in KVAHNLGFYF

            Total:        9
            9-mer:        4
            10-mer:       5

OUTPUT:
            >final seq
            LSDSGRISYGDKKDPNISAVFQTYYNEQDQPTTMPSGFELYEDDQKDASDWFAPRYGDNP
            RTAPNEIAFGDKKDPRTAIGTPVYEEEDDQVYERGCRWYDQEEDGKIFRFGSHKWNDENP
            KVAHNLGFYF

            Final ID order:
            ID19-V1-S++-?-ID23-V1-S+-?-ID43-V0-S+-?-ID25-V1-S++-?-ID24-V
            0-S++-?-ID17-V1-S++-?-ID7-V1-S+-?-ID22-V1-S+-?-ID10-V1-S+

JUNCTION OVERVIEW:
g?d: 0-14                           0         10        20
            Final Seq:              LSDSGRISYGDKKDPNISAVFQTYYNEQDQ
            Code:                   ggggggggg??????ddddddddddd?????
            SLA-2*0401 10:          000000000000001---------------- <= False neoepitope - unsolvable

d?e: 15-30                          15        25        35
            Final Seq:              NISAVFQTYYNEQDQPTTMPSGFELYEDDQ
            Code:                   ddddddddddd??????eeeeeeeeee????
            SLA-2*1101 9:           --00000000000010--------------
            SLA-2*1101 11:          0000000000000010--------------

e?i: 31-46                          31        41        51
            Final Seq:              TTMPSGFELYEDDQKDASDWFAPRYGDNPR
            Code:                   eeeeeeeeee??????iiiiiiiii????h
            SLA-1*0702 9:           --00000000000001--------------- <= Solvable by: AQGKP (incl.)
            SLA-1*0702 10:          -000000000000001--------------- <= False neoepitope - unsolvable
            SLA-1*1201 9:           --00000000000001--------------- <= False neoepitope - unsolvable
            SLA-2*0401 10:          -000000000000001--------------- <= False neoepitope - unsolvable


PROCESSING HISTORY:
            Rec:Itr       Unfixed
            Origin        8/8         a?c c?b b?e e?d d?g g?f f?i i?h
            *0:0          7/8         a?c c?b b?e e?d d?g g?f f?i
             0:1          6/8         c?b b?e e?d d?g g?f f?i
             0:2          5/8         b?e e?d d?g g?f f?i
             0:3          5/8         b?e e?d d?g g?f f?i
             0:4          5/8         b?e e?d d?g g?f f?i
            *1:0          5/8         d?f f?a b?i h?g g?e
             1:1          4/8         d?f b?i h?g g?e
             1:2          4/8         d?f b?i h?g g?e
             1:3          4/8         d?f b?i h?g g?e
             1:4          4/8         d?f b?i h?g g?e
            *2:0          4/8         g?d d?e e?i h?f
```

2:1	4/8	g?d d?e e?i h?f	
2:2	4/8	g?d d?e e?i h?f	
2:3	4/8	g?d d?e e?i h?f	
2:4	3/8	g?d d?e e?i	
*3:0	3/8	e?g g?i b?d	
3:1	3/8	e?g g?i b?d	
3:2	3/8	e?g g?i b?d	
3:3	3/8	e?g g?i b?d	
3:4	3/8	e?g g?i b?d	

EPITOPE ORDER:
gdeihfacb

CLEARING SPACERS:

SPCR	frag	percent	
c?b	3/570	0%	qadgp (54.85); dkggpp (60.86); ndenp (61.36);
f?a	1/413	0%	eeedd (60.98);
i?h	3/171	1%	deegn (61.49); nnnp (63.57); gdnp (65.64);
h?f	1/1351	0%	gdkkdp (63.53);
a?c	4/357	1%	neeank (53.16); nqegde (58.85); ndege (55.75); dqeedg (60.75);
g?d	1/1351	0%	gdkkdp (56.03);

####################################

BEST SPACERS#{"b?i": {"rankmean": 38.16, "score": "4", "seq": "eddqkd"}, "c?b": {"rankmean": 61.36, "score": "0", "seq": "ndenp"}, "f?a": {"rankmean": 60.98, "score": "0", "seq": "eeedd"}, "i?h": {"rankmean": 65.64, "score": "0", "seq": "gdnp"}, "b?d": {"rankmean": 54.07, "score": "1", "seq": "gdkkdp"}, "b?e": {"rankmean": 54.92, "score": "2", "seq": "neqdqp"}, "g?i": {"rankmean": 37.64, "score": "4", "seq": "eddqkd"}, "f?i": {"rankmean": 37.88, "score": "4", "seq": "eddqkd"}, "h?f": {"rankmean": 63.53, "score": "0", "seq": "gdkkdp"}, "h?g": {"rankmean": 59.59, "score": "3", "seq": "eddqkd"}, "a?c": {"rankmean": 60.75, "score": "0", "seq": "dqeedg"}, "e?d": {"rankmean": 52.7, "score": "3", "seq": "gdkdp"}, "g?e": {"rankmean": 53.8, "score": "1", "seq": "gekpp"}, "g?d": {"rankmean": 56.03, "score": 0, "seq": "gdkkdp"}, "e?i": {"rankmean": 37.78, "score": 1, "seq": "eddqkd"}, "g?f": {"rankmean": 60.32, "score": "1", "seq": "gpkdqp"}, "d?f": {"rankmean": 58.87, "score": "2", "seq": "edqedp"}, "d?g": {"rankmean": 58.48, "score": "3", "seq": "eddqkd"}, "e?g": {"rankmean": 58.76, "score": "3", "seq": "eddqkd"}, "d?e": {"rankmean": 53.6, "score": "2", "seq": "neqdqp"}}

ALL SPACERS#["gne", "n", "", "epe", "pkde", "qeek", "qen", "dned", "q", "e", "eaggd", "dnagp", "gp", "a", "pen", "qn", "keqg", "qaa", "qepn", "qge", "ggdnkq", "eaaek", "gndn", "eqgaq", "d", "ed", "pak", "nakdad", "ddkq", "eeaaan", "dqga", "egp", "deegn", "kdd", "nnd", "gq", "gpddaq", "apdq", "kage", "gnp", "ndg", "gkqaa", "dd", "eedd", "nakgdk", "p", "dqk", "qp", "ddadp", "akqg", "kae", "aene", "qeg", "gan", "aeee", "dkkkg", "qaapap", "ganqq", "pekad", "gaeka", "qegpkq", "kpddge", "qd", "engqk", "ped", "gen", "aapepk", "kpe", "gnq", "addgq", "na", "apqqak", "agq", "pnk", "gpp", "kap", "nkpan", "g", "aa", "eap", "qgedn", "qaeaq", "pqd", "kng", "pqkdde", "ap", "ppk", "ae", "k", "dknan", "kaaden", "nnnp", "nq", "gkg", "qdaqk", "pgpgeq", "kded", "nke", "qka", "qk", "ang", "qdn", "qeqa", "kqgepq", "npaa", "qpq", "ea", "qdqndd", "dk", "ekeq", "aeagap", "dn", "nqdaa", "qeqga", "qaae", "qadkk", "qdpe", "edqe", "nqpg", "dnpa", "nqd", "gqa", "kge", "qkpdk", "ppa", "akqea", "ppgn", "gkk", "geqn", "kkdgpd", "dagda", "pnqngn", "kkkp", "qepd", "dkenng", "pkee", "depgga", "qqnkd", "ep", "kkpaa", "aqaa", "ndp", "papd", "kp", "pe", "gggan", "kapa", "ppka", "dqpng", "ggegpa", "knedn", "ndkek", "aqakde", "knpp", "ek", "ked", "pqengk", "kaaeg", "ka", "kpdpng", "nqaa", "gdnp", "eda", "pan", "angda", "nqekg", "dgpe", "gk", "ppnkg", "da", "epnkkn", "pd", "qpdkge", "kkpqag", "napnq", "neeank", "enaan", "agapnd", "nap", "gnepe", "kdepkn", "kn", "pk", "nqegde", "gpag", "qppa", "aaepnq", "kdqed", "gpkp", "ned", "kkp", "dqe", "nkp", "pq", "npg", "apa", "ge", "pkk", "ddpdeq", "dadggg", "agd", "dde", "nenap", "dqna", "qqd", "qdeaqp", "qgeqp", "paqe", "aege", "qpnnda", "nqqge", "pege", "ndgk", "ngkn", "qdpa", "qgepgd", "kpaqa", "keqqpg", "eddn", "pdqa", "peeng", "paqpep", "dnea", "qa", "adgeka", "nekn", "ngdq", "en", "edek", "ekedae", "pnkqn", "npgpkp", "gdne", "qaadq", "pngqdn", "kpne", "qkgeaa", "nega", "pnaqpp", "aqekp", "ggq", "epag", "kqnk", "pqnen", "qdk", "kgpek", "qqpqdq", "pkpaa", "gqe", "eega", "an", "gdgg", "ngg", "akk", "pkged", "kag", "qdnp", "ak", "gad", "pggga", "ggnqnd", "kndd", "pp", "gqeaa", "kqnn", "kpaea", "kde", "kd", "ekaak", "ndakp", "qegp", "pagp", "enkkk", "edg", "eeen", "ndege", "egdaan", "qnppn", "paedd", "qnan", "npaqd", "gn", "eang", "eg", "ddggq", "annngq", "ggna", "qpqnp", "dg", "kg", "kgepp", "dqeedg", "egea", "nnag", "dkea", "andgad", "epg", "kk", "daade", "denn", "gddggd", "gqeana", "qqaagd", "kkepp", "eqen", "npgenq", "nakqe", "ke", "kpk", "ng", "nadn", "kppq", "nakpqn", "epp", "ddnk", "pagag", "aakneg", "gnaen", "qkkqp", "pnn", "ppqea", "akn", "anndqq", "nepg", "dedn", "dgakgg", "eqak", "qek", "eddqkd", "ndqeaq", "dkkp", "dnak", "aggd", "npeq", "gkpq", "adk", "ddqggg", "nqnqda", "qgp", "npnee", "apn", "qdagga", "kkqkpd", "kek", "anakk", "aak", "qkpadd", "gqag", "gqaepd", "dqane", "nqqd", "enqada", "neqdqp", "aaa", "nd", "denq", "gqkedp", "paedqd", "nkkaq", "kneqq", "gpd", "akq", "gnqeg", "agggp", "dgkg", "eq", "pqenpg", "adqq", "pkqkag", "gakda", "pkqep", "kknanq", "kqda", "napgg", "qpad", "ad", "qedkek", "pndeg", "naekn", "eqn", "nnenqn", "pkkn", "andkgp", "qgqq", "eeedd", "ddk", "kaeakk", "knqd", "ekd", "ga", "dkeka", "dngkn", "qkg", "eqa", "qadgp", "gaqekg", "nnpd", "knaa", "gg", "enqndd", "kenp", "kngkak", "kqae", "pnkaeq", "akaq", "akkde", "kqadq", "neg", "neked", "gage", "gggka", "eppnq", "kaap", "de", "qpqeq", "pdd", "gnn", "naeedq", "ppeed", "gd", "ddkp", "epnage", "kddpdq", "ee", "kepgek", "eqqae", "pgqkd", "akqn", "dnkd", "nqak", "eqan", "pqp", "nnnn", "nea", "pn", "gpda", "ndnade", "qde", "pegaeg", "dkpneg", "qekn", "kengp", "qe", "dkggpp", "dden", "dpkkpe", "knepqg", "ppp", "qegppa", "pqqq", "qdp", "edd", "aq", "genenk", "kqqdk", "pqaee", "ndkpgq", "qepae", "ndenp", "qqpaa", "dakpg", "dkdkae", "dp", "aaqqan", "panka", "agk", "kqgen", "pkqad", "dqek", "annpea", "anenaa", "gqggk", "kqg", "kepq", "dakd", "gqpk", "neepe", "nppna", "qap", "dqgd", "kqee", "ageaa", "kan", "ndad", "ppeaqq", "nqdadq", "apppdq", "nkqq", "gnpdnq", "egq", "aqngq", "epaa", "degkk", "dppqkd", "dnkk", "gdnq", "egnn", "ekka", "gnkgn", "aqqe", "pde", "nda", "ppgnng", "pkakna", "adgpk", "dnqa", "kaank", "ddnp",

"qqakaq", "pkpag", "geank", "npkp", "qppn", "nqkan", "agn", "eqe", "ngnkd", "geqqd", "kka", "nae", "qne",
"dpg", "enn", "deep", "pdggqk", "eank", "qnaegn", "pdkdn", "aedkag", "apq", "kpkqq", "add", "gqqg", "gddp",
"gdn", "dka", "annnd", "kq", "nn", "nnaeq", "dagpqg", "qenp", "qq", "qqgqde", "engd", "gagnkg", "ddkk",
"ppkk", "ppd", "aeeg", "pkna", "qdqpq", "qqk", "ppggad", "gkkg", "nkqadd", "aepqa", "pqde", "ngaapg",
"pepked", "kaddpg", "ggagg", "nqpq", "knd", "qakga", "kegqea", "qnke", "gkaqek", "enpp", "dagq", "egakde",
"anaae", "npekd", "gngq", "nqe", "kaed", "edae", "ekean", "gapd", "gke", "kpndd", "ggg", "pdp", "enp",
"akgg", "aqe", "epd", "pagdnn", "aqedda", "nqp", "qake", "gng", "qdd", "qqg", "nnadqg", "deegg", "nga",
"naa", "pgedqq", "qgkkk", "qpekn", "enpk", "pda", "kngak", "keped", "een", "akg", "pnkn", "egapea", "dqegn",
"nk", "ppadd", "kpdge", "ppdde", "ngpk", "epda", "keeaqp", "apeq", "paddp", "gek", "nng", "gnaegq",
"dadneg", "qkq", "kgqqq", "qkaa", "pgqaea", "pdqd", "agp", "qgq", "gqqqdk", "adgk", "peqdqe", "nkgqea",
"dgend", "ppaq", "nqgd", "qkaae", "ppqnp", "nengq", "naka", "qkqd", "pke", "pdada", "nken", "ggadp",
"gdeng", "ngqqa", "nqqpk", "knnaa", "dqq", "gapadn", "pkq", "aaqnd", "akeqq", "pgpdn", "qkkpq", "nkqqnk",
"aae", "knadaq", "gekpp", "nkqe", "ppnekq", "edqqa", "pqgke", "gaqkn", "gegn", "nnkq", "pqqeag", "dnk",
"nkadn", "naadqg", "gap", "ppndpq", "kdedne", "qedn", "pedq", "knn", "ekqeke", "ppgnpe", "eag", "eeg",
"pqqkng", "qpe", "kdpan", "pnad", "gkdap", "ppea", "gkqe", "qakqpa", "nekpq", "adnep", "pgq", "ddkn", "kpp",
"kkqad", "nddge", "ggekk", "kada", "dpgn", "epdp", "qpgpdn", "apkqdn", "dqne", "apd", "dkddd", "nnaqe",
"qdaddg", "eegeqe", "anagpe", "paq", "dpdqgg", "ankna", "daaq", "qped", "pqg", "aeqgn", "agke", "adan",
"pnqpg", "eggkge", "dnd", "dqn", "gpndg", "dapna", "ppqq", "edgnk", "ggek", "keag", "keq", "gkqgee", "pqkg",
"eeqa", "gnkqnk", "eennen", "qkgqgn", "gaaq", "nadpp", "qqe", "qke", "adag", "anaqn", "qaadk", "eaqqaq",
"knp", "adeeg", "eadda", "aad", "kadqnp", "pepqq", "gqgqdk", "eagnge", "qnndde", "knqe", "nknane", "nkqpq",
"qkppd", "pqan", "eakq", "adad", "np", "gkdkpn", "nepppq", "kegn", "gaena", "npd", "pddp", "aegdg", "png",
"nadp", "kedadd", "qqg", "ggnnad", "agnaeg", "akkp", "dkqdeq", "gea", "gqage", "dppa", "aek", "apkekg",
"daap", "ngqpd", "akdnn", "gep", "aqka", "gdaa", "gpkkgn", "gpgdaa", "ekq", "gqke", "epenne", "keg",
"eqngdp", "pkp", "qaekp", "ngnakq", "nqeg", "kapqp", "dqag", "gpdq", "ekp", "knq", "qaedkp", "kdg",
"gaeagq", "ggpdae", "ppegek", "ddg", "qkgkd", "kpqqd", "adpae", "edaked", "qknak", "gkeek", "ndan", "nnaea",
"pdndd", "egdd", "agpqp", "knenpe", "gengnq", "enenk", "gpkdqp", "kdgqpd", "deepeg", "ngagg", "gpeka",
"gdakd", "needak", "eaqpak", "qnpa", "aaq", "kkgda", "kpgegk", "dqqne", "ngkd", "qdep", "qddpap", "dgnnd",
"pqn", "edpe", "gaekag", "kknka", "qgggq", "eea", "dngeg", "qnqqak", "pdeq", "qagqa", "dkk", "qpp", "annp",
"dkkgd", "epagg", "kpapk", "ene", "edag", "kdkdde", "pdgn", "ngknk", "kqaad", "dgpaed", "deg", "epgk",
"dqg", "gqeep", "qeqn", "geeaa", "ag", "padn", "dkqge", "gge", "apnd", "panggk", "nqapaa", "nep", "pegdq",
"nana", "ndkg", "npppn", "pepqa", "qqpa", "epgeqp", "nqdd", "ppapde", "gnen", "gapa", "aqgapn", "dgnag",
"gdkdp", "gapg", "kqag", "aadea", "qea", "dag", "appgp", "kqgeq", "qedkk", "qpnn", "qqaddk", "aaenq",
"nqnk", "gkd", "ppngd", "npn", "eekn", "qnk", "agek", "dpe", "aqad", "agkqkg", "ekddqd", "ennpde", "dgn",
"pkggp", "ggnag", "gpap", "dqpe", "nege", "pged", "dpenkd", "gqgkk", "dege", "anekg", "gaed", "gdapne",
"qkknqq", "qdpqa", "ade", "pngke", "dnneqq", "dgdee", "kegd", "gngp", "nakpn", "qkpeg", "anng", "adng",
"ppn", "qkggn", "eaa", "qqpdqk", "dgqpke", "gappee", "kgkk", "dqpae", "nagep", "eka", "epke", "qqkg", "pek",
"nagd", "neapd", "eadeek", "nnnng", "ddgpa", "qqgnqe", "edqedp", "ppq", "kgqpn", "dkde", "ndq", "deede",
"ggag", "penn", "pg", "egnd", "akdned", "dqdgqp", "ndkag", "nnpdkk", "nqn", "gag", "ndnka", "gqngaq",
"pgdpng", "eenap", "pnnaqn", "eaep", "dkndd", "dnp", "kpdegp", "akdeqp", "egaad", "egaqk", "nkqge", "qqga",
"danq", "qnknad", "egnaa", "ndekke", "ekad", "dgnpda", "kaqn", "pneq", "ggkqq", "nkeak", "qpddgp", "knnng",
"gggq", "npnkdk", "nkgk", "deq", "agpeka", "qgqgka", "edpdpd", "gnqn", "gnggnq", "egppke", "gedke",
"adegpg", "qkpkn", "kaa", "dke", "qggq", "dqed", "qnadkq", "qkda", "qqq", "qakgan", "nka", "aeg", "pdng",
"pgp", "pdk", "adppp", "eakd", "qdddad", "qpap", "depgp", "ngk", "ppqnne", "addek", "kege", "gdg", "pnp",
"pggen", "gqdeap", "aggdae", "aeqen", "pa", "paa", "qggpq", "qpk", "kepggp", "dge", "pdgp", "paka", "ggd",
"qqdakn", "gqnep", "daeand", "gdneek", "nqad", "keenkq", "pdga", "npgpk", "nkpq", "gdkk", "nakk", "kdne",
"dpqak", "geed", "kaeka", "qep", "dpkde", "qgqnqd", "anqdnk", "pkgpna", "kgeeqp", "qkqqk", "eean", "aepa",
"pep", "qad", "kdknng", "ankk", "dekng", "akaag", "gpggq", "enepqg", "qg", "kpkqqg", "dgqapp", "aekanq",
"eqdenq", "aqn", "daqd", "pgak", "akegdd", "pankeq", "akeekn", "gpgnq", "qqpnn", "ne", "pdkgap", "ddek",
"eqgp", "dndggk", "gndnae", "qqqag", "adane", "naagpq", "pkddkn", "ddan", "dpkeq", "egeena", "qkk", "nded",
"qdagkp", "epn", "ead", "pggk", "adkeg", "gkdnnd", "eakdn", "kdngd", "dgd", "ngaegq", "qnqdn", "gpaea",
"qkqak", "dnq", "kdgag", "ggnn", "qpee", "ekdpd", "naeed", "peae", "knpg", "agqa", "qadq", "dqee", "dknpk",
"kgqgd", "qaeded", "qnppp", "kqep", "kqa", "ggndk", "aqq", "kddpe", "gdqek", "nadnk", "dpdd", "gka",
"aggdga", "qee", "peqqk", "naeqee", "ngggpa", "nqkeeq", "dnkae", "daqqa", "nkanak", "dqaed", "nnqnqg",
"qdaqak", "peddg", "pqe", "npae", "paee", "edead", "dppqe", "dqkg", "aeqgg", "qkqpa", "epq", "nkpaa", "kgd",
"pened", "dpqd", "gpqgka", "apk", "pkkpe", "gqnkqn",
"papa", "gpgqdq", "gknn", "aaqnn", "pdndn", "gdkkdp", "qaep", "egpeqa", "aqan", "gaq", "pnq", "gpkn",
"agepae", "eegnn", "agpq", "qepqak", "dngggd", "kgqepd", "gnkkk", "agkg", "aqdapq", "pgqek", "enang",
"kkpea", "anpn", "pqqgqd", "gdd", "ggeeg", "ean", "ggaedn", "nkkdpn", "aaka", "eqnd", "neq", "dkedg",
"pdqe", "ddgkge", "kgedak", "dqggpa", "gpdeeq", "dan", "qdg", "qqqdad", "kakqd", "qdapdq", "peg", "gdan",
"gqg", "dkae", "gaad", "dqaek", "dndnda", "nkna", "aqpq", "nnkng", "endan", "eapg", "naee", "akpak",
"gaanq", "dqgqe", "npadkn", "paqeq", "daknpd", "eapk", "eae", "qngp", "gnk", "kdegp", "qgqgq", "nann",
"enkq", "qndgq", "geg", "gaeqqp", "nqdegd", "ppgkka", "pkpqgg", "kpkqdp", "qqde", "aapdek", "ppgagk",
"nandp", "agkde", "gkpg", "pppg", "nddqe", "adgken", "adpaa", "nadqda", "pagedk", "endnkd", "deqgp",
"egqdeg", "qgn", "qeanpp", "kkd", "nkaqdg", "kgkkg", "adkk", "edpdg", "nepka", "qdpn", "dnn", "ekpn",
"dadq", "apnk", "aaenqd", "qeeenq", "gnaae", "aaan", "qkgpd", "gnnnnk", "dgpd", "eaqg", "gqgnpg", "aepn",
"dpnkq", "dpnn", "dnqeqa", "aqggp", "pqpnen", "angp", "eqq", "qkqdk", "edegn", "dqgaek", "knk", "kkqag",
"pka", "qkgp", "andang", "peeqe", "nqge", "gekqak", "gpqk", "akeaae", "andqkp", "adp", "enk", "aganpe",
"nqdpkg", "aeq", "dqak", "nqegk", "geka", "npde", "qgqpgp", "qng", "nkaagk", "ppqk", "knng", "aqkak",
"kqpgnq", "aaqpq", "ppkkqa", "ddgg", "aakqq", "gqdq", "ngkdq", "nnae", "eknn", "nknnqq", "aagkkq", "qdkna",
"nkgq", "akgqan", "naann", "eggk", "ppgpkg", "deakd", "ana", "egqkd", "negd", "ekg", "gqeq", "qga", "ngak",
"dee", "ekde", "qkkpgp", "qgapd", "pgdnke", "kqge", "egn", "npkdn", "gqapkk", "qkpagd", "agpan", "kqk",
"qdnek", "aqpgpk", "gkdkke", "nqkd", "pkd", "qnqe", "genn", "keed", "ekepd", "neqn", "panq", "gdpan",
"npngaa", "dpq", "qagpg", "dpnqg", "eqeqk", "eqakd", "ppdggp", "qqaa", "nnnaq", "aeeq", "gkkpag", "age",
"dakepa", "npknan", "dgnqk", "den", "dnnadn", "apkda", "gqpek", "dga", "kqnpgp", "naqed", "kkqqn", "qgea",
"kedn", "gneka", "nqq", "qqpd", "gnkdnp", "adg", "anka", "knka", "egpgg", "kgqeen", "qqkd", "paaqp",
"ekppnk", "dqapp", "ddeek", "apqaka", "eqgqeg", "nen", "qene", "ppkngn", "agdppg", "eqaa", "aednd", "gppaq",
"nkdqe", "pap", "deaeag", "dgdq", "pgpgqp", "ddnq", "dkkk", "qaede", "qana", "dpeage", "gqn", "pqgn",
"akpp", "enq", "qqkpp", "qaaeag", "qqnkq", "nnqpgp", "dq", "edqqpq", "qknga", "pddqaa", "dndpad", "nake",
"enap", "qega", "eed", "qdknn", "gekd", "pgng", "qndeqe", "qpnpna", "akqdg", "qpeg", "kne", "dakkn", "dad",
"ngkeap", "edqkk", "ddgdeg", "pdap", "qpdpqq", "gpg", "ednqep", "adq", "kdedaa", "kkaad", "kkkqpa", "pdg",
"kkpkad", "kkge", "aggn", "eqakp", "aenk", "dndd", "qpddke", "kankd", "kpene", "dqdnp", "epekk", "aeke",
"ddd", "dgan", "ekkkn", "kpgkg", "egegpq", "qgkpq", "kpad", "nddq", "adee", "keaap", "kda", "pdkeqq",

"qepkeq", "kaek", "qna", "ekkk", "agad", "pgqad", "dkqan", "pnpd", "qddkaq", "epqnk", "dne", "ngne", "ddpg", "gegqkp", "qpdad", "pgpea", "aeqkd", "qeeke", "gnpk", "geqddq", "kkgeq", "eanadq", "agdkkq", "ggdgk", "naeq", "ede", "eaqndg", "kad", "ekga", "qnadd", "agekep", "kqd", "qgqndk", "qpnepg", "aaapeq", "aqd", "gnnaqq", "dnaqpe", "nedn", "gepqe", "nknp", "qagqp", "naep", "pkga", "knek", "kqq", "gkngnk", "gqaa", "dagqp", "eepk", "ndkpe", "pdkag", "anee", "ggeqnd", "qgnae", "nngkak", "akag", "dddp", "nde", "nqapg", "eapdne", "kqgdk", "gqkd", "nedeek", "ddgdq", "angg", "ake", "naqq", "ndagn", "pgeepn", "apeaqn", "ngqqe", "nedpdd", "daa", "npkk", "aegng", "qnn", "pnpan", "ppan", "pndk", "pakdk", "apap", "naeaag", "pqkqaq", "nppaka", "qqn", "qdkdng", "ged", "eqea", "pqgkp", "ken", "epqe", "agnegg", "nadngg", "aagk", "agknd", "ane", "qan", "dgqggd", "kppp", "ngqgq", "dpa", "gnnd", "kdekdk", "ggenp", "kqqank", "pknppa", "kgqeqn", "qpgk", "eqpgng", "gaekk", "neeegq", "aed", "kkgek", "dpdgk", "agankg", "aqqpa", "addg", "nnk", "pqekae", "eengp", "ekeddd", "aggp", "kpgade"]

EPIDATA#{"a": {"length": 10, "code": "aaaaaaaaaa", "ID": "ID7-V1-S+", "seq": "QVYERGCRWY"}, "c": {"length": 10, "code": "cccccccccc", "ID": "ID22-V1-S+", "seq": "KIFRFGSHKW"}, "b": {"length": 10, "code": "bbbbbbbbbb", "ID": "ID10-V1-S+", "seq": "KVAHNLGFYF"}, "e": {"length": 10, "code": "eeeeeeeeee", "ID": "ID43-V0-S+", "seq": "TTMPSGFELY"}, "d": {"length": 10, "code": "dddddddddd", "ID": "ID23-V1-S+", "seq": "NISAVFQTYY"}, "g": {"length": 9, "code": "ggggggggg", "ID": "ID19-V1-S++", "seq": "LSDSGRISY"}, "f": {"length": 9, "code": "fffffffff", "ID": "ID17-V1-S++", "seq": "RTAIGTPVY"}, "i": {"length": 9, "code": "iiiiiiiii", "ID": "ID25-V1-S++", "seq": "ASDWFAPRY"}, "h": {"length": 9, "code": "hhhhhhhhh", "ID": "ID24-V0-S++", "seq": "RTAPNEIAF"}}

EPIORDER#"gdeihfacb"

MHC WEIGHT#{"SLA-1*0702": 100, "SLA-2*0401": 100, "SLA-1*1101": 100, "SLA-2*0202": 100, "SLA-2*1101": 100, "SLA-3*0401": 100, "SLA-1*1201": 100, "SLA-3*0302": 100, "SLA-2*0601": 100, "SLA-2*1001": 100, "SLA-1*0501": 100, "SLA-6*0101": 100, "SLA-1*0801": 100, "SLA-2*0701": 100, "SLA-3*0502": 100, "SLA-1*0401": 100, "SLA-3*0101": 100, "SLA-2*0301": 100, "SLA-2*0502": 100}

NEOTOPE WEIGHT#{"8": 25, "9": 100, "10": 100, "11": 50}

SPACEORDER#["d?e", "e?i"]

ENDORDER#["g", "g?d", "d", "d?e", "e", "e?i", "i", "i?h", "h", "h?f", "f", "f?a", "a", "a?c", "c", "c?b", "b"]

SPACERDICT#{"b?i": {"ranks": [], "score": []}, "c?b": {"ranks": [], "score": []}, "f?a": {"ranks": [], "score": []}, "i?h": {"ranks": [], "score": []}, "sequence": [], "b?d": {"ranks": [], "score": []}, "b?e": {"ranks": [], "score": []}, "f?i": {"ranks": [], "score": []}, "h?f": {"ranks": [], "score": []}, "h?g": {"ranks": [], "score": []}, "g?i": {"ranks": [], "score": []}, "g?d": {"ranks": [], "score": []}, "e?d": {"ranks": [], "score": []}, "g?e": {"ranks": [], "score": []}, "a?c": {"ranks": [], "score": []}, "e?i": {"ranks": [], "score": []}, "g?f": {"ranks": [], "score": []}, "d?f": {"ranks": [], "score": []}, "d?g": {"ranks": [], "score": []}, "e?g": {"ranks": [], "score": []}, "d?e": {"ranks": [], "score": []}}

POST#"\tNeotopes left:\t\t3 real, 4 false\n\tJunctions:\t\t3\n\n\tDist matrix (incl. FNs):\t8-mer\t9-mer\t10-mer\t11-mer\t\n\tSLA-1*0401:\t\t 0\t 0\t 0\t 0\t\n\tSLA-1*0501:\t\t 0\t 0\t 0\t 0\t\n\tSLA-1*0702:\t\t 0\t 1\t 1\t 0\t\n\tSLA-1*0801:\t\t 0\t 0\t 0\t 0\t\n\tSLA-1*1101:\t\t 0\t 0\t 0\t 0\t\n\tSLA-1*1201:\t\t 0\t 1\t 0\t 0\t\n\tSLA-2*0202:\t\t 0\t 0\t 0\t 0\t\n\tSLA-2*0301:\t\t 0\t 0\t 0\t 0\t\n\tSLA-2*0401:\t\t 0\t 0\t 2\t 0\t\n\tSLA-2*0502:\t\t 0\t 0\t 0\t 0\t\n\tSLA-2*0601:\t\t 0\t 0\t 0\t 0\t\n\tSLA-2*0701:\t\t 0\t 0\t 0\t 0\t\n\tSLA-2*1001:\t\t 0\t 0\t 0\t 0\t\n\tSLA-2*1101:\t\t 0\t 1\t 0\t 1\t\n\tSLA-3*0101:\t\t 0\t 0\t 0\t 0\t\n\tSLA-3*0302:\t\t 0\t 0\t 0\t 0\t\n\tSLA-3*0401:\t\t 0\t 0\t 0\t 0\t\n\tSLA-3*0502:\t\t 0\t 0\t 0\t 0\t\n\tSLA-6*0101:\t\t 0\t 0\t 0\t 0\t\n"

SOLVED#{"h?f": {"ranks": 63.53, "seq": "gdkkdp"}, "c?b": {"ranks": 61.36, "seq": "ndenp"}, "a?c": {"ranks": 60.75, "seq": "dqeedg"}, "f?a": {"ranks": 60.98, "seq": "eeedd"}, "i?h": {"ranks": 65.64, "seq": "gdnp"}}

TESTEDSPCS#{"b?i": 1124, "b?d": 1624, "f?i": 1070, "b?e": 1070, "h?g": 1124, "g?i": 1624, "e?d": 1070, "g?e": 1124, "e?g": 1624, "e?i": 1351, "g?f": 1070, "d?f": 1124, "d?g": 1070, "d?e": 1351}

Appendix D - "Juncitope" - code

```
# 1
### INPUT VARIABLES
username = 'Simon'
Min_spacer_aa = 0 # 0 er en mulighed for spacere mellem fragmenter, da disse ikke testes i for-analysen
Max_spacer_aa = 9
spacersPerItr = max #skriv enten et tal eller 'max', hvilket laver den længst tilladte streng
runthru = 5 # Allowed number of iterations where no junction clearance is obtained
AminoAcids = 'adegknpq'#'arndcqeghilkmfpstwyv'
ReRun = 0 # 0=no, 1=yes
maxtime = 100000 #minutes
SaveToFile = 1 # 0=no, 1=yes
include_spacers = 0 # 0=no, 1=yes

############## Hvis include_spacers == 1 ##########
spcfile = "BEST OF - 24Jul2015 - 02:49:16 - V1 - neo:1070->75.txt"
spcpath = "/home/siwel/Documents/neoepitope log/"

############## Hvis ReRun == 0 ####################
neo_in = {8: 25,
          9: 100,
          10: 100,
          11: 50} # vægtning i procent - OBS! Neotoper længere end len(epitope)+1
    # kan i teorien overlappe 3 peptider, hvorfor placeringen af et neotop kan være tvetydig. Brug evt kun neotoplængder op til
    # len(korteste epitop)+1 til den initielle screening (AllCombis).
MHC_in = {'SLA-1*0101': 0,
          'SLA-1*0201': 0,
          'SLA-1*0202': 0,
          'SLA-1*0401': 100,
          'SLA-1*0501': 100,
          'SLA-1*0601': 0,
          'SLA-1*0701': 0,
          'SLA-1*0702': 100,
          'SLA-1*0801': 100,
          'SLA-1*1101': 100,
          'SLA-1*1201': 100,
          'SLA-1*1301': 0,
          'SLA-2*0101': 0,
          'SLA-2*0102': 0,
          'SLA-2*0201': 0,
          'SLA-2*0202': 100,
          'SLA-2*0301': 100,
          'SLA-2*0302': 0,
          'SLA-2*0401': 100,
          'SLA-2*0402': 0,
          'SLA-2*0501': 0,
          'SLA-2*0502': 100,
          'SLA-2*0601': 100,
          'SLA-2*0701': 100,
          'SLA-2*1001': 100,
          'SLA-2*1002': 0,
          'SLA-2*1101': 100,
          'SLA-2*1201': 0,
          'SLA-3*0101': 100,
          'SLA-3*0301': 0,
          'SLA-3*0302': 100,
          'SLA-3*0303': 0,
          'SLA-3*0304': 0,
          'SLA-3*0401': 100,
          'SLA-3*0501': 0,
          'SLA-3*0502': 100,
          'SLA-3*0503': 0,
          'SLA-3*0601': 0,
          'SLA-3*0602': 0,
          'SLA-3*0701': 0,
          'SLA-6*0101': 100,
          'SLA-6*0102': 0,
          'SLA-6*0103': 0,
          'SLA-6*0104': 0,
          'SLA-6*0105': 0,
          'SLA-2*CDY.AA': 0,
          'SLA-2*HB01': 0,
          'SLA-2*LWH.AA': 0,
          'SLA-2*TPK.AA': 0,
          'SLA-2*YC.AA': 0,
          'SLA-2*YDL.AA': 0,
          'SLA-2*YDY.AA': 0,
          'SLA-2*YTH.AA': 0,
          'SLA-1*es11': 0,
          'SLA-2*es22': 0,
          'SLA-1-CHANGDA': 0,
          'SLA-1-HB01': 0,
          'SLA-1-HB02': 0,
          'SLA-1-HB03': 0,
          'SLA-1-HB04': 0,
          'SLA-1-LWH': 0,
          'SLA-1-TPK': 0,
          'SLA-1-YC': 0,
          'SLA-1-YDL01': 0,
          'SLA-1-YTH': 0,
          'SLA-2-YDL02': 0,
          'SLA-3-CDY': 0,
          'SLA-3-HB01': 0,
          'SLA-3-LWH': 0,
          'SLA-3-TPK': 0,
          'SLA-3-YC': 0,
          'SLA-3-YDL': 0,
          'SLA-3-YDY01': 0,
          'SLA-3-YDY02': 0,
          'SLA-3-YTH': 0}

RnkThr = 4 # neotoper med rank højere end denne værdi tælles ikke med
EpiList = "/home/siwel/Documents/SLA-10401.txt" #Ingelvac slas 10401, 10702, 20401, 30401.txt"

############## Hvis ReRun == 1 ####################
```

```
Logfile = "21Jul2015 - 19:10:50 - V0 - neo:179->8.txt"
Logpath = "/home/siwel/Documents/neoepitope log/1*0401/"



--(new block)--


# 2

print 'PREPARATIONS: (#1-#17)'

import subprocess, os, random, itertools, math, time, json
from collections import OrderedDict
from random import randrange
from scipy import stats


starttime = time.time()
PS = {}
PS['end'] = ""

tried_spacers = []
recombined = 0
oldspacers = []
RECOMBINE = 0
TOBEST = 0
MAKESPACERS = 0
TOEND = 0

codestring = "abcdefghijklmnopqrstuvwxyzABCDEFGHIJKLMNOPQRSTUVWXYZ" # '?' and numbers are NOT allowed in this string
if len(codestring) != len(set(codestring)):
    print 'Signs in "codestring" not unique'

if ReRun == 1:
    print 'Proceding from logfile: '+Logfile
    OptiSeq = {'epiOrder': [], 'workOrder': [], 'workEpiOrder': [],'spaceOrder': [], 'endOrder': []}
    MAKESPACERS = 1
    ufstring = ""
    read = "stop"
    PS['epitopes'] = ""
    PS['pre'] = ""
    PS['last'] = ""
    with open(Logpath+Logfile,'r') as handle:
        for line in handle:
            line = line.rstrip()
            if 'INPUT' in line:
                read = 'input'
            if 'PRE PROCESSING' in line:
                read = 'pre'
            if 'PROCESSING SUMMARY' in line or 'OUTPUT' in line:
                read = 'stop'
            if read == 'input':
                PS['epitopes'] += line+'\n'
            if read == 'pre':
                PS['pre'] += line+'\n'
            if 'Rank threshold' in line:
                line = line.split()
                RnkThr = int(line[2])
            elif 'Neotopes:' in line:
                line = line.split()
                stotSum = int(line[1])
            elif 'BEST SPACERS#' in line:
                line = line.split('#')
                oldbest = json.loads(line[1])
            elif 'ALL SPACERS#' in line:
                line = line.split('#')
                oldspacers = json.loads(line[1])
            elif 'EPIDATA#' in line:
                line = line.split('#')
                EpiData = json.loads(line[1])
            elif 'EPIORDER#' in line:
                line = line.split('#')
                OptiSeq['epiOrder'].append(json.loads(line[1]))
            elif 'MHC WEIGHT#' in line:
                line = line.split('#')
                MHC_weight = json.loads(line[1])
            elif 'NEOTOPE WEIGHT#' in line:
                line = line.split('#')
                nw = json.loads(line[1])
            elif 'SPACEORDER#' in line:
                line = line.split('#')
                OptiSeq['spaceOrder'].append(json.loads(line[1]))
            elif 'ENDORDER#' in line:
                line = line.split('#')
                OptiSeq['endOrder'].append(json.loads(line[1]))
            elif 'SPACERDICT#' in line:
                line = line.split('#')
                OptiSeq['spacers'] = json.loads(line[1])
            elif 'POST#' in line:
                line = line.split('#')
                PS['last'] = json.loads(line[1])
            elif 'SOLVED#' in line:
                line = line.split('#')
                solved = json.loads(line[1])
            elif 'TESTEDSPCS#' in line:
                line = line.split('#')
                testedSpcs = json.loads(line[1])
    for x in OptiSeq['spaceOrder'][recombined]:
        ufstring += x+" "
    neotope_weight = {}
    for key in nw:
        neotope_weight[int(key)] = nw[key]




### Creates dicts that contains only the MHCs and neotopes that weigh > 0
```

```
if ReRun == 0:
    neotope_weight = {}
    MHC_weight = {}
    for neo in neo_in:
        if neo_in[neo] > 0:
            neotope_weight[neo] = neo_in[neo]
    for MHC in MHC_in:
        if MHC_in[MHC] > 0:
            MHC_weight[MHC] = MHC_in[MHC]



### Returns list of rank scores for the n-mers of a given aa-sequence
# output can be printet if p=True

def getnetrank(episize, MHC, inputstring, p=False):
    list =[]
    oput = subprocess.Popen(['/home/siwel/netMHCpan-2.8/netMHCpan','--', '-l '+str(episize), '-a '+MHC.replace('*',':')], stdout=subprocess.PIPE,
stdin=subprocess.PIPE)
    oput.stdin.write('>input\n'+inputstring.upper())
    oput = oput.communicate()[0]
    oput = oput.rsplit('\n')
    for line in range(len(oput)):
        if '#' not in oput[line]:
            if p==True:
                print oput[line]
            oput[line] = oput[line].rsplit()
            if '%Rank' in oput[line]:
                RNKindex = oput[line].index('%Rank')
            try:
                if oput[line].index(MHC)==1:
                    list.append(oput[line][int(RNKindex)])
            except:pass
    return list


### Returns a string indicating where potential neotopes may be found
# '1' = potential neotope
# '0' = within original epitope
# '-' = out of score - end of codestring

def neoloc(neosize, codestring):
    olap = ""
    for inc in range(len(codestring)):
        incprod=1
        for cnt in range(int(neosize)):
            if codestring[inc]=='?':
                incprod *= 2
            else:
                try:
                    if codestring[inc]==codestring[inc+cnt] :
                        incprod *= 1
                    else:
                        incprod *= 2
                except:
                    incprod *= 0
        if incprod ==1:
            olap += str(0)
        if incprod > 1:
            olap += str(1)
        if incprod ==0:
            olap += str("-")
    return str(olap)


### Returns a string locating actual neotopes as defined by NetMHCpan and the user defined thresholds
# '1' = real neotope
# '0' = not real neotope
# '-' = out of scope - within epitope or at end of sequence

def realneos(NeoLocString, RankList, MHC, neosize):
    binders = ""
    for pep in range(len(NeoLocString)):
        try:
            if NeoLocString[pep]==str(1): # 1 hvis neotop, 0 hvis epitope
                if float(RankList[pep])*10000/float(MHC_weight[MHC])/float(neotope_weight[neosize]) <= RnkThr:
                    binders += str(1) # 1 hvis rank <= rnkthr
                else:
                    binders += str(0) # 0 hvis rank > rnkthr
            else:
                binders += str("-")
        except:
            binders += str("-")
    return binders


### Returns list providing the number of real neotopes in the junction of two epitopes for a given MHC

def neosum(codestring, workEpiOrder, realNeoString):
    epicount = 0
    countneos = {}
    neocount = 0
    for aa in range(len(codestring)):
        if codestring[aa] == workEpiOrder[epicount] or codestring[aa] =='?':
            if realNeoString[aa] == str(1):
                neocount += 1
        else:
            countneos[str(workEpiOrder[epicount])+'?'+str(workEpiOrder[epicount+1])] = neocount
            epicount += 1
            neocount = 0
            if realNeoString[aa] == str(1):
                neocount += 1
    return countneos

def neorank(codestring, workEpiOrder, neolocstring, ranklist, MHC, neosize):
    epicount = 0
    countneos = {}
    neoscore = []
    for aa in range(len(codestring)):
```

```
        if codestring[aa] == workEpiOrder[epicount] or codestring[aa] =='?':
            if neolocstring[aa] == '1':
                try: #Nødvendigt da neolocstring kan være out of range ifht ranklist.
                    neoscore.append(float(ranklist[aa])*10000/float(MHC_weight[MHC])/float(neotope_weight[neosize]))
                except: pass
        else:
            countneos[str(workEpiOrder[epicount])+'?'+str(workEpiOrder[epicount+1])] = neoscore
            epicount += 1
            neoscore = []
            if neolocstring[aa] == '1':
                neoscore.append(float(ranklist[aa])*10000/float(MHC_weight[MHC])/float(neotope_weight[neosize]))
    return countneos



### REPORT - spacers
PS['spacers'] = "\tSpacer aa's:\t\t"+AminoAcids.upper()+'\n'
PS['spacers'] += "\tSpacer length:\t\t"+str(Min_spacer_aa)+'-'+str(Max_spacer_aa)+" aa's\n"
if spacersPerItr == max:
    PS['spacers'] += "\tSpacers per iteration:\tMaximum allowed\n"
else:
    PS['spacers'] += "\tSpacers per iteration:\t"+str(spacersPerItr)+'\n'
PS['spacers'] += "\tIterations:\t"+str(runthru)+'\n'

### REPORT - neotopes
PS['neotopes'] = "\tNeotope weight:\t\t"
for neo in sorted(neotope_weight):
    PS['neotopes'] += str(neo)+'-mer:\t\t'+str(neotope_weight[neo])+'%\n\t\t\t\t'

### REPORT - MHCs
PS['MHC'] = "\tMHC weight:\t\t"
for MHC in sorted(MHC_weight):
    PS['MHC'] += MHC+':\t'+str(MHC_weight[MHC])+'%\n\t\t\t\t'

# 3
### IMPORT AF EPITOPER ###

# Laver dict 'EpiData', der indeholder epitopernes stamdata (længde, sekvens, tegnsekvens) identificeret ved unikt tegn
# OBS: antal epitoper er begrænset af len(codestring)
if ReRun == 0:
    print '\tImporting epitopes...'
    PS['epitopes'] = "INPUT:\n\tEpitopes\tID\n"
    ls = {}
    EpiData = {}
    intermed = []
    PS['nested'] = "\tExcluded\n"

    with open(EpiList, "r") as handle:
        for line in handle:
            line = line.rstrip().split()
            if len(line) > 0: #1
                intermed.append(line)
    num = 0
    for l in intermed:
        x = 0
        if 1==1:
            for m in intermed:
                if l[0] in m[0] and len(l[0]) < len(m[0]):
                    print '\tRemoving epitope '+l[0]+' nested in '+m[0]
                    PS['nested'] += '\t'+l[0]+' nested in '+m[0]
                    x = 1
        if x == 0:
            if num == len(codestring): #2
                print '\n\nNot enough signs in "codestring"\n\n'
                break
            if len(l[0]) not in ls:
                ls[(len(l[0]))] = 1
            else:
                ls[(len(l[0]))] += 1
            EpiData[str(codestring[num])] = {"length": len(l[0]), "seq": l[0], "code": len(l[0])*codestring[num]}
            PS['epitopes'] += '\t'+str(l[0])
            if len(l) == 2:
                EpiData[str(codestring[num])]['ID'] = l[1]
                PS['epitopes'] += '\t'+str(l[1])+'\n'
            else: PS['epitopes'] += '\n'
            num += 1


    ### REPORT - EPITOPES
    PS['epitopes'] += '\n'+PS['nested']+'\n'
    PS['epitopes'] += "\n\tTotal:\t"+str(len(EpiData))+'\n'
    for l in sorted(ls):
        PS['epitopes'] += '\t'+str(l)+'-mer:\t'+str(ls[l])+'\n'


    # Opdeler epitoper i grupper a 10, der herefter skal kombineres
    # 10 epitoper = 8 sekunder - stiger med ca en faktor 10 pr ekstra epitop.

    ################################################################################

    ### Max antal epitoper, der skal testes for bedste kombination. Hvis over dette tal, opdeles i fragmenter, der testes individuelt.

    seq = list(EpiData)
    size = int(math.ceil(len(seq)/math.ceil(len(seq)/float(10)))) # max længde på 10 epitoper, da dette giver en processeringstid på ca 8
sekunder. Denne øges med en faktor 10 for hvert ekstra epitop.
    elists = [seq[i:i+size] for i in range(0, len(seq), size)]

    # 4 ny - med flere fragmenter
    ### ALLE EPITOP KOMBINATIONER ###

    # Kombinerer epitoperne i ét enkelt rækkefølge, hvor alle mulige sammenføjninger er tilstede.
    # Denne rækkefølge gemmes i dict 'AllCombis > base > order'

    AllCombis = {"base": {'order': ""}, 'neotopes': {}, 'NetMHCpan': {}}
    for l in range(len(elists)):
        order = elists[l][-1]
        for epi1 in range(len(elists[l])):
            for epi2 in range(len(elists[l])):
                if epi1<epi2:
```

```
                order += str(elists[l][epi1])+str(elists[l][epi2])
        AllCombis["base"]["order"] += order

    # 5
    ### STAM POLYTOP og KODE SEKVENS ###

    # Baseret på rækkefølgen ovenfor kombineres epitoperne og deres kodesekvens og gemmes i hhv 'AllCombis > base > seq'
    # og 'AllCombis > base > code'

    seq = ""
    code = ""
    seqlen = 0
    for sign in AllCombis["base"]["order"]:
        seq += str(EpiData[sign]["seq"])
        code += str(EpiData[sign]["code"])
        seqlen += EpiData[sign]['length']
    AllCombis["base"]["seq"] = seq
    AllCombis["base"]["code"] = code
    if seqlen > 20000: # hvis sekvensen er større end 20.000 aa (max for NetMHCpan) stoppes processen.
        print '\nAllCombis sequence too long for NetMHCpan'
        PS['end'] += 'AllCombis sequence too long for NetMHCpan'
        stop = 1

    print '\t'+str(len(EpiData))+' imported'
    # 6
    ### NEOTOP Lokation ###
    # se func 'neoloc'

    # Laver en sekvens for hver neotop test størrelse (angivet i neotopeSize ovenfor), hvor 0 angiver et reelt epitope (intet overlap),
    # 1 angiver et neotope (overlap), og '-' angiver at sekvensen slutter indenfor teststørrelsen og er derfor ikke relevant.
    # Sekvenserne gemmes i 'AllCombis > neotopes > [neotopstørrelse] (8-mer, 9-mer, etc)

    for neo in neotope_weight: # Angiver locations for pot neotoper for neotopstørrelser op til +1 for epitopestørrelsen
        AllCombis["neotopes"][str(neo)+"-mer"] = neoloc(neo,AllCombis['base']['code'])

    # 7-9 ny
    ### Kører sekvens gennem NetMHCpan - se func 'getnetrank'
    ### Laver string, der angiver sande neotoper - se func 'realneos'
    ### Laver list, der angiver hvor mange sande neotoper en given fusion mellem
        # 2 epitoper findes for en given MHC - se func 'neosum'

    print '\tTesting combinations:'

    for sla in sorted(MHC_weight):
        print '\t\t'+sla,
        AllCombis['NetMHCpan'][sla] = {'rank': {"8-mer": [], "9-mer": [], "10-mer": [], "11-mer": []}} # Denne skal være på denne måde så de
efterfølgende kan tilføjes på gjorte måde
        AllCombis["NetMHCpan"][sla]["realNeos"] = {}
        AllCombis["NetMHCpan"][sla]["NeoSum"] = {}
        for neo in sorted(neotope_weight):
            print str(neo),
            AllCombis['NetMHCpan'][sla]['rank'][str(neo)+'-mer'] = getnetrank(neo, sla, AllCombis['base']['seq'])
            AllCombis["NetMHCpan"][sla]["realNeos"][str(neo)+"-mer"] = realneos(AllCombis['neotopes'][str(neo)+'-
mer'],AllCombis['NetMHCpan'][sla]['rank'][str(neo)+'-mer'], sla, neo)
            AllCombis["NetMHCpan"][sla]["NeoSum"][str(neo)+"-mer"] =
neosum(AllCombis['base']['code'],AllCombis['base']['order'],AllCombis['NetMHCpan'][sla]['realNeos'][str(neo)+'-mer'])
        print 'done'

    # 10

    pSum = []
    for pos in range(len(AllCombis["base"]["order"])-1):
        position = str(AllCombis["base"]["order"][pos])+"?"+str(AllCombis["base"]["order"][pos+1])
        posSum = 0
        for sla in MHC_weight:
            slaSum = 0
            for neo in neotope_weight:
                if AllCombis["NetMHCpan"][str(sla)]["NeoSum"][str(neo)+"-mer"][position] > 0:
                    slaSum += 1
            if slaSum > 0:
                posSum =1
        pSum.append([str(position), posSum])
    AllCombis["NetMHCpan"]["slaPosSum"] = pSum

    ### KOMBINERER EPITOPER TIL BEDSTE UDGANGSPUNKT

    tstring = ""
    for l in range(len(elists)):
        slist = []
        elements = []
        converter = {}
        for item in AllCombis["NetMHCpan"]["slaPosSum"]:
            if item[0][0] in elists[l] and item[0][2] in elists[l]:
                slist.append(item[:])
        cnt = 0
        for sign in elists[l]:
            elements.append(str(cnt))
            converter[cnt] = sign
            for spacer in slist:
                if sign in spacer[0]:
                    spacer[0] = spacer[0].replace(sign,str(cnt))
            cnt += 1

        s = dict(slist)
        string = ""
        ss = list(min(itertools.permutations(elements), key=lambda p: sum(s[a+'?'+b] for a, b in zip(p, p[1:]))))
        for x in ss:
            string += converter[int(x)]
        tstring += string

    OptiSeq = {'epiOrder': [tstring], 'workOrder': [], 'workEpiOrder': [], 'before': {'neotopes': {}, 'NetMHCpan': {}}}
    # 12
    ### Laver optimal sekvens i aminosyre sekvens og kodesekvens


    seq = ""
    code = ""
    for sign in OptiSeq["epiOrder"][recombined]:
        seq += str(EpiData[sign]["seq"])
```

```
        code += str(EpiData[sign]["code"])
    OptiSeq["before"]["seq"] = seq
    OptiSeq["before"]["code"] = code

    # 13
    for neo in neotope_weight: # Angiver locations for pot neotoper for neotopstørrelser op til +1 for epitopestørrelsen
        OptiSeq["before"]["neotopes"][str(neo)+"-mer"] = neoloc(neo,OptiSeq["before"]['code'])

    print '\tAnalysing optimal sequence:'
    #14-16
    for sla in sorted(MHC_weight):
        print '\t\t'+sla,
        OptiSeq["before"]['NetMHCpan'][sla] = {'rank': {"8-mer": [], "9-mer": [], "10-mer": [], "11-mer": []}}
        OptiSeq["before"]["NetMHCpan"][sla]["realNeos"] = {}
        OptiSeq["before"]["NetMHCpan"][sla]["NeoSum"] = {}
        for neo in sorted(neotope_weight):
            print str(neo),
            OptiSeq["before"]['NetMHCpan'][sla]['rank'][str(neo)+'-mer'] = getnetrank(neo, sla, OptiSeq["before"]['seq'])
            OptiSeq["before"]["NetMHCpan"][sla]["realNeos"][str(neo)+"-mer"] = realneos(OptiSeq["before"]['neotopes'][str(neo)+'-
mer'],OptiSeq["before"]['NetMHCpan'][sla]['rank'][str(neo)+'-mer'], sla, neo)
            OptiSeq["before"]["NetMHCpan"][sla]["NeoSum"][str(neo)+"-mer"] =
neosum(OptiSeq["before"]['code'],OptiSeq['epiOrder'][recombined],OptiSeq["before"]['NetMHCpan'][sla]['realNeos'][str(neo)+'-mer'])
        print 'done'

    # ny
    # pdict tæller hvor mange x-mer neotoper, der findes for hver sla.
    newpSum = []
    pdict = {}
    stotSum = 0
    for pos in range(len(OptiSeq['epiOrder'][recombined])-1):
        position = str(OptiSeq['epiOrder'][recombined][pos])+"?"+str(OptiSeq['epiOrder'][recombined][pos+1])
        posSum = 0
        for sla in MHC_weight:
            if sla not in pdict:
                pdict[sla] = {}
            slaSum = 0
            for neo in neotope_weight:
                if OptiSeq["before"]["NetMHCpan"][sla]["NeoSum"][str(neo)+"-mer"][position] > 0:
                    if neo not in pdict[sla]:
                        pdict[sla][neo] = OptiSeq["before"]["NetMHCpan"][sla]["NeoSum"][str(neo)+"-mer"][position]
                    else:
                        pdict[sla][neo] += OptiSeq["before"]["NetMHCpan"][sla]["NeoSum"][str(neo)+"-mer"][position]
                    slaSum += 1
                    stotSum += OptiSeq["before"]["NetMHCpan"][sla]["NeoSum"][str(neo)+"-mer"][position]
            if slaSum > 0:
                posSum =1
        newpSum.append([str(position), posSum])
    #itrscores = [stotSum]


    #17 - ny
    ### LISTE OVER SPACERE, hvilket er synonym med positioner, der indeholder neotoper

    OptiSeq['spacers'] = {'sequence': []}
    solved = {}
    order = []
    endOrder = []
    for x in range(len(OptiSeq['epiOrder'][recombined])-1):
        endOrder.append(OptiSeq['epiOrder'][recombined][x])
        pos = str(OptiSeq['epiOrder'][recombined][x]+"?"+OptiSeq['epiOrder'][recombined][x+1])
        for score in range(len(newpSum)):
            if pos == newpSum[score][0]:
                if newpSum[score][1] > 0:
                    OptiSeq['spacers'][pos] = {} #{'sequence': [], 'score': []}
                    order.append(pos)
                    endOrder.append(pos)
                elif newpSum[score][1] == 0:
                    solved[pos] = {'seq': "", 'ranks': None} # indeholder kun positioner, uden neotoper, og den pågældende spacer (her "")
    endOrder.append(OptiSeq['epiOrder'][recombined][len(OptiSeq['epiOrder'][recombined])-1])
    OptiSeq['spaceOrder']=[order]
    OptiSeq['endOrder']=[endOrder]
    if len(order)==0:
        RECOMBINE = 0
        TOBEST = 0
        MAKESPACERS = 0
        TOEND = 1
        print 'Optimal sequence obtained by combining - No spacers needed'
        PS['end'] += 'Optimal sequence obtained by combining - No spacers needed'
        finalSeq = OptiSeq["before"]['seq']
        etotSum = 0
        if 'ID' in EpiData[str(codestring[0])]:
            finalIDorder = ""
            for sign in OptiSeq["epiOrder"][recombined]:
                finalIDorder += EpiData[sign]['ID']+'-'
            finalIDorder = finalIDorder.rstrip('-')

    else:
        RECOMBINE = 0
        TOBEST = 0
        MAKESPACERS = 1
        TOEND = 0

    countunfix = [0]
    ufstring = ""
    for x in OptiSeq['spaceOrder'][recombined]:
        countunfix[0] += 1
        ufstring += x+" "
    ufstring = ufstring.rstrip(' ')
    print '\t'+str(len(OptiSeq['spaceOrder'][recombined]))+'/'+str(len(EpiData)-1),
    print 'junctions contain neotopes'
    print '\tJunctions: '+ufstring


    ### REPORT - Pre processing analysis
    PS['pre'] = 'PRE PROCESSING:\n'
    PS['pre'] += "\tNeotopes:\t\t"+str(stotSum)+"\n"
    if stotSum > 0:
        PS['pre'] += "\tJunctions:\t\t"+str(len(OptiSeq['spaceOrder'][recombined]))+"\n"
    PS['pre'] += "\n\tDist matrix:\t\t"
```

```
    for neo in sorted(neotope_weight):
        PS['pre'] += str(neo)+'-mer\t'
    PS['pre'] += '\n'
    for MHC in sorted(MHC_weight):
        PS['pre'] += '\t'+MHC+':\t\t'
        for neo in sorted(neotope_weight):
            try: PS['pre'] += '  '+str(pdict[MHC][neo])+'\t'
            except: PS['pre'] += '  '+str(0)+'\t'
        PS['pre'] += '\n'



PS['history'] = '\tOrigin\t'+str(len(OptiSeq['spaceOrder'][recombined]))+'/'+str(len(EpiData)-1)+'\t'+ufstring+'\n'
unfixed = []
cntFN = 0

if include_spacers == 1:
    incnt = 0
    with open(spcpath+spcfile,'r') as handle:
        for line in handle:
            line = line.rstrip()
            OptiSeq['spacers']['sequence'].append(line)
            incnt += 1
    print '\t'+str(incnt)+' spacers imported from file:\n\t'+spcfile
# 18
### GENERERER WORKSEQ, SOM ER ARBEJDSSEKVENSEN,
### DER SKAL TESTES FOR FUNKTIONELLE SPACERE

while MAKESPACERS == 1: # starter herfra efter recombination
    print '\nFINDING SPACERS'
    countunfix = [0]
    ufstring = ""
    for x in OptiSeq['spaceOrder'][recombined]:
        countunfix[0] += 1
        ufstring += x+" "
    print '\n\tSolving: '+str(countunfix[0])+'/'+str(len(EpiData)-1)+' ('+ufstring.strip(' ')+')'
    workseq = []
    uworkseq = []
    weorder = ""
    OptiSeq['workOrder'].append([])
    OptiSeq['workEpiOrder'].append([])
    for x in OptiSeq['spaceOrder'][recombined]:
        OptiSeq['spacers'][x] = {'score': [], 'ranks': []}
        workseq.append(x[0])
        workseq.append(x)
        workseq.append(x[2])
    [uworkseq.append(y) for y in workseq if y not in uworkseq]
    OptiSeq['workOrder'][recombined].append(uworkseq)
    for aa in OptiSeq['workOrder'][recombined][0]:
        if '?' not in aa:
            weorder += aa
    OptiSeq['workEpiOrder'][recombined].append(weorder)

### forsøger at lave kun én spacer pr iteration

    PS['history'] += '\t*'
    thruPan = 0
    passed_itrs = 0
    allgood = 0
    stopiter = 0
    while MAKESPACERS == 1: # starter herfra efter kørsel gennem netMHCpan
        print '\t'+str(recombined)+':'+str(thruPan)+' (Recombination:ThruPan)'
        PS['history'] += str(recombined)+':'+str(thruPan)

        ### Oprettelse af diverse lister, dics og strings
        workString = ""
        worklength = 0
        OptiSeq['NetMHCpan'] = {}
        OptiSeq['workstring'] = []
        OptiSeq['codestring'] = []
        OptiSeq['neoloc'] = {}
        OptiSeq['neoMHC'] = []
        OptiSeq['neosum'] = {}
        OptiSeq['realNeos'] = {}
        OptiSeq['neoranks'] = {}

        for sla in MHC_weight:
            OptiSeq['neosum'][sla] = {}
            OptiSeq['realNeos'][sla] = {}
            OptiSeq['NetMHCpan'][sla] = {}
            OptiSeq['neoranks'][sla] = {}
            for neo in neotope_weight:
                OptiSeq['neosum'][sla][str(neo)+'-mer'] = []
                OptiSeq['realNeos'][sla][str(neo)+'-mer'] = []
                OptiSeq['NetMHCpan'][sla][str(neo)+'-mer'] = {}
                OptiSeq['neoranks'][sla][str(neo)+'-mer'] = []
        for neo in neotope_weight:
            OptiSeq['neoloc'][str(neo)+'-mer'] = []



        #max # iteration will stop after this number of rounds
        itr = 0
        retry = 0
        limlen = 0
        stopitr = 0

        while stopitr == 0: # forbereder string til at køre gennem netMHCpan
            for sla in MHC_weight:
                for neo in neotope_weight:
                    OptiSeq['NetMHCpan'][sla][str(neo)+'-mer'][itr] = []


    # 19
        ### GENERERER RANDOM SPACER SEKVENSER
            if itr+passed_itrs == len(OptiSeq['spacers']['sequence']): # for ikke automatisk at lave flere spacers ved ny recombination
                ct = 0
                while ct == 0:
```

```
                spseq = ""
                for c in range(randrange(Min_spacer_aa,Max_spacer_aa)):
                    spseq += AminoAcids[randrange(len(AminoAcids))]
                if spseq in OptiSeq['spacers']['sequence'] or spseq in oldspacers:
                    retry += 1
                    if retry == 1000:
                        print '\nRandom generator stopped due to lack of unique spacer combinations'
                        stopitr = 1
                        ct = 1
                        RECOMBINE = 1
                else:
                    OptiSeq['spacers']['sequence'].append(spseq)
                    ct = 1

    # 20
        ### Kombinerer random spacere og epitoper for at få workstrings og codestrings
            cstring = ""
            wstring = ""
            for unit in OptiSeq['workOrder'][recombined][thruPan]:
                if '?' in unit:
                    wstring += OptiSeq['spacers']['sequence'][itr+passed_itrs]
                    cstring += len(OptiSeq['spacers']['sequence'][itr+passed_itrs])*'?'
                    worklength += len(OptiSeq['spacers']['sequence'][itr+passed_itrs])
                    if itr == 0:
                        limlen += Max_spacer_aa
                else:
                    wstring += EpiData[unit]['seq']
                    cstring += EpiData[unit]['code']
                    worklength += EpiData[unit]['length']
                    if itr == 0:
                        limlen += EpiData[unit]['length']


            OptiSeq['workstring'].append(wstring)
            OptiSeq['codestring'].append(cstring)

            if 1==0:
                if itr == 0:
                    print 'Limlen:',limlen
                    print 'Workorder:',OptiSeq['workOrder'][recombined][thruPan]
                    print 'workEpiOrder:', OptiSeq['workEpiOrder'][recombined][thruPan]
                    print 'len(workEpiOrder):', len(OptiSeq['workEpiOrder'][recombined][thruPan])
                print OptiSeq['spacers']['sequence'][itr+passed_itrs],

        ### Stops iteration
            if spacersPerItr == max:
                if worklength > 20000-limlen:
                    stopitr = 1
            elif spacersPerItr < 1:
                stopitr = 1
                print '\nAdjust "spacersPerItr"\n'
            elif itr == spacersPerItr-1:
                    stopitr = 1
            else:
                if not type(spacersPerItr) == int:
                    print '\nAdjust "spacersPerItr"\n'
                    stopitr = 1

    # 21
        ### Identificerer placeringen af potentielle nye neotoper
        # se func 'neoloc'
            for neo in neotope_weight:
                OptiSeq['neoloc'][str(neo)+'-mer'].append(neoloc(neo,cstring))

        ### Samler alle sekvenser i én samlet sekvens, der så skal analyseres af NetMHCpan,
            # for derefter at blive delt op i individuelle sekvenser efterfølgende.
            workString += wstring

            itr += 1
        passed_itrs += itr
        print '\n\tSpacers:\t',itr, '(curr.)\t',passed_itrs,'(total)\t', retry, '(retrys)'
        print '\tWorklength:\t'+str(worklength)


        #Kører workString gennem NetMHCpan og deler den derefter op i rank lister, der svarer til hver iteration


    # 22
        for sla in sorted(MHC_weight):
            print '\t\t',sla,
            for neo in sorted(neotope_weight):
                ranklist = getnetrank(neo, sla, workString)
                i = 0
                passed = 0
                for x in range(len(ranklist)):
                    if x-passed < len(OptiSeq['workstring'][i]):
                        OptiSeq['NetMHCpan'][sla][str(neo)+'-mer'][i].append(ranklist[x])
                    else:
                        OptiSeq['NetMHCpan'][sla][str(neo)+'-mer'][i+1].append(ranklist[x])
                        passed = x
                        i += 1



    # 23-24
            ### Kører hver sekvens gennem NetMHCpan - se func 'getnetrank'
            ### Laver string, der angiver sande neotoper - se func 'realneos'
                # Heri tages højde for sla og neo vægtningerne
            ### Laver list, der angiver hvor mange sande neotoper en given fusion mellem
                # 2 epitoper findes for en given MHC - se func 'neosum'
                for iter in range(itr):
                    realn = realneos(OptiSeq['neoloc'][str(neo)+'-mer'][iter], OptiSeq['NetMHCpan'][sla][str(neo)+'-mer'][iter], sla, neo)
                    #print itr, sla, neo,'\t',realn
                    OptiSeq['realNeos'][sla][str(neo)+'-mer'].append(realn)
                    nsum = neosum(OptiSeq['codestring'][iter], OptiSeq['workEpiOrder'][recombined][thruPan], realn)
                    #print itr, sla, neo, nsum
                    OptiSeq['neosum'][sla][str(neo)+'-mer'].append(nsum)
                    rnk = neorank(OptiSeq['codestring'][iter],OptiSeq['workEpiOrder'][recombined][thruPan], OptiSeq['neoloc'][str(neo)+'-
mer'][iter], OptiSeq['NetMHCpan'][sla][str(neo)+'-mer'][iter], sla, neo)
```

```
                OptiSeq['neoranks'][sla][str(neo)+'-mer'].append(rnk)
            print str(neo),
        print 'done'


    # 25
        ### Laver liste der angiver det totale antal ægte neotoper for hver position
        for iter in range(itr):
            itrsum = 0
            for pos in OptiSeq['workOrder'][recombined][thruPan]:
                if '?' in pos:
                    posSum = 0
                    ranks = []
                    for sla in MHC_weight:
                        for neo in neotope_weight:
                            posSum += OptiSeq["neosum"][sla][str(neo)+"-mer"][iter][pos]
                            ranks += OptiSeq['neoranks'][sla][str(neo)+'-mer'][iter][pos]
                    itrsum += posSum
                    OptiSeq['spacers'][pos]['score'].append(posSum)
                    OptiSeq['spacers'][pos]['ranks'].append(round(stats.hmean(ranks),2))
            #itrscores.append(itrsum)



    #26
        # Finder postition, der endnu ikke er helt uden neotoper
        newWorkOrder = []
        unewWorkOrder = []
        newEpiOrder = ""
        countunfix.append(0)
        fixed = []
        uf = []
        ufstring = ""
        for pos in OptiSeq['spaceOrder'][recombined]:
            if min(OptiSeq['spacers'][pos]['score']) != 0:
                uf.append(pos)
                countunfix[thruPan+1] += 1
                ufstring += pos+' '
                posIndex = OptiSeq['workOrder'][recombined][0].index(pos)
                newWorkOrder.append(OptiSeq['workOrder'][recombined][0][posIndex-1])
                newWorkOrder.append(OptiSeq['workOrder'][recombined][0][posIndex])
                newWorkOrder.append(OptiSeq['workOrder'][recombined][0][posIndex+1])
            else:
                fixed.append(pos)
                ########## solved[pos] =
        print '\t'+str(countunfix[thruPan+1])+'/'+str(len(OptiSeq['epiOrder'][recombined])-1),'still missing ('+ufstring+')'
        [unewWorkOrder.append(y) for y in newWorkOrder if y not in unewWorkOrder]
        PS['history'] += '\t'+str(countunfix[thruPan+1])+'/'+str(len(OptiSeq['epiOrder'][recombined])-1)+'\t'+ufstring+'\n'


        if maxtime > 0:
            intertime = time.time()
            if intertime-starttime > maxtime*60:
                PS['end'] += 'Time Out'
                print '\n\nTIME OUT\n\n'
                RECOMBINE = 0
                TOBEST = 1
                MAKESPACERS = 0
                TOEND = 0
                unfixed.append(uf)
        if TOBEST == 0:
            if RECOMBINE == 1 or thruPan == runthru-1:
                RECOMBINE = 1
                TOBEST = 0
                MAKESPACERS = 0
                TOEND = 0
            elif len(unewWorkOrder) != 0:
                for pos in unewWorkOrder:
                    if not '?' in pos:
                        newEpiOrder += pos
                thruPan += 1 # Får besked på at lave ny workstring, der skal køres i pan
                OptiSeq['workOrder'][recombined].append(unewWorkOrder)
                OptiSeq['workEpiOrder'][recombined].append(newEpiOrder)
                RECOMBINE = 0
                TOBEST = 0
                MAKESPACERS = 1
                TOEND = 0
                PS['history'] += '\t '
            else:
                RECOMBINE = 0
                TOBEST = 1
                MAKESPACERS = 0
                TOEND = 0
                unfixed.append(uf)
                print 'No more neotopes - Ending process\n'



# 27
### Splitter OptiSeq['endOrder'][recombined] op i fragmenter, de steder hvor en passende spacer ikke kunne findes.
    if RECOMBINE == 1:
        print '\nRECOMBINING',
        unfixed.append(uf)
        tlist = {}
        for x in range(len(unfixed[recombined])+1):
            tlist[x] = []

        y = 0
        for item in OptiSeq['endOrder'][recombined]:
            if item in unfixed[recombined]:
                tried_spacers.append(item)
                y += 1
            else:
                tlist[y].append(item)

        s = list(range(len(tlist)))
        recombis = 0
        end = 0
        while end == 0:
```

```
            random.shuffle(s)
            xlist = []
            for x in range(len(s)-1):
                xlist.append(tlist[s[x]][len(tlist[s[x]])-1]+'?'+tlist[s[x+1]][0])
            redo = 0
            for y in xlist:
                if y in tried_spacers or y in solved:
                    redo = 1
            if redo == 1:
                recombis += 1
                if recombis == 10000:
                    print '- failed - No more combinations'
                    PS['end'] += 'No more combinations'
                    end = 1
                    TOBEST = 1
                    RECOMBINE = 0
                    MAKESPACERS = 0
                    TOEND = 0
            else:
                nlist = []
                k = 0
                for z in s:
                    nlist.append(tlist[z])
                    try:
                        nlist.append([xlist[k]])
                    except: pass
                    k += 1
                zlist = []
                for n in nlist:
                    zlist += n
                #itrscores = [itrscores[len(itrscores)-1]]
                OptiSeq['endOrder'].append(zlist)
                OptiSeq['spaceOrder'].append(xlist)
                recombined += 1
                end = 1
                RECOMBINE = 0
                TOBEST = 0
                MAKESPACERS = 1
                TOEND = 0
                print '- completed - Testing spacers'

                epistring = ""
                for epi in OptiSeq['endOrder'][recombined]:
                    if not '?' in epi:
                        epistring += epi
                OptiSeq['epiOrder'].append(epistring)

### return to 18
#################################################################################################33
# 28
### Printer de af alle testede spacersekvenser, der giver færrest neotoper, og er kortest
if 1==0:
    if TOBEST == 1:
        best = {}
        recombis = {'recSeq': [], 'recCode': [], 'recIDorder': [], 'recScore': []}
        for rec in range(recombined+1):
            for pos in OptiSeq['spaceOrder'][rec]:
                best[pos] = {}
                minimums = {'seq': [], 'len': [], 'ind' : []}
                min_score = min(OptiSeq['spacers'][pos]['score'])
                for spcr in range(len(OptiSeq['spacers'][pos]['score'])):
                    if OptiSeq['spacers'][pos]['score'][spcr] == min_score:
                        minimums['seq'].append(OptiSeq['spacers']['sequence'][spcr])
                        minimums['len'].append(len(OptiSeq['spacers']['sequence'][spcr]))
                min_len = min(minimums['len'])
                for cand in range(len(minimums['seq'])):
                    if minimums['len'][cand] == min_len:
                        best[pos]['seq'] = minimums['seq'][cand]
                        best[pos]['score'] = str(min_score)
                        #best[pos]['index'] = OptiSeq['spacers']['sequence'].index(minimums['seq'][cand])
                        if min_score == 0:
                            solved[pos] = minimums['seq'][cand]

# 28
### Printer de af alle testede spacersekvenser, der giver færrest neotoper, og er har højest harmean(ranks[sla][neo])
if TOBEST == 1: # ny
    best = {}
    for rec in range(recombined+1):
        for pos in OptiSeq['spaceOrder'][rec]:
            best[pos] = {}
            minimums = {'seq': [], 'len': [], 'ranks': [], 'ind' : []}
            min_score = min(OptiSeq['spacers'][pos]['score'])
            for spcr in range(len(OptiSeq['spacers'][pos]['score'])):
                if OptiSeq['spacers'][pos]['score'][spcr] == min_score: # Samler de spacere, der giver færrest neotoper for en given position
                    minimums['seq'].append(OptiSeq['spacers']['sequence'][spcr])
                    minimums['len'].append(len(OptiSeq['spacers']['sequence'][spcr]))
                    minimums['ranks'].append(OptiSeq['spacers'][pos]['ranks'][spcr])
            for cand in range(len(minimums['ranks'])):
                if minimums['ranks'][cand] == max(minimums['ranks']): # vælger den spacer, der har højest harmean(ranks)
                    best[pos]['seq'] = minimums['seq'][cand]
                    best[pos]['score'] = str(min_score)
                    best[pos]['rankmean'] = minimums['ranks'][cand]
                    if min_score == 0:
                        solved[pos] = {'seq': minimums['seq'][cand],'ranks': minimums['ranks'][cand]}

    ### Sammenholder nuværende og tidligere bedste til en samlet best liste
    if 1==0: # gl
        try:
            for key in oldbest:
                if key in best:
                    if int(oldbest[key]['score']) < int(best[key]['score']):
                        best[key] = {'score': int(oldbest[key]['score']), 'seq': oldbest[key]['seq']}
                    elif int(oldbest[key]['score']) == int(best[key]['score']):
                        if len(oldbest[key]['seq']) < len(best[key]['seq']):
                            best[key] = {'score': int(oldbest[key]['score']), 'seq': oldbest[key]['seq']}
                else:
                    best[key] = {'score': int(oldbest[key]['score']), 'seq': oldbest[key]['seq']}
        except: pass
```

```
    ### Sammenholder nuværende og tidligere bedste til en samlet best liste
    # Ny: tager højde for rankmean i stedet for længde
    try:
        for key in oldbest:
            if key in best:
                if int(oldbest[key]['score']) < int(best[key]['score']):
                    best[key] = {'score': int(oldbest[key]['score']), 'seq': oldbest[key]['seq'], 'rankmean': float(oldbest[key]['rankmean'])}
                elif int(oldbest[key]['score']) == int(best[key]['score']):
                    if float(oldbest[key]['rankmean']) > float(best[key]['rankmean']):
                        best[key] = {'score': int(oldbest[key]['score']), 'seq': oldbest[key]['seq'], 'rankmean':
float(oldbest[key]['rankmean'])}
            else:
                best[key] = {'score': int(oldbest[key]['score']), 'seq': oldbest[key]['seq'], 'rankmean': float(oldbest[key]['rankmean'])}
    except: pass

# gl 29 - her finder den den bedste af de testede recombinationer.
    recombis = {'recSeq': [], 'recCode': [], 'recIDorder': [], 'recScore': [], 'recRNK': []}
    for rec in range(recombined+1):
        if len(unfixed[recombined]) == min(len(x) for x in unfixed): # vælger den rekombination med færrest neotop junctions
            recSeq = ""
            recCode = ""
            recIDorder = ""
            recRNK = 0
            recScore = 0
            for pos in OptiSeq['endOrder'][rec]:
                if '?' in pos:
                    try:
                        recSeq += best[pos]['seq']
                        recCode += len(best[pos]['seq'])*'?'
                        recScore += int(best[pos]['score'])
                        recRNK += best[pos]['rankmean']
                        if 'ID' in EpiData[codestring[0]]:
                            recIDorder += '?-'
                    except:
                        recSeq += solved[pos]
                        recCode += len(solved[pos])*'?'
                        recScore += 0
                        recRNK += solved[pos]['ranks']
                        if 'ID' in EpiData[codestring[0]]:
                            recIDorder += '?-'
                else:
                    recSeq += EpiData[pos]['seq']
                    recCode += EpiData[pos]['code']
                    if 'ID' in EpiData[codestring[0]]:
                        recIDorder += EpiData[pos]['ID']+'-'
            try: recIDorder = recIDorder.rstrip('-')
            except: pass
            recombis['recSeq'].append(recSeq)
            recombis['recCode'].append(recCode)
            recombis['recIDorder'].append(recIDorder)
            recombis['recScore'].append(recScore)
            recombis['recRNK'].append(recRNK)
    recombinations = recombined

    bestscore = {}
    for rec in range(recombined+1):
        if recombis['recScore'][rec] == min(recombis['recScore']):
            bestscore[rec] = recombis['recRNK'][rec]
    for num in bestscore:
        if recombis['recRNK'][num] == max(bestscore[x] for x in bestscore):
            recombined = num #fixerer 'recombined' til bedste rekombination
    finalSeq = recombis['recSeq'][recombined]
    finalCode = recombis['recCode'][recombined]
    finalIDorder = recombis['recIDorder'][recombined]



# 30

    print '\nEND SEQUENCE\n'
    final = {'neotopes':{},'rank':{},'realNeos': {}, 'NeoSum':{}}
    for neo in neotope_weight:
        final['neotopes'][str(neo)+'-mer'] = neoloc(neo,finalCode)
        final['rank'][str(neo)+'-mer'] = {}
        final['realNeos'][str(neo)+'-mer'] = {}
        final['NeoSum'][str(neo)+'-mer'] = {}
        for sla in MHC_weight:
            final['rank'][str(neo)+'-mer'][sla] = getnetrank(neo, sla, finalSeq)
            final["realNeos"][str(neo)+"-mer"][sla] = realneos(final['neotopes'][str(neo)+'-mer'],final['rank'][str(neo)+'-mer'][sla], sla, neo)
            final["NeoSum"][str(neo)+"-mer"][sla] = neosum(finalCode,OptiSeq['epiOrder'][recombined],final['realNeos'][str(neo)+'-mer'][sla])

    # ny
    newpSum = []
    pdict = {}
    etotSum = 0
    for pos in range(len(OptiSeq['epiOrder'][recombined])-1):
        position = str(OptiSeq['epiOrder'][recombined][pos])+"?"+str(OptiSeq['epiOrder'][recombined][pos+1])
        slalist = {}
        for sla in sorted(MHC_weight):
            neolist = []
            if sla not in pdict:
                pdict[sla] = {}
            for neo in sorted(neotope_weight):
                if final["NeoSum"][str(neo)+"-mer"][sla][position] > 0:
                    if neo not in pdict[sla]:
                        pdict[sla][neo] = final["NeoSum"][str(neo)+"-mer"][sla][position]
                    else:
                        pdict[sla][neo] += final["NeoSum"][str(neo)+"-mer"][sla][position]
                    neolist.append(str(neo))
                    etotSum += final["NeoSum"][str(neo)+"-mer"][sla][position]
            if len(neolist) > 0:
                slalist[sla] = neolist
        if len(slalist) > 0:
            newpSum.append([str(position), slalist])

    ufstring = ""
    for spc in unfixed[recombined]:
        ufstring += spc+' '
    print '\tBest recombination:\t'+ufstring
```

```
print '\tNeotopes still present:\t'+str(etotSum)


### REPORT - Junctions
PS['junc'] = ""
for pos in newpSum:
    start = finalCode.index(pos[0][0])
    stop = finalCode.index(pos[0][2])
    l=30 #linelength
    xtra = l-stop+start
    for i in range(start,stop+xtra,l):
        PS['junc'] += pos[0]+': '+str(start)+'-'+str(stop-1)+'\t\t'
        for x in range(l/10):
            y = i+x*10
            PS['junc'] += str(y)+' '*(10-len(str(y)))
        PS['junc'] += '\n'
        PS['junc'] += '\tFinal Seq:\t'+finalSeq.upper()[0+i:l+i]+'\n'
        PS['junc'] += '\tCode:\t\t'+finalCode[0+i:l+i]+'\n'
        for sla in sorted(pos[1]):
            for neo in pos[1][sla]:
                PS['junc'] += '\t'+str(sla)+' '+str(neo)+':\t'+str(final["realNeos"][str(neo)+"-mer"][sla][0+i:l+i-xtra])+'-'*xtra
                nt = final["realNeos"][str(neo)+"-mer"][sla][0+i:l+i-xtra].rfind(str(1))+start
                endepi2 = stop+EpiData[pos[0][2]]['length']
                if nt+int(neo) > endepi2:
                    PS['junc'] += ' <= double overlapper\n'
                if nt == stop-1:
                    print '\t\tTesting for false neoepitopes at position '+str(nt)+' ('+pos[0]+') '+sla, str(neo)
                    string = ""
                    allaa = 'arndcqeghilkmfpstwyv' # all 20 aminoacids
                    for aa in allaa:
                        string += aa+EpiData[pos[0][2]]['seq'][0:int(neo)-1]
                    lst = getnetrank(neo,sla,string)
                    slvrs = []
                    for aa in range(len(allaa)):
                        if float(lst[aa*int(neo)])*10000/float(MHC_weight[sla])/float(neotope_weight[int(neo)]) > RnkThr:
                            slvrs.append(allaa[aa])
                    sstring = " <= "
                    if len(slvrs) == 0:
                        sstring += 'False neoepitope - unsolvable'
                        cntFN += 1
                        if int(best[pos[0]]['score']) > 0:
                            if best[pos[0]]['seq'] in OptiSeq['spacers']['sequence']:
                                best[pos[0]]['score'] = int(best[pos[0]]['score'])-1 # ændrer i pos, så falske neoepitoper ikke tælles med.
                                nmr = OptiSeq['spacers']['sequence'].index(best[pos[0]]['seq'])
                                OptiSeq['spacers'][pos[0]]['score'][nmr] = OptiSeq['spacers'][pos[0]]['score'][nmr]-1
                                if best[pos[0]]['score'] == 0:
                                    unfixed[recombined].remove(pos[0])
                    else:
                        sstring += 'Solvable by: '
                        inc = ""
                        ex = ""
                        for aas in slvrs:
                            if aas in AminoAcids:
                                inc += aas.upper()
                            else:
                                ex += aas.upper()
                        if not len(inc) == 0:
                            sstring += inc+' (incl.) '
                        if not len(ex) == 0:
                            sstring += ex+' (excl.)'
                    PS['junc'] += sstring+'\n'
                else:
                    PS['junc'] += '\n'
    PS['junc'] += '\n'

print '\tFalse neoepitopes found: '+str(cntFN)
print '\tReal neoepitopes:\t\t'+ str(etotSum-cntFN)



### REPORT - post processing analysis
PS['post'] = "\tNeotopes left:\t\t"+str(etotSum-cntFN)+" real, "+str(cntFN)+" false\n"
if etotSum > 0:
    PS['post'] += "\tJunctions:\t\t"+str(len(newpSum))+"\n"
PS['post'] += "\n\tDist matrix (incl. FNs):\t"
for neo in sorted(neotope_weight):
    PS['post'] += str(neo)+'-mer\t'
PS['post'] += '\n'
for MHC in sorted(MHC_weight):
    PS['post'] += '\t'+MHC+':\t\t'
    for neo in sorted(neotope_weight):
        try: PS['post'] += '  '+str(pdict[MHC][neo])+'\t'
        except: PS['post'] += '  '+str(0)+'\t'
    PS['post'] += '\n'


### REPORT - clearing spacers
PS['clearers'] = '\tSPCR\tfrag\tpercent\n'
if ReRun == 0:
    testedSpcs = {}
for spc in OptiSeq['spacers']:
    if '?' in spc:
        zeros = 0
        zspacers = ""
        for s in range(len(OptiSeq['spacers'][spc]['score'])):
            if OptiSeq['spacers'][spc]['score'][s] == 0:
                zeros += 1
                zspacers += OptiSeq['spacers']['sequence'][s]+' ('+str(OptiSeq['spacers'][spc]['ranks'][s])+'); '
        length = len(OptiSeq['spacers'][spc]['score'])
        if spc in testedSpcs:
            length = length + testedSpcs[spc]
        if zeros > 0:
            PS['clearers'] += '\t'+spc+'\t'+str(zeros)+'/'+str(length)
            PS['clearers'] += '\t'+str(int((zeros/float(length)*100))).rjust(2)+'%'
            PS['clearers'] += '\t'+zspacers+'\n'
        if zeros == 0:
            testedSpcs[spc] = length
```

```
### Processing time
endtime = time.time()
ptime = time.ctime(endtime-starttime-3600).split(' ')[4]
print '\tProcessing time:\t',ptime
print '\n>final sequence\n'+finalSeq.upper()

### REPORT - User ID, date and time
s = time.ctime(starttime).split()
e = time.ctime(endtime).split()
PS['ID'] = '\tUser:\t\t\t'+username+'\n\tStart time:\t\t'+s[2]+'-'+s[1]+'-'+s[4]+', '+s[3]
PS['ID'] += '\n\tEnd time:\t\t'+e[2]+'-'+e[1]+'-'+e[4]+', '+e[3]
PS['ID'] += '\n\tProcessing time:\t'+ptime



# write filestring
ostr = 'PROCESSING ID:\n'+PS['ID']
if ReRun == 1:
    ostr += '\n\tRerun of logfile:\t'+Logfile+'\n'
else:
    ostr += '\n\tInputfile:\t\t'+EpiList+'\n'
ostr += '\n\nSETTINGS:\n'
ostr += '\tRank threshold:\t\t'+str(RnkThr)+'\n'
ostr += PS['neotopes']+'\n'
ostr += PS['MHC']+'\n'
ostr += PS['spacers']+'\n'
ostr += PS['pre']
if ReRun == 1:
    ostr += 'LATEST PROCESSING SUMMARY:\n'
    ostr += PS['last']
ostr += '\nCURRENT PROCESSING SUMMARY:\n'
if TOEND == 0:
    ostr += PS['post']
ostr += '\n\tEnd reason:\t\t'+PS['end']+'\n'
if TOEND == 0:
    ostr += '\tRandom spacers tried:\t'
    if ReRun == 1:
        ostr += str(len(OptiSeq['spacers']['sequence'])+len(oldspacers))
        ostr += '\t(current: '+str(len(OptiSeq['spacers']['sequence']))+')'
        ostr += '\t(former: '+str(len(oldspacers))+')\n'
    else:
        ostr += str(len(OptiSeq['spacers']['sequence']))+'\n'
    ostr += '\tCombinations tried:\t'+str(recombinations+1)+'\n\n'
ostr += PS['epitopes'].strip('\n')+'\n\n' #INPUT
ostr += 'OUTPUT:\n'
ostr += '\t>final seq\n'
l=60 #linelength of finalSeq in log
for i in range(0, len(finalSeq),l):
    ostr += '\t'+finalSeq.upper()[0+i:l+i]+'\n'
if 'ID' in EpiData[str(codestring[0])]:
    ostr += '\n\tFinal ID order:\n'
    for i in range(0, len(finalIDorder),l):
        ostr += '\t'+finalIDorder[0+i:l+i]+'\n'
if TOEND == 0:
    ostr += '\nJUNCTION OVERVIEW:\n'
    ostr += PS['junc']
    ostr += '\nPROCESSING HISTORY:\n'
    ostr += '\tRec:Itr\tUnfixed\n'
    ostr += PS['history']+'\n'
    ostr += '\nEPITOPE ORDER:\n'
    ostr += '\t'+OptiSeq['epiOrder'][recombined]+'\n'
    ostr += '\nCLEARING SPACERS:\n'
    ostr += PS['clearers']+'\n'
    ostr += '\n\n########################################\n\n'
    ostr += '\nBEST SPACERS#'
    ostr += json.dumps(best)+'\n'
    ostr += '\nALL SPACERS#'
    ostr += json.dumps(OptiSeq['spacers']['sequence']+oldspacers)+'\n'
    ostr += '\nEPIDATA#'
    ostr += json.dumps(EpiData)+'\n'
    ostr += '\nEPIORDER#'
    ostr += json.dumps(OptiSeq['epiOrder'][recombined])+'\n'
    ostr += '\nMHC WEIGHT#'
    ostr += json.dumps(MHC_weight)+'\n'
    ostr += '\nNEOTOPE WEIGHT#'
    ostr += json.dumps(neotope_weight)+'\n'
    ostr += '\nSPACEORDER#'
    ostr += json.dumps(unfixed[recombined])+'\n'
    ostr += '\nENDORDER#'
    ostr += json.dumps(OptiSeq['endOrder'][recombined])+'\n'
    spacerDict = {'sequence': []}
    for key in OptiSeq['spacers']:
        if '?' in key:
            spacerDict[key] = {'score': [], 'ranks': []}
    ostr += '\nSPACERDICT#'
    ostr += json.dumps(spacerDict)+'\n'
    ostr += '\nPOST#'
    ostr += json.dumps(PS['post'])+'\n'
    ostr += '\nSOLVED#'
    ostr += json.dumps(solved)+'\n'
    ostr += '\nTESTEDSPCS#'
    ostr += json.dumps(testedSpcs)+'\n'



# writing file
if SaveToFile == 1:
    if ReRun == 1:
        f = Logfile.split(' - ')
        v = f[2]
        neo = f[3].split('>')[0]+'>'
        nv = 'V'+str(int(v[1:])+1)
        filename = f[0]+' - '+f[1]+' - '+nv+' - '+neo+str(etotSum-cntFN)
    else:
        filename = e[2]+e[1]+e[4]+' - '+e[3]+' - V0 - neo:'+str(stotSum)+'->'+str(etotSum-cntFN)
    file = open(Logpath+filename+'.txt','w')
    file.write(ostr)
    file.close()
```

Appendix E - *Ex vivo* analysis of pigs vaccinated with Ingelvac PRRS Vet

Materials and Methods

Animals, maintenance and experimental design

Six vacant contingency pigs (438-443) already present in a stable at DTU, Frederiksberg, were used for the experiment as they had no other current purpose. The pigs were vaccinated with Ingelvac PRRS Vet (Boehringer Ingelheim, W245-E81BE) according to the manufacturer's instruction. At days post vaccination (dpv) -1, 7, 14, 21, 28, 35 and 42 heparinized blood was sampled from the jugular vein of each animal for the purification PBMC. During the whole period, the pigs were kept in an isolated stable with free access to water and daily feeding. From dpv 42 and on, the pigs resumed their role as contingency pigs, and I am unaware of their fates. The experiment was approved by the Danish Animal Experiments Inspectorate (2014-15-0201-00091).

SLA typing

The pigs were SLA genotyped using the DNA based SLA genotyping described in section 2.4.1, based on genomic DNA purified from ethylenediaminetetraacetic acid (EDTA) stabilized blood.

Purification, cryopreservation and thawing of PBMCs

PBMCs were purified from heparinized blood sampled at dpv -1, 7, 14, 21, 28, 35 and 42, by density centrifugation on Ficoll-Pague Plus (GE Healthcare) in 50 ml Falkon tubes at 2500 rpm for 15 minutes. Purified PBMCs were counted on a NucleoCounter NC-200 (Chemometec) and cryopreserved in liquid nitrogen in vials containing 1E7 PBMCs suspended in 50% fetal bovine serum (FBS)\40% RPMI-1640 (Sigma)\10% DMSO. Thawing of PBMCs was performed by transferring half-frozen cells to 20 ml 37 °C RPMI-1640\10% FBS followed by centrifugation and washing. Thawed PBMCs were counted prior to analysis on a NucleoCounter NC-200.

Peptide pools

Three pools of six peptides each were used in this setup. Pool 1 contained the peptides (with IDs referring to table 2 in paper 1, page 87) 2, 10, 13, 19, 36 and 38; pool 2 contained the peptides 7, 12, 17, 21, 25 and 28; and pool 3 contained the peptides 4, 24, 34, 43, 44 and 45. All peptides of pools 1 and 2 were encoded by the parental strain of the used vaccine, VR-2332 (acc. U87392), while the peptides of pool 3 differed by single amino acids from the homologous sequences of VR-2332 (table E1)

Peptide ID	Peptid sequence	VR-2332 sequence
4	YSFPGPPFF	YSFPG**T**PFF
24	RTAPNEIAF	RTAPNE**V**AF
34	SSEGHLTSVY	S**N**EGHLTSVY
43	TTMPSGFELY	TTMP**P**GFELY
44	MSWRYSCTRY	MSWRY**A**CTRY
45	SSAFFLRYF	S**A**AFFLRYF

***Table E1**: Peptides included in pool 3 compared their homologous sequences encoded by VR-2332. Single amino acid polymorphisms are highlighted with bold and underscore.*

Expansion of PBMCs

Thawed PBMCs isolated from pigs 440 and 442 from all sample dates were expanded in wells of a 96-well cell culture plate in the presence of IL-2, peptide pools and/and not IL-18 according to table E2.

	- IL-18	+ IL-18
Pool 1	well 1	well 5
Pool 2	well 2	well 6
Pool 3	well 3	well 7
No peptide	well 4	well 8

***Table E2**: Generalized setup used for expanding PBMC isolated at different 7 days from the two pigs, 440 and 442.*

Each well contained 4E5 PBMCs suspended in 250 µl RPMI-1640\10% FBS containing the final concentrations of 100 nM peptide (partial concentration if included), 50 U/ml IL-2 and 50 ng/ml IL-18, if included. Cells were left to expand for six days at 37 °C, 5% CO_2, medium changed at day 3. Following this, they were put on ice for 15 minutes to detach, collected, washed and counted before being subjected to analysis with ELISPOT.

IFN-γ ELISPOT setup

96-well MultiScreen IP filter plates (Millipore, MSIPS4510) were pre-treated with 25 µl 35% ethanol for no more than 60 seconds before being washed three times in phosphate buffered saline (PBS) and coated with 250 ng/well mouse anti-porcine IFN-γ monoclonal antibody (P2F6, ThermoFisher) in PBS at 4 ˚C overnight. Plates were washed three times in PBS and blocked with RPMI-1640 (11875093, ThermoFisher) at 37 ˚C, 5% CO_2 for at least 1 hour, after which cells and stimuli were seeded. Following 1 day of incubation at 37 ˚C, 5% CO_2, the plates were emptied and the cells were lysed by two times washing with MilliQ, then three times with washing buffer (PBS\0.01% Tween 20). Plates were incubated with 100 ng/well biotinylated mouse anti-porcine IFN-γ antibody (P2C11, BD Biosciences) in reaction buffer (PBS\0.01% Tween 20\0.1% bovine serum albumin) on a shaker at room temperature (RT) for 1 hour. The plates were washed four times and incubated with 50 mU/well streptavidin-AP-conjugate (11089161001, Sigma-Aldrich) in reaction buffer on a shaker at RT for 1 hour. Plates were washed three times with washing buffer followed by two times with PBS. Spots were developed in the dark at RT for 5 min using 100 µl/well BCIP/NBT Liquid Substrate System (B1911, Sigma-Aldrich), and the development was stopped under running tab water while the underdrain was removed. After having dried in the dark, the spots were counted on an AID iSpot Reader Spectrum (Autoimmun diagnostika GmbH) with the counting parameters size > 60, intensity > 10, gradient > 0.

Both expanded and freshly thawed PBMCs were subjected to analysis. For the expanded PBMCs, these were restimulated with their respective peptide pools used during expansion at final partial concentrations of 5 uM. 50 ng/ml IL-18 was included for the cells that had expanded in the presence of IL-18. Freshly thawed cells were also restimulated with the respective peptide pools and/and not IL-18 using the same concentrations as with the expanded cells. Samples restimulated with peptides were performed in triplicates and unstimulated samples were performed in duplicates. A single well for each isolation date/pig was stimulated with 1 µg/ml staphylococcal enterotoxin B (SEB) as a positive control for cell viability. All wells contained 1E5 suspended in 200 µl RPMI-1640\10% FBS.

RESULTS

SLA typing

Based on the preliminary low resolution SLA typing, amplicons for high resolution SLA typing of SLA-1*04, SLA-2*04 and SLA-3*04 were generated from five of the six pigs (438, 440-443). In addition, amplicons for SLA-1*07 were generated from pigs 438 and 441. No amplicons were made from pig 439. Sequencing and analysis was performed as described in section 2.4.1. The results are presented in table E3.

SLAs	Pigs					
	438	439	440	441	442	443
SLA-1*0401	●		●	●	●	●
SLA-1*0702	●			●		
SLA-2*0401	●		●	●	●	●
SLA-3*0401	●		●	●	●	●

***Table E3**: Results from the SLA genotyping of the six pigs with respect to the four SLAs.● indicates a match.*

ELISPOT data

The ELISPOT data is summarized in the figure E1.

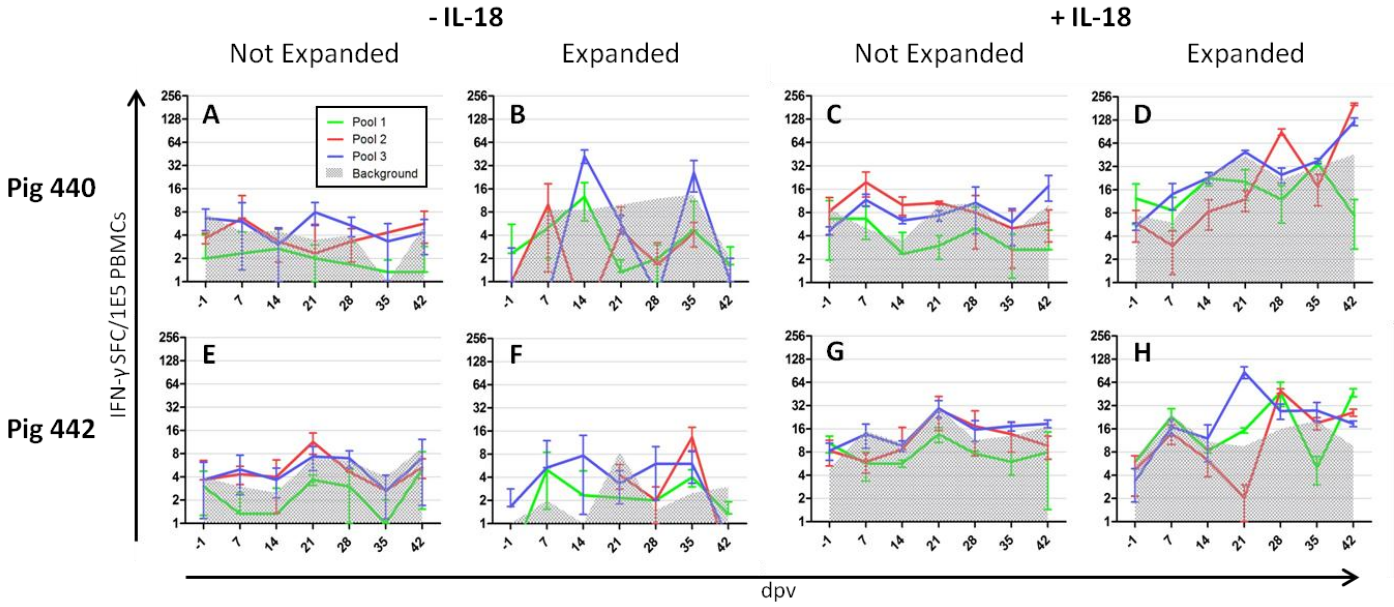

***Figure E1**: ELISPOT results. X-axis represents the isolation date of PBMCs, Y-axis represents the number of IFN-γ spot forming cells (SFC) per 1E5 PBMCs presented in Log2. The curves represent the average spot counts for the respective peptide pools, and the gray area represents the background. Error bars represent the standard deviation based on triplicate measurements. Pig and treatment of cells with respect to expansion and IL-18 are indicated in rows and columns, respectively.*

DISCUSSION AND CONCLUSIONS

For both pigs, the general spot counts were relatively low for the unexpanded PBMCs without IL-18 stimulation (graphs A and D). I would estimate this to be below the limit of detection. Expansion of these cells not treated with IL-18 (graphs B and F), results in more irregular signals, especially for pig 440 (graph B), in which pool 3 exhibits some dramatic changes across dates. One explanation for this could be that the expansion of PBMCs in the presence of peptides, by chance have nurtured and expanded T cells cognate for peptides in the pool that are so infrequent that only few vials contain them. In that case, they are less likely to be caused by the vaccine, but more likely to be the result of T-cell receptor promiscuity. For pig 442 the expansion of PBMCs without IL-18 did not result in any noticeable changes, although the background was slightly lower. The addition of IL-18 (graphs C and G) to unexpanded cells adds a little more spots than without IL-18, which is also expected since IL-18 is a general inducer of IFN-γ. This also affects the background, especially for pig 442 (graph G). For pig 440, PBMCs stimulated with pools 2 and 3 reach above the background at dpv 7 and 14, while this is only the case for pool 3 at later dates. The cells expanded in the presence of IL-18 (graphs D and H) exhibit the strongest response. Both pigs respond in a way that on average increases with dpi, thus indicating an effect of the vaccination. Also several data points are much higher than the background, suggesting non-artifact differences.

Originally, pool 3 was included as a negative control, assuming that the vaccination would not induce a response against these peptides. In retrospect, this was not thought through since the single amino acid differences between the included peptides and the homologue sequences encoded by the vaccine strain may not have had a big impact on SLA binding and or T-cell receptor recognition (Mokhtar et al. 2016). Hence, it could be speculated that CTLs primed by the vaccine were able to recognize the peptides of this pool, which would explain the relatively strong signals. A correctly composed peptide pool for negative control should instead have contained completely unrelated peptides.

In summary, the lack of a proper negative control pool prevented the conclusion of whether or not peptides recognized by vaccine-primed CTLs were contained in the tested pools. The expansion and treatment with IL-18 showed promising results that should be investigated in more details. Such future analyses should not only include a better negative control, but should also examine the effects of expansion without the presence of peptides that may skew the relative composition of T cells in favor of peptide-specific cells. Identifying peptide responses in such a setup would provide strong indications of the presence of immunodominant epitopes. Additionally, restimulations with single peptides should be performed.

REFERENCES

Ahmed R, Butler LD, Bhatti L (1988) T4+ T helper cell function in vivo: differential requirement for induction of antiviral cytotoxic T-cell and antibody responses. J Virol 62:2102–6.

Allan GM, McNeilly F, Kennedy S, et al (2000) Immunostimulation, PCV-2 and PMWS. Vet Rec 147:170–1.

Allende R, Laegreid WW, Kutish GF, et al (2000) Porcine Reproductive and Respiratory Syndrome Virus: Description of Persistence in Individual Pigs upon Experimental Infection. J Virol 74:10834–10837. doi: 10.1128/JVI.74.22.10834-10837.2000

Allende R, Lewis TL, Lu Z, et al (1999) North American and European porcine reproductive and respiratory syndrome viruses differ in non-structural protein coding regions. J Gen Virol 80 (Pt 2):307–15.

An T, Zhou Y, Liu G, et al (2007) Genetic diversity and phylogenetic analysis of glycoprotein 5 of PRRSV isolates in mainland China from 1996 to 2006: coexistence of two NA-subgenotypes with great diversity. Vet Microbiol 123:43–52. doi: 10.1016/j.vetmic.2007.02.025

Ansari IH, Kwon B, Osorio FA, Pattnaik AK (2006) Influence of N-linked glycosylation of porcine reproductive and respiratory syndrome virus GP5 on virus infectivity, antigenicity, and ability to induce neutralizing antibodies. J Virol 80:3994–4004. doi: 10.1128/JVI.80.8.3994-4004.2006

Assarsson E, Sidney J, Oseroff C, et al (2007) A quantitative analysis of the variables affecting the repertoire of T cell specificities recognized after vaccinia virus infection. J Immunol 178:7890–901.

Barber LD, Parham P (1994) The essence of epitopes. J Exp Med 180:1191–4.

Barthold SW, Bowen RA, Hedrick RP, et al (2011) Virus Replication. In: MacLachlan NJ, Dubovi EJ (eds) Fenner's Veterinary Virology, 4th edn. Elsevier Inc., London, pp 21–42

Bauhofer O, Summerfield A, McCullough KC, Ruggli N (2005) Role of double-stranded RNA and Npro of classical swine fever virus in the activation of monocyte-derived dendritic cells. Virology 343:93–105. doi: 10.1016/j.virol.2005.08.016

Bauhofer O, Summerfield A, Sakoda Y, et al (2007) Classical Swine Fever Virus Npro Interacts with Interferon Regulatory Factor 3 and Induces Its Proteasomal Degradation. J Virol 81:3087–3096. doi: 10.1128/JVI.02032-06

Bautista E, Molitor T (1997) Cell-mediated immunity to porcine reproductive and respiratory syndrome virus in swine. Viral Immunol 10:83–94.

Bautista EM, Goyal SM, Yoon IJ, et al (1993) Comparison of porcine alveolar macrophages and CL 2621 for the detection of porcine reproductive and respiratory syndrome (PRRS) virus and anti-PRRS antibody. J Vet Diagn Invest 5:163–5.

Beauvillain C, Delneste Y, Scotet M, et al (2007) Neutrophils efficiently cross-prime naive T cells in vivo. Blood 110:2965–73. doi: 10.1182/blood-2006-12-063826

Beilage E, Nathues H, Meemken D, et al (2009) Frequency of PRRS live vaccine virus (European and North American genotype) in vaccinated and non-vaccinated pigs submitted for respiratory tract diagnostics in North-Western Germany. Prev.Vet.Med. 92:31–37.

Belsham G, Nielsen I, Normann P, et al (2008) Monocistronic mRNAs containing defective hepatitis C virus-like picornavirus internal ribosome entry site elements in their 5' untranslated regions are efficiently translated in cells by a cap-dependent mechanism. RNA 14:1671–80.

Benfield DA, Nelson E, Collins JE, et al (1992) Characterization of swine infertility and respiratory syndrome (SIRS) virus (isolate ATCC VR-2332). J Vet Diagn Invest 4:127–33.

Bentzen AK, Marquard AM, Lyngaa R, et al (2016) Large-scale detection of antigen-specific T cells using peptide-

MHC-I multimers labeled with DNA barcodes. Nat Biotechnol 34:1037–1045. doi: 10.1038/nbt.3662

Bergtold A, Desai DD, Gavhane A, Clynes R (2005) Cell surface recycling of internalized antigen permits dendritic cell priming of B cells. Immunity 23:503–14. doi: 10.1016/j.immuni.2005.09.013

Beura LK, Sarkar SN, Kwon B, et al (2010) Porcine reproductive and respiratory syndrome virus nonstructural protein 1beta modulates host innate immune response by antagonizing IRF3 activation. J Virol 84:1574–84. doi: 10.1128/JVI.01326-09

Bhati M, Cole DK, McCluskey J, et al (2014) The versatility of the αβ T-cell antigen receptor. Protein Sci 23:260–72. doi: 10.1002/pro.2412

Binjawadagi B, Dwivedi V, Manickam C, et al (2014a) Adjuvanted poly(lactic-co-glycolic) acid nanoparticle-entrapped inactivated porcine reproductive and respiratory syndrome virus vaccine elicits cross-protective immune response in pigs. Int J Nanomedicine 9:679–94. doi: 10.2147/IJN.S56127

Binjawadagi B, Dwivedi V, Manickam C, et al (2014b) An innovative approach to induce cross-protective immunity against porcine reproductive and respiratory syndrome virus in the lungs of pigs through adjuvanted nanotechnology-based vaccination. Int J Nanomedicine 9:1519–35. doi: 10.2147/IJN.S59924

Bogdan C (2001) Nitric oxide and the immune response. Nat Immunol 2:907–916. doi: 10.1038/ni1001-907

Bonneville M, O'Brien RL, Born WK (2010) γδ T cell effector functions: a blend of innate programming and acquired plasticity. Nat Rev Immunol 10:467–478. doi: 10.1038/nri2781

Botner A, Strandbygaard B, Sorensen KJ, et al (1997) Appearance of acute PRRS-like symptoms in sow herds after vaccination with a modified live PRRS vaccine. Vet.Rec. 141:497–499.

Bourgeois C, Rocha B, Tanchot C (2002) A Role for CD40 Expression on CD8+ T Cells in the Generation of CD8+ T Cell Memory. Science (80-) 297:2060–2063. doi: 10.1126/science.1072615

Britten CM, Gouttefangeas C, Welters MJP, et al (2008) The CIMT-monitoring panel: a two-step approach to harmonize the enumeration of antigen-specific CD8+ T lymphocytes by structural and functional assays. Cancer Immunol Immunother 57:289–302. doi: 10.1007/s00262-007-0378-0

Brockmeier SL, Halbur PG, Thacker EL (2002) Porcine Respiratory Disease Complex. In: Brogden K, Guthmiller J (eds) Polymicrobial Diseases. ASM Press, Washington (DC),

Brockmeier SL, Palmer M V, Bolin SR (2000) Effects of intranasal inoculation of porcine reproductive and respiratory syndrome virus, Bordetella bronchiseptica, or a combination of both organisms in pigs. Am J Vet Res 61:892–9.

Buller RML, Holmes KL, Hügin A, et al (1987) Induction of cytotoxic T-cell responses in vivo in the absence of CD4 helper cells. Nature 328:77–79. doi: 10.1038/328077a0

Butz EA, Bevan MJ (1998) Massive expansion of antigen-specific CD8+ T cells during an acute virus infection. Immunity 8:167–75.

Bøtner A, Nielsen J, Bille-Hansen V (1994) Isolation of porcine reproductive and respiratory syndrome (PRRS) virus in a Danish swine herd and experimental infection of pregnant gilts with the virus. Vet Microbiol 40:351–60.

Calis JJA, Maybeno M, Greenbaum JA, et al (2013) Properties of MHC class I presented peptides that enhance immunogenicity. PLoS Comput Biol 9:e1003266. doi: 10.1371/journal.pcbi.1003266

Cano JP, Dee SA, Murtaugh MP, et al (2007) Effect of vaccination with a modified-live porcine reproductive and respiratory syndrome virus vaccine on dynamics of homologous viral infection in pigs. Am J Vet Res 68:565–71. doi: 10.2460/ajvr.68.5.565

Cao J, Grauwet K, Vermeulen B, et al (2013) Suppression of NK cell-mediated cytotoxicity against PRRSV-infected porcine alveolar macrophages in vitro. Vet Microbiol 164:261–9. doi: 10.1016/j.vetmic.2013.03.001

Carding SR, Egan PJ (2002) γδ T CELLS: FUNCTIONAL PLASTICITY AND HETEROGENEITY. Nat Rev Immunol 2:336–345. doi: 10.1038/nri797

Cardozo C, Kohanski RA (1998) Altered properties of the branched chain amino acid-preferring activity contribute to increased cleavages after branched chain residues by the "immunoproteasome". J Biol Chem 273:16764–70.

Carrasco CP, Rigden RC, Vincent IE, et al (2004) Interaction of classical swine fever virus with dendritic cells. J Gen Virol 85:1633–1641. doi: 10.1099/vir.0.19716-0

Cecere TE, Todd SM, LeRoith T (2012) Regulatory T Cells in Arterivirus and Coronavirus Infections: Do They Protect Against Disease or Enhance it? Viruses 4:833–846. doi: 10.3390/v4050833

Cha S-H, Choi E-J, Park J-H, et al (2006) Molecular characterization of recent Korean porcine reproductive and respiratory syndrome (PRRS) viruses and comparison to other Asian PRRS viruses. Vet Microbiol 117:248–57. doi: 10.1016/j.vetmic.2006.05.007

Chand RJ, Trible BR, Rowland RR (2012) Pathogenesis of porcine reproductive and respiratory syndrome virus. Curr Opin Virol 2:256–263. doi: 10.1016/j.coviro.2012.02.002

Chang H-C, Peng Y-T, Chang H-L, et al (2008) Phenotypic and functional modulation of bone marrow-derived dendritic cells by porcine reproductive and respiratory syndrome virus. Vet Microbiol 129:281–93. doi: 10.1016/j.vetmic.2007.12.002

Chapiro J, Claverol S, Piette F, et al (2006) Destructive cleavage of antigenic peptides either by the immunoproteasome or by the standard proteasome results in differential antigen presentation. J Immunol 176:1053–61.

Chappell P, Meziane EK, Harrison M, et al (2015) Expression levels of mhc class i molecules are inversely correlated with promiscuity of peptide binding. Elife 2015:1–22. doi: 10.7554/eLife.05345

Charerntantanakul W, Platt R, Roth JA (2006) Effects of Porcine Reproductive and Respiratory Syndrome Virus-Infected Antigen-Presenting Cells on T Cell Activation and Antiviral Cytokine Production. Viral Immunol 19:646–661. doi: 10.1089/vim.2006.19.646

Charley B, Laverne S, Lavenant L (1990) Recombinant porcine interferon-gamma activates in vitro porcine adherent mononuclear cells to produce interleukin 1. Vet Immunol Immunopathol 25:117–124. doi: 10.1016/0165-2427(90)90029-R

Chen C, Li J, Bi Y, et al (2013) Synthetic B- and T-cell epitope peptides of porcine reproductive and respiratory syndrome virus with Gp96 as adjuvant induced humoral and cell-mediated immunity. Vaccine 31:1838–47. doi: 10.1016/j.vaccine.2013.01.049

Chen J, Liu T, Zhu C-G, et al (2006) Genetic Variation of Chinese PRRSV Strains Based on ORF5 Sequence. Biochem Genet 44:421–431. doi: 10.1007/s10528-006-9039-9

Chen Z, Lawson S, Sun Z, et al (2010) Identification of two auto-cleavage products of nonstructural protein 1 (nsp1) in porcine reproductive and respiratory syndrome virus infected cells: nsp1 function as interferon antagonist. Virology 398:87–97. doi: 10.1016/j.virol.2009.11.033

Chen Z, Li M, He Q, et al (2014) The amino acid at residue 155 in nonstructural protein 4 of porcine reproductive and respiratory syndrome virus contributes to its inhibitory effect for interferon-β transcription in vitro. Virus Res 189:226–234. doi: 10.1016/j.virusres.2014.05.027

Choi K, Park C, Jeong J, et al (2016) Comparison of commercial type 1 and type 2 PRRSV vaccines against heterologous dual challenge. Vet Rec 178:291. doi: 10.1136/vr.103529

Correia D V., Fogli M, Hudspeth K, et al (2011) Differentiation of human peripheral blood Vδ1+ T cells expressing the natural cytotoxicity receptor NKp30 for recognition of lymphoid leukemia cells.

Costers S, Lefebvre DJ, Delputte PL, Nauwynck HJ (2008) Porcine reproductive and respiratory syndrome virus modulates apoptosis during replication in alveolar macrophages. Arch Virol 153:1453–1465. doi: 10.1007/s00705-008-0135-5

Costers S, Lefebvre DJ, Goddeeris B, et al (2009) Functional impairment of PRRSV-specific peripheral CD3+CD8high cells. Vet Res 40:46. doi: 10.1051/vetres/2009029

Cox JH, Ferrari G, Kalams SA, et al (2005) Results of an ELISPOT proficiency panel conducted in 11 laboratories participating in international human immunodeficiency virus type 1 vaccine trials. AIDS Res Hum Retroviruses 21:68–81. doi: 10.1089/aid.2005.21.68

Crowther JR (2000) ELISA Guidebook, The. Humana Press, New Jersey

Dalchau N, Phillips A, Goldstein LD, et al (2011) A peptide filtering relation quantifies MHC class I peptide optimization. PLoS Comput Biol 7:e1002144. doi: 10.1371/journal.pcbi.1002144

Dalton DK, Pitts-Meek S, Keshav S, et al (1993) Multiple defects of immune cell function in mice with disrupted interferon-gamma genes. Science 259:1739–42.

Das PB, Dinh PX, Ansari IH, et al (2010) The minor envelope glycoproteins GP2a and GP4 of porcine reproductive and respiratory syndrome virus interact with the receptor CD163. J Virol 84:1731–40. doi: 10.1128/JVI.01774-09

de Saint Basile G, Ménasché G, Fischer A (2010) Molecular mechanisms of biogenesis and exocytosis of cytotoxic granules. Nat Rev Immunol 10:568–579. doi: 10.1038/nri2803

Dee S (2003) Principles of Prevention, Control, and Eradication. In: Zimmerman J, Yoon K-J, Neumann E (eds) 2003 PRRS Compendium Producers Edition: A Reference for Pork Producers. National Pork Board, pp 78–87

Dee S, Deen J, Rossow K, et al (2003) Mechanical transmission of porcine reproductive and respiratory syndrome virus throughout a coordinated sequence of events during warm weather. Can J Vet Res 67:12–9.

Dee S, Deen J, Rossow K, et al (2002) Mechanical transmission of porcine reproductive and respiratory syndrome virus throughout a coordinated sequence of events during cold weather. Can J Vet Res 66:232–9.

Dee S, Joo HS, Pijoan C (1995) Controlling the spread of PRRS virus in the breeding herd through management of the gilt pool.

Dee S, Otake S, Deen J (2010) Use of a production region model to assess the efficacy of various air filtration systems for preventing airborne transmission of porcine reproductive and respiratory syndrome virus and Mycoplasma hyopneumoniae: results from a 2-year study. Virus Res 154:177–84. doi: 10.1016/j.virusres.2010.07.022

Dee S, Otake S, Oliveira S, Deen J (2009) Evidence of long distance airborne transport of porcine reproductive and respiratory syndrome virus and *Mycoplasma hyopneumoniae*. Vet Res 40:39. doi: 10.1051/vetres/2009022

Dee SA, Deen J, Otake S, Pijoan C (2004) An experimental model to evaluate the role of transport vehicles as a source of transmission of porcine reproductive and respiratory syndrome virus to susceptible pigs. Can J Vet Res 68:128–33.

Delputte PL, Costers S, Nauwynck HJ (2005) Analysis of porcine reproductive and respiratory syndrome virus attachment and internalization: Distinctive roles for heparan sulphate and sialoadhesin. J Gen Virol 86:1441–1445. doi: 10.1099/vir.0.80675-0

Delputte PL, Vanderheijden N, Nauwynck HJ, Pensaert MB (2002) Involvement of the matrix protein in attachment of porcine reproductive and respiratory syndrome virus to a heparinlike receptor on porcine alveolar macrophages. J Virol 76:4312–20. doi: 10.1128/jvi.76.9.4312-4320.2002

Denyer MS, Wileman TE, Stirling CMA, et al (2006) Perforin expression can define CD8 positive lymphocyte subsets in pigs allowing phenotypic and functional analysis of Natural Killer, Cytotoxic T, Natural Killer T and MHC un-restricted cytotoxic T-cells. Vet Immunol Immunopathol 110:279–292. doi: 10.1016/j.vetimm.2005.10.005

Doherty PC (1998) The numbers game for virus-specific CD8+ T cells. Science 280:227.

Dubois B, Caux C (2005) Critical role of ITIM-bearing FcgammaR on DCs in the capture and presentation of native antigen to B cells. Immunity 23:463–4. doi: 10.1016/j.immuni.2005.10.005

Dustin ML, Cooper J a (2000) The immunological synapse and the actin cytoskeleton: molecular hardware for T cell signaling. Nat Immunol 1:23–29. doi: 10.1038/76877

Dwivedi V, Manickam C, Binjawadagi B, et al (2012) Evaluation of immune responses to porcine reproductive and respiratory syndrome virus in pigs during early stage of infection under farm conditions. Virol J 9:45. doi: 10.1186/1743-422X-9-45

Eisen HN, Sykulev Y, Tsomides TJ (1996) Antigen-specific T-cell receptors and their reactions with complexes formed by peptides with major histocompatibility complex proteins. Adv Protein Chem 49:1–56.

Ewer KJ, O'Hara GA, Duncan CJA, et al (2013) Protective CD8+ T-cell immunity to human malaria induced by chimpanzee adenovirus-MVA immunisation. Nat Commun 4:2836. doi: 10.1038/ncomms3836

Fairbairn L, Kapetanovic R, Sester DP, Hume DA (2011) The mononuclear phagocyte system of the pig as a model for understanding human innate immunity and disease. J Leukoc Biol 89:855–71. doi: 10.1189/jlb.1110607

Fairchild PJ, Wraith DC (1996) Lowering the tone: mechanisms of immunodominance among epitopes with low affinity for MHC. Immunol Today 17:80–85.

Fan B, Liu X, Bai J, et al (2015) The amino acid residues at 102 and 104 in GP5 of porcine reproductive and respiratory syndrome virus regulate viral neutralization susceptibility to the porcine serum neutralizing antibody. Virus Res 204:21–30. doi: 10.1016/j.virusres.2015.04.015

Fang Y, Snijder EJ (2010) The PRRSV replicase: exploring the multifunctionality of an intriguing set of nonstructural proteins. Virus Res 154:61–76. doi: 10.1016/j.virusres.2010.07.030

Fang Y, Treffers EE, Li Y, et al (2012) Efficient -2 frameshifting by mammalian ribosomes to synthesize an additional arterivirus protein. Proc Natl Acad Sci U S A 109:E2920-8. doi: 10.1073/pnas.1211145109

Feng W, Tompkins MB, Xu J-S, et al (2002) Thymocyte and Peripheral Blood T Lymphocyte Subpopulation Changes in Piglets Following in Utero Infection with Porcine Reproductive and Respiratory Syndrome Virus. Virology 302:363–372. doi: 10.1006/viro.2002.1650

Flores-Mendoza L, Silva-Campa E, Reséndiz M, et al (2008) Porcine reproductive and respiratory syndrome virus infects mature porcine dendritic cells and up-regulates interleukin-10 production. Clin Vaccine Immunol 15:720–5. doi: 10.1128/CVI.00224-07

Forsberg R (2005) Divergence time of porcine reproductive and respiratory syndrome virus subtypes. Mol Biol Evol 22:2131–4. doi: 10.1093/molbev/msi208

Forsberg R, Oleksiewicz MB, Petersen a M, et al (2001) A molecular clock dates the common ancestor of European-type porcine reproductive and respiratory syndrome virus at more than 10 years before the emergence of disease. Virology 289:174–9. doi: 10.1006/viro.2001.1102

Frahm N, Kiepiela P, Adams S, et al (2006) Control of human immunodeficiency virus replication by cytotoxic T lymphocytes targeting subdominant epitopes. Nat Immunol 7:173–8. doi: 10.1038/ni1281

Fremont DH, Matsumura M, Stura EA, et al (1992) Crystal structures of two viral peptides in complex with murine MHC class I H-2Kb. Science 257:919–27.

Frey CF, Bauhofer O, Ruggli N, et al (2006) Classical swine fever virus replicon particles lacking the Erns gene: a potential marker vaccine for intradermal application. Vet Res 37:655–70. doi: 10.1051/vetres:2006028

Frossard JP, Hughes GJ, Westcott DG, et al (2012) Porcine reproductive and respiratory syndrome virus: genetic

diversity of recent British isolates. Vet.Microbiol. 162:507–518.

Fuerst TR, Niles EG, Studier FW, Moss B (1986) Eukaryotic transient expression system based on recombinant vaccinia virus that synthesizes bacteriophage T7 RNA polymerase. ProcNatlAcadSci 83:8122–8126.

Fulwyler MJ (1965) Electronic Separation of Biological Cells by Volume.

Geissmann F, Gordon S, Hume DA, et al (2010) Unravelling mononuclear phagocyte heterogeneity. Nat Rev Immunol 10:453–460. doi: 10.1038/nri2784

Genini S, Delputte PL, Malinverni R, et al (2008) Genome-wide transcriptional response of primary alveolar macrophages following infection with porcine reproductive and respiratory syndrome virus. J Gen Virol 89:2550–2564. doi: 10.1099/vir.0.2008/003244-0

Gerner W, Käser T, Saalmüller A (2009) Porcine T lymphocytes and NK cells - An update. Dev Comp Immunol 33:310–320. doi: 10.1016/j.dci.2008.06.003

Goldszmid RS, Trinchieri G (2012) The price of immunity. Nat Immunol 13:932–938. doi: 10.1038/ni.2422

Gordon S, Brown G, Gordon S, et al (2002) Pattern recognition receptors: doubling up for the innate immune response. Cell 111:927–30. doi: 10.1016/S0092-8674(02)01201-1

Gordon S, Martinez FO, Agapov E, et al (2010) Alternative activation of macrophages: mechanism and functions. Immunity 32:593–604. doi: 10.1016/j.immuni.2010.05.007

Grakoui A, Bromley SK, Sumen C, et al (1999) The immunological synapse: a molecular machine controlling T cell activation. Science 285:221–7.

Greiser-Wilke I, Fiebig K, Drexler C, grosse Beilage E (2010) Genetic diversity of Porcine reproductive and respiratory syndrome virus (PRRSV) in selected herds in a pig-dense region of North-Western Germany. Vet Microbiol 143:213–23. doi: 10.1016/j.vetmic.2009.12.006

Guillaume B, Chapiro J, Stroobant V, et al (2010) Two abundant proteasome subtypes that uniquely process some antigens presented by HLA class I molecules. Proc Natl Acad Sci 107:18599–18604. doi: 10.1073/pnas.1009778107

Guo R, Katz BB, Tomich JM, et al (2016) Porcine reproductive and respiratory syndrome virus utilizes nanotubes for intercellular spread. J Virol 90:5163–5175. doi: 10.1128/JVI.00036-16

Halstead SB, Mahalingam S, Marovich MA, et al (2010) Intrinsic antibody-dependent enhancement of microbial infection in macrophages: disease regulation by immune complexes. Lancet Infect Dis 10:712–22. doi: 10.1016/S1473-3099(10)70166-3

Hamerman JA, Ogasawara K, Lanier LL (2005) NK cells in innate immunity. Curr Opin Immunol 17:29–35. doi: 10.1016/j.coi.2004.11.001

Han J, Rutherford MS, Faaberg KS (2010) Proteolytic products of the porcine reproductive and respiratory syndrome virus nsp2 replicase protein. J Virol 84:10102–12. doi: 10.1128/JVI.01208-10

Han J, Wang Y, Faaberg KS (2006) Complete genome analysis of RFLP 184 isolates of porcine reproductive and respiratory syndrome virus. Virus Res 122:175–82. doi: 10.1016/j.virusres.2006.06.003

Hanada K, Suzuki Y, Nakane T, et al (2005) The Origin and Evolution of Porcine Reproductive and Respiratory Syndrome Viruses. Mol Biol Evol 22:1024–1031. doi: 10.1093/molbev/msi089

Harndahl M, Justesen S, Lamberth K, et al (2009) Peptide binding to HLA class I molecules: homogenous, high-throughput screening, and affinity assays. J Biomol Screen 14:173–80. doi: 10.1177/1087057108329453

Harndahl M, Rasmussen M, Roder G, et al (2012) Peptide-MHC class I stability is a better predictor than peptide affinity of CTL immunogenicity. Eur J Immunol 42:1405–16. doi: 10.1002/eji.201141774

Harndahl M, Rasmussen M, Roder G, Buus S (2011) Real-time, high-throughput measurements of peptide-MHC-I dissociation using a scintillation proximity assay. J Immunol Methods 374:5–12. doi: 10.1016/j.jim.2010.10.012

Heink S, Ludwig D, Kloetzel P-M, Krüger E (2005) IFN-gamma-induced immune adaptation of the proteasome system is an accelerated and transient response. Proc Natl Acad Sci U S A 102:9241–6. doi: 10.1073/pnas.0501711102

Ho C-S, Lunney JK, Franzo-Romain MH, et al (2009) Molecular characterization of swine leucocyte antigen class I genes in outbred pig populations. Anim Genet 40:468–478. doi: 10.1111/j.1365-2052.2009.01860.x

Ho C-S, Rochelle ES, Martens GW, et al (2006) Characterization of swine leukocyte antigen polymorphism by sequence-based and PCR-SSP methods in Meishan pigs. Immunogenetics 58:873–882. doi: 10.1007/s00251-006-0145-y

Holtkamp DJ, Kliebenstein JB, Neumann EJ, et al (2013) Assessment of the economic impact of porcine reproductive and respiratory syndrome virus on United States pork producers. J Swine Heal Prod 21:72–84.

Holtkamp DJ, Morrison B, Classen DM, et al (2011) Terminology for Classifying Swine Herds by PRRS Status. J Swine Heal Prod 19:44–56.

Honda K, Yanai H, Negishi H, et al (2005) IRF-7 is the master regulator of type-I interferon-dependent immune responses. Nature 434:772–777. doi: 10.1038/nature03464

Hoof I, Peters B, Sidney J, et al (2009) NetMHCpan, a method for MHC class I binding prediction beyond humans. Immunogenetics 61:1–13. doi: 10.1007/s00251-008-0341-z

Hou J, Wang L, He W, et al (2012a) Highly pathogenic porcine reproductive and respiratory syndrome virus impairs LPS- and poly(I:C)-stimulated tumor necrosis factor-alpha release by inhibiting ERK signaling pathway.

Hou J, Wang L, Quan R, et al (2012b) Induction of interleukin-10 is dependent on p38 mitogen-activated protein kinase pathway in macrophages infected with porcine reproductive and respiratory syndrome virus. Virol J 9:165. doi: 10.1186/1743-422X-9-165

Howarth M, Williams A, Tolstrup AB, Elliott T (2004) Tapasin enhances MHC class I peptide presentation according to peptide half-life. Proc Natl Acad Sci U S A 101:11737–42. doi: 10.1073/pnas.0306294101

Huang C, Zhang Q, Guo X, et al (2014) Porcine reproductive and respiratory syndrome virus nonstructural protein 4 antagonizes beta interferon expression by targeting the NF-κB essential modulator. J Virol 88:10934–45. doi: 10.1128/JVI.01396-14

Huo Y, Fan L, Yin S, et al (2013) Involvement of unfolded protein response, p53 and Akt in modulation of porcine reproductive and respiratory syndrome virus-mediated JNK activation. Virology 444:233–240. doi: 10.1016/j.virol.2013.06.015

Iwasaki A, Medzhitov R (2004) Toll-like receptor control of the adaptive immune responses. Nat Immunol 5:987–995. doi: 10.1038/ni1112

Janetzki S, Britten CM (2012) The impact of harmonization on ELISPOT assay performance. Methods Mol Biol 792:25–36. doi: 10.1007/978-1-61779-325-7_2

Janetzki S, Panageas KS, Ben-Porat L, et al (2008) Results and harmonization guidelines from two large-scale international Elispot proficiency panels conducted by the Cancer Vaccine Consortium (CVC/SVI). Cancer Immunol Immunother 57:303–15. doi: 10.1007/s00262-007-0380-6

Janetzki S, Price L, Schroeder H, et al (2015) Guidelines for the automated evaluation of Elispot assays. Nat Protoc 10:1098–1115. doi: 10.1038/nprot.2015.068

Janssen EM, Lemmens EE, Wolfe T, et al (2003) CD4+ T cells are required for secondary expansion and memory in CD8+ T lymphocytes. Nature 421:852–856. doi: 10.1038/nature01441

Jiang W, Jiang P, Wang X, et al (2007) Influence of porcine reproductive and respiratory syndrome virus GP5 glycoprotein N-linked glycans on immune responses in mice. Virus Genes 35:663–71. doi: 10.1007/s11262-007-0131-y

Jiang Y, Xia T, Zhou Y, et al (2015) Characterization of three porcine reproductive and respiratory syndrome virus isolates from a single swine farm bearing strong homology to a vaccine strain. Vet Microbiol 179:242–249. doi: 10.1016/j.vetmic.2015.06.015

Johnson CR, Griggs TF, Gnanandarajah J, Murtaugh MP (2011) Novel structural protein in porcine reproductive and respiratory syndrome virus encoded by an alternative ORF5 present in all arteriviruses. J Gen Virol 92:1107–16. doi: 10.1099/vir.0.030213-0

Kaech SM, Wherry EJ, Ahmed R (2002) Effector and memory T-cell differentiation: implications for vaccine development. Nat Rev Immunol 2:251–62. doi: 10.1038/nri778

Kaech SM, Ahmed R (2001) Memory CD8+ T cell differentiation: initial antigen encounter triggers a developmental program in naïve cells. Nat Immunol 2:415–422. doi: 10.1016/j.pestbp.2011.02.012.Investigations

Kalergis AM, Boucheron N, Doucey M-A, et al (2001) Efficient T cell activation requires an optimal dwell-time of interaction between the TCR and the pMHC complex. Nat Immunol 2:229–234. doi: 10.1038/85286

Kappes MA, Faaberg KS (2015) PRRSV structure, replication and recombination: Origin of phenotype and genotype diversity. Virology 479–480:475–86. doi: 10.1016/j.virol.2015.02.012

Kappes MA, Miller CL, Faaberg KS (2015) Porcine reproductive and respiratory syndrome virus nonstructural protein 2 (nsp2) topology and selective isoform integration in artificial membranes. Virology 481:51–62. doi: 10.1016/j.virol.2015.01.028

Kappes MA, Miller CL, Faaberg KS (2013) Highly divergent strains of porcine reproductive and respiratory syndrome virus incorporate multiple isoforms of nonstructural protein 2 into virions. J Virol 87:13456–65. doi: 10.1128/JVI.02435-13

Karniychuk UU, Geldhof M, Vanhee M, et al (2010) Pathogenesis and antigenic characterization of a new East European subtype 3 porcine reproductive and respiratory syndrome virus isolate. BMC Vet Res 6:30. doi: 10.1186/1746-6148-6-30

Karniychuk UU, Nauwynck HJ (2013) Pathogenesis and prevention of placental and transplacental porcine reproductive and respiratory syndrome virus infection. Vet Res 44:95. doi: 10.1186/1297-9716-44-95

Kast WM, Brandt RM, Sidney J, et al (1994) Role of HLA-A motifs in identification of potential CTL epitopes in human papillomavirus type 16 E6 and E7 proteins. J Immunol 152:3904–12.

Kaufman J, Völk H, Wallny HJ (1995) A "minimal essential Mhc" and an "unrecognized Mhc": two extremes in selection for polymorphism. Immunol Rev 143:63–88.

Keffaber KK (1989) Reproductive Failure of Unknown Etiology. AASP Newsl 1:1–10.

Kersh GJ, Kersh EN, Fremont DH, Allen PM (1998) High- and low-potency ligands with similar affinities for the TCR: the importance of kinetics in TCR signaling. Immunity 9:817–26.

Kim HS, Kwang J, Yoon IJ, et al (1993) Enhanced replication of porcine reproductive and respiratory syndrome (PRRS) virus in a homogeneous subpopulation of MA-104 cell line. Arch Virol 133:477–83.

Kim J-K, Fahad A-M, Shanmukhappa K, Kapil S (2006) Defining the cellular target(s) of porcine reproductive and respiratory syndrome virus blocking monoclonal antibody 7G10. J Virol 80:689–96. doi: 10.1128/JVI.80.2.689-696.2006

Kim W-I, Kim J-J, Cha S-H, et al (2013) Significance of genetic variation of PRRSV ORF5 in virus neutralization and molecular determinants corresponding to cross neutralization among PRRS viruses. Vet Microbiol 162:10–22.

doi: 10.1016/j.vetmic.2012.08.005

Klemke M, Wabnitz GH, Funke F, et al (2008) Oxidation of cofilin mediates T cell hyporesponsiveness under oxidative stress conditions. Immunity 29:404–13. doi: 10.1016/j.immuni.2008.06.016

Kovacsovics-Bankowski M, Rock KL (1995) A phagosome-to-cytosol pathway for exogenous antigens presented on MHC class I molecules. Science 267:243–6.

Kristensen C, Jensen P, Christiansen M (2014a) Udbredelse af PRRS-negative besætninger i Danmark 2013.

Kristensen CS, Lorenzen B, Bækbo P, Nymark K (2014b) PRRS manual.

Kumar V, Sharma A (2010) Neutrophils: Cinderella of innate immune system. Int Immunopharmacol 10:1325–1334. doi: 10.1016/j.intimp.2010.08.012

Kvisgaard LK, Hjulsager CK, Kristensen CS, et al (2013) Genetic and antigenic characterization of complete genomes of Type 1 Porcine Reproductive and Respiratory Syndrome viruses (PRRSV) isolated in Denmark over a period of 10 years. Virus Res 178:197–205. doi: 10.1016/j.virusres.2013.10.009

Kwong GPS, Poljak Z, Deardon R, Dewey CE (2013) Bayesian analysis of risk factors for infection with a genotype of porcine reproductive and respiratory syndrome virus in Ontario swine herds using monitoring data. Prev Vet Med 110:405–417. doi: 10.1016/j.prevetmed.2013.01.004

Kärre K, Ljunggren HG, Piontek G, Kiessling R (1986) Selective rejection of H–2-deficient lymphoma variants suggests alternative immune defence strategy. Nature 319:675–678. doi: 10.1038/319675a0

Käser T, Gerner W, Hammer SE, et al (2008) Phenotypic and functional characterisation of porcine CD4+CD25high regulatory T cells.

Käser T, Gerner W, Saalmüller A (2011) Porcine regulatory T cells: Mechanisms and T-cell targets of suppression. Dev Comp Immunol 35:1166–1172. doi: 10.1016/j.dci.2011.04.006

Käser T, Müllebner A, Hartl RT, et al (2012) Porcine T-helper and regulatory T cells exhibit versatile mRNA expression capabilities for cytokines and co-stimulatory molecules. Cytokine 60:400–409. doi: 10.1016/j.cyto.2012.07.007

Lager KM, Mengeling WL, Brockmeier SL (1997a) Homologous challenge of porcine reproductive and respiratory syndrome virus immunity in pregnant swine. Vet Microbiol 58:113–25.

Lager KMM, Mengeling WLL, Brockmeier SLL (1997b) Duration of homologous porcine reproductive and respiratory syndrome virus immunity in pregnant swine. VetMicrobiol 58:127–133. doi: 10.1016/S0378-1135(97)00159-4

Lamontagne L, Pagé C, Larochelle R, Magar R (2003) Porcine reproductive and respiratory syndrome virus persistence in blood, spleen, lymph nodes, and tonsils of experimentally infected pigs depends on the level of CD8high T cells. Viral Immunol 16:395–406. doi: 10.1089/088282403322396181

Lanier LL (2005) NK CELL RECOGNITION. Annu Rev Immunol 23:225–274. doi: 10.1146/annurev.immunol.23.021704.115526

Lanzavecchia A, Iezzi G, Viola A (1999) From TCR engagement to T cell activation: a kinetic view of T cell behavior. Cell 96:1–4.

Laouar Y, Sutterwala FS, Gorelik L, Flavell RA (2005) Transforming growth factor-β controls T helper type 1 cell development through regulation of natural killer cell interferon-γ. Nat Immunol 6:600–607. doi: 10.1038/ni1197

Lazarski CA, Chaves FA, Jenks SA, et al (2005) The kinetic stability of MHC class II:peptide complexes is a key parameter that dictates immunodominance. Immunity 23:29–40. doi: 10.1016/j.immuni.2005.05.009

Lee J, Choi K, Olin MR, et al (2004) Gammadelta T cells in immunity induced by Mycobacterium bovis bacillus Calmette-Guérin vaccination. Infect Immun 72:1504–11. doi: 10.1128/IAI.72.3.1504-1511.2004

Lei B, Abdul Hameed MDM, Hamza A, et al (2010) Molecular basis of the selectivity of the immunoproteasome catalytic subunit LMP2-specific inhibitor revealed by molecular modeling and dynamics simulations. J Phys Chem B 114:12333–9. doi: 10.1021/jp1058098

LeRoith T, Hammond S, Todd SM, et al (2011) A modified live PRRSV vaccine and the pathogenic parent strain induce regulatory T cells in pigs naturally infected with Mycoplasma hyopneumoniae.

Lim K, Hyun Y-M, Lambert-Emo K, et al (2015) Neutrophil trails guide influenza-specific $CD8^+$ T cells in the airways. Science 349:aaa4352. doi: 10.1126/science.aaa4352

Linhares DCL, Cano JP, Torremorell M, Morrison RB (2014) Comparison of time to PRRSv-stability and production losses between two exposure programs to control PRRSv in sow herds. Prev Vet Med 116:111–9. doi: 10.1016/j.prevetmed.2014.05.010

Linhares DCL, Cano JP, Wetzell T, et al (2012) Effect of modified-live porcine reproductive and respiratory syndrome virus (PRRSv) vaccine on the shedding of wild-type virus from an infected population of growing pigs. Vaccine 30:407–13. doi: 10.1016/j.vaccine.2011.10.075

Liu J, Wei S, Liu L, et al (2016) The role of porcine reproductive and respiratory syndrome virus infection in immune phenotype and Th1/Th2 balance of dendritic cells. Dev Comp Immunol 65:245–252. doi: 10.1016/j.dci.2016.07.012

Liu Y-J (2005) IPC: professional type 1 interferon-producing cells and plasmacytoid dendritic cell precursors. Annu Rev Immunol 23:275–306. doi: 10.1146/annurev.immunol.23.021704.115633

Ljunggren HG, Kärre K (1985) Host resistance directed selectively against H-2-deficient lymphoma variants. Analysis of the mechanism.

Lohse L, Nielsen J, Eriksen L (2004) Temporary CD8+ T-cell depletion in pigs does not exacerbate infection with porcine reproductive and respiratory syndrome virus (PRRSV). Viral Immunol 17:594–603. doi: 10.1089/vim.2004.17.594

Lopez OJ, Osorio FA (2004) Role of neutralizing antibodies in PRRSV protective immunity. Vet Immunol Immunopathol 102:155–63. doi: 10.1016/j.vetimm.2004.09.005

López Fuertes L, Doménech N, Alvarez B, et al (1999) Analysis of cellular immune response in pigs recovered from porcine respiratory and reproductive syndrome infection. Virus Res 64:33–42.

Loving CL, Brockmeier SL, Sacco RE (2007) Differential type I interferon activation and susceptibility of dendritic cell populations to porcine arterivirus. Immunology 120:217–29. doi: 10.1111/j.1365-2567.2006.02493.x

Ludewig B, Krebs P, Junt T, et al (2004) Determining control parameters for dendritic cell-cytotoxic T lymphocyte interaction. Eur J Immunol 34:2407–18. doi: 10.1002/eji.200425085

Lundegaard C, Karlsson A, Perez C, et al (2010) PopCover: A method for selecting of peptides with optimal Population and Pathogen Coverage. BCB ’10 Proc First ACM Int Conf Bioinforma Comput Biol 658–659.

Ma Z, Wang Y, Zhao H, et al (2013) Porcine Reproductive and Respiratory Syndrome Virus Nonstructural Protein 4 Induces Apoptosis Dependent on Its 3C-Like Serine Protease Activity. PLoS One 8:e69387. doi: 10.1371/journal.pone.0069387

MacLennan I, Vinuesa C (2002) Dendritic cells, BAFF, and APRIL: innate players in adaptive antibody responses. Immunity 17:235–8.

Madden DR, Gorga JC, Strominger JL, Wiley DC (1992) The three-dimensional structure of HLA-B27 at 2.1 A resolution suggests a general mechanism for tight peptide binding to MHC. Cell 70:1035–48.

Madsen KG, Hansen CM, Madsen ES, et al (1998) Sequence analysis of porcine reproductive and respiratory syndrome virus of the American type collected from Danish swine herds. Arch.Virol. 143:1683–1700.

Mair KH, Essler SE, Patzl M, et al (2012) NKp46 expression discriminates porcine NK cells with different functional properties. Eur J Immunol 42:1261–1271. doi: 10.1002/eji.201141989

Mair KH, Müllebner A, Essler SE, et al (2013) Porcine CD8αdim/-NKp46high NK cells are in a highly activated state. Vet Res 44:13. doi: 10.1186/1297-9716-44-13

Manickam C, Dwivedi V, Patterson R, et al (2013) Porcine reproductive and respiratory syndrome virus induces pronounced immune modulatory responses at mucosal tissues in the parental vaccine strain VR2332 infected pigs. Vet Microbiol 162:68–77. doi: 10.1016/j.vetmic.2012.08.021

Martens GW, Lunney JK, Baker JE, Smith DM (2003) Rapid assignment of swine leukocyte antigen haplotypes in pedigreed herds using a polymerase chain reaction-based assay. Immunogenetics 55:395–401. doi: 10.1007/s00251-003-0596-3

Mateu E, Diaz I (2008) The challenge of PRRS immunology. Vet J 177:345–51. doi: 10.1016/j.tvjl.2007.05.022

Matsumura M, Fremont DH, Peterson PA, Wilson IA (1992) Emerging principles for the recognition of peptide antigens by MHC class I molecules. Science 257:927–34.

McCaw M (2003) Management Changes to Reduce Exposure to Bacteria and Eliminate Losses (McREBEL). In: Zimmerman J, Yoon K-J, Neumann E (eds) 2003 PRRS Compendium Producers Edition: A Reference for Pork Producers. National Pork Board, pp 91–95

McCullough KC, Bassi I, Milona P, et al (2014) Self-replicating Replicon-RNA Delivery to Dendritic Cells by Chitosan-nanoparticles for Translation In Vitro and In Vivo. Mol Ther Acids 3:e173. doi: 10.1038/mtna.2014.24

McKeithan TW (1995) Kinetic proofreading in T-cell receptor signal transduction. Proc Natl Acad Sci U S A 92:5042–6.

Meier T, Eulenbruch H-P, Wrighton-Smith P, et al (2005) Sensitivity of a new commercial enzyme-linked immunospot assay (T SPOT-TB) for diagnosis of tuberculosis in clinical practice. Eur J Clin Microbiol Infect Dis 24:529–36. doi: 10.1007/s10096-005-1377-8

Mempel TR, Henrickson SE, Von Andrian UH (2004) T-cell priming by dendritic cells in lymph nodes occurs in three distinct phases. Nature 427:154–9. doi: 10.1038/nature02238

Mengeling WL, Lager KM, Vorwald AC (1998) Clinical consequences of exposing pregnant gilts to strains of porcine reproductive and respiratory syndrome (PRRS) virus isolated from field cases of "atypical" PRRS. Am J Vet Res 59:1540–4.

Merad M, Sathe P, Helft J, et al (2013) The Dendritic Cell Lineage: Ontogeny and Function of Dendritic Cells and Their Subsets in the Steady State and the Inflamed Setting. Annu Rev Immunol 31:563–604. doi: 10.1146/annurev-immunol-020711-074950

Meraviglia S, El Daker S, Dieli F, et al (2011) γδ T cells cross-link innate and adaptive immunity in Mycobacterium tuberculosis infection. Clin Dev Immunol 2011:587315. doi: 10.1155/2011/587315

Mercado R, Vijh S, Allen SE, et al (2000) Early programming of T cell populations responding to bacterial infection. J Immunol 165:6833–9.

Meulenberg JJ, Hulst MM, de Meijer EJ, et al (1993) Lelystad virus, the causative agent of porcine epidemic abortion and respiratory syndrome (PEARS), is related to LDV and EAV. Virology 192:62–72. doi: 10.1006/viro.1993.1008

Miller JC, Brown BD, Shay T, et al (2012) Deciphering the transcriptional network of the dendritic cell lineage. Nat Immunol 13:888–899. doi: 10.1038/ni.2370

Miller MJ, Wei SH, Cahalan MD, Parker I (2003) Autonomous T cell trafficking examined in vivo with intravital two-photon microscopy. Proc Natl Acad Sci U S A 100:2604–9. doi: 10.1073/pnas.2628040100

Mokhtar H, Eck M, Morgan SB, et al (2014) Proteome-wide screening of the European porcine reproductive and

respiratory syndrome virus reveals a broad range of T cell antigen reactivity. Vaccine 32:6828–37. doi: 10.1016/j.vaccine.2014.04.054

Mokhtar H, Pedrera M, Frossard J-P, et al (2016) The Non-structural Protein 5 and Matrix Protein Are Antigenic Targets of T Cell Immunity to Genotype 1 Porcine Reproductive and Respiratory Syndrome Viruses. Front Immunol 7:40. doi: 10.3389/fimmu.2016.00040

Moodie Z, Huang Y, Gu L, et al (2006) Statistical positivity criteria for the analysis of ELISpot assay data in HIV-1 vaccine trials. J Immunol Methods 315:121–32. doi: 10.1016/j.jim.2006.07.015

Moore KW, de Waal Malefyt R, Coffman RL, O'Garra A (2001) Interleukin-10 and the interleukin-10 receptor. Annu Rev Immunol 19:683–765. doi: 10.1146/annurev.immunol.19.1.683

Mortensen S, Stryhn H, Søgaard R, et al (2002) Risk factors for infection of sow herds with porcine reproductive and respiratory syndrome (PRRS) virus. Prev Vet Med 53:83–101.

Murali-Krishna K, Altman JD, Suresh M, et al (1998) Counting antigen-specific CD8 T cells: a reevaluation of bystander activation during viral infection. Immunity 8:177–87.

Murtaugh MP, Stadejek T, Abrahante JE, et al (2010) The ever-expanding diversity of porcine reproductive and respiratory syndrome virus. Virus Res 154:18–30. doi: 10.1016/j.virusres.2010.08.015

Nagata S, Golstein P (1995) The Fas death factor. Science 267:1449–56.

Nathues C, Perler L, Bruhn S, et al (2014) An Outbreak of Porcine Reproductive and Respiratory Syndrome Virus in Switzerland Following Import of Boar Semen. Transbound Emerg Dis 63:e251-61. doi: 10.1111/tbed.12262

Natoli G, Costanzo A, Guido F, et al (1998) Apoptotic, non-apoptotic, and anti-apoptotic pathways of tumor necrosis factor signalling. Biochem Pharmacol 56:915–920. doi: 10.1016/S0006-2952(98)00154-3

Nelsen CJ, Murtaugh MP, Faaberg KS (1999) Porcine reproductive and respiratory syndrome virus comparison: divergent evolution on two continents. J Virol 73:270–80.

Norbury CC, Chambers BJ, Prescott AR, et al (1997) Constitutive macropinocytosis allows TAP-dependent major histocompatibility complex class I presentation of exogenous soluble antigen by bone marrow-derived dendritic cells. Eur J Immunol 27:280–8. doi: 10.1002/eji.1830270141

Norbury CC, Hewlett LJ, Prescott AR, et al (1995) Class I MHC presentation of exogenous soluble antigen via macropinocytosis in bone marrow macrophages. Immunity 3:783–91.

Olin MR, Batista L, Xiao Z, et al (2005a) γδ Lymphocyte Response to Porcine Reproductive and Respiratory Syndrome Virus. Viral Immunol 18:490–499. doi: 10.1089/vim.2005.18.490

Olin MR, Hwa Choi K, Lee J, Molitor TW (2005b) γδ T-lymphocyte cytotoxic activity against Mycobacterium bovis analyzed by flow cytometry. J Immunol Methods 297:1–11. doi: 10.1016/j.jim.2004.10.002

Osorio FAA, Galeota JAA, Nelson E, et al (2002) Passive Transfer of Virus-Specific Antibodies Confers Protection against Reproductive Failure Induced by a Virulent Strain of Porcine Reproductive and Respiratory Syndrome Virus and Establishes Sterilizing Immunity. Virology 302:9–20. doi: 10.1006/viro.2002.1612

Ostrowski M, Galeota JA, Jar AM, et al (2002) Identification of neutralizing and nonneutralizing epitopes in the porcine reproductive and respiratory syndrome virus GP5 ectodomain. J Virol 76:4241–50.

Otake S, Dee S, Corzo C, et al (2010) Long-distance airborne transport of infectious PRRSV and Mycoplasma hyopneumoniae from a swine population infected with multiple viral variants. Vet Microbiol 145:198–208. doi: 10.1016/j.vetmic.2010.03.028

Overgaard NH, Frøsig TM, Welner S, et al (2015) Establishing the pig as a large animal model for vaccine development against human cancer. Front Genet. doi: 10.3389/fgene.2015.00286

Pandya M, Rasmussen M, Hansen A, et al (2015) A modern approach for epitope prediction: identification of foot-and-mouth disease virus peptides binding bovine leukocyte antigen (BoLA) class I molecules. Immunogenetics 67:691–703. doi: 10.1007/s00251-015-0877-7

Park C, Choi K, Jeong J, Chae C (2015) Cross-protection of a new type 2 porcine reproductive and respiratory syndrome virus (PRRSV) modified live vaccine (Fostera PRRS) against heterologous type 1 PRRSV challenge in growing pigs. Vet Microbiol 177:87–94. doi: 10.1016/j.vetmic.2015.02.020

Parker KC, DiBrino M, Hull L, Coligan JE (1992) The beta 2-microglobulin dissociation rate is an accurate measure of the stability of MHC class I heterotrimers and depends on which peptide is bound. J Immunol 149:1896–904.

Patel D, Nan Y, Shen M, et al (2010) Porcine reproductive and respiratory syndrome virus inhibits type I interferon signaling by blocking STAT1/STAT2 nuclear translocation. J Virol 84:11045–55. doi: 10.1128/JVI.00655-10

Pedersen KW, van der Meer Y, Roos N, Snijder EJ (1999) Open reading frame 1a-encoded subunits of the arterivirus replicase induce endoplasmic reticulum-derived double-membrane vesicles which carry the viral replication complex. J Virol 73:2016–26.

Pedersen LE, Harndahl M, Rasmussen M, et al (2011) Porcine major histocompatibility complex (MHC) class I molecules and analysis of their peptide-binding specificities. Immunogenetics 63:821–34. doi: 10.1007/s00251-011-0555-3

Pedersen LE, Jungersen G, Sorensen MR, et al (2014) Swine Leukocyte Antigen (SLA) class I allele typing of Danish swine herds and identification of commonly occurring haplotypes using sequence specific low and high resolution primers. Vet Immunol Immunopathol 162:108–16. doi: 10.1016/j.vetimm.2014.10.007

Pedersen LE, Rasmussen M, Harndahl M, et al (2016) A combined prediction strategy increases identification of peptides bound with high affinity and stability to porcine MHC class I molecules SLA-1*04:01, SLA-2*04:01, and SLA-3*04:01. Immunogenetics 68:157–165. doi: 10.1007/s00251-015-0883-9

Pileri E, Mateu E (2016) Review on the transmission porcine reproductive and respiratory syndrome virus between pigs and farms and impact on vaccination. Vet Res 47:108. doi: 10.1186/s13567-016-0391-4

Pirzadeh B, Dea S (1997) Monoclonal antibodies to the ORF5 product of porcine reproductive and respiratory syndrome virus define linear neutralizing determinants. J Gen Virol 78 (Pt 8):1867–73. doi: 10.1099/0022-1317-78-8-1867

Plagemann PGW (2003) Porcine Reproductive and Respiratory Syndrom Virus: Origin Hypothesis. Emerg Infect Dis 9:903–908.

Plagemann PGW (2004a) GP5 ectodomain epitope of porcine reproductive and respiratory syndrome virus, strain Lelystad virus. Virus Res 102:225–230. doi: 10.1016/j.virusres.2004.01.031

Plagemann PGW (2004b) The primary GP5 neutralization epitope of North American isolates of porcine reproductive and respiratory syndrome virus. Vet Immunol Immunopathol 102:263–75. doi: 10.1016/j.vetimm.2004.09.011

Prajeeth CK, Haeberlein S, Sebald H, et al (2011) Leishmania-infected macrophages are targets of NK cell-derived cytokines but not of NK cell cytotoxicity. Infect Immun 79:2699–708. doi: 10.1128/IAI.00079-11

Prlic M, Hernandez-Hoyos G, Bevan MJ (2006) Duration of the initial TCR stimulus controls the magnitude but not functionality of the CD8+ T cell response. J Exp Med 203:2135–43. doi: 10.1084/jem.20060928

Provost C, Jia JJ, Music N, et al (2012) Identification of a new cell line permissive to porcine reproductive and respiratory syndrome virus infection and replication which is phenotypically distinct from MARC-145 cell line. Virol.J. 9:267-.

Pujhari S, Baig TT, Zakhartchouk AN (2014) Potential role of porcine reproductive and respiratory syndrome virus structural protein GP2 in apoptosis inhibition. Biomed Res Int 2014:160505. doi: 10.1155/2014/160505

Rahemtulla A, Fung-Leung WP, Schilham MW, et al (1991) Normal development and function of CD8+ cells but markedly decreased helper cell activity in mice lacking CD4. Nature 353:180–4. doi: 10.1038/353180a0

Regoes RR, Barber DL, Ahmed R, Antia R (2007) Estimation of the rate of killing by cytotoxic T lymphocytes in vivo. Proc Natl Acad Sci U S A 104:1599–603. doi: 10.1073/pnas.0508830104

Reinhold B, Keskin DB, Reinherz EL (2010) Molecular Detection of Targeted Major Histocompatibility Complex I-Bound Peptides Using a Probabilistic Measure and Nanospray MS ^{3} on a Hybrid Quadrupole-Linear Ion Trap. Anal Chem 82:9090–9099. doi: 10.1021/ac102387t

Reis e Sousa C (2001) Dendritic cells as sensors of infection. Immunity 14:495–8.

Renukaradhya GJ, Meng X-J, Calvert JG, et al (2015a) Inactivated and subunit vaccines against porcine reproductive and respiratory syndrome: Current status and future direction. Vaccine 33:3065–72. doi: 10.1016/j.vaccine.2015.04.102

Renukaradhya GJ, Meng X-J, Calvert JG, et al (2015b) Live porcine reproductive and respiratory syndrome virus vaccines: Current status and future direction. Vaccine 33:4069–80. doi: 10.1016/j.vaccine.2015.06.092

Rock KL, Shen L (2005) Cross-presentation: underlying mechanisms and role in immune surveillance. Immunol Rev 207:166–183. doi: 10.1111/j.0105-2896.2005.00301.x

Rodríguez-Gómez IM, Gómez-Laguna J, Carrasco L (2013) Impact of PRRSV on activation and viability of antigen presenting cells. World J Virol 2:146–51. doi: 10.5501/wjv.v2.i4.146

Rosendal T, Dewey C, Friendship R, et al (2014) Spatial and temporal patterns of porcine reproductive and respiratory syndrome virus (PRRSV) genotypes in Ontario, Canada, 2004–2007. BMC Vet Res 10:83. doi: 10.1186/1746-6148-10-83

Rossow KD (1998) Porcine Reproductive and Respiratory Syndrome. Vet Pathol l:1–20.

Rothkötter HJ (2009) Anatomical particularities of the porcine immune system-A physician's view. Dev Comp Immunol 33:267–272. doi: 10.1016/j.dci.2008.06.016

Rothoeft T, Balkow S, Krummen M, et al (2006) Structure and duration of contact between dendritic cells and T cells are controlled by T cell activation state. Eur J Immunol 36:3105–17. doi: 10.1002/eji.200636145

Rowley T (2012) Flow Cytometry - A Survey and the Basics. Mater Methods. doi: 10.13070/mm.en.2.125

Sabat R, Grütz G, Warszawska K, et al (2010) Biology of interleukin-10. Cytokine Growth Factor Rev 21:331–44. doi: 10.1016/j.cytogfr.2010.09.002

Sagong M, Lee C (2011) Porcine reproductive and respiratory syndrome virus nucleocapsid protein modulates interferon-β production by inhibiting IRF3 activation in immortalized porcine alveolar macrophages. Arch Virol 156:2187–95. doi: 10.1007/s00705-011-1116-7

Saletti G, Çuburu N, Yang JS, et al (2013) Enzyme-linked immunospot assays for direct ex vivo measurement of vaccine-induced human humoral immune responses in blood. Nat Protoc 8:1073–87. doi: 10.1038/nprot.2013.058

Samsom JN, de Bruin TG, Voermans JJ, et al (2000) Changes of leukocyte phenotype and function in the broncho-alveolar lavage fluid of pigs infected with porcine reproductive and respiratory syndrome virus: a role for CD8(+) cells. J Gen Virol 81:497–505. doi: 10.1099/0022-1317-81-2-497

Saurer L, McCullough KC, Summerfield A (2007) In vitro induction of mucosa-type dendritic cells by all-trans retinoic acid. J Immunol 179:3504–14.

Sedgwick JD, Holt PG (1983) A solid-phase immunoenzymatic technique for the enumeration of specific antibody-secreting cells. J Immunol Methods 57:301–9.

Sedlak C, Patzl M, Saalmüller A, Gerner W (2014) CD2 and CD8α define porcine γδ T cells with distinct cytokine production profiles. Dev Comp Immunol 45:97–106. doi: 10.1016/j.dci.2014.02.008

Sercarz EE, Lehmann P V, Ametani A, et al (1993) Dominance and Crypticity of T Cell Antigenic Determinants. Annu Rev Immunol 11:729–766. doi: 10.1146/annurev.iy.11.040193.003501

Shanmukhappa K, Kim JK, Kapil S (2007) Role of CD151, A tetraspanin, in porcine reproductive and respiratory syndrome virus infection. VirolJ 4:62. doi: 10.1186/1743-422X-4-62

Shedlock DJ, Shen H (2003) Requirement for CD4 T Cell Help in Generating Functional CD8 T Cell Memory. Science (80-) 300:337–339. doi: 10.1126/science.1082305

Shen Z, Reznikoff G, Dranoff G, Rock KL (1997) Cloned dendritic cells can present exogenous antigens on both MHC class I and class II molecules. J Immunol 158:2723–30.

Shi K, Li H, Guo X, et al (2008) Changes in peripheral blood leukocyte subpopulations in piglets co-infected experimentally with porcine reproductive and respiratory syndrome virus and porcine circovirus type 2.

Shi M, Lam TT-Y, Hon C-C, et al (2010a) Phylogeny-Based Evolutionary, Demographical, and Geographical Dissection of North American Type 2 Porcine Reproductive and Respiratory Syndrome Viruses. J Virol 84:8700–8711. doi: 10.1128/JVI.02551-09

Shi M, Lam TT-Y, Hon C-C, et al (2010b) Molecular epidemiology of PRRSV: a phylogenetic perspective. Virus Res 154:7–17. doi: 10.1016/j.virusres.2010.08.014

Šinkora M, Šinkora J, Reháková Z, Butler JE (2000) Early Ontogeny of Thymocytes in Pigs: Sequential Colonization of the Thymus by T Cell Progenitors.

Sinkora M, Sinkorová J, Cimburek Z, Holtmeier W (2007) Two groups of porcine TCRgammadelta+ thymocytes behave and diverge differently. J Immunol 178:711–9.

Sinkora M, Sinkorová J, Holtmeier W (2005) Development of gammadelta thymocyte subsets during prenatal and postnatal ontogeny. Immunology 115:544–55. doi: 10.1111/j.1365-2567.2005.02194.x

Slifka MK, Blattman JN, Sourdive DJD, et al (2003) Preferential escape of subdominant CD8+ T cells during negative selection results in an altered antiviral T cell hierarchy. J Immunol 170:1231–9.

Smith-Garvin JE, Koretzky GA, Jordan MS (2009) T cell activation. Annu Rev Immunol 27:591–619. doi: 10.1146/annurev.immunol.021908.132706

Smith CA, Farrah T, Goodwin RG, et al (1994) The TNF receptor superfamily of cellular and viral proteins: activation, costimulation, and death. Cell 76:959–62. doi: 10.1016/0092-8674(94)90372-7

Solano GI, Segalés J, Collins JE, et al (1997) Porcine reproductive and respiratory syndrome virus (PRRSv) interaction with Haemophilus parasuis. Vet Microbiol 55:247–57.

Song C, Krell P, Yoo D (2010) Nonstructural protein 1α subunit-based inhibition of NF-κB activation and suppression of interferon-β production by porcine reproductive and respiratory syndrome virus. Virology 407:268–280. doi: 10.1016/j.virol.2010.08.025

Song S, Bi J, Wang D, et al (2013) Porcine reproductive and respiratory syndrome virus infection activates IL-10 production through NF-κB and p38 MAPK pathways in porcine alveolar macrophages. Dev Comp Immunol 39:265–272. doi: 10.1016/j.dci.2012.10.001

Song T, Fang L, Wang D, et al (2016) Quantitative interactome reveals that porcine reproductive and respiratory syndrome virus nonstructural protein 2 forms a complex with viral nucleocapsid protein and cellular vimentin. J Proteomics 142:70–81. doi: 10.1016/j.jprot.2016.05.009

Spilman MS, Welbon C, Nelson E, Dokland T (2009) Cryo-electron tomography of porcine reproductive and

respiratory syndrome virus: organization of the nucleocapsid. J Gen Virol 90:527–535. doi: 10.1099/vir.0.007674-0

Stadejek T, Oleksiewicz MB, Scherbakov A V., et al (2008) Definition of subtypes in the European genotype of porcine reproductive and respiratory syndrome virus: nucleocapsid characteristics and geographical distribution in Europe. ArchVirol 153:1479–1488. doi: 10.1007/s00705-008-0146-2

Stadejek T, Stankevicius A, Murtaugh MP, Oleksiewicz MB (2013) Molecular evolution of PRRSV in Europe: current state of play. VetMicrobiol 165:21–28. doi: 10.1016/j.vetmic.2013.02.029

Stanke J, Hoffmann C, Erben U, et al (2010) A flow cytometry-based assay to assess minute frequencies of CD8+ T cells by their cytolytic function. J Immunol Methods 360:56–65. doi: 10.1016/j.jim.2010.06.005

Stein M, Keshav S (1992) The versatility of macrophages. Clin Exp Allergy 22:19–27.

Steinbrink K, Graulich E, Kubsch S, et al (2002) CD4(+) and CD8(+) anergic T cells induced by interleukin-10-treated human dendritic cells display antigen-specific suppressor activity. Blood 99:2468–76.

Steinman RM (1991) The Dendritic Cell System and its Role in Immunogenicity. Annu Rev Immunol 9:271–296. doi: 10.1146/annurev.iy.09.040191.001415

Štěpánová K, Šinkora M (2012) The expression of CD25, CD11b, SWC1, SWC7, MHC-II, and family of CD45 molecules can be used to characterize different stages of γδ T lymphocytes in pigs. Dev Comp Immunol 36:728–740. doi: 10.1016/j.dci.2011.11.003

Stetson DB, Mohrs M, Reinhardt RL, et al (2003) Constitutive Cytokine mRNAs Mark Natural Killer (NK) and NK T Cells Poised for Rapid Effector Function.

Stevenson GW, Van Alstine WG, Kanitz CL, Keffaber KK (1993) Endemic porcine reproductive and respiratory syndrome virus infection of nursery pigs in two swine herds without current reproductive failure. JVetDiagnInvest 5:432–434.

Streeck H, Frahm N, Walker BD (2009) The role of IFN-γ Elispot assay in HIV vaccine research. Nat Protoc 4:461–469. doi: 10.1038/nprot.2009.7

Stryhn A, Pedersen LO, Romme T, et al (1996) Peptide binding specificity of major histocompatibility complex class I resolved into an array of apparently independent subspecificities: quantitation by peptide libraries and improved prediction of binding. EurJImmunol 26:1911–1918. doi: 10.1002/eji.1830260836

Subramaniam S, Kwon B, Beura LK, et al (2010) Porcine reproductive and respiratory syndrome virus non-structural protein 1 suppresses tumor necrosis factor-alpha promoter activation by inhibiting NF-κB and Sp1. Virology 406:270–279. doi: 10.1016/j.virol.2010.07.016

Summerfield A, McCullough KC (2009) The porcine dendritic cell family. Dev Comp Immunol 33:299–309. doi: 10.1016/j.dci.2008.05.005

Sun JC, Bevan MJ (2003) Defective CD8 T Cell Memory Following Acute Infection Without CD4 T Cell Help. Science (80-) 300:339–342. doi: 10.1126/science.1083317

Sun L, Li Y, Liu R, et al (2013) Porcine reproductive and respiratory syndrome virus ORF5a protein is essential for virus viability. Virus Res 171:178–185. doi: 10.1016/j.virusres.2012.11.005

Sun Y, Li D, Giri S, et al (2014) Differential host cell gene expression and regulation of cell cycle progression by nonstructural protein 11 of porcine reproductive and respiratory syndrome virus. Biomed Res Int 2014:430508. doi: 10.1155/2014/430508

Sun Z, Chen Z, Lawson SR, Fang Y (2010) The cysteine protease domain of porcine reproductive and respiratory syndrome virus nonstructural protein 2 possesses deubiquitinating and interferon antagonism functions. J Virol 84:7832–46. doi: 10.1128/JVI.00217-10

Sun Z, Li Y, Ransburgh R, et al (2012) Nonstructural protein 2 of porcine reproductive and respiratory syndrome virus inhibits the antiviral function of interferon-stimulated gene 15. J Virol 86:3839–50. doi: 10.1128/JVI.06466-11

Suradhat S, Wongyanin P, Kesdangsakonwut S, et al (2015a) A novel DNA vaccine for reduction of PRRSV-induced negative immunomodulatory effects: A proof of concept. Vaccine 33:3997–4003. doi: 10.1016/j.vaccine.2015.06.020

Suradhat S, Wongyanin P, Sirisereewan C, et al (2015b) Transdermal delivery of plasmid encoding truncated nucleocapsid protein enhanced PRRSV-specific immune responses. Vaccine 34:609–615. doi: 10.1016/j.vaccine.2015.12.043

Suter R, Summerfield A, Thomann-Harwood LJ, et al (2011) Immunogenic and replicative properties of classical swine fever virus replicon particles modified to induce IFN-α/β and carry foreign genes. Vaccine 29:1491–503. doi: 10.1016/j.vaccine.2010.12.026

Sykulev Y, Joo M, Vturina I, et al (1996) Evidence that a single peptide-MHC complex on a target cell can elicit a cytolytic T cell response. Immunity 4:565–71.

Sylvester-Hvid C, Kristensen N, Blicher T, et al (2002) Establishment of a quantitative ELISA capable of determining peptide - MHC class I interaction. Tissue Antigens 59:251–8.

Saalmüller A, Reddehase MJ, Bühring H-J, et al (1987) Simultaneous expression of CD4 and CD8 antigens by a substantial proportion of resting porcine T lymphocytes. Eur J Immunol 17:1297–1301. doi: 10.1002/eji.1830170912

Takamatsu H-H, Denyer M., Wileman T. (2002) A sub-population of circulating porcine γδ T cells can act as professional antigen presenting cells. Vet Immunol Immunopathol 87:223–224. doi: 10.1016/S0165-2427(02)00083-1

Takamatsu H-H, Denyer MS, Stirling C, et al (2006) Porcine γδ T cells: Possible roles on the innate and adaptive immune responses following virus infection. Vet Immunol Immunopathol 112:49–61. doi: 10.1016/j.vetimm.2006.03.011

Talker SC, Käser T, Reutner K, et al (2013) Phenotypic maturation of porcine NK- and T-cell subsets. Dev Comp Immunol 40:51–68. doi: 10.1016/j.dci.2013.01.003

Thacker EL, Halbur PG, Ross RF, et al (1999) Mycoplasma hyopneumoniae potentiation of porcine reproductive and respiratory syndrome virus-induced pneumonia. J Clin Microbiol 37:620–7.

Thomson BJ (2001) Viruses and apoptosis. Int J Exp Pathol 82:65–76.

Tian D, Wei Z, Zevenhoven-Dobbe JC, et al (2012) Arterivirus minor envelope proteins are a major determinant of viral tropism in cell culture. J Virol 86:3701–12. doi: 10.1128/JVI.06836-11

Tian K, Yu X, Zhao T, et al (2007) Emergence of fatal PRRSV variants: unparalleled outbreaks of atypical PRRS in China and molecular dissection of the unique hallmark. PLoS One 2:e526. doi: 10.1371/journal.pone.0000526

Tingstedt J-E, Nielsen J (2004) Cellular immune responses in the lungs of pigs infected in utero with PRRSV: an immunohistochemical study. Viral Immunol 17:558–64. doi: 10.1089/vim.2004.17.558

Torremorell M, Moore C, Christianson WT (2002) Establishment of a herd negative for porcine reproductive and respiratory syndrome virus (PRRSV) from PRRSV-positive sources. J Swine Heal Prod 10:153–160.

Torremorell M, Pijoan C, Janni K, et al (1997) Airborne transmission of Actinobacillus pleuropneumoniae and porcine reproductive and respiratory syndrome virus in nursery pigs. Am J Vet Res 58:828–32.

Tousignant SJP, Perez AM, Lowe JF, et al (2015) Temporal and spatial dynamics of porcine reproductive and respiratory syndrome virus infection in the United States. Am J Vet Res 76:70–76. doi: 10.2460/ajvr.76.1.70

Trolle T, Metushi IG, Greenbaum JA, et al (2015) Automated benchmarking of peptide-MHC class I binding predictions. Bioinformatics 31:2174–81. doi: 10.1093/bioinformatics/btv123

Turner SJ, Doherty PC, McCluskey J, Rossjohn J (2006) Structural determinants of T-cell receptor bias in immunity. Nat Rev Immunol 6:883–894. doi: 10.1038/nri1977

Uenishi H, Eguchi-Ogawa T, Toki D, et al (2009) Genomic sequence encoding diversity segments of the pig TCR δ chain gene demonstrates productivity of highly diversified repertoire. Mol Immunol 46:1212–1221. doi: 10.1016/j.molimm.2008.11.010

Valitutti S, Lanzavecchia A (1997) Serial triggering of TCRs: a basis for the sensitivity and specificity of antigen recognition. Immunol Today 18:299–304.

Valitutti S, Müller S, Cella M, et al (1995) Serial triggering of many T-cell receptors by a few peptide-MHC complexes. Nature 375:148–51. doi: 10.1038/375148a0

Van Breedam W, Van Gorp H, Zhang JQ, et al (2010) The M/GP5 Glycoprotein Complex of Porcine Reproductive and Respiratory Syndrome Virus Binds the Sialoadhesin Receptor in a Sialic Acid-Dependent Manner. PLoS Pathog 6:e1000730. doi: 10.1371/journal.ppat.1000730

van der Burg SH, Visseren MJ, Brandt RM, et al (1996) Immunogenicity of peptides bound to MHC class I molecules depends on the MHC-peptide complex stability. J Immunol 156:3308–14.

Van Doorsselaere J, Brar MS, Shi M, et al (2012) Complete genome characterization of a East European Type 1 subtype 3 porcine reproductive and respiratory syndrome virus. Virus Genes 44:51–54. doi: 10.1007/s11262-011-0665-x

Van Gorp H, Van Breedam W, Delputte PL, Nauwynck HJ (2008) Sialoadhesin and CD163 join forces during entry of the porcine reproductive and respiratory syndrome virus. J Gen Virol 89:2943–2953. doi: 10.1099/vir.0.2008/005009-0

Van Gorp H, Van Breedam W, Delputte PL, Nauwynck HJ (2009) The porcine reproductive and respiratory syndrome virus requires trafficking through CD163-positive early endosomes, but not late endosomes, for productive infection. Arch Virol 154:1939–1943. doi: 10.1007/s00705-009-0527-1

van Hemert MJ, de Wilde AH, Gorbalenya AE, Snijder EJ (2008) The in vitro RNA synthesizing activity of the isolated arterivirus replication/transcription complex is dependent on a host factor. J Biol Chem 283:16525–36. doi: 10.1074/jbc.M708136200

van Marle G, Dobbe JC, Gultyaev AP, et al (1999) Arterivirus discontinuous mRNA transcription is guided by base pairing between sense and antisense transcription-regulating sequences. Proc Natl Acad Sci U S A 96:12056–61. doi: 10.1073/PNAS.96.21.12056

Van Reeth K, Nauwynck H, Pensaert M (1996) Dual infections of feeder pigs with porcine reproductive and respiratory syndrome virus followed by porcine respiratory coronavirus or swine influenza virus: a clinical and virological study. Vet Microbiol 48:325–35.

Vanderheijden N, Delputte PL, Favoreel HW, et al (2003) Involvement of sialoadhesin in entry of porcine reproductive and respiratory syndrome virus into porcine alveolar macrophages. J Virol 77:8207–15. doi: 10.1128/JVI.77.15.8207-8215.2003

Vanhee M, Van Breedam W, Costers S, et al (2011) Characterization of antigenic regions in the porcine reproductive and respiratory syndrome virus by the use of peptide-specific serum antibodies. Vaccine 29:4794–804. doi: 10.1016/j.vaccine.2011.04.071

Vidović D, Matzinger P (1988) Unresponsiveness to a foreign antigen can be caused by self-tolerance. Nature 336:222–225. doi: 10.1038/336222a0

Vivier E (2006) What is natural in natural killer cells? Immunol Lett 107:1–7. doi: 10.1016/j.imlet.2006.07.004

von Andrian UH, Mackay CR, von Andrian UH, Mackay CR (2000) T-cell function and migration. Two sides of the same coin. N Engl J Med 343:1020–34. doi: 10.1056/NEJM200010053431407

Vu HLX, Kwon B, Yoon K-J, et al (2011) Immune evasion of porcine reproductive and respiratory syndrome virus through glycan shielding involves both glycoprotein 5 as well as glycoprotein 3. J Virol 85:5555–64. doi: 10.1128/JVI.00189-11

Walker BA, Hunt LG, Sowa AK, et al (2011) The dominantly expressed class I molecule of the chicken MHC is explained by coevolution with the polymorphic peptide transporter (TAP) genes. Proc Natl Acad Sci 108:8396–8401. doi: 10.1073/pnas.1019496108

Walzer T, Dalod M, Robbins SH, et al (2005) Natural-killer cells and dendritic cells: “l’union fait la force.”

Wang R, Nan Y, Yu Y, Zhang Y-J (2013) Porcine reproductive and respiratory syndrome virus Nsp1β inhibits interferon-activated JAK/STAT signal transduction by inducing karyopherin-α1 degradation. J Virol 87:5219–28. doi: 10.1128/JVI.02643-12

Wang X, Eaton M, Mayer M, et al (2007) Porcine reproductive and respiratory syndrome virus productively infects monocyte-derived dendritic cells and compromises their antigen-presenting ability. Arch Virol 152:289–303. doi: 10.1007/s00705-006-0857-1

Wei Z, Lin T, Sun L, et al (2012a) N-linked glycosylation of GP5 of porcine reproductive and respiratory syndrome virus is critically important for virus replication in vivo. J Virol 86:9941–51. doi: 10.1128/JVI.07067-11

Wei Z, Tian D, Sun L, et al (2012b) Influence of N-linked glycosylation of minor proteins of porcine reproductive and respiratory syndrome virus on infectious virus recovery and receptor interaction. Virology 429:1–11. doi: 10.1016/j.virol.2012.03.010

Wells KD, Bardot R, Whitworth KM, et al (2017) Replacement of Porcine CD163 Scavenger Receptor Cysteine-Rich Domain 5 with a CD163-Like Homolog Confers Resistance of Pigs to Genotype 1 but Not Genotype 2 Porcine Reproductive and Respiratory Syndrome Virus. J Virol 91:1–11.

Wensvoort G, de Kluyver EP, Luijtze EA, et al (1992) Antigenic comparison of Lelystad virus and swine infertility and respiratory syndrome (SIRS) virus. J Vet Diagn Invest 4:134–8.

Wensvoort G, Terpstra C, Pol JM, et al (1991) Mystery swine disease in The Netherlands: the isolation of Lelystad virus. Vet Q 13:121–130. doi: 10.1080/01652176.1991.9694296

Williams AP, Peh CA, Purcell AW, et al (2002) Optimization of the MHC class I peptide cargo is dependent on tapasin. Immunity 16:509–20.

Williams MA, Bevan MJ (2007) Effector and Memory CTL Differentiation. Annu Rev Immunol 25:171–192. doi: 10.1146/annurev.immunol.25.022106.141548

Wills RW, Doster AR, Galeota JA, et al (2003) Duration of infection and proportion of pigs persistently infected with porcine reproductive and respiratory syndrome virus. J Clin Microbiol 41:58–62.

Wills RW, Zimmerman JJ, Yoon KJ, et al (1997) Porcine reproductive and respiratory syndrome virus: a persistent infection. VetMicrobiol 55:231–240.

Wissink EHJ, Kroese M V, van Wijk HAR, et al (2005) Envelope protein requirements for the assembly of infectious virions of porcine reproductive and respiratory syndrome virus. J Virol 79:12495–506. doi: 10.1128/JVI.79.19.12495-12506.2005

Witherden DA, Havran WL (2013) Cross-talk between intraepithelial T cells and epithelial cells. J Leukoc Biol 94:69–76. doi: 10.1189/jlb.0213101

Wongyanin P, Buranapraditkul S, Yoo D, et al (2012) Role of porcine reproductive and respiratory syndrome virus nucleocapsid protein in induction of interleukin-10 and regulatory T-lymphocytes (Treg). J Gen Virol 93:1236–

46. doi: 10.1099/vir.0.040287-0

Wongyanin P, Buranapraditkun S, Chokeshai-usaha K, et al (2010) Induction of inducible CD4+CD25+Foxp3+ regulatory T lymphocytes by porcine reproductive and respiratory syndrome virus (PRRSV). Vet Immunol Immunopathol 133:170–182. doi: 10.1016/j.vetimm.2009.07.012

Wu WH, Fang Y, Farwell R, et al (2001) A 10-kDa structural protein of porcine reproductive and respiratory syndrome virus encoded by ORF2b. Virology 287:183–91. doi: 10.1006/viro.2001.1034

Wykes M, Pombo A, Jenkins C, MacPherson GG (1998) Dendritic cells interact directly with naive B lymphocytes to transfer antigen and initiate class switching in a primary T-dependent response. J Immunol 161:1313–9.

Xiao Z, Batista L, Dee S, et al (2004) The level of virus-specific T-cell and macrophage recruitment in porcine reproductive and respiratory syndrome virus infection in pigs is independent of virus load. J Virol 78:5923–33. doi: 10.1128/JVI.78.11.5923-5933.2004

Xu X-G, Wang Z-S, Zhang Q, et al (2012) Baculovirus as a PRRSV and PCV2 bivalent vaccine vector: baculovirus virions displaying simultaneously GP5 glycoprotein of PRRSV and capsid protein of PCV2. J Virol Methods 179:359–66. doi: 10.1016/j.jviromet.2011.11.023

Yamazaki S, Patel M, Harper A, et al (2006) Effective expansion of alloantigen-specific Foxp3+ CD25+ CD4+ regulatory T cells by dendritic cells during the mixed leukocyte reaction. Proc Natl Acad Sci 103:2758–2763. doi: 10.1073/pnas.0510606103

Yewdell JW, Bennink JR (1999) Immunodominance in major histocompatibility complex class I-restricted T lymphocyte responses. Annu Rev Immunol 17:51–88. doi: 10.1146/annurev.immunol.17.1.51

Yewdell JW, Haeryfar SMM (2005) Understanding presentation of viral antigens to CD8+ T cells in vivo: the key to rational vaccine design. Annu Rev Immunol 23:651–82. doi: 10.1146/annurev.immunol.23.021704.115702

Yokosuka T, Sakata-Sogawa K, Kobayashi W, et al (2005) Newly generated T cell receptor microclusters initiate and sustain T cell activation by recruitment of Zap70 and SLP-76. Nat Immunol 6:1253–62. doi: 10.1038/ni1272

Yoon SH, Kim H, Kim J, et al (2013) Complete genome sequences of porcine reproductive and respiratory syndrome viruses: perspectives on their temporal and spatial dynamics. Mol Biol Rep 40:6843–6853. doi: 10.1007/s11033-013-2802-1

Zhang L, Zhou L, Ge X, et al (2016) The Chinese highly pathogenic porcine reproductive and respiratory syndrome virus infection suppresses Th17 cells response in vivo. Vet Microbiol 189:75–85. doi: 10.1016/j.vetmic.2016.05.001

Zhang W, Caspell R, Karulin AY, et al (2009) ELISPOT assays provide reproducible results among different laboratories for T-cell immune monitoring—even in hands of ELISPOT-inexperienced investigators. J Immunotoxicol 6:227–234. doi: 10.3109/15476910903317546

Zhang Y, Zhou Y, Yang Q, et al (2012) Ligation of Fc gamma receptor IIB enhances levels of antiviral cytokine in response to PRRSV infection in vitro.

Zhou J-X, Xue J-D, Yu T, et al (2010) Immune responses in pigs induced by recombinant canine adenovirus 2 expressing the glycoprotein 5 of porcine reproductive and respiratory syndrome virus. Vet Res Commun 34:371–80. doi: 10.1007/s11259-010-9364-7

Zhou L, Yang H (2010) Porcine reproductive and respiratory syndrome in China. Virus Res 154:31–37. doi: 10.1016/j.virusres.2010.07.016

Zhou Y, Bai J, Li Y, et al (2012) Suppression of immune responses in pigs by nonstructural protein 1 of porcine reproductive and respiratory syndrome virus. Can J Vet Res 76:255–60.

Zhou Y, Lin G, Baarsch MJ, et al (1994) Interleukin-4 suppresses inflammatory cytokine gene transcription in porcine

macrophages. J Leukoc Biol 56:507–13.

Zimmerman JJ, Yoon K-J, Wills RW, Swenson SL (1997) General overview of PRRSV: A perspective from the United States. Vet Microbiol 55:187–196. doi: 10.1016/S0378-1135(96)01330-2

Zuckermann FA (1999) Extrathymic CD4/CD8 double positive T cells. Vet Immunol Immunopathol 72:55–66.

Zuckermann FA, Garcia EA, Luque ID, et al (2007) Assessment of the efficacy of commercial porcine reproductive and respiratory syndrome virus (PRRSV) vaccines based on measurement of serologic response, frequency of gamma-IFN-producing cells and virological parameters of protection upon challenge. Vet Microbiol 123:69–85. doi: 10.1016/j.vetmic.2007.02.009

Don’t be a pig!

Simon Welner
PhD thesis 2017

DTU Vet
National Veterinary Institute
Technical University of Denmark

Kemitorvet, Building 202
DK-2800 Kgs. Lyngby
www.vet.dtu.dk